



TECHNISCHE UNIVERSITÄT WIEN

DISSERTATION

Modeling of a human spinal pattern generator for locomotion and its activation by electrical epidural stimulation

ausgeführt zum Zwecke der Erlangung des akademischen Grades eines
Doktors der technischen Wissenschaften unter der Leitung von

Ao. Univ. Prof. DDr. Frank Rattay
E101
Institut für Analysis und Scientific Computing

Eingereicht an der Technischen Universität Wien,
Fakultät für Mathematik und Geoinformation

von

Dipl.-Ing. Karen Minassian
9225637
Blechturmstraße 15–17/3
A-1050 Wien

Wien, im Mai 2004

Handwritten signature of Karen Minassian in black ink, underlined.

Kurzfassung der Dissertation

Modellierung eines spinalen Mustergenerators für Lokomotion im Menschen und dessen Aktivierung mittels elektrischer, epiduraler Rückenmarksstimulation

Motivation und Ziele der Dissertation

Der erste direkte Hinweis auf die Existenz eines spinalen Mustergenerators für Lokomotion im Menschen gelang 1998 in Patienten mit traumatischen Rückenmarksverletzungen nach Setzen einer epiduralen Rückenmarkselektrode zur Kontrolle der Spastizität. Bei kontinuierlicher, elektrischer Stimulation der posterioren Strukturen des lumbalen Rückenmarks konnten unwillkürliche Schrittbewegungen der unteren Extremitäten ausgelöst werden. Die theoretischen Grundlagen waren zu diesem Zeitpunkt weitgehend unerforscht.

Basierend auf dieser Beobachtung wurde in der vorliegenden Dissertation eine systematische Untersuchung der zugrunde liegenden neuronalen Mechanismen mittels mathematischen Modellen und neurophysiologischen Methoden durchgeführt. Konkrete Ziele waren (i) die Identifizierung der durch die elektrische Rückenmarksstimulation angeregten neuronalen Strukturen zur Auslösung der schrittähnlichen Bewegungen; (ii) Hinweise zu erbringen, dass autonome interneuronale Netzwerke an der Initiierung und Kontrolle der evozierten rhythmischen Bewegung beteiligt sind; (iii) festzustellen, ob das durch elektrische Stimulation aktivierte Lokomotionszentrum im Rückenmark afferentes Feedback ausgelöst durch manuell assistiertes Laufband-Gehen verarbeiten kann, um funktionelle Aktivitätsmuster der Beinmuskeln in paraplegischen Patienten zu generieren.

Methodik

Datensätze von siebzehn Patienten mit traumatischen, kompletten Rückenmarksverletzungen wurden analysiert. Diese Patienten hatten implantierte Elektroden im dorsalen Epiduralraum auf der Höhe zwischen den Wirbelkörpern BWK10–LWK1 zur Behandlung der spinalen Spastizität. Die Wirkung der Stimulation mit verschiedenen Parametern wurde durch die Aufzeichnung der evozierten elektromyographischen (EMG) Aktivität der Beinmuskeln dokumentiert. Diese neurophysiologischen Daten über das Input-Output Verhalten des lumbalen Rückenmarks wurden retrospektiv ausgewertet.

Um die direkte Wirkung der epiduralen Stimulation zu untersuchen, wurden die Rekrutierungsfolgen der Hauptmuskelgruppen der unteren Extremitäten in Abhängigkeit der Kathodenlage der epiduralen Elektrode ermittelt. Die gewonnenen neurophysiologischen Erkenntnisse wurden mit Computersimulationen zur Ermittlung der direkt angeregten neuronalen Strukturen kombiniert.

Um aktivierte zentrale Mechanismen zu studieren, wurden Stimulus-getriggerte Zeitfenster der EMG-Aktivitäten bei kontinuierlich applizierter Stimulation mit 1–10 V und 5–50 Hz analysiert. Es wurden Latenzzeit, Amplitude und Morphologie von EMG-Antworten zu einzelnen Pulsen bei Stimulation mit unterschiedlichen Parametern untersucht.

Der Effekt der elektrischen Rückenmarksstimulation wurde auch in zwei komplett paraplegischen Patienten während manuell assistiertem Laufband-Gehen untersucht.

Ergebnisse

Epidurale 2.2 Hz Stimulation der posterioren Strukturen des Lumbalmarks löste Muskelzuckungen in den unteren Extremitäten aus. Die entsprechenden EMG-Signale (zusammengesetzte Muskelaktionspotentiale) zeigten kurze Latenzzeiten, welche für die verschiedenen Muskelgruppen charakteristisch waren. Die rostrocaudale Lage der Kathode bestimmte die Rekrutierungsfolge der Muskelgruppen und dadurch den segmentalen Ursprung der aktivierten neuronalen Strukturen. Diese Selektivität der Stimulation war ein Hinweis für die direkte Anregung von Hinterwurzelfasern durch die epidurale Elektrode. Computersimulationen bestätigten die Hinterwurzelfasern als unmittelbar angeregte Strukturen, welche zu den induzierten Muskelaktivitäten führten.

Kontinuierliche Stimulation der lumbalen Hinterwurzelfasern mit Frequenzen von 5–15 Hz evozierte eine tonische EMG Aktivität mit charakteristisch modulierten Amplituden in den Beinmuskeln und führte zu einer Extensionsbewegung der Beine.

Direkte elektrische Anregung der gleichen Strukturen mit 25–50 Hz induzierte schrittähnliche Bewegungen mit alternierenden EMG-„bursts“ der Flexoren und Extensoren der Ober- und Unterschenkel. Die Muskelaktionspotentiale, welche die „burst“-Phasen zusammensetzten, zeigten um 10 ms längere Latenzen als jene einfacher Muskelzuckungen.

Bei Applikation elektrischer Rückenmarksstimulation während manuell assistiertem Laufband-Gehen konnten rhythmische, mit dem Gangzyklus synchronisierte EMG Aktivitäten evoziert werden. Alle effektiven Stimulationsparameter lagen im Bereich von 20–50 Hz und 6–10 V.

Schlussfolgerungen

Muskelzuckungen, ausgelöst durch epidurale Stimulation der posterioren Strukturen des Lumbalmarks mit Einzelpulsen, sind monosynaptische Reflexantworten auf Anregung afferenter Axone in den Hinterwurzeln. Diese Muskelantworten wurden als „Posterior Root Muscle Reflex Responses“ (PRMRRs) bezeichnet. Dieselben afferenten Nervenimpulse werden synaptisch an Interneurone im Lumbalmark weitergeleitet, mit denen die Hinterwurzelfasern anatomisch verbunden sind. Bei kontinuierlicher epiduraler Stimulation der lumbalen Hinterwurzeln mit Frequenzen von 5–50 Hz können synaptische und presynaptische Mechanismen aktiviert werden, welche zur Induktion von Extension und schrittähnlichen Bewegungen führen. Die Selektion der funktionellen Wirkung der interneuronalen Strukturen ist frequenzabhängig. Aktivierte spinale Interneurone formen nicht nur das Muster des Motoroutputs, sie leiten die eintreffenden afferenten Impulse über längere, oligosynaptische Pfade und inhibieren die entsprechenden monosynaptischen Bahnen. Die durch epidurale Stimulation mit 25–50 Hz konfigurierten interneuronalen Netzwerke haben Eigenschaften von Mustergeneratoren für Lokomotion und wurden „Lumbar Locomotor Pattern Generator“ (LLPG) genannt. Der LLPG kann durch kontinuierliche elektrische Stimulation während manuell assistierter Laufbandlokomotion aktiviert werden und dabei afferentes Feedback funktionell verarbeiten.

Die Ergebnisse der vorliegenden Dissertation untermauern die empirische Beobachtung der Induktion eines LLPGs durch kontinuierliche Rückenmarksstimulation. Trotz der Einfachheit des äußeren Reizes, ein anhaltender Input durch die Hinterwurzeln mit konstanter Frequenz, wird eine komplexe Muskelaktivierung ausgelöst. Basierend auf den gefundenen Ergebnissen liegt es nahe, die Einbeziehung des LLPG gezielt therapeutisch einzusetzen.

Summary

Modeling of a human spinal pattern generator for locomotion and its activation by electrical epidural stimulation

Motivation and objectives

While evaluating the effect of electrical epidural spinal cord stimulation on spasticity in patients with complete spinal cord injury, it was discovered that the sustained non-patterned stimulation could induce stepping-like lower limb movements. This observation was regarded as evidence for the existence of a spinal locomotor pattern generator in humans. At this early stage the mechanisms underlying the stimulus-evoked stepping-like movements were not clear.

This thesis aimed at studying the capability of the human lumbar spinal cord isolated from brain control to generate stepping-like motor output. Systematic research should establish the existence of a human spinal pattern generator for locomotion by providing further evidence. Particular objectives were (i) to identify the neural structures which are stimulated by the epidural electrode initiating stepping-like movements of the paralyzed lower limbs, (ii) to supply evidence that epidurally evoked stepping-like movement is due to activation of central spinal structures, (iii) to find out if the human spinal pattern generator activated by non-patterned epidural stimulation can process peripheral feedback input related to passive stepping to generate functional electromyographic (EMG) patterns.

Material and Methods

Neurophysiological data on the input-output behavior of the lumbar cord in isolation from supraspinal input but with well-defined input delivered by externally controlled spinal cord stimulation was analyzed. The data was derived from seventeen subjects with complete spinal cord injury. They had implanted electrodes placed in the posterior, epidural space at vertebral levels T10–L1 for the control of spasticity. The effect of stimulation had been assessed by surface EMG recording of induced muscle activity in the lower limbs.

To examine the direct effect of spinal cord stimulation, muscle twitch distribution patterns of the lower limbs with respect to the cathode site of the epidural electrode were evaluated. The results were combined with computer simulations of epidural spinal cord stimulation to calculate the spatial distributions of the electric fields generated by the electrodes.

To study central effects induced by spinal cord stimulation, EMG responses to stimulation with 1–10 V at 5–50 Hz were analyzed. Stimulus-triggered 50 ms time windows from the original EMG traces were evaluated. Stimulus-evoked compound muscle action potentials (CMAPs) were analyzed with reference to latency, amplitude, and shape.

Epidural stimulation was applied during manually assisted stepping on a treadmill in two paralyzed subjects to consider the capabilities of the spinal locomotor pattern generator to process peripheral feedback input to generate functional motor output.

Results

Epidural stimulation of the human lumbar cord caudal to the complete spinal cord injury level elicited single twitch responses and different patterns of tonic and rhythmic EMG

activity in the lower limb muscles depending on the site, frequency and amplitude of stimulation.

Stimulation at 2.2 Hz induced stimulus-coupled CMAPs of short latency. The recruitment order of quadriceps and triceps surae twitch responses was related to the rostrocaudal position of the cathode with respect to spinal cord segments. This segmental-selectivity of stimulation indicated that the stimulus-evoked muscle activity was initiated in the posterior roots. The comparison of calculated electric potential distributions generated by the epidural electrode with the topographical anatomy of neural target structures provided an independent evidence for the direct stimulation of posterior roots.

Sustained stimulation at 5–15 Hz evoked a tonic EMG activity with characteristic amplitude modulations and could initiate an extension movement of the paralyzed lower limbs.

Stimulation at 25–50 Hz with predominant activation of the L2–L4 posterior roots induced alternating burst-style EMG activity in the lower limb muscles leading to stepping-like movements in supine individuals with complete spinal cord injury. Successive stimulus-evoked CMAPs were subject to well-defined amplitude modulations resulting in burst-like envelopes of the EMG activity. A significant increase of CMAP latencies by about 10 ms during burst-style phases was found.

Epidural stimulation applied during manually assisted, weight-bearing treadmill stepping evoked functional EMG bursts in the paralyzed lower limb muscles, which were temporally synchronized to specific phases of the step cycle. All effective stimulation parameters were within the range of 20–50 Hz and 6–10 V.

Conclusion

Single pulse (2.2 Hz-) stimulation of posterior lumbar cord structures activated large afferent fibers within the posterior roots and recruited motoneurons through monosynaptic connections in the spinal cord. The resulting stimulus-evoked muscle activity was termed Posterior Roots Muscle Reflex Responses (PRMRRs). The same afferent input was synaptically transmitted to spinal interneurons. Sustained stimulation of the posterior roots at higher frequencies activated lumbar neuronal circuits that modulated the afferent flow through monosynaptic pathways by presynaptic inhibitory mechanism and controlled motoneuronal discharge by mono- and oligosynaptic excitatory pathways. The responses could be organized to result in either limb extension or stepping-like movements. Inducing these patterns was a function of different frequencies of the applied train of electrical stimuli. The EMG responses during the rhythmical movements elicited by the sustained, non-patterned stimulation were dynamically modulated with respect to both amplitude and latency. It is proposed to consider the described capabilities of the human lumbar cord isolated from brain control and tested by repetitively induced PRMRRs at 25–50 Hz as evidence for the existence of a Lumbar Locomotor Pattern Generator (LLPG). The LLPG could be activated during weight-bearing, manually assisted treadmill stepping by electrically-evoked tonic input and could integrate and interpret peripheral feedback input in order to generate functional locomotor patterns.

The possibility of activating the human spinal pattern generator for locomotion raises the possibility to partially overcome the loss of supraspinal input in patients with spinal cord injury by appropriate electrical stimulation.

Acknowledgements

I wish to acknowledge the invaluable support of Professor Milan R. Dimitrijevic to the work presented in this thesis. His visionary approach to understanding human motor control has inspired and guided me throughout my work. He motivated me to work to my full potential. Thank you for being a teacher and a mentor.

I am grateful to Professor Frank Rattay for introducing me to the field of neuromathematics and "Brain modeling". Thank you for establishing an environment enabling interdisciplinary research. Your support and supervision accompanied me from the very beginning.

I am also thankful to Dozent Dr. Michaela M. Pinter for her extensive effort to allow neurophysiological studies in humans as part of well-established clinical programs.

Many thanks to Ms. Preinfalk, Ms. Auer, and Ms. Alesch for their excellent technical support.

Table of Contents

Kurzfassung der Dissertation	2
Summary	4
Acknowledgements	6
Table of Contents	7
Abbreviations	10
Chapter 1	
Introduction	11
Background and Motivation	11
An autonomous spinal pattern generator for locomotion in humans?	11
Model and Methodology	13
An approach to conduct human neurosciences	13
The model of the lower spinal cord under the condition of well-defined inputs	15
Surface-EMG as an approach to indicate the function and state of activation of the central nervous system	16
Stimulation-response paradigms	17
Computer modeling	18
Computer modeling – Volume conductor model	20
Computer modeling – Nerve fiber model	23
Design of the thesis	27
References	29
Chapter 2	
Posterior Roots Muscle Reflex Responses elicited by epidural stimulation of the human lumbar cord	33
Summary	33
Introduction	34
Material and methods	34
Subjects	34
Stimulation setup	36
Recording procedure	36
Data analysis – Data based on incremental pulse amplitudes	36
Data analysis – Data based on incremental pulse frequencies	37
Computer simulation of the electric potential distribution	38
Results	38
Muscle responses to single stimuli (2.2 Hz stimulation)	38

Relationships between cathode levels, stimulation amplitudes and activated muscle groups – Stimulation frequency: 2.2 Hz	41
Muscle responses to trains of stimuli	43
Relationships between cathode levels, stimulation amplitudes and activated muscle groups – Stimulation frequencies: 2.2, 25, 50 Hz	45
Stimulation of neuronal structures at the level of the cathode	47
Stimulation of neuronal structures distant from the cathode level	50
Discussion	50
Muscle responses to epidural lumbosacral cord stimulation are initiated in the posterior roots	52
Posterior Roots Muscle Reflex Responses	55
Differences between Posterior Roots Muscle Reflex Responses and the H-reflex	56
Posterior Roots Muscle Reflex Responses to trains of stimuli at higher frequencies	58
Significance of the results	60
References	62
Chapter 3	
Stepping-like movements in humans with complete spinal cord injury induced by epidural stimulation of the lumbar cord: Electromyographic study of compound muscle action potentials	66
Summary	66
Introduction	67
Material and methods	68
Subjects	68
Stimulation and recording setup	69
Data analysis – Data based on incremental pulse amplitudes	71
Data analysis – Data based on incremental pulse frequencies	71
Results	72
Epidurally evoked segmental twitch responses	72
Stimulation with pairs of stimuli	74
Stimulation with trains of stimuli	76
Discussion	81
Directly stimulated structures which should be considered as inputs resulting in the CMAPs	81
Epidural stimulation induces Posterior Roots Muscle Reflex Responses	84
Posterior Roots Muscle Reflex Responses and induced central effects	85
Posterior Roots Muscle Reflex Responses and the Lumbar Locomotor Pattern Generator	86
Significance of the results	88
References	89

Chapter 4

Effect of peripheral afferent and central afferent input to the isolated human lumbar spinal cord	94
Summary	94
Introduction	95
Material and methods	96
Subjects	96
Stimulation procedure	96
Recording procedure	98
Data analysis	99
Results	99
Effect of spinal cord stimulation on lower limb EMG patterns induced during passive treadmill stepping	99
Contributions of mechanical (phasic) and electrical (tonic) stimulation to the induced EMG activities	101
The effect of epidural cathode position on the induced EMG patterns	104
The effect of different frequencies of spinal cord stimulation on the induced EMG patterns	105
Discussion	107
Effect of phasic peripheral feedback input to the isolated lumbar cord	107
Effect of tonic input to the lumbar cord generated by spinal cord stimulation	107
Effect of spinal cord stimulation-evoked tonic input in conjunction with phasic peripheral feedback input to the lumbar cord	108
Significance of the results	110
References	112
<i>Curriculum vitae</i>	113
<i>List of scientific publications</i>	115

Abbreviations

A	adductor
ASIA	American Spinal Cord Injury Association
BMCA	brain motor control assessment
CMAP	compound muscle action potential
CPG	central pattern generator
EMG	electromyography, electromyographic
FES	functional electrical stimulation
H	hamstrings
ISI	interstimulus interval
KJA	knee joint angle
KM	knee movement
L	lumbar
LLPG	Lumbar Locomotor Pattern Generator
Mn	motoneuron
PARA	paraspinal trunk muscles
PRMRR	Posterior Roots Muscle Reflex Response
Q	quadriceps
S	sacral
SCI	spinal cord injury, spinal cord injured
SCS	spinal cord stimulation
T	thoracic
TA	tibialis anterior
TS	triceps surae

Chapter 1

Introduction

Background and Motivation

An autonomous spinal pattern generator for locomotion in humans?

Vertebrate locomotion is characterized by rhythmic activity and the utilization of multiple degrees of freedom, i.e. multiple joints and muscles. Motion is generated by the musculoskeletal system in which torques are created by antagonist muscles at the joints of articulated systems composed of rigid bones. By rhythmically applying forces to the ground, reaction forces are generated which move the body forward. This type of locomotion is in contrast to the propulsion of most manmade machines, which usually rely on few degrees of freedom (e.g. a limited number of powered wheels) and continuous rather than rhythmic actuation. From a technological point of view, vertebrate locomotion is significantly more difficult to control than that of wheeled machines. To generate efficient locomotion, the frequencies, amplitudes, and phases of the signals sent to the multiple muscles must be well coordinated. Complex coordination is required not only between different joints and limbs, but also between antagonist muscles which combine periods of co-activation for modulating the stiffness of the joint and periods of alternation for actuating the joint.

While locomotion is highly complex, animal experiments and recent findings in humans have documented, that it is to some degree an automated movement. Vertebrate locomotion control appears to be organized such that autonomous neural networks in the spinal cord generate the basic rhythmic patterns necessary for locomotion. Higher control centers interact with the spinal circuits for posture control and accurate limb movements. This means that the control signals sent to the spinal cord by supraspinal centers do not need to specify all the details of when and how much the multiple muscles must contract, but rather specify higher level commands such as stop and go signals, speed, and heading of motion.

Autonomous neural circuits which can generate a rhythmic motor output without receiving rhythmic input are called "central pattern generators" (CPGs). The hallmark for identification of a locomotor CPG within the spinal cord is the production of recognizable and reproducible patterns of rhythmic output in the absence of instructive external drive from higher levels of the central nervous system or from peripheral sensory feedback.

Definite evidence for spinal CPGs for locomotion exists in lower mammals. Investigations on animals (rat, rabbit, cat, dog) demonstrated that the lumbar spinal cord harbors a pacemaker capable of inducing locomotor-movements. This pacemaker acts autonomously since it had been separated from suprasegmental and peripheral influences by experimentally induced trauma (Grillner, 1981). The existence of a CPG in primates first remained unclear. Eidelberg and colleagues (1981) reported that in acute and chronic spinal macaque monkeys it was not possible to evoke locomotor movement. On the other hand,

Hultborn and colleagues (Hultborn *et al.* 1993; Fedirchuk *et al.* 1998) demonstrated fictive locomotion in spinal marmoset monkeys.

The existence of a spinal CPG in humans according to the definition originally established in animal preparations (as aforementioned to have the capacity to produce movement in the absence of phasic, movement-related sensory input and in the absence of supraspinal input) is more difficult to demonstrate and evidence is, by necessity, indirect. While it is possible to rule out supraspinal inputs to the lower human spinal cord due to complete spinal cord injuries, peripheral segmental input cannot be completely removed (e.g. by posterior rhizotomy) like in the experimental animal model.

Nevertheless, recent observations in patients with spinal cord lesions suggest that there is an autonomous network in the human spinal cord which has the capacity of generating rhythmic alternating muscle activity similar to that seen during active walking.

Calancie and co-workers (1994) documented an indirect evidence for the existence of a human spinal locomotor pattern generator in an individual with incomplete spinal cord injury and periathritic changes in the hip. This individual exhibited involuntary stepping movements of the lower extremities when he was positioned supine with the hip extended. The strength, rate, and rhythmicity of these movements exceeded those that the subject was able to produce voluntarily. The temporal relationships of the electromyographic (EMG) patterns were consistent both within and between testing sessions. The investigators contended that afferent input to the spinal cord due to active osteoarthritis at the hip was a primary factor allowing the central pattern-generated movement to manifest in this individual with spinal cord injury. Bussel and colleagues discussed that some elements of the spinal circuitry in the acute spinal cat, on which the generation of stepping rhythms relies, also exist in man (Roby-Brami & Bussel, 1987; Bussel *et al.* 1996). Gurfinkel and colleagues (1998) used tonic peripheral afferent stimulation to elicit involuntary stepping in able-bodied individuals. They found that continuous lower limb muscle vibration gave rise to involuntary locomotion-like movements in suspended legs and suggested that the non-specific afferent input induced by vibration activated central structures governing stepping movements. Another approach to generate stepping-like oscillating EMG patterns in the paralyzed lower limbs is manually assisted stepping of complete spinal cord injured subjects over a moving treadmill belt (Dietz *et al.* 1995; Dobkin *et al.* 1995). These findings suggested that pattern generating spinal networks can be activated by means of peripheral afferent feedback from muscles, tendon, cutaneous and articular receptors related to passive stepping.

Dimitrijevic *et al.* (1998) were among the first who provided direct evidence for the presence of a human spinal locomotor pattern generator. They discovered that repetitive and regular electrical stimulation of the posterior structures of the lumbar spinal cord could initiate and maintain rhythmic stepping-like flexion/extension movements of the subject's paralyzed limbs. To illustrate their findings, they chose surface-recorded EMG activity of agonist-antagonist muscles of thigh and leg that lasted for 30 s without changes in the rhythmical patterns (Fig. 1.1). The authors demonstrated that the lumbar cord, isolated from brain control, could respond to a sustained, non-patterned train of stimuli with the generation of rhythmic stepping-like motor output. This result was regarded as evidence for the existence of a spinal locomotor pattern generator in humans, which can generate a rhythmic motor output without receiving rhythmic input with spatially and temporally complex patterns.

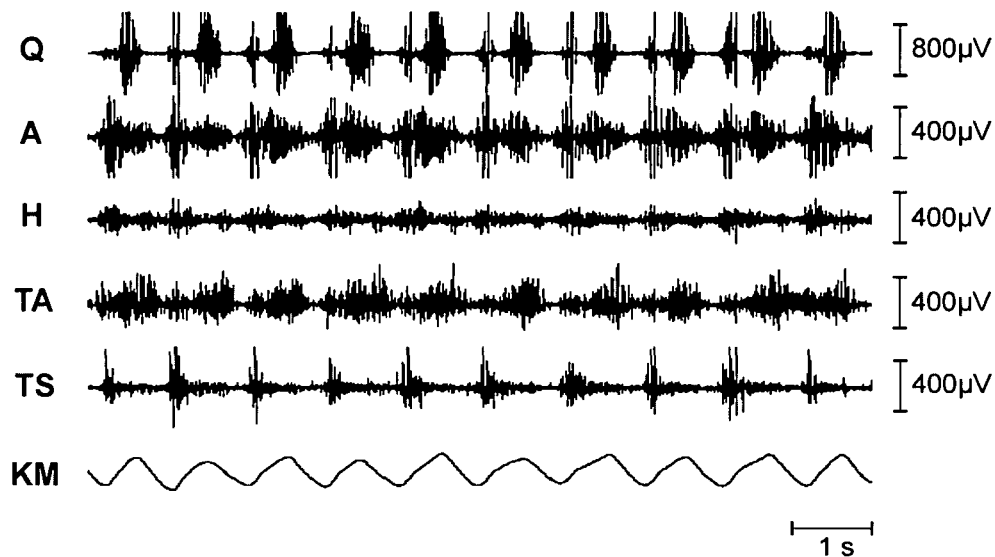


Figure 1.1 Stepping-like modulated EMG activity in response to repetitive and regular epidural lumbar cord stimulation

Surface EMG recordings from the right quadriceps (Q), adductor (A), hamstrings (H), tibialis anterior (TA), and triceps surae (TS) muscles and knee movement (KM, deflection up is flexion, deflection down is extension) in a complete paraplegic. Epidural stimulation was applied over the posterior structures of the L2 cord segment with a train of 30 Hz and stimulus strength of 9 V (Dimitrijevic *et al.* 1998).

At this early stage of Dimitrijevic's initial studies it was not clear which neural structures were stimulated by the electrical epidural stimulation. The mechanisms underlying the stimulus-evoked stepping-like movements were not clear.

The aim of this thesis was to further advance the encouraging findings of Dimitrijevic's pioneering work. Systematic research should establish the existence of a human central pattern generator for locomotion by providing further evidence. The thesis was motivated by the unique opportunity to study human motor control of locomotion on the basis of neurophysiological data. The studied model is the human lumbosacral spinal cord in complete (subclinical) isolation from supraspinal input. Externally controlled spinal cord stimulation provides a well-defined input. A computer model of epidural spinal cord stimulation was applied to identify the directly stimulated neural structures and thus the pathways mediating the activating input to the pattern generating neural circuits. Stimulus-evoked and surface recorded EMG data were analyzed to reveal features of the input-output processing capabilities of the activated spinal neural networks and to investigate the nature of the muscle responses.

Model and Methodology

An approach to conduct human neurosciences


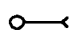
Definite evidence for a CPG in lower mammals was repeatedly demonstrated in acute animal preparations. Thereby, neuronal networks in the spinal cord were completely isolated from sensory input (deafferentation) and separated from suprasegmental influences (spinalization or decerebration) by experimentally induced trauma (transection). The CPG

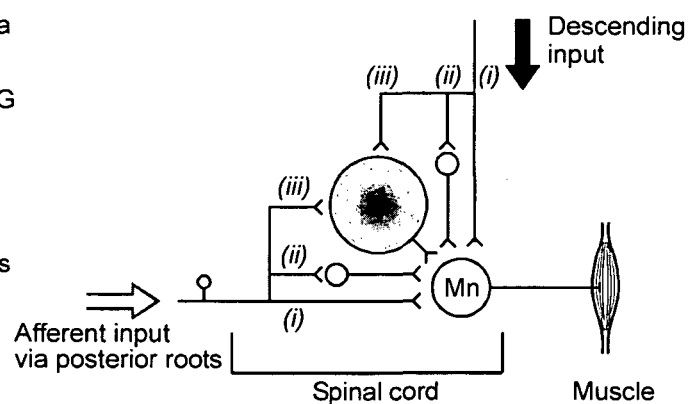
was activated by injection of drugs or application of electrical stimulation. The generated complex coordinated patterns of efferent output were recorded intracellularly from motoneurons during the so-called “fictive locomotion” (Figs. 1.2A and B).

Obviously, this experimental approach is not possible in humans. However, there is the possibility of neurophysiological studies in humans in parallel to well-established clinical programs. Epidural spinal cord stimulation is a clinical method to control severe spasticity in chronic spinal cord injured individuals (Dimitrijevic *et al.* 1986 *a,b*; Barolat *et al.* 1995). In a clinical program of restorative neurology carried out in the Neurological Hospital Maria Theresien Schlössel (Vienna, Austria), the effect of epidural spinal cord stimulation on spasticity of the lower limbs in patients with traumatic spinal cord injury was evaluated. Clinical protocols were conducted to define optimal electrode positions and stimulation parameters, thereby applying stimulation strengths of 1–10 V at frequencies of 2–100 Hz and testing different contact combinations of an epidurally placed electrode array. The effect of stimulation was assessed by surface EMG recordings of lower limb muscle

A

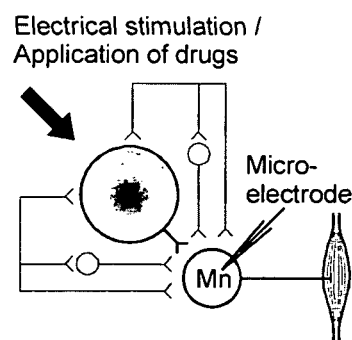
Control of motoneurons (Mn) via
 (i) direct pathways
 (ii) interneurons outside the CPG
 (iii) interneurons capable of
 building-up CPG networks

 CPG / locomotor networks
 Interneurons



B

Animal preparation



C

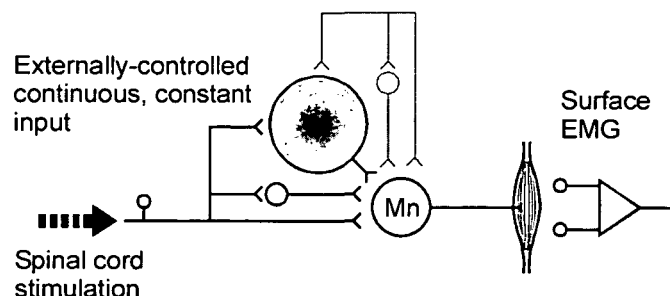
Human lumbar cord model
of the present study

Figure 1.2 Models of the lumbar cord: Schematic drawings of afferent and descending pathways projecting to motoneurons via different pathways

A, Lumbar cord under the influence of (residual) supraspinal input and afferent feedback. B, Experimental animal preparations with the CPG completely isolated from descending and afferent input. Non-functional pathways are displayed gray. C, Model of the human lumbar cord deprived of descending influence and under the condition of well-defined external input.

activity. In a period of six years, more than 1000 recordings were carried out. It was demonstrated that spinal cord stimulation was effective to *suppress* the excitability within particular motor nuclei – and thus reduce spinal spasticity – if the stimulating electrode was located at upper lumbar segmental levels, and the applied stimulus train had an amplitude of 2–7 V at frequencies of 50–100 Hz (Pinter *et al.* 2000). Stimulation at frequencies below 50 Hz *enhanced* the excitability of lumbosacral motor nuclei and *induced* single twitch responses, sustained contractions or even rhythmical activity of the lower limb muscles. These EMG data of stimulus-evoked muscle response patterns was anonymized and made available for the present study. The data analyzed in the present study was derived from subjects with complete spinal cord injuries.

The model of the lower spinal cord under the condition of well-defined inputs

Unlike the studies of animals with deafferentation and complete isolation of the spinal cord from descending input, it is difficult to provide evidence in humans that initiation and maintenance of automated stepping-like activity is due to spinal mechanisms alone. In individuals with incomplete spinal cord injury as well as with clinically complete ones, there is clearly a potential for some influence of remaining supraspinal descending input on the lumbar spinal cord. Furthermore, due to intact sensory input to the spinal cord, some groups of researches proposed simpler mechanisms than the contribution of pattern generating spinal networks to account for stepping-like activity in paralyzed lower limbs. Some researchers initially suggested that rhythmical EMG-activity in lower limb muscles induced during passive treadmill-walking could be due to periodically imposed muscle stretches. Regarding Dimitrijevic's observation, there were even critics considering that repeated induction of fatigue induced by the high frequency stimulation of peripheral nerves might explain the rhythmical activity. The suggestion that stretch reflexes were the sole source of the phasic EMG activity induced in flexors and extensors during manually assisted stepping of paraplegic subjects has meanwhile been discarded (Harkema *et al.* 1997). It is now more and more accepted that sensory information associated with weight-bearing passive stepping can activate and coordinate human spinal locomotor networks. In this thesis evidence will be presented that the epidurally evoked stepping-like activities is due to activation of central spinal structures. Peripheral feedback-input can reinforce the pattern generator activities and has a timing function.

A rather unique approach in this thesis is the attempt to study the locomotor capabilities of the lower spinal cord under the condition of well-defined inputs. All data which was analyzed in this thesis were derived from complete spinal cord injured subjects. Within the clinical program of restorative neurology carried out in the Neurological Hospital Maria Theresien Schlössel, a neurologist examined the subjects' spinal cord functions and assessed their functional status (*clinical* assessment). In addition, non-invasive techniques for the neurophysiological assessment of *sub-clinical* spinal cord functions were applied. The „brain motor control assessment“ (BMCA) protocol was carried out for the examination of residual functional capabilities, i.e., of the degree to which brain influence is preserved below a spinal cord lesion (Sherwood *et al.* 1996). By using this method, a comprehensive multichannel surface EMG recording, it is possible to register objective, quantitative and reproducible data on the altered motor control after an upper motoneuron trauma. The results of the BMCA protocol demonstrate the presence of any trans-lesional brain influence over spinal motor activity and reveal features of motor control that are not apparent in the clinical examination. Furthermore, lumbosacral evoked potentials were used

to assess the functions of the spinal gray matter below the lesion level. They were recorded after tibial nerve stimulation with surface electrodes placed at the S1, L4, L2, and T12 spinous processes referenced to an electrode at T6 (Lehmkuhl, 1984; Beric, 1988).

The results presented in the following chapters were derived from complete spinal cord injured subjects with intact functions of the posterior structures and gray matter of the spinal cord below the lesion level and with preserved stretch and cutaneomuscular reflexes. All results illustrating the successful activation of stepping-like EMG activity and corresponding alternating flexion/extension movements were recorded in subjects with a *sub-clinical* complete spinal cord injury (i.e. no brain influence preserved below the lesion level).

Consequently, actual stepping-like movements were *initiated* under well-defined input conditions to the spinal cord (Fig. 1.2C), namely:

- (i) no supraspinal input
- (ii) minimized and insignificant afferent feedback input (no conditioning by leg movement before the stimulus-evoked movement was initiated) and
- (iii) externally-controlled repetitive and regular input generated by spinal cord stimulation with implanted electrodes.

This is in contrast to the studies of assisted treadmill-stepping of clinically complete spinal cord injured subjects. It was demonstrated there that EMG activity can be generated in response to passive limb movement combined with loading – but there was no *independent stepping*, only *passive leg motion*.

Surface-EMG as an approach to indicate the function and state of activation of the central nervous system

The basis of this thesis was the analysis of surface-recorded electromyographic (sEMG) activities from four main lower limb muscle groups induced under externally-controlled input conditions to the spinal cord. The recording electrodes were placed over the quadriceps (anterior thigh), hamstrings (posterior thigh), tibialis anterior (anterior leg), and triceps surae (posterior leg) muscles. It is important to keep in mind that sEMG were not analyzed to study movement. The sEMG recording was interpreted as a non-invasive technique that provided a measure of central nervous system output to the muscle and as a window to reveal features of the spinal motor control strategies (Fig. 1.2C). Thus, the information contained in the sEMG was investigated to find out how the epidural stimulation affected the circuitries in the spinal cord. Special consideration was given to the EMG activities of the quadriceps and triceps surae muscle groups, because they are the only ones of the recorded muscle groups with separate segmental innervations. Responses in quadriceps and triceps surae were taken as an estimate of the spinal motor neuron pool activity over time of the L2, L3, L4 segments and L5, S1, S2 segments, respectively.

When analyzing the EMG recordings, we assumed that the EMG activity was predominantly related to the epidural stimulation. Motor neuron pool activation by supraspinal input could be ruled out. When the subject was lying in a supine position and no lower limb movements were initiated by the stimulation, afferent feedback input certainly played an insignificant role. When stepping-like movements were induced by the electrical spinal cord stimulation, conditions were set to minimize afferent feedback-input from articular and cutaneous receptors. It was shown that afferent feedback input associated

with “air-stepping” (assisted stepping with the limbs bearing no load) is ineffective to induce rhythmic EMG-activity in the paralyzed lower limbs (Harkema *et al.* 1997, Dietz *et al.* 2002).

Indeed, the analyzed EMG activities consisted of separate compound muscle action potentials (CMAPs) which could unequivocally be related to the stimulus-pulse which had triggered it. EMG potentials of consecutively evoked CMAPs did not interfere with each other when the stimulus frequency did not exceed 30 Hz. The moments when stimulus pulses were applied were indicated by stimulus artifacts recorded by surface electrodes which were placed over the subject’s lower back (paraspinal muscles). Due to the close distance of these paraspinal-electrodes to the epidural electrode, volume-conducted artifacts of the stimulus pulses delivered by the stimulating electrode were picked up by the recording surface electrode. This allowed analyzing stimulus-triggered time windows of the original continuous EMG-recordings, each containing a CMAP. We examined the single surface-recorded CMAPs for latencies (quantitatively), peak-to-peak amplitudes, and shapes (qualitatively). Modulations of the response latency, EMG-amplitude and potential shape of the CMAPs evoked by stimulation with constant parameters could be attributed to activation of premotorneural spinal mechanisms that control motoneuronal discharge and the transmission through reflex pathways (see chapters 2 and 3).

Stimulation-response paradigms

When describing the neurophysiological characteristics of motor control in spinal cord injury, two different paradigms can be used as an investigative tool, single stimulus-response and repetitive stimulus-response measurements. Thereby, analyzing the motor responses reveals information about the excitability of the motoneurons, changes in transmission of spinal pathways, and the organization of spinal interneurons into functional circuits. Muscle responses are clinically evoked by muscle stretch delivered manually or by a reflex hammer or vibrator, and through different modalities of electrical stimulation applied to peripheral nerves. Single impulse input to the spinal cord typically produces a single twitch in the muscle corresponding to the stimulated nerve. However, repeated impulses at increasing frequency as would be generated by passive stretch of a muscle or, in the laboratory using strong vibration of the muscle, recruit additional spinal cord internuncial and propriospinal neurons and can build up some regularities in the control of motor output (Kern *et al.* 2004).

Using an electrode which had been percutaneously inserted into the posterior epidural space for the control of severe spasticity, provided a technique to deliver input to the human lumbar cord from a localized and stable region. The advantage of this method is the possibility to

- (i) stimulate different segments in certain isolation with single stimuli
- (ii) continuously and simultaneously stimulate all segments which contain the cell bodies of motoneurons innervating all main lower limb muscles as well as elements of the spinal circuitry involved in generating rhythmic locomotor activity.

Besides recruiting motoneurons, spinal cord stimulation also produces postsynaptic potentials in spinal interneurons. The analysis of the stimulus-responses is based on the concept that the externally applied pulse train could be regarded as conditioning the spinal cord premotorneural structures. In parallel, each single pulse within the train is a test

stimulus eliciting an EMG response, which reveals the conditioning effect of the train applied prior to the arbitrarily chosen test stimulus.

Testing the spinal cord circuitries with low frequency stimulation (2 Hz) demonstrated a functional resting state of the spinal interneurons. Due to the long interstimulus interval (0.5 s), a given response is not influenced by the elicited activity of the preceding stimulus. Thus, the effect of 2 Hz-stimulation is similar to the effect of single applied stimulus pulses and can be used to examine the segmental effects of spinal cord stimulation. Particularly, information on the immediately activated structures that generate postsynaptic potentials in lower limb motoneurons can be derived from this “single pulse” stimulation (Murg *et al.* 2000).

Analysis of the responses to the first two stimuli of the applied trains was carried out to describe the refractory behavior of the epidurally evoked muscle responses. Thereby, long-lasting, stimulus-strength dependent conditioning effects of the first stimulus on the excitability of the activated structures is revealed by the second (test) response. The range of the refractory periods and its dependency on stimulation parameters gives further information on the immediately stimulated structures (see chapter 3).

EMG responses to trains of electrical stimuli of 1–10 V and 5–50 Hz were examined to learn how the sustained stimulation causes lumbar cord neurons to shape different types of sustained tonic or patterned rhythmical motor output.

Computer modeling

A central question of the thesis was to identify the directly stimulated neural structures which led to the observed motor effects. Since the directly stimulated pathways are mediating the activating input to the pattern generating neural circuits, recognizing these structures is a precondition for understanding the mechanisms underlying the stepping-like movements activated by electrical epidural stimulation. Their identification is essential to localize the locomotor pattern generating networks within the human spinal cord. Once identified, other methods less invasive than epidural stimulation can target the input structures to the spinal structures for enhancing locomotor capabilities in people with impaired central nervous system functions.

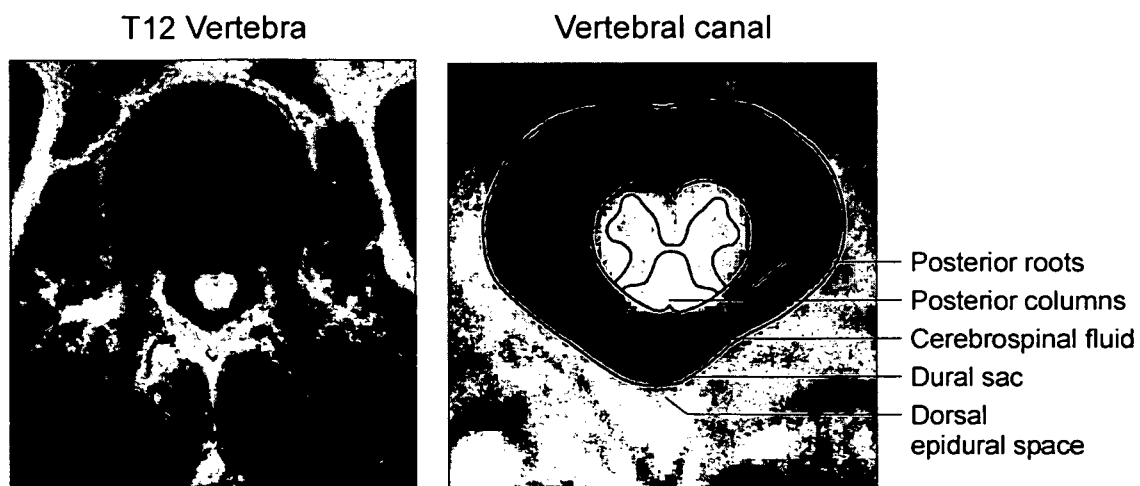


Figure 1.3 Cross-sectional anatomy of the lower spinal cord and its surrounding structures at the level of the twelfth thoracic (T12) vertebra (Bulling *et al.* 1997)

Epidural electrical stimulation is delivered by an array of electrode contacts which is inserted into the epidural space between the inner wall of the spinal canal and the dural sac. The dural sac is a membranous covering containing the spinal cord bathed in cerebrospinal fluid (Fig. 1.3).

In principle, the epidural electrode can directly stimulate any neural structures within the different quadrants of the spinal cord and within the spinal roots if the stimulus amplitude is sufficiently high. Even recruitment of structures dorsal to the epidural space was suggested, such as of small fibers in the ligamentum flavum (North *et al.* 1997).

The immediate effects of spinal cord stimulation are muscle contractions and paresthesiae (felt as tingling sensation on the skin in individuals with intact sensory functions), that are referred to the body parts corresponding to the activated neurons. From the beginning of spinal cord stimulation it has been assumed that primarily the dorsal columns are stimulated, as expressed by the terminology 'Dorsal Column Stimulation' used in many papers. This assumption originally derived from empirical studies based on the main application of epidural spinal cord stimulation, which is chronic pain management. For this application the electrode is placed dorsally in the epidural space, generally between cervical and mid-thoracic vertebral levels. Most work was concentrated in understanding the stimulation of large cutaneous fibers which are the structures initiating paresthesiae, and which were postulated to inhibit spinal cord neurons transmitting noxious information (Melzack & Wall, 1965). Although paresthesiae sometimes starts as segmental sensation, it spreads to dermatomes corresponding with low spinal levels when stimulus amplitude is increased. This widespread distribution of paresthesiae may even occur at the perception threshold (He *et al.* 1994) and can be attributed to activation of the dorsal columns (Barolat *et al.* 1993).

On the other hand, less attention was paid to the mechanisms underlying motor effects, which were regarded as side effects limiting the therapeutic efficacy in pain control stimulation. From previous studies, direct ventral motor root activation (DiMarco *et al.* 1999), direct stimulation of the dorsal columns (Hunter & Ashby, 1994; Regnaud *et al.* 2000), or even of the gray matter seemed a plausible explanation for muscle activation. Initially, rhythmical motor patterns activated by epidural stimulation were attributed to the direct activation of the dorsolateral funiculi (Gerasimenko *et al.* 2000, 2002; Dimitrijevic *et al.* 2001). This hypothesis was influenced by animal experimental work of Kazennikov and colleagues. They showed that stepping movements could be elicited in the decerebrate cat by microstimulation of a particular portion of fibers in the dorsolateral funiculus at the cervical or thoracic level, the so-called "locomotor strip" (see abstract of Kazennikov *et al.* 1983). In the clinical application of epidural stimulation with dorsal electrode placement for control of pain or spasticity, it was repeatedly observed that evoked muscle activity is typically a segmental effect, which, with increasing amplitude, only spreads to adjacent levels. This finding suggested dorsal roots as initiation sites of motor effects (Struijk *et al.* 1993; Murg *et al.* 2000).

A better understanding of this discrepancy of the direct effect of epidural spinal cord stimulation required a better knowledge in the electrical phenomena involved. These phenomena include two main aspects. First, the potential difference between the contacts of the epidural electrode during a stimulation pulse causes ionic current to flow from the anode to the cathode via the intermediate anatomical structures. These structures can be considered as a volume conductor. The resulting three-dimensional distribution of the electric potential and current density are determined by the geometrical relations and

electrical conductivities of the anatomical structures composing the volume conductor. Secondly, the stimulation-induced electrical field causes current to flow across nerve cell membranes, thereby eliciting local depolarization and hyperpolarization of these membranes. If a nerve fiber membrane is sufficiently depolarized, an action potential will be generated that propagates in both orthodromic and antidromic directions. The two separate aspects of the involved electrical phenomena can be represented by a volume conductor model and a nerve fiber model, respectively. Thus, computer modeling was recognized to be an appropriate method to identify the direct effects of epidural stimulation.

Computer modeling –Volume conductor model

The first computer models of spinal cord stimulation were established by Coburn in the late '70s (Coburn, 1980). Since 1986 similar modeling studies were initiated by Holsheimer and colleagues (Holsheimer & Struijk, 1987). Both groups were mainly interested in the mechanism underlying the effect of stimulation for pain control, and to improve the efficiency of spinal cord stimulation, primarily by the design of new epidural electrodes (Struijk & Holsheimer, 1996). Accordingly, the computer models were based on the spinal cord anatomy and geometrical relations at cervical and mid-thoracic vertebral levels. Three-dimensional volume conductor models were defined by prismatically extending a single two-dimensional cross-section of the gray matter, white matter, cerebrospinal fluid, dura mater, epidural fat, vertebral bone, and a surrounding layer. These models are appropriate for these rostral vertebral levels.

The purpose of this thesis was to explore motor effects induced by electrodes placed at low thoracic or first lumbar vertebral levels. Therefore the volume conductor model had to be representative for the terminal spinal cord and had to include the relevant anatomical structures at these levels. The lower spinal cord has a region with enlarged diameter, from which the nerve fibers supply the lower limb muscles. Below this region at the twelfth thoracic vertebral level, the spinal cord tapers to form the conus medullaris and terminates between the first and second lumbar vertebral level. The diameter of the dural sac does not change notably at these vertebral levels. This results in an increasing dorsal thickness of the cerebrospinal fluid layer surrounding the terminal spinal cord. This specific structure of the lower spinal cord required a three-dimensional volume conductor model composed of varying cross-sections (Fig. 1.4).

As indicated, the volume conductor model represents the anatomical structures and related conductivities, and the stimulating electrode contacts. The transverse geometry of the model is based on magnetic resonance images, on an interactive program on the human cross-sectional anatomy ('Visible Human Male', Bulling *et al.* 1997), and on quantitative measurements of the intradural geometry (Wall *et al.* 1990; Holsheimer *et al.* 1994; Kameyama *et al.* 1996). The stylized cross-sections describe the boundaries between gray matter, white matter, cerebrospinal fluid, dura mater, epidural space, vertebral bone, and a surrounding layer.

The first response of a long homogeneous fiber to an electric field is related to the second-order difference of the electric potential ('activating function') along the fiber (Rattay, 1990). Thus, the electric potential along the fiber trajectory has to be computed first. This electric potential is generated during the stimulation pulse of the implanted electrode. In order to obtain the electric potential Φ it is necessary to solve the volume conductor

problem $\nabla \cdot \mathbf{J} = I_V$ subject to specified boundary conditions, where \mathbf{J} is the current density and I_V the current per unit volume defined within the solution domain Ω .

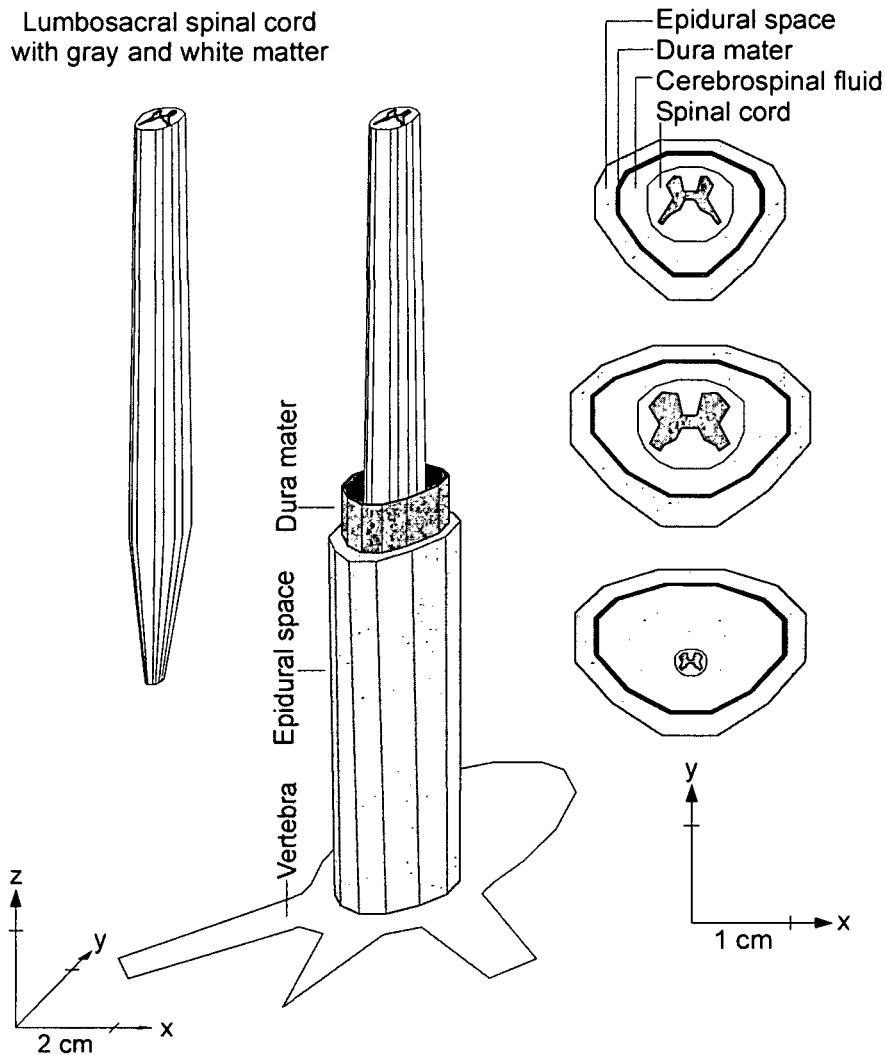


Figure 1.4 Finite-element geometry

Three-dimensional representation of the lumbosacral spinal cord. The geometry of the surrounding compartments (cerebrospinal fluid, dura mater, epidural space and vertebral bone) are only partially displayed. The layer surrounding the vertebrae is not shown. Right side: cross-sections demonstrating the varying geometrical relations within the spinal canal. The y-axis is showing in ventral direction.

With $\mathbf{J} = \sigma \mathbf{E}$ and $\mathbf{E} = -\nabla \Phi$, where \mathbf{E} is the electric field strength and σ is the electrical conductivity tensor, the bioelectric volume conductor can be formulated as the following boundary value problem

$$\nabla \cdot \sigma \nabla \Phi = -I_V \quad \text{in } \Omega. \quad (1.1)$$

Since the imposed current densities are zero ($I_V = 0$, electrodes will be considered as boundary conditions), $\nabla \cdot \mathbf{J} = I_V$ is equivalent to the Laplace equation

$$\nabla \cdot \sigma \nabla \Phi = 0 \quad \text{in } \Omega. \quad (1.2)$$

The original boundary value problem (1.2) can then be replaced with an equivalent integral formulation:

$$\int_{\Omega} (\nabla \cdot \sigma \nabla \Phi) \bar{\Phi} d\Omega = 0 \quad (1.3)$$

where $\bar{\Phi}$ is an arbitrary test function. This equation must hold for all test functions $\bar{\Phi}$. Applying Green's theorem, Eq. (1.3) can be written as

$$\int_{\Omega} \sigma \nabla \Phi \nabla \bar{\Phi} d\Omega - \int_S \sigma \bar{\Phi} \frac{\partial \Phi}{\partial n} dS = 0 \quad (1.4)$$

where S is the boundary of the solution domain Ω . When Dirichlet, $\Phi = \Phi_0$, or Neumann, $\sigma \nabla \Phi \cdot \mathbf{n} = 0$, boundary conditions are specified on S , the weak form of Eq. (1.4) is obtained:

$$\int_{\Omega} \sigma \nabla \Phi \nabla \bar{\Phi} d\Omega = 0. \quad (1.5)$$

The finite element method was applied to turn the continuous problem (1.5) into a discrete formulation. First, the solution domain is discretized into a mesh of finite volume elements which may have various shapes and which are connected via N nodes. Each element represents a part of an anatomical structure and has a constant conductivity.

Furthermore, a finite dimensional subspace V_N is defined. If the basis functions $\Psi_i \in V_N$ are defined as linear piecewise continuous functions that take the value 1 at node points x_i and zero at all other node points, then the function $\bar{\Phi} \in V_N$ can be represented as

$$\bar{\Phi}(x) = \sum_{i=0}^N \alpha_i \Psi_i(x) \quad \alpha_i = \bar{\Phi}(x_i), \quad i = 0, 1, \dots, N \quad (1.6)$$

such that each $\bar{\Phi} \in V_N$ can be written in a unique way as a linear combination of the basis functions $\Psi_i \in V_N$. Now the finite-element approximation of the original boundary value problem can be stated as:

$$\text{Find } \Phi_N \in V_N \text{ such that } \int_{\Omega} \sigma \nabla \Phi_N \nabla \bar{\Phi} d\Omega = 0. \quad (1.7)$$

Furthermore, if $\Phi_N \in V_N$ satisfies problem (1.7), then

$$\int_{\Omega} \sigma \nabla \Phi_N \nabla \Psi_i d\Omega = 0 \quad (1.8)$$

holds. This equation must hold for all (i.e. for a finite number N) basis functions $\Psi_i \in V_N$. Finally, since Φ_N itself can be expressed as the linear combination

$$\Phi_N = \sum_{i=0}^N \xi_i \Psi_i(x) \quad \xi_i = \Phi_N(x_i) \quad (1.9)$$

problem (1.7) can be written as

$$\sum_{i=1}^N \xi_i \int_{\Omega} (\sigma_{ij} \nabla \Psi_i) \nabla \Psi_j d\Omega = 0 \quad j = 0, 1, \dots, N \quad (1.10)$$

Then the finite-element approximation of Eq. (1.2) can equivalently be expressed as a system of N equations with N unknowns ξ_0, \dots, ξ_N , which are the electrostatic potentials at the node points x_i . In matrix form, the preceding system can be written as $A\xi = 0$ where $A = a_{ij}$

has the elements

$$a_{ij} = \int_{\Omega} (\sigma_{ij} \nabla \Psi_i) \nabla \Psi_j \, d\Omega. \quad (1.11)$$

The matrix A contains all geometry and conductivity information of the model. A is symmetric and positive definite and thus is nonsingular and has a unique solution. Since the basis function differs from zero for only a few intervals, A is sparse (only a few of its entries are nonzero). $A\xi = 0$ is subsequently solved for the unknown variable ξ . The finite element software package ANSYS was used to solve this bioelectric volume conductor problem.

The epidural electrode contacts were considered as boundaries with constant voltages (voltage sources, Dirichlet boundary conditions). The electrode had a realistic geometry representing a quadripolar lead with cylindrical, circumferentially exposed electrode contacts (PISCES-QUAD electrode, Model 3487A, MEDTRONIC, Minneapolis, MN, USA). The four independent contacts of the quadripolar lead were labeled 0, 1, 2, 3, such that contact #0 was at the top and contact #3 at the bottom. The epidural electrode was operated as a bipolar electrode with a contact separation of 27 mm. Dirichlet boundary condition of 0.5 Volt was applied to the 0-contact, and -0.5 Volt to the 3-contact. This represented a potential difference of one Volt for the '0+3-' electrode configuration. To obtain the potential distribution along the nerve fiber trajectories for any stimulation voltage strength or the other polarity ('0-3+'), the results calculated by the finite element method were multiplied by the corresponding factor.

The electrical conductivities of the anatomical structures were taken from the compendium by Geddes and Baker (1967). All structures have an isotropic conductivity, except nerve fiber bundles. In the latter structure the conductivity parallel to the constituent fibers exceeds the value in direction normal to these fibers, as is the case for the spinal white matter.

The output of the volume conductor model is the electric potential Φ within the whole, three-dimensional solution domain Ω . To quantitatively calculate the effect of an externally generated electric field on a nerve fiber, the potential distribution computed by the finite element method had to be evaluated along the trajectories of representative target neurons. These voltage profiles then served as the input data V_e (extracellular potential) for the nerve fiber model. Therefore the assumed geometry of the simulated target neurons has an essential influence on the results (Struijk *et al.* 1993). Clinical findings based on the distributions of stimulus-evoked muscle twitches on the lower limb muscle suggested that the predominantly stimulated structures resulting in motor effects were posterior roots of the lumbar spinal cord. Thus, computer modeling was concentrated on these nerve structures. However, there is no anatomical data on posterior root trajectories in humans, which is directly applicable to the computer simulation. Discussions with anatomists, information from anatomical photographs and from Wall *et al.* (1990) and Hasegawa *et al.* (1996) were used to define standard trajectories of the simulated fibers (for details see Minassian, 2000).

Computer modeling – Nerve fiber model

The fundamental unit of information in the nervous system is the action potential. An action potential is an electrical signal that propagates along a nerve fiber from the place of its

generation to the end of the nerve fiber. A neuron consists of three main parts, the soma (the cell body), the dendrites and the axon. From the soma a large number of branching processes called dendrites spread out. Dendrites are specialized for receiving signals from other neurons. The soma also gives rise to a thin and long fiber, called axon. The axon transmits action potentials to other neurons or to muscles. At the end region of an axon called synapse the neuron is in very close contact with other cells and, via the release of chemical substances, the neural information is passed on. The axon consists of a long cylinder of axoplasm, which is surrounded by an electrically excitable membrane. The specific properties of this membrane are the basis for the propagation of action potentials along all nerve fibers. The membrane consists of a lipid bilayer, which contains large protein molecules that penetrate through the membrane. Some of these protein molecules are ion channels. They selectively allow ions and other small hydrophilic molecules to cross the membrane which would otherwise be unable to do so. The ion channels are essential for the generation of action potentials.

The intracellular and the extracellular fluids of the neuron are separated by the membrane. Different ionic concentrations in these fluids cause a voltage gradient across the membrane. When the cell is at rest, the inside potential is about 70 mV lower than the outside. This state is called polarized. During an action potential, the membrane voltage changes from the resting potential of -70 mV up to $+50$ mV. This phase is called depolarization. After reaching the peak value the voltage decreases again to the resting state, commonly with an overshoot to values less than -70 mV being called hyperpolarization.

The neural structures considered in the computer model of epidural spinal cord stimulation were posterior roots of the lumbar cord. Posterior roots at their proximal sites, where the epidural electrodes were placed, contain long axons of sensory neurons, also called dorsal root ganglion cells or sensory afferents. They transmit sensory information to the central nervous system. The somata of the posterior root fibers are contained in the dorsal root ganglia, which are enlargements of the posterior roots at the intervertebral foramen (bony canals formed by two adjacent vertebrae). The main posterior roots containing sensory afferents from the lower limbs are of the spinal cord segments L2–S2. The ganglia of these spinal roots are all situated below the termination of the spinal cord and thus are several centimeters away from the epidural electrodes as positioned in the subjects studied in this thesis. In contrast, the axons within the posterior roots of the segments L2–S2 are in a close distance to the electrode (minimum 3–5 mm). Thus, the nerve model of dorsal root ganglion cells is restricted to a model of a myelinated axon.

In the electrical network model the axon is divided into identical compartments of the length Δx . The first approach is to assume that the myelinated parts of the axon are ideal insulators. Therefore the membrane currents of these internodes are neglected. One compartment per node of Ranvier is considered. The n -th compartment is represented electrically as a single point on the axon's length-coordinate x_n by its mean inside potential $V_{i,n}$, the capacity C_m and the ion current across the membrane $I_{ion,n}$ (Fig. 1.5). The extracellular potential $V_{e,n}$ at the positions x_n is caused by the stimulating electrode current. It is calculated by the finite element method and is the input data for the electrical network model.

Since the spatial axon model is represented by an electrical network where the current efflux of one segment is the current influx for the next, Kirchhoff's law can be used for the n -th compartment to obtain current equations for the capacitive current $I_{C,n}$, the ion current $I_{ion,n}$ and the axonal current $I_{axon,n}$:

$I_{C,n} + I_{ion,n} + I_{axon,n} = 0$ or, in more detail:

$$C_m \frac{d(V_{i,n} - V_{e,n})}{dt} + I_{ion,n} + G_a(V_{i,n} - V_{i,n-1}) + G_a(V_{i,n} - V_{i,n+1}) = 0$$

where C_m and G_a are the membrane capacity and the axonal conductance, respectively.

For a cylindrical axon (Fig. 1.5A), if the membrane currents of the internodes are neglected, C_m , $I_{ion,n}$ and G_a can be substituted by

$$C_m = c_m \pi d L$$

$$I_{ion,n} = i_{ion} \pi d L$$

$$G_a = \frac{\pi d^2}{4 \Delta x \rho_i}$$

where c_m is the membrane capacity per cm^2 , i_{ion} is the ion current density across the membrane and ρ_i is the axoplasmatic resistivity.

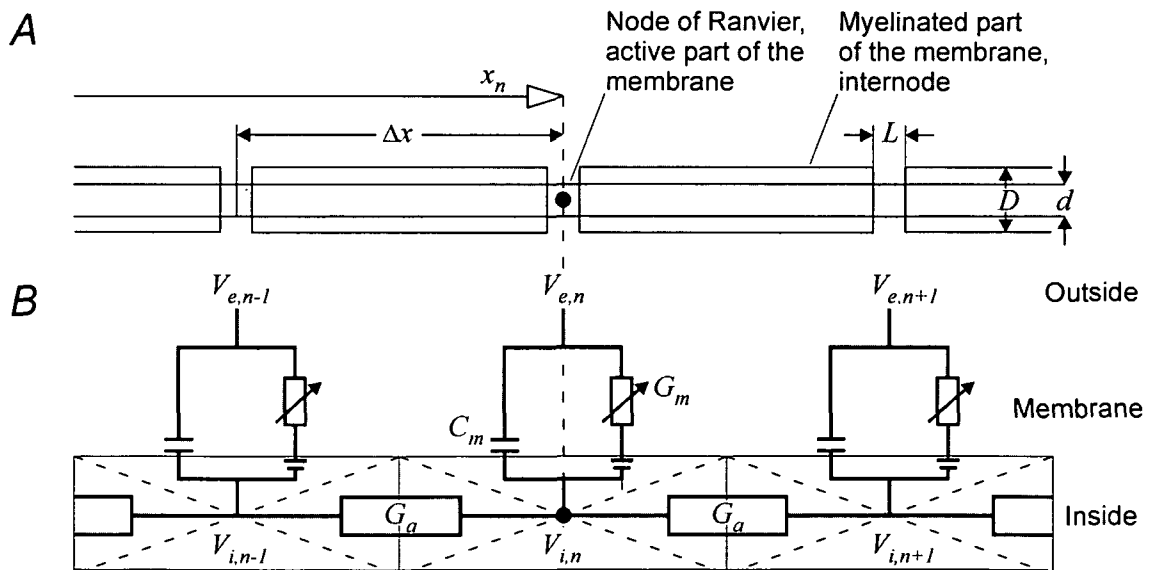


Figure 1.5 Distributed cable network model of myelinated nerve fiber

A, Geometric parameters of a myelinated axon, x_n is the axon's length coordinate. B, Electrical network to simulate the currents in a homogeneous axon with identical, cylindrical compartments of length Δx . Membrane currents are assumed to pass only through the area of active membranes, the internodes are ideal insulators.

Using the reduced membrane potential $V_n = V_{i,n} - V_{e,n} - V_{rest}$, where V_{rest} is the resting membrane potential ($V_{rest} \sim -70\text{mV}$), the following equation will be obtained

$$\frac{dV_n}{dt} = \left[\frac{d\Delta x}{4\rho_i L} \left(\frac{V_{n-1} - 2V_n + V_{n+1}}{\Delta x^2} + \frac{V_{e,n-1} - 2V_{e,n} + V_{e,n+1}}{\Delta x^2} \right) - i_{ion,n} \right] / c_m$$

The influence of an applied electric field on each of the compartments is proportional to the activating function f , which is the second spatial difference quotient of the extracellular potential V_e along the axon (Rattay, 1990):

$$f = \frac{V_{e,n-1} - 2V_{e,n} + V_{e,n+1}}{\Delta x^2}$$

An axon which is in the resting state before an electric field is applied becomes depolarized (stimulated) in regions with $f > 0$ and hyperpolarized in regions with $f < 0$. The origin of an artificially generated action potential is expected in the region where f has its maximum value.

The activating function concept is obvious when derived from the model shown in Fig. 1.5. However, a neuron model of a myelinated axon with additional compartments representing the myelinated parts of the axon (one compartment per internode) was used, because the membrane currents of these parts of the axon can not be neglected completely. Then, the main equation for the n -th compartment is:

$$\frac{dV_n}{dt} = \left[-I_{ion,n} + \frac{V_{n-1} - 2V_n + V_{n+1}}{R_a} + \frac{V_{e,n-1} - 2V_{e,n} + V_{e,n+1}}{R_a} \right] / C_{m,n}$$

where R_a is the axonal resistance, $R_a = l/G_a$ (Fig. 1.6).

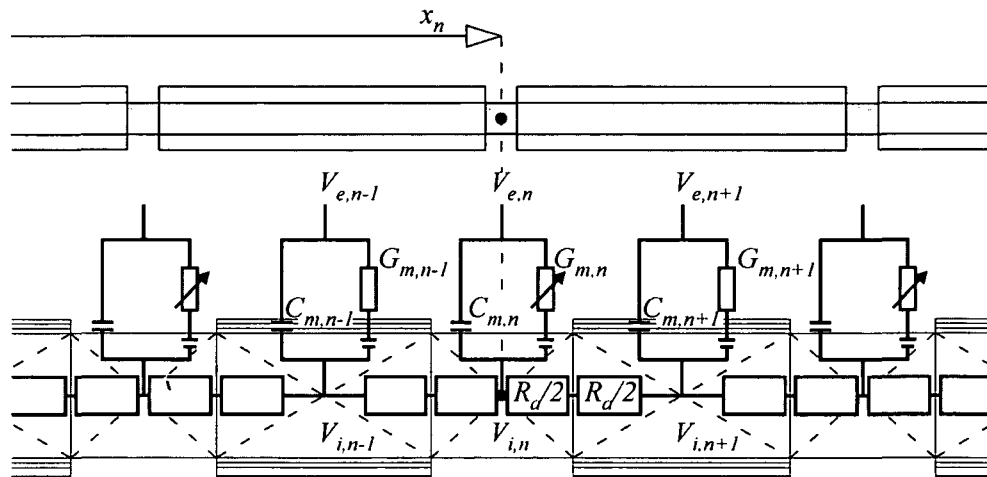


Figure 1.6 Electrical network model of an axon with subunits

Internodes are considered as single compartments with a constant membrane conductance G_m . The active parts of the membrane require an adequate membrane model. The batteries are resulting from differences in ion concentrations between the intracellular and extracellular fluid.

The influence of the extracellular potential can now be described by the generalized activating function f_n :

$$f_n = \left[\frac{V_{e,n-1} - 2V_{e,n} + V_{e,n+1}}{R_a} \right] / C_{m,n}$$

The physical dimension of the generalized activating function f_n is [V/s] or [mV/ms]. Thus, this form of the generalized activating function represents the temporal voltage change in every compartment influenced by the extracellular field.

The internodal compartments are elements with passive membranes and are assumed to have a constant membrane conductance G_m . In these cases $I_{ion,n}$, $C_{m,n}$ and G_m can be substituted by

$$I_{ion,n} = G_m V_n$$

$$G_m = g_m \pi D \Delta x$$

$$C_{m,n} = c_m \pi D \Delta x$$

where c_m is the specific membrane capacity, g_m the specific membrane conductance and $\pi D \Delta x$ the surface of the passive membrane. Note that g_m and c_m are proportional to $1/N$, with N being the number of myelin sheets of the passive membrane.

To describe the membrane kinetics of the nodal compartments, additional differential equations have to be solved to calculate $I_{ion,n}$, the ion current across the membrane at the nodes of Ranvier. The CRRSS (Chiu-Ritchie-Rogart-Stagg-Sweeney) model was used to simulate the nonlinear gating mechanism of the ionic channels in the active parts of the neuron membrane (Sweeney *et al.* 1987). The CRRSS model considers that the potassium current is negligible in mammalian axon membranes and is directly applicable for a temperature of 37°C . An ACSL (Advanced Continuous Simulation Language) program was applied to implement the nerve fiber model and to analyze the excitability of the target fibers. The following standard data for simulation was used: posterior root fiber diameter $D = 22 \mu\text{m}$, $d = 0.64D$, internodal length $\Delta x = 100D$, nodal length $L = 1.5 \mu\text{m}$.

The cable model including ion channel dynamics was applied to identify the thresholds of posterior roots when stimulated by different positioned epidural electrodes (Minassian 2000; Rattay *et al.* 2000). With this expertise, particular emphasis was given to the geometric relations between the calculated isopotential lines and the topographic anatomy of afferent fiber systems in this thesis (chapter 2). This approach is supported by the activating function concept. As aforementioned, the activating function gives a qualitative indication of the effect of an externally applied electric field on a target fiber. The first response of every node and every internode to a stimulus pulse can be estimated with the activating function, which describes the local change of membrane voltage. The activating function uses the extracellular voltage along the neuron as input data, but the complicated ion channel mechanisms are not required in order to find the position of strongest depolarization along a fiber. For a regular myelinated nerve fiber the activating function is related to the second difference quotient of the external potential. When a stimulus pulse is applied to a fiber which has been in resting state before, largest nodal depolarization and thus spike initiation is expected in the region with the highest positive values of the activating function. The value of the activating function is related to the curvature of the extracellular voltage profile along the fiber. For a given stimulus intensity the curvature of the extracellular voltage profile is mostly influenced by the distance to the electrode, the curvature of the fiber and changes of electrical conductivity along the trajectory of the fiber (e.g. the interface between cerebrospinal fluid and white matter at the entry points of the posterior roots into the spinal cord).

Design of the thesis

The following chapters 2–4 are written as independent articles, since they were the outcome of research to be published in peer-reviewed scientific journals.

Chapter 2, Posterior Roots Muscle Reflex Responses elicited by epidural stimulation of the human lumbar cord.

This chapter provides several independent approaches to identify the directly stimulated structures by epidural lumbar cord stimulation leading to single muscle twitches, continuous muscle contractions or alternating flexion/extension movements of the lower limbs. Information on muscle twitch distribution patterns were combined with calculated electric potential distributions and the topographical anatomy of posterior columns and roots. It is concluded that muscle responses to bipolar stimulation from the dorsal epidural space were initiated in large afferent fibers within the posterior roots. It is emphasized that the possibility to selectively elicit these Posterior Roots Muscle Reflex Responses (PRMRRs) is due to the unique anatomical architecture of the terminal spinal cord which determines the resultant electrical field characteristics and its effect on excitable structures. Work from this chapter was also submitted to the *Journal of Physiology*.

Chapter 3, Stepping-like movements in humans with complete spinal cord injury induced by epidural stimulation of the lumbar cord: Electromyographic study of compound muscle action potentials

This chapter provides evidence for the involvement of lumbar interneuronal structures in the generation and control of epidurally induced stepping-like movements. Stimulus-triggered time windows from the original EMG traces were analyzed to reveal features of the intrinsic organization of human spinal networks activated by sustained external stimulation. It is proposed to consider the described processing capabilities of the lumbar cord isolated from brain control and tested by PRMRRs as evidence for the existence of a human Lumbar Locomotor Pattern Generator (LLPG). A shortened version of chapter 3 is published in the journal *Spinal Cord* (Minassian *et al.* 2004a).

Chapter 4, Effect of peripheral afferent and central afferent input to the isolated human lumbar spinal cord

While in the preceding chapters it is demonstrated that sustained stimulation of the posterior roots can activate the LLPG in supine spinal cord injured individuals, the topic of chapter 4 addresses whether the LLPG can be activated during manually assisted treadmill stepping. It is shown that the LLPG activated by a “central” peripheral input (provided by epidural stimulation) can integrate and interpret the proprioceptive input associated with passive stepping to generate functional locomotor patterns. This finding is considered as further evidence that lumbar interneurons can be temporarily incorporated into pattern generating networks for stepping-like activity. The encouraging results of chapter 4 will be presented in the 34th Annual Meeting of the Society for Neuroscience (Minassian *et al.* 2004b).

REFERENCES

- Barolat G, Massaro F, He J, Zeme S & Ketcik B (1993). Mapping of sensory responses to epidural stimulation of the intraspinal neural structures in man. *J Neurosurg* **78**, 233-239.
- Barolat G, Singh-Sahni K, Staas WE, Shatin D, Ketcik B & Allen K (1995). Epidural spinal cord stimulation in the management of spasms in spinal cord injury. A prospective study. *Stereotact Funct Neurosurg* **64**, 153-164.
- Beric A (1988). Stability of lumbosacral somatosensory evoked potentials in a long-term follow-up. *Muscle Nerve* **11**, 621-626.
- Bulling A, Castrop F, Agneskirchner J, Rumitz M, Ovtscharoff W, Wurzinger LJ, Gratzl M (1997). Body Explorer 2.0, An interactive program on the cross-sectional anatomy of the Visible Human Male. Springer Verlag, Heidelberg.
- Bussel B, Roby-Brami A, Neris OR & Yakovlev A (1996). Evidence for a spinal stepping generator in man. *Paraplegia* **34**, 91-92.
- Calancie B, Needham-Shropshire B, Jacobs P, Willer K, Zych G & Green BA (1994). Involuntary stepping after chronic spinal cord injury. Evidence for a central rhythm generator for locomotion in man. *Brain* **117**, 1143-1159.
- Coburn B (1980). Electrical stimulation of the spinal cord: two-dimensional finite element analysis with particular reference to epidural electrodes. *Med Biol Eng Comput* **18**, 573-584.
- Dietz V, Colombo G, Jensen L & Baumgartner L (1995). Locomotor capacity of spinal cord in paraplegic patients. *Ann Neurol* **37**, 574-582.
- Dietz V, Muller R & Colombo G (2002). Locomotor activity in spinal man: significance of afferent input from joint and load receptors. *Brain* **125**, 2626-2634.
- DiMarco AF, Romaniuk JR, Kowalski KE & Supinski G (1999). Pattern of expiratory muscle activation during lower thoracic spinal cord stimulation. *J Appl Physiol* **86**, 1881-1889.
- Dimitrijevic MR, Prevec TS, Sherwood AM (1983) Somatosensory perception and cortical evoked potentials in established paraplegia. *J Neurol Sci* **60**, 253-265
- Dimitrijevic MM, Dimitrijevic MR, Illis LS, Nakajima K, Sharkey PC & Sherwood AM (1986a). Spinal cord stimulation for the control of spasticity in patients with chronic spinal cord injury: I. Clinical observations. *Cent Nerv Syst Trauma* **3**, 129-144.
- Dimitrijevic MR, Illis LS, Nakajima K, Sharkey PC & Sherwood AM (1986b). Spinal cord stimulation for the control of spasticity in patients with chronic spinal cord injury: II. Neurophysiologic observations. *Cent Nerv Syst Trauma* **3**, 145-152.
- Dimitrijevic MR, Gerasimenko Y & Pinter MM (1998). Evidence for a spinal central pattern generator in humans. In *Neural Mechanisms for Generating Locomotor Activity*. *Ann N Y Acad Sci Vol. 860*, ed. Kiehn O, Harris-Warrik RM, Jordan LM, Hultborn H & Kudo N, pp. 360-376. New York Academy of Sciences, New York.
- Dimitrijevic MR, Minassian K, Murg M, PinterMM, Rattay F, Gerasimenko Y & Binder H (2001). Study of locomotor capabilities induced by spinal cord stimulation (SCS) of the

human lumbar cord isolated from the brain control by posttraumatic spinal cord injury (SCI). *Soc Neurosci Abstr*; 27: Program No. 935.6.

Dobkin BH, Harkema S, Requejo P & Edgerton VR (1995). Modulation of locomotor-like EMG activity in subjects with complete and incomplete spinal cord injury. *J Neurol Rehabil* 9, 183-190.

Fedirchuk B, Nielsen J, Petersen N & Hultborn H (1998). Pharmacologically evoked fictive motor patterns in the acutely spinalized marmoset monkey (*Callithrix jacchus*). *Exp Brain Res* 122, 351-361.

Geddes LA & Baker LE (1967). The specific resistance of biological material—a compendium of data for the biomedical engineer and physiologist. *Med Biol Eng* 5, 271-293.

Gerasimenko YP, Dimitrijevic MR, Bussel B, Daniel O, Regnaud JP, Combeaud M, Pinter MM (2000). The mechanisms of central pattern generator activation by means of epidural spinal cord stimulation. *Proceedings of the 5th Annual Conference of the International Functional Electrical Stimulation Society*, pp. 129-131, Aalborg, Denmark.

Gerasimenko YP, Makarovskii AN & Nikitin OA (2002). Control of locomotor activity in humans and animals in the absence of supraspinal influences. *Neurosci Behav Physiol* 32, 417-423.

Grillner S (1981). Control of locomotion in bipeds, tetrapods and fish. In *Handbook of Physiology. The Nervous System. Motor Control. sect. 1, vol. II, part 2*, pp. 1179-1236. Am Physiol Soc, Washington, DC.

Gurfinkel VS, Levik YS, Kazennikov OV & Selionov VA (1998). Locomotor-like movements evoked by leg muscle vibration in humans. *Eur J Neurosci* 10, 1608-1612.

Eidelberg E, Walden JG & Nguyen LH (1981) Locomotor control in macaque monkeys. *Brain* 104, 647-663.

Harkema SJ, Hurley SL, Patel UK, Requejo PS, Dobkin BH & Edgerton VR (1997). Human lumbosacral spinal cord interprets loading during stepping. *J Neurophysiol* 77: 797-811.

Hasegawa T, Mikawa Y & Watanabe R (1996). Morphometric analysis of the lumbosacral nerve roots and dorsal root ganglia by magnetic resonance imaging. *Spine* 21, 1005-1009.

He J, Barolat G, Holsheimer J & Struijk JJ (1994). Perception threshold and electrode position for spinal cord stimulation. *Pain* 59, 55-63.

Holsheimer & Struijk (1987). Electrode combination and specificity in spinal cord stimulation. *Proc. 9th Int Symp 'Advances in external control of human extremities'*, pp. 383-404. Dubrovnik.

Holsheimer J, den Boer JA, Struijk JJ & Rozeboom AR (1994). MR assessment of the normal position of the spinal cord in the spinal canal. *AJNR Am J Neuroradiol* 15, 951-995.

Holsheimer J (1998). Computer modelling of spinal cord stimulation and its contribution to therapeutic efficacy. *Spinal Cord* 36, 531-540.

Holsheimer J (2002). Which neuronal elements are activated directly by spinal cord stimulation. *Neuromodulation* 5, 25-31.

Hultborn H et al. (1993) Evidence of fictive spinal locomotion in the marmoset (*Callithrix jacchus*). *Soc Neurosci Abstr* 19: 539.

Kameyama T, Hashizume Y & Sobue G (1996). Morphologic features of the normal human cadaveric spinal cord. *Spine* 21, 1285-1290.

Kazennikov OV, Shik ML, Yakovleva GV (1983) Stepping elicited by stimulation of the dorsolateral funiculus in the cat spinal cord. *Biull Eksp Biol Med (Bulletin of Experimental Biology and Medicine)* 96, 8-10. [Article in Russian with English abstract]

Kern H, McKay WB, Dimitrijevic MM & Dimitrijevic MR (2004). Motor control in the human spinal cord and the repair of cord function. *Current Pharmaceutical Design* (in press).

Lehmkuhl D, Dimitrijevic MR & Renouf F (1984). Electrophysiological characteristics of lumbosacral evoked potentials in patients with established spinal cord injury. *Electroencephalogr Clin Neurophysiol* 59, 142-155.

Melzack R & Wall PD (1965). Pain mechanisms: a new theory. *Science* 150, 971-979.

Minassian (2000). Excitation of lower spinal cord structures with implanted electrodes: 3D finite element analysis and simulation of neural responses. Diploma Thesis, Vienna University of Technology.

Minassian K, Jilge B, Rattay F, Pinter MM, Binder H, Gerstenbrand F & Dimitrijevic MR (2004a). Stepping-like movements in humans with complete spinal cord injury induced by epidural stimulation of the lumbar cord: Electromyographic study of compound muscle action potentials. *Spinal Cord* May 4 [Epub ahead of print].

Minassian K, Persy I, Rattay F, Binder H, Pinter MM & Dimitrijevic MR (2004b). Output induced by manually assisted treadmill stepping of paraplegic individuals can be enhanced by epidural stimulation of the Lumbar Locomotor Pattern Generator. Abstract No. 4770, 34th Annual Meeting of the Society for Neuroscience, San Diego, CA.

North RB, Lanning A, Hessels R & Cutchis PN (1997). Spinal cord stimulation with percutaneous and plate electrodes: side effects and quantitative comparisons. *Neurosurg Focus* 2(1):ARTICLE.

Pinter MM, Gerstenbrand F & Dimitrijevic MR (2000). Epidural electrical stimulation of posterior structures of the human lumbosacral cord: 3. Control of spasticity. *Spinal Cord* 38, 524-531.

Rattay F (1990). *Electrical Nerve Stimulation: Theory, Experiments and Applications*. Springer, Wien-New York.

Rattay F, Minassian K & Dimitrijevic MR (2000). Epidural electrical stimulation of posterior structures of the human lumbosacral cord: 2. quantitative analysis by computer modeling. *Spinal Cord* 38, 473-489.

Regnaud JP, Daniel O, Combeaud M, Denys P, Remy Neris O, Gerasimenko Y & Busses B (2000). Evidence for a monosynaptic response after low thoracic spinal cord epidural stimulation in paraplegic humans. *Proceedings of the 5th Annual Conference of the International Functional Electrical Stimulation Society*, pp. 171, Aalborg, Denmark.

Roby-Brami A & Bussel B (1987). Long-latency spinal reflex in man after flexor reflex afferent stimulation. *Brain* 110, 707-725.

Sherwood AM, McKay WB & Dimitrijevic MR (1996). Motor control after spinal cord injury: Assessment using surface EMG. *Muscle Nerve* **19**, 966-979.

Struijk JJ, Holsheimer J & Boom HB (1993). Excitation of dorsal root fibers in spinal cord stimulation: A theoretical study. *IEEE Trans Biomed Eng* **40**, 632-639.

Struijk JJ & Holsheimer J (1996). Transverse tripolar spinal cord stimulation: theoretical performance of a dual channel system. *Med Biol Eng Comput* **34**, 273-279.

Sweeney JD, Mortimer JT & Durand D (1987). Modeling of mammalian myelinated nerve for functional neuromuscular electrostimulation. *Proceedings of the IEEE 9th Annual Conference Eng Med Biol Soc*, pp 1577-1578, Boston.

Wall EJ, Cohen MS, Abitbol JJ & Garfin SR (1990). Organization of intrathecal nerve roots at the level of the conus medullaris. *J Bone Joint Surg Am* **72**, 1495-1499.

Chapter 2

Posterior Roots Muscle Reflex Responses elicited by epidural stimulation of the human lumbar cord

Summary

While evaluating the effect of epidural spinal cord stimulation on spasticity of lower limbs in patients with complete spinal cord injury, we found that sustained non-patterned stimulation of posterior lumbar cord structures can induce sustained extension-standing like and alternating stepping-like lower limb movements. In the present paper we identify the stimulated lumbar neural structures which resulted in the evoked muscle activity.

We analyzed surface-recorded electromyographic (EMG) responses of the quadriceps, hamstrings, tibialis anterior, and triceps surae muscles elicited by epidural stimulation of the posterior lumbar cord at 1–10 V and 2.2–50 Hz. Seventeen subjects with motor complete, chronic spinal cord injury at levels rostral to the lumbar cord were included in the study. We examined the relationship between the segmental cathode level of the epidural electrode and the corresponding recruitment order of the quadriceps and triceps surae muscles. We applied a computer model of epidural spinal cord stimulation to calculate the spatial distributions of the electric fields generated by the electrodes. The results were combined with patterns of segmental organization of the posterior columns and roots which are the most obvious targets of stimulation.

We found that EMG signals associated with twitch responses to 2.2 Hz stimulation were stimulus-coupled short-latency compound muscle action potentials (CMAPs). We present evidence that these CMAPs were initiated in large fibers within the posterior roots and refer to this type of stimulus-evoked muscle activity as Posterior Roots Muscle Reflex Responses (PRMRRs). Amplitudes of PRMRRs to 2.2 Hz stimulation were determined by cathode position and stimulus strength. At 5–50 Hz different patterns of tonic and rhythmic EMG activity in the lower limbs were elicited by non-patterned stimulation. The tonic EMG responses as well as the "burst-style" EMG phases during epidurally induced flexion/extension movements consisted of stimulus-triggered CMAPs with similar EMG features as single twitch responses.

We hypothesize that the modulation of PRMRR amplitudes during 5–50 Hz stimulation is due to the fact that in addition to recruitment of motoneurons through monosynaptic connection in the spinal cord the afferent input also produces postsynaptic potentials in spinal interneurons. We argue that at particular higher frequencies the tonic afferent input activates spinal mechanisms that control motoneuronal discharge and the transmission through reflex pathways thereby generating potentially functional lower limb movements.

INTRODUCTION

When a stimulating electrode is placed in the epidural space over the dorsum of the human spinal cord, a variety of neural structures are located in the vicinity of the electrode and are potential sites for direct electrical stimulation. Axons which originate from receptors and free nerve endings in muscles, tendons, joints, and cutaneous and subcutaneous tissues enter the cord via the posterior roots in close proximity to the posterior aspect of the epidural space. Upon entering the spinal cord the axons bifurcate to rostral and caudal branches in the posterior columns, which are close to a midline epidural electrode as well. The immediate effects of epidural electrical stimulation of the spinal cord in humans with intact sensory functions are tingling sensations within the skin (paresthesiae) and muscle contractions that are referred to the body parts corresponding to the activated neurons.

Clinical programs for modifying altered sensations, pain (Shealy *et al.* 1967) or impaired motor control in neurological disorders (Barolat *et al.* 1988; Waltz, 1998) by epidural spinal cord stimulation can provide the possibility of parallel neurophysiological studies to investigate the induced sensory and motor effects.

While evaluating the effect of epidural spinal cord stimulation on spasticity of lower limbs in patients with complete, long-standing spinal cord injury we found that the sustained non-patterned stimulation of posterior lumbar cord structures could induce stepping-like alternating flexion and extension movements (Dimitrijevic *et al.* 1998). We advanced these studies of the locomotor capabilities of the human lumbar cord and examined the mechanisms activated by epidural stimulation which resulted in stepping-like movements in subjects with motor complete spinal cord injury (Minassian *et al.* 2004). Furthermore we provided evidence that epidural stimulation of posterior lumbar cord structures can initiate and retain lower limb extension in paraplegic subjects (Jilge *et al.* 2004).

The purpose of the present study is to find out which posterior lumbar cord structures were stimulated, inducing motor effects and potentially functional movements of the paralyzed lower limbs and to elucidate what the electrophysiological components of the responses are.

MATERIAL AND METHODS

Subjects

The EMG data of stimulus-evoked muscle response patterns which was made available for the present retrospective study was derived from seventeen patients with long-standing motor complete spinal cord injury (SCI). They had participated in a program of restorative neurology for the control of spasticity with epidural spinal cord stimulation, since they did not have a satisfactory response to other therapeutical modalities. Clinical protocols had been conducted to define optimal electrode positions and stimulation parameters. The effect of stimulation had been assessed by surface EMG recordings of induced muscle activity in the lower limbs.

At the time of data collection all subjects met the following criteria: (1) They were healthy adults with closed, post-traumatic spinal cord lesions; (2) all patients were in a chronic (more than 1 year post-onset) and stable condition; (3) no antispastic medication was being used; (4) the stretch and cutaneomuscular reflexes were preserved; (5) there was no voluntary activation of motor units below the level of the lesion as confirmed by brain

motor control assessment (Sherwood *et al.* 1996); while (6) surface recorded lumbosacral evoked potentials – used to assess the functions of the posterior structures and gray matter of the spinal cord below the level of the lesion – were present (Beric, 1988; Lehmkuhl *et al.* 1984).

To control their spasticity all subjects had an electrode array placed in the dorsomedial epidural space (see "*Stimulation setup*"). The implantation procedure has been described in detail previously (Murg *et al.* 2000). The position of the epidurally placed electrodes relative to the vertebral bodies was obtained from postoperative X-rays. The estimated, functional segmental level of the cathode was derived from a neurophysiological technique for electrode positioning in subjects with impaired sensory function (Murg *et al.* 2000). Additionally, information on average spatial relations between the cord segments and the vertebral bodies was used (Lang, 1984a). The implantations as well as the clinical protocol to evaluate the optimal stimulation parameters were approved by the local ethics committee. All patients gave their informed consent. Pertinent patient-related data are listed in Table 2.1.

Table 2.1 Demographic and clinical data.

Subject No.	Sex	Born in	Accident in	Implantation of electrode in	Type of accident	Level of SCI	ASIA Class.
1	m	1970	1996	1999	Car accident	C6	B
2	m	1977	1994	1999	Motorbike accident	C6	A
3	m	1970	1991	1999	Car accident	T4	A
4	m	1973	1995	1998	Car accident	C4	A
5	m	1981	1996	1999	Car accident	C4	A
6	m	1973	1997	1998	Ski accident	C7	B
7	f	1966	1996	1997	Car accident	T5	A
8	m	1974	1993	2001	Fall accident	T2	A
9	f	1976	1992	1998	Fall accident	T2	B
10	m	1978	1996	1999	Car accident	T10	B
11	f	1978	1994	1996	Car accident	T4	A
12	f	1975	1996	2000	Car accident	T6	A
13	m	1967	1987	2001	Motorbike accident	T5	A
14	f	1965	1996	1998	Car accident	T5	A
15	m	1971	1991	1999	Car accident	C6	B
16	m	1939	1994	1997	Fall accident	T7	A
17	m	1973	1996	1997	Car accident	T4	A

Stimulation setup

Stimulation was delivered via a quadripolar lead with cylindrical electrode design (PISCES-QUAD electrode, Model 3487A, MEDTRONIC, Minneapolis, MN, USA) placed in the dorsomedial epidural space at vertebral levels ranging from T10 to L1. The data analyzed in the present study was recorded when the electrode array was operated as a bipolar electrode, the most rostral and caudal electrode contacts being connected to the positive and negative outputs, respectively, of the implanted pulse generator (ITREL 3, Model 7425, MEDTRONIC). The separation of the active electrode contacts was 27 mm. The bipolar impedance was generally about 1000 Ω . The stimulus pulses were biphasic and actively charge balanced. The first dominant phase was about rectangular with a width of 210 μ s, the amplitude in the much longer second phase was small and irrelevant to the stimulation process but avoided charge accumulation. Thus, stimulation was virtually monophasic and the stimulating effect of the epidural electrode based on its polarity during the first dominant phase, i.e. on the electrode contact which had a negative potential during the first phase. Cathodal stimulation of spinal neural structures results in lower thresholds than anodal stimulation. For posterior root fibers the calculated thresholds for cathodal excitation are about three times lower than anodal thresholds (Struijk *et al.* 1993a; Holsheimer, 2002). Reversing the polarity of the bipolar epidural electrode shifted the effective cathode site to a different rostrocaudal level. Thus, setting the electrode polarity allowed for stimulation of posterior structures of the spinal cord at different segmental levels, determined by the cathode site, with a single epidural electrode array.

Recording procedure

To assess the effect of spinal cord stimulation, stimulus-evoked muscle activity of quadriceps, hamstring, tibialis anterior, and triceps surae were recorded with silver-silver chloride surface electrodes. The bipolar electrodes were placed centrally over the muscle bellies spaced 3 cm apart and oriented along the long axis of the muscles. Additionally, electromyographic activity of the lumbar paraspinal trunk muscles was recorded. The skin was slightly abraded to obtain an electrode impedance below 5 k Ω . The EMG signals were amplified with the Grass 12D-16-OS NEURODATA ACQUISITION SYSTEM (GRASS INSTRUMENTS, Quincy, MA) adjusted to a gain of 2000 over a bandwidth of 30–1000 Hz and digitized at 2048 samples/s/channel using a CODAS ADC system (DATAQ INSTRUMENTS, Akron, OH). All recordings were conducted with the patients in a comfortable supine position. The EMG data was analyzed off-line using WINDAQ Waveform Browser playback software (DATAQ INSTRUMENTS).

Data analysis – Data based on incremental pulse amplitudes

The first set of EMG data had originally been collected to define the rostrocaudal level of the electrode relative to the lumbosacral cord segments based on muscle twitch distribution patterns (Murg *et al.* 2000). For this purpose, a frequency of 2.2 Hz was used, and the stimulation strength was intensified in 1-Volt increments from 1 to 10 V.

We examined single stimulus-evoked and surface-recorded compound muscle action potentials (CMAPs) associated with the twitch responses for latencies (quantitatively), peak-to-peak amplitudes, and shapes (qualitatively) of the same data set. The latencies were read off-line from the EMG traces using the playback software and measured as the time

between stimulation onset – identified by stimulus artifacts – and the first deflection of the EMG potential from baseline. Mean latency times based on all subjects were calculated for the threshold stimulus strengths eliciting responses in each muscle group and for the maximum strengths applied.

Furthermore, the recruitment order of the quadriceps and triceps surae muscles was examined by establishing the threshold voltages at which they responded – i.e. the lowest whole-numbered stimulation voltage inducing an unequivocal EMG activity (about $\pm 10 \mu\text{V}$). To this end, EMG data of the subjects 1–15 were analyzed. Quadriceps and triceps surae were considered in this analysis, because they are the only ones of the recorded muscle groups with separate segmental innervations (L2–L4 vs. L5–S2). For each subject and given electrode array position, data of two different recording sets were examined, where first the most rostral and then the most caudal electrode of the array had been operated as the effective cathode. Four subjects had two epidural electrode arrays positioned at different rostrocaudal levels or had a single one repositioned during participation in the clinical program. Moreover, threshold values for right and left side were frequently different (in 62% of all cases), thus each lower extremity was taken as a separate case. In this way, a total of 76 (19 electrode array positions) \times (2 cathode positions each) \times (2 cases: left and right side) muscle recruitment orders and corresponding threshold voltages were obtained, 75 of the 76 cases could be assigned to one of four distinct groups. In group 1, only the thigh muscles were recruited even with the stimulation strength at its maximum level of 10 V. Group 2 was characterized by a lower threshold for quadriceps than for triceps surae responses. In group 3, quadriceps and triceps surae had the same (whole-numbered) threshold. In group 4, triceps surae responded at lower voltages than quadriceps, i.e. the recruitment order was reversed in comparison with group 2.

The rostrocaudal position of the active cathode was entered into a chart of vertebral body levels that also featured a spinal cord with "standard" spatial relations of the cord segments to the vertebral bodies (adapted from Lang, 1984a) to estimate the geometric segmental level of the cathode. Additional information about relative heights of the vertebral bodies (Panjabi *et al.* 1991; Panjabi *et al.* 1992) and the mean position of the termination of the spinal cord (Saifuddin *et al.* 1998) were also considered in this model. For each of the four groups of subjects with different muscle recruitment patterns, the mean cathode level relative to the spine was established, based on the positions in the chart.

Data analysis – Data based on incremental pulse frequencies

The second set of EMG data that was analyzed had originally been collected to assess the effect of trains of electrical stimuli at 5–100 Hz on spasticity (Pinter *et al.* 2000). The same data was used to examine the motor output patterns induced by sustained trains over a frequency range of 5–50 Hz. To examine the components of the overall EMG pattern the time scale of the EMG traces was subsequently enlarged. This allowed us to address the question of how far individual responses to the single pulses within the applied stimulus train were reflected in the EMG output pattern. Separate successive responses to these pulses were analyzed for characteristic patterns of relative EMG amplitudes.

Again, the data was analyzed for the recruitment order of the quadriceps and triceps surae muscles as was done for 2.2 Hz stimulation. Recruitment properties of stimulation with 2.2 Hz, 25 Hz and 50 Hz were compared in the same subject and for a given cathode position. For this retrospective analysis, data were available from the subjects 1, 2, 5, 7, 10, 12, 13

and 16. The recruitment orders were classified in groups according to the relative threshold voltages at which quadriceps and triceps surae responded to the 2.2 Hz stimulation.

Computer simulation of the electric potential distribution

A computer model was established to learn more about the potential distribution within the spinal cord and its surrounding tissues, focusing on the geometric relations between the calculated isopotential lines and the topographic anatomy of posterior root and posterior column fibers of different segmental origins. This model consisted of 3-dimensional volume conductors representing the spinal cord, cerebrospinal fluid, dura mater, epidural space, vertebral bone, and a compartment surrounding the spine. The potential distribution was determined by the geometry and electric conductivities of the anatomical structures. The finite-element method was applied to calculate the steady-state solutions of this volume conductor problem, which included inhomogeneity, anisotropy and a complex geometry. This finite-element model based on varying cross-sections to represent the lumbosacral spinal cord, including the lumbar enlargement and the lower end of the cord, which tapers to form the conus medullaris. For further details of the volume conductor model to calculate the generated potential distributions see Rattay *et al.* (2000).

RESULTS

Muscle responses to single stimuli (2.2 Hz stimulation)

Electrical stimulation of the lumbosacral cord delivered from the dorsomedial epidural space at 2.2 Hz and 1–10 V elicited twitch responses in the lower limb muscles. Figure 2.1A shows characteristic EMG features associated with these stimulus-evoked responses of the quadriceps (Q), triceps surae (TS) and lumbar paraspinal trunk (PARA) muscles displayed with different time scales. The rostrocaudal position of the active cathode was at the center level of the twelfth thoracic vertebra, the estimated segmental cathode level was L3/L4 (subject 5). Stimulation strength was 5 V. On the left side of Fig. 2.1A, 10-second traces of EMG recordings are displayed. Twenty-two separate responses of quadriceps and triceps surae were elicited within this time. The EMG activity of successive single responses demonstrated only minor variation of the peak-to-peak amplitudes. There was no EMG activity between two consecutive twitch responses. The EMG trace derived from the paraspinal muscles showed more deflections than those from the lower limb muscles. Their origins can be identified in the middle column of Fig. 2.1A, where the last second of the EMG recordings is shown in a time scale extended 10 times. The deflections are artifacts which are superimposed on the recordings of the stimulus-evoked EMG activity of the paraspinal muscle. Due to the close distance of the paraspinal-electrode to the epidural electrode, volume-conducted artifacts of the stimulus pulses are picked up by the recording surface electrode. Three of these stimulus artifacts can be seen within the one-second trace, each followed by single low-amplitude paraspinal EMG response. The prominent potential with long duration between the first two stimulus artifacts is an electrocardiographic activity.

Each pulse within the sustained stimulus train which is identifiable by the stimulus artifacts triggered a single compound muscle action potential (CMAP) in quadriceps and triceps surae. The EMG features of these CMAPs can be seen on the right side of Fig. 2.1A, where

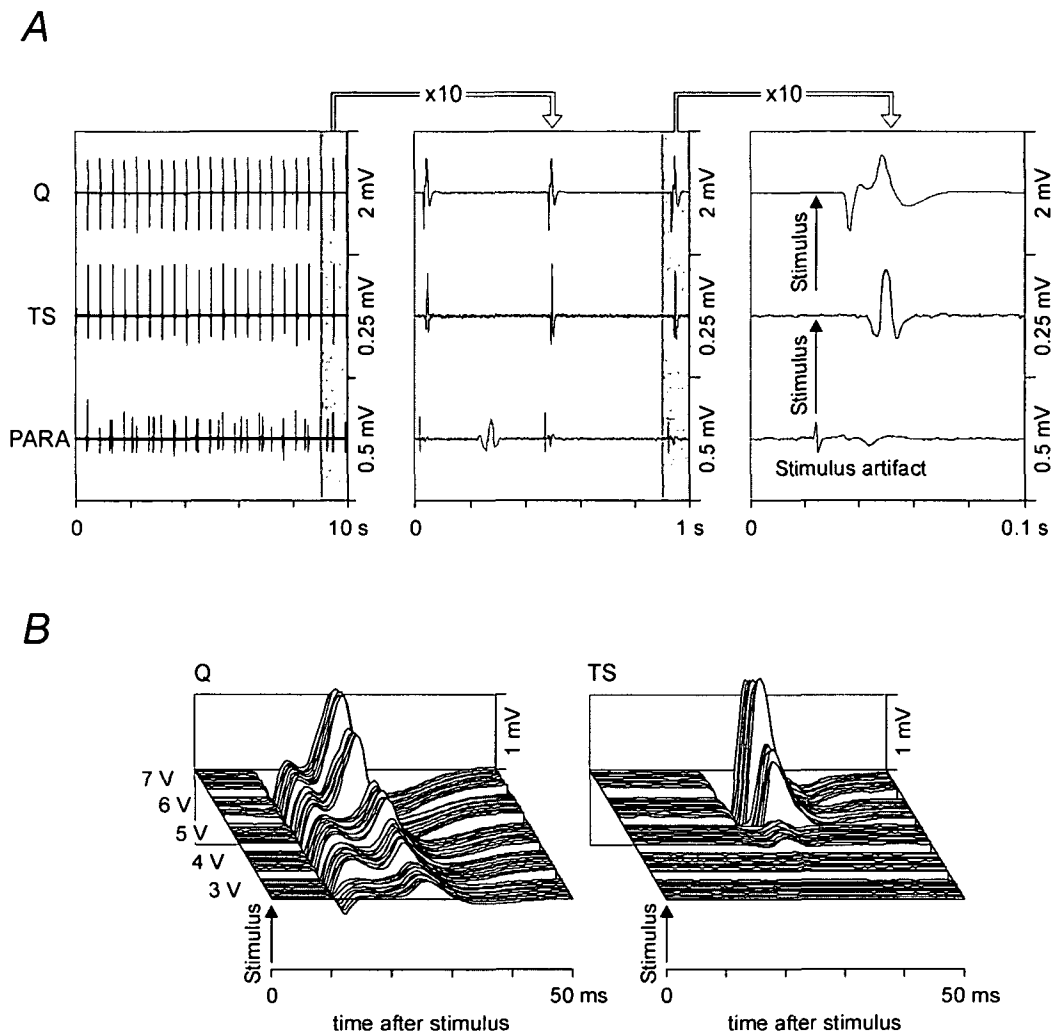


Figure 2.1 EMG responses to 2.2 Hz stimulation

A, EMG responses of the quadriceps (Q), triceps surae (TS) and lumbar paraspinal (PARA) muscles presented with different time scales (subject 5). Stimulus strength was 5 V, cathode was located at the center level of the T12 vertebral body. Stimulus artifacts captured by the paraspinal-surface electrodes allow the identification of the onsets of applied voltage pulses. *B*, stimulus-triggered sequential presentation of EMG potentials induced in the Q and TS. The graph shows the first 50 ms following the onset of each stimulus pulse. Same subject and cathode position as in *A*, but the stimulation strength was increased in steps of 1 V (3–7 V). Ten single EMG potentials of successive twitch responses are shown for each incremental voltage.

the last 100 milliseconds of the original recording are shown. The latency times of the different muscle groups were rather short. The quadriceps twitch had a latency of 9.5 ms, the more distal triceps surae muscle responded with a latency of 18.5 ms.

Figure 2.1*B* compares single surface recorded CMAPs of quadriceps and triceps surae muscles induced by stimuli at 3–7 V and 2.2 Hz in the same subject as in Fig. 2.1*A* (same cathode position). The figure is a stimulus-triggered sequential presentation of successively elicited CMAPs in which the original continuous EMG traces are shown as time windows of 50 ms that are arranged behind each other (compare with right side of Fig. 2.1*A*). The left

margins of the windows indicate the onsets of the stimuli. CMAPs associated with ten single twitch responses are shown for each incremental voltage. In the presented case, muscle responses could not be elicited in the lower limbs at 1–2 V. At 3 V, single CMAPs with short (9.5 ms) and constant latencies were recorded in quadriceps, while triceps surae showed no activity. At 4 V, quadriceps CMAPs had higher amplitudes than at 3 V while the latencies remained unchanged. Faint activity was also observed in triceps surae at 4 V, involving latencies of 18.5 ms. At higher stimulation strengths, EMG amplitudes of the twitch responses further increased for both muscle groups. The results shown in Fig. 2.1 are representative for subjects with cathodes positioned at T12 vertebral body level.

The latencies of successive responses remained constant in both muscle groups, while no additional EMG components with longer latencies or later potential-peaks emerged at higher stimulus strengths. In each subject and for a given muscle group, latency times were rather invariable regardless of stimulus strength and site. The mean latency times for quadriceps, hamstrings, tibialis anterior and triceps surae at threshold level and maximum applied stimulation strength (generally 8–10 V) are compiled in Table 2.2. They were about 10 ms for the thigh muscles and 17 ms for the leg muscles. Note that the weak responses induced at threshold stimulation had low CMAP amplitudes and slight onset slopes of the potentials, thus making the precise identification of the onset of the CMAPs difficult. This may partially account for the longer latencies of muscle responses at threshold level in Table 2.2.

Table 2.2 Mean latencies (ms \pm SD) of CMAPs evoked by 2.2 Hz stimulation based on all subjects at threshold and maximum stimulation strength

	Threshold	Maximum
Q	9.7 \pm 1.7	9.3 \pm 1.2
H	10.2 \pm 1.6	9.7 \pm 1.1
TA	16.8 \pm 1.6	16.6 \pm 1.1
TS	17.1 \pm 1.4	16.9 \pm 0.9

Consecutive CMAPs to continuous stimulation of the same strength and at 2.2 Hz exhibited essentially identical potential shapes. The shape of the EMG responses of a given muscle group was alike in different subjects. The CMAPs showed mainly increased amplitudes at suprathreshold strengths, with only minor changes of the EMG shape.

To summarize, the EMG signals associated with the twitch responses elicited by 2.2 Hz stimulation were separate, stimulus coupled CMAPs with short latency. Equal-voltage stimuli yielded only negligible variations in CMAP amplitudes and shapes. Thus, a given response demonstrated no influence on following responses to the stimulus train. For a given cathode position the CMAP amplitudes were governed by the stimulus strength. The effect of 2.2 Hz stimulation was like the effect of single applied stimulus pulses.

Relationships between cathode levels, stimulation amplitudes and activated muscle groups – Stimulation frequency: 2.2 Hz

Figure 2.2A illustrates the four different groups of muscle recruitment patterns as described in Methods under "*Data analysis – Data based on incremental pulse amplitudes*". The left margins of the black bars of the vertical-bar diagrams indicate the mean threshold voltages eliciting quadriceps (Q) and triceps surae (TS) responses at 2.2 Hz in the subjects 1–15. In group 1, quadriceps had a rather high mean threshold of 7.9 V, while triceps surae could not be recruited at stimulus strengths up to 10 V. In this group the lumbar paraspinal trunk muscles responded to the stimulation on average at 4.5 V and thus demonstrated lower response thresholds than the lower limb muscles. In group 2, the mean threshold of quadriceps was lower than of triceps surae responses (3.9 V vs. 5.9 V). Thus, similarly to group 1, stimulation was selective to a certain degree, i.e. it was possible to activate quadriceps without activating triceps surae, which required an additional increase of 51% of the stimulus strength to respond. In group 3, the whole-numbered thresholds of quadriceps and triceps surae were rather low and identical (mean 3.0 V). In group 4, triceps surae responded at lower voltages than quadriceps (2.5 V vs. 3.4 V), i.e. the recruitment order was reversed in comparison with group 2 and activation of triceps surae without eliciting quadriceps twitch responses was possible.

Note that the limited accuracy of our methodology to identify thresholds by increasing the stimulus strength in 1 Volt-steps may partially account for the "non-selective" effect of stimulation in group 3. However, stimulation was also selective to a certain degree in this group as reflected by the EMG amplitudes of the muscle responses at threshold level: in 44% of the cases classified as group 3, the mean ratio of quadriceps and triceps surae amplitudes was 33:1, in the remaining cases the ratio was 1:12. Thus, two subgroups within group 3 could be revealed, one related more to group 2, the other more to group 4.

Figure 2.2B shows the cathode levels of the four groups with respect to the vertebral body levels T10 to L1. First, the total distribution of rostrocaudal cathode positions in the subjects 1–15 is indicated (black diamonds). Then, the mean cathode level (black rectangle), the calculated average distance between the cathode positions and the mean cathode level (shaded rectangle), and the rostrocaudal range (white rectangle) within each group are illustrated.

It turns out that the four different groups – originally defined according to the recruitment order of the L2–L4 innervated quadriceps and the L5–S2 innervated triceps surae muscles – have considerably different rostrocaudal cathode levels. The most rostral cathode positions mainly belonged to the group 1, while responses elicited by the most caudal positions were recruited according to the pattern of group 4.

Mean thresholds of quadriceps responses considerably increased to more than 200% with cathode site in caudorostral direction from the group 2 to the group 1 position. Thresholds of triceps surae activation steadily increased the more rostrally the cathode was located. The lower third of the T10 vertebral body was the most rostral position from which lower limb muscle responses could be evoked at a stimulation strength of 10 V – in fact solely in the thigh muscles. From the upper third of the vertebral body T10 none of the studied lower limb muscles could be activated with strengths up to 10 V (see the cathode position marked by the most rostral black diamond in the chart displayed in Fig. 2.2B). At this rostral level segmental twitch responses could be elicited in the lumbar paraspinal trunk muscles at a moderate threshold of 5 V.

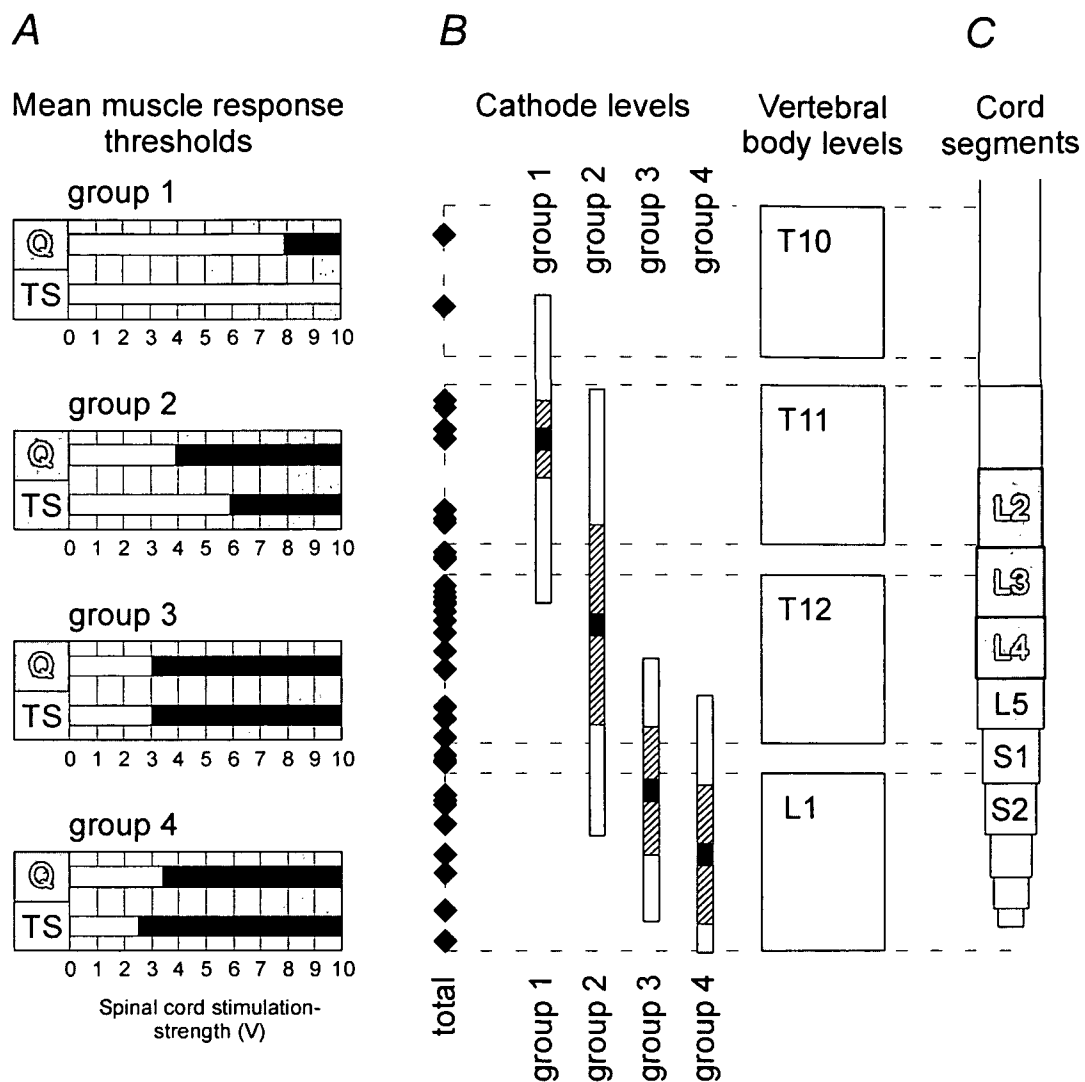


Figure 2.2 Mean response threshold voltages and corresponding cathode positions of quadriceps (Q) and triceps surae (TS) of the subjects 1–15

A, the threshold voltages are indicated by the left margins of the black bars. In group 1, Q was recruited but not TS with strengths up to 10 V ($n = 8$). In group 2, the thresholds were lower for Q than for TS ($n = 47$). In group 3, the whole-numbered thresholds were identical for both muscle groups ($n = 9$). In group 4, they were higher for Q than for TS ($n = 11$). *B*, the total distribution of cathode positions relative to vertebral body levels T10–L1 (black diamonds) are indicated, and for each group the mean cathode level (black rectangle), the averaged distance between the cathode positions and the mean cathode level (shaded rectangle), and the rostrocaudal range (white rectangle) are shown. *C*, spinal cord model adapted from Lang (1984a) showing average segmental lengths and positions relative to the vertebral body levels T10–L1 shown on the left side. The designated segments L2–L4 and L5–S2 provide innervation of Q and TS, respectively.

The lowest whole-numbered threshold of lower extremity muscle responses was 1 V and was found in three subjects (subjects 1, 4, and 8), all with cathodes at L1 vertebral body levels, corresponding to the average position of the conus medullaris. In a single case (subject 4, cathode at the lower third of the vertebral body level L1), muscle twitch

thresholds had been identified by increasing the stimulus strength in 0.1 V-steps. The threshold for eliciting CMAPs in triceps surae was as low as 0.5 V.

Figure 2.2C gives an average model of spatial relations between the spinal cord segments L2–S2 and the rostrocaudal vertebral body levels introduced in Fig. 2.2B. This model can be used to get information about the cathode levels relative to lumbosacral cord segments. The segmental innervations of quadriceps (L2–L4) and triceps surae (L5–S2) are indicated by different shades of gray. Comparison between Figs. 2.2A–C demonstrates the following mean segmental cathode levels for the groups with different muscle recruitment orders – group 1: rostral to L2, group 2: L3/L4, group 3: S1/S2, group 4: caudal to S2.

Figure 2.2 exposes a strong relationship between the rostrocaudal position of the cathode relative to spinal cord segments and the recruitment order of quadriceps and triceps surae twitch responses. The cathode level and the stimulation amplitude determine a segmental-selective recruitment of lower limb muscles.

Muscle responses to trains of stimuli

Figure 2.3A displays 0.5-second traces of induced tonic EMG activity of the antagonistic muscles quadriceps (Q) and hamstrings (H) derived from subject 2. The active cathode was at upper T12 vertebral level (estimated L3/L4 segmental level), stimulation strength was 6 V and left unchanged when switching frequencies from 16 Hz to 22 Hz. At both frequencies, each single pulse of the sustained train of electrical stimuli, marked by black diamonds in the figure, elicited a separate CMAP. Successive stimuli evoked alternately strong and weak responses. At 16 Hz, strong responses occurred simultaneously in Q and H, while increasing the stimulation frequency to 22 Hz changed the pattern of the muscle activity. In this case, each stimulus pulse induced a strong response in one muscle and a weaker one in its antagonist indicating mutual influences of the responses. The CMAP amplitudes were subject to a modulatory influence and were not solely governed by the stimulation strength, like in case of 2.2 Hz stimulation. Moreover, the trains of stimulus-evoked CMAPs of a given muscle had one of only two different characteristic types of EMG shapes.

Mutual influence of responses in different muscle groups could not be observed only in the time base of single responses. Figure 2.3B shows surface EMG recordings from the right quadriceps (Q), hamstrings (H), tibialis anterior (TA) and triceps surae (TS), and position sensor recordings showing knee flexion/extension movements (KM – knee movement). The data were derived from a complete paraplegic (subject 17). The rostrocaudal cathode site was at the T12-L1 intervertebral level, the segmental level was estimated as L4/L5. Stimulation parameters were 9 V and 30 Hz and constant during the continuous recording. The EMG traces demonstrate alternating phases of burst-style activity in the lower limb muscles. The corresponding position sensor trace confirms that the induced muscle activity led to actual flexion/extension movements of the lower limb. Deflection up indicates flexion and deflection down extension of the lower limb, the range of knee movement (rotation of the longitudinal axis of the thigh around the hip) was about 65°.

To identify whether individual responses to single pulses within the applied stimulus train were reflected in the EMG output pattern, the first of the burst-style phases of quadriceps is displayed in extended time scale at the bottom of Fig. 2.3B. Corresponding stimulus artifacts derived from the paraspinal muscle indicate the onset of the stimulus pulses. It can be seen that each pulse of the stimulus train triggered a separate CMAP. Thus, the burst-

style phase consisted of stimulus-triggered CMAPs that were subject to well-defined amplitude modulations resulting in a burst-like shape of the EMG activity.

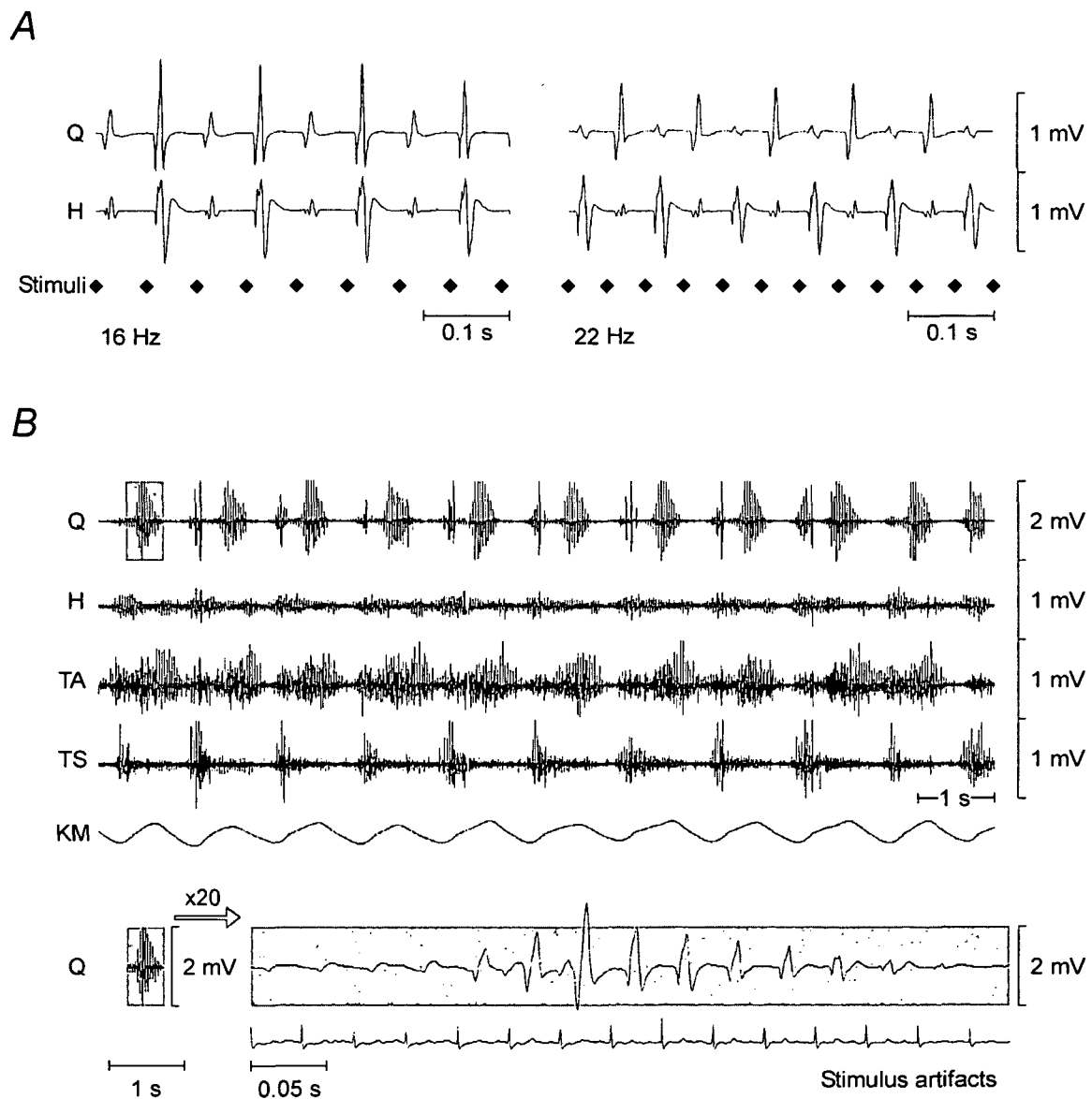


Figure 2.3 EMG responses to trains of stimuli showing modulations of amplitudes

A, 0.5 seconds of induced EMG activity of quadriceps (Q) and hamstrings (H), single pulses of the sustained electrical stimulation (black diamonds). The cathode was at upper T12 vertebral level, stimulation strength was 6 V, and frequency was changed from 16 Hz to 22 Hz (subject 2). *B*, surface EMG recordings from the right quadriceps (Q), hamstrings (H), tibialis anterior (TA), and triceps surae (TS); position sensor traces demonstrating flexion/extension movements of the knee (KM). The cathode was at the T12-L1 intervertebral level. Stimulation parameters were 9 V and 30 Hz (subject 17). The first "burst-style" phase of quadriceps marked by gray background is shown in extended time scale on the bottom of the original EMG. Note that some peaks of the quadriceps activity displayed in the original trace are cut at ± 1 mV.

A discussion of the great variety of responses to epidural stimulation with patterned amplitude modulations is beyond the scope of the present study. Figure 2.3 is to demonstrate that at higher stimulation frequencies the amplitudes of the evoked EMG

responses were not determined solely by the stimulus strength. Applying trains of electrical stimuli with constant parameters to the posterior lumbosacral cord structures at 5–50 Hz yielded well-defined EMG patterns of amplitude modulation in lower limb muscles. Moreover, it turns out that the different tonic, patterned tonic (Fig. 2.3A) and rhythmic EMG activity and even "burst-style" phases (Fig. 2.3B) consist of separate stimulus-triggered CMAPs.

Relationships between cathode levels, stimulation amplitudes and activated muscle groups – Stimulation frequencies: 2.2, 25, 50 Hz

Figure 2.4A displays approximately 16 seconds of surface EMG recordings from the left lower limb muscles along with a recording of a position sensor measuring flexion/extension movements of the knee (subject 16). The effective cathode was located at upper lumbar segmental level. The stimulation frequency was 25 Hz and constant, while the stimulation strength was increased in 0.5-Volt steps during continuous recording. At the threshold level of 3.5 V, low amplitude EMG activity was induced in quadriceps. At 4 V the quadriceps activity increased in amplitude and additionally hamstrings responses of smaller amplitudes were induced. A further increase in stimulation strength to 4.5 V elicited faint activity in the tibialis anterior and triceps surae muscles. The EMG activity of the previously recruited quadriceps muscle decreased, while hamstrings showed approximately reciprocal temporal changes in EMG amplitudes. This is substantially different from the findings derived from EMG data of stimulus-evoked responses at 2.2 Hz, where CMAP amplitudes showed progressive increase with increasing stimulus strength. Another increase in stimulation amplitude to 5 V induced rhythmic EMG activity in the recruited lower limb muscles and flexion/extension movements. The sustained stimulus train at 25 Hz and strengths of 3.5–4.5 V induced a tonic EMG activity consisting of separate, frequency following single EMG responses. Also at 5 V during the phases of burst-style activity, which alternated with phases of inactivity/low activity, each pulse of the stimulus train triggered a single CMAP.

Figure 2.4A demonstrated that once a muscle group was recruited by the epidural stimulation, the EMG amplitudes of the stimulus-evoked CMAPs elicited at 25 Hz were not solely governed by the stimulus strength. However, the muscle recruitment sequence was quite similar to the one at the lower stimulation frequency of 2.2 Hz. The EMG activity displayed in Fig. 2.4A was evoked by an epidural electrode with a cathode located at the T11-T12 intervertebral level, thus similar to the mean rostrocaudal cathode level of the group 2 introduced in Fig. 2.2. It also shows the characteristic muscle recruitment order of group 2. This finding prompted us to perform the same analysis as conducted for Fig. 2.2 for higher stimulation frequencies.

In Fig. 2.4B the recruitment properties of sustained epidural stimulation at 2.2 Hz, 25 Hz and 50 Hz are compared. Less data were available for this analysis than for the one presented in Fig. 2.2. In all available cases the rostrocaudal positions of the effective cathodes were located between the T11-T12 intervertebral level and the lower third of the L1 vertebral body. All cases could be classified into two groups with characteristic recruitment order of the quadriceps and triceps surae muscles for stimulation with 2.2 Hz – group 2' and group 3'. In group 2', quadriceps responded at lower stimulation strengths (mean 3.1 V) than triceps surae (4.5 V). The mean cathode level of group 2' was located more caudally than that of group 2 (Fig. 2.2), since no data were available from subjects with cathodes positioned rostrally to the T11-T12 intervertebral level for this retrospective

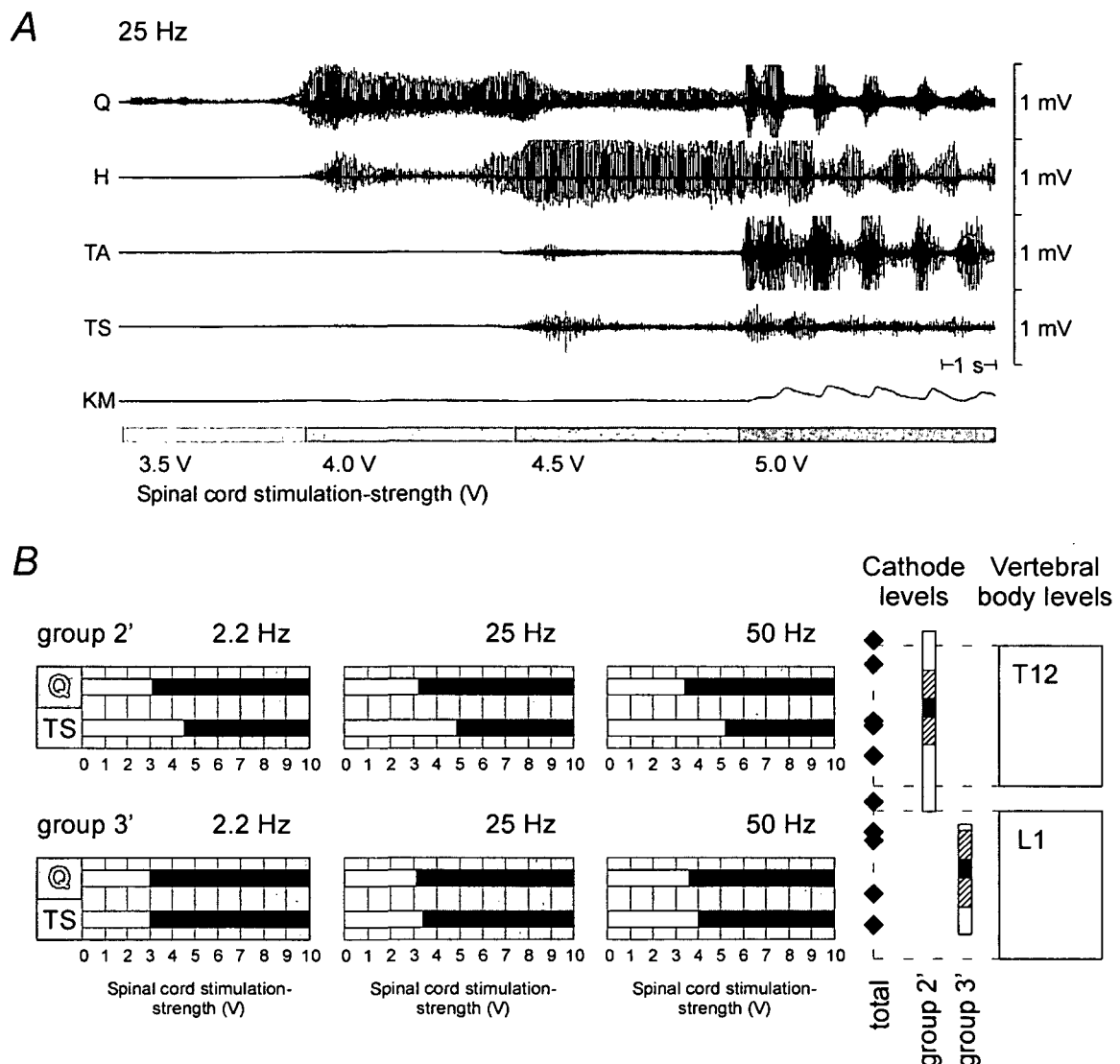


Figure 2.4 Muscle recruitment properties of sustained epidural stimulation

A, continuous surface EMG recordings from the left quadriceps (Q), hamstrings (H), tibialis anterior (TA), and triceps surae (TS); position sensor traces measuring flexion/extension movements of the knee (KM). The cathode was at the T11-T12 intervertebral level. The stimulation frequency was 25 Hz, stimulation strength was intensified in 0.5-Volt increments from 3.5 V to 5 V (subject 16). *B*, mean thresholds of quadriceps (Q) and triceps surae (TS) responses to stimulation frequencies at 2.2, 25 and 50 Hz. Data were derived from subjects 1, 2, 5, 7, 10, 12, 13 and 16. Cases were classified in groups 2' and 3' according to characteristic recruitment orders, the corresponding mean vertebral cathode levels of the two groups are shown on the right side of the figure.

analysis to contribute to the calculated mean value. Increasing the frequency of the sustained stimulation in the same subjects and for the same cathode positions resulted in higher muscle response thresholds for all muscle groups. This was mainly due to the fact that EMG activity generally decreased in amplitude at higher stimulation frequencies. When the EMG activity elicited at the threshold level for stimulation at 2.2 Hz were of low amplitudes, it could frequently not be evoked at all at 25 Hz or 50 Hz, unless the stimulation strength was increased. No single case was found where response thresholds

became lower when stimulation frequency was increased from 2.2 Hz to 25 or 50 Hz. Moreover, rhythmical flexion/extension movements were never induced at stimulation voltages less than the strength required to induce twitch responses in both quadriceps and triceps. The recruitment pattern of this group 2' was independent of the stimulation frequency. The ratios of the quadriceps and triceps surae thresholds were 1:1.45, 1:1.53 and 1:1.53 for stimulation at 2.2 Hz, 25 Hz and 50 Hz, respectively. The same ratio was 1:1.51 for the cases classified as group 2 in Fig. 2.2.

In group 3', quadriceps and triceps surae were recruited at the same stimulus strength (mean 3.0 V) when stimulation frequency was 2.2 Hz. The mean cathode level was somewhat more caudally than for group 3 (Fig. 2.2). As in the case for group 2', thresholds increased at stimulation frequencies of 25 Hz and 50 Hz. The ratios of the quadriceps and triceps surae thresholds were 1:1 at 2.2 Hz and 1:1.10 and 1:1.11 for stimulation at 25 Hz and 50 Hz, respectively.

In summary, epidural stimulation could elicit muscle activity in response to frequencies of 2.2, 25, and 50 Hz. At 25 and 50 Hz, CMAP amplitudes of induced activity did not increase systematically with increasing stimulus strengths as was seen in case of 2.2 Hz stimulation. The thresholds for initiation of muscle activity at 25 and 50 Hz were higher than for evoking single twitch responses to 2.2 Hz stimulation. Stimulation with higher frequencies and also with parameters which induced coordinated flexion/extension movements in the lower limbs showed the segmental-selective recruitment of muscle responses, as demonstrated for 2.2 Hz stimulation.

Stimulation of neuronal structures at the level of the cathode

Due to the dorsomedial position of the epidural electrode, the sensory afferents in the posterior roots and their axonal branches in the posterior columns are the largest fibers closest to the cathode. These "dorsal root fibers" and "dorsal column fibers" – which are part of the same afferent fiber system – are the most apparent among the various possible neural targets. To address the question whether our findings of segmental-selective muscle activation that depended on the segmental cathode level can be explained by stimulation of posterior root or column fibers, we established a three-dimensional computer model of electric potential distributions in the spinal cord and its surrounding tissues, generated by the epidural electrode. The spatial distributions of calculated fields were then compared with the topographic relationships between fibers of different segmental origins in the posterior roots and columns.

The computed isopotential lines in Fig. 2.5A illustrate how a field generated by a bipolar epidural electrode placed over the upper lumbar cord, penetrates the dorsal columns in a transversal plane at the level of the cathode. The isopotential lines are not circular around the electrode as would be expected in a homogeneous medium. The potential distribution spreads in accordance with the geometry and electric conductivities of the anatomical structures around the electrode. Initially the isopotential lines are rounder, but then become flatter as they enter the dorsal columns as a consequence of the higher electric resistance of the spinal cord compared to the cerebrospinal fluid. In the dorsal columns, the isopotential lines are perpendicular to the median septum. The direction of current flow is perpendicular to the isopotential lines. The current density is inversely proportional to the distance between the isopotential lines and proportional to the conductivity of the medium. The transverse electric conductivity of the white matter is about 20 times lower than that of the

cerebrospinal fluid (Geddes & Baker, 1967; Holsheimer, 2002) and restricts current flow into the spinal cord. Consequently in ventral direction the current density is reduced markedly when entering the dorsal columns.

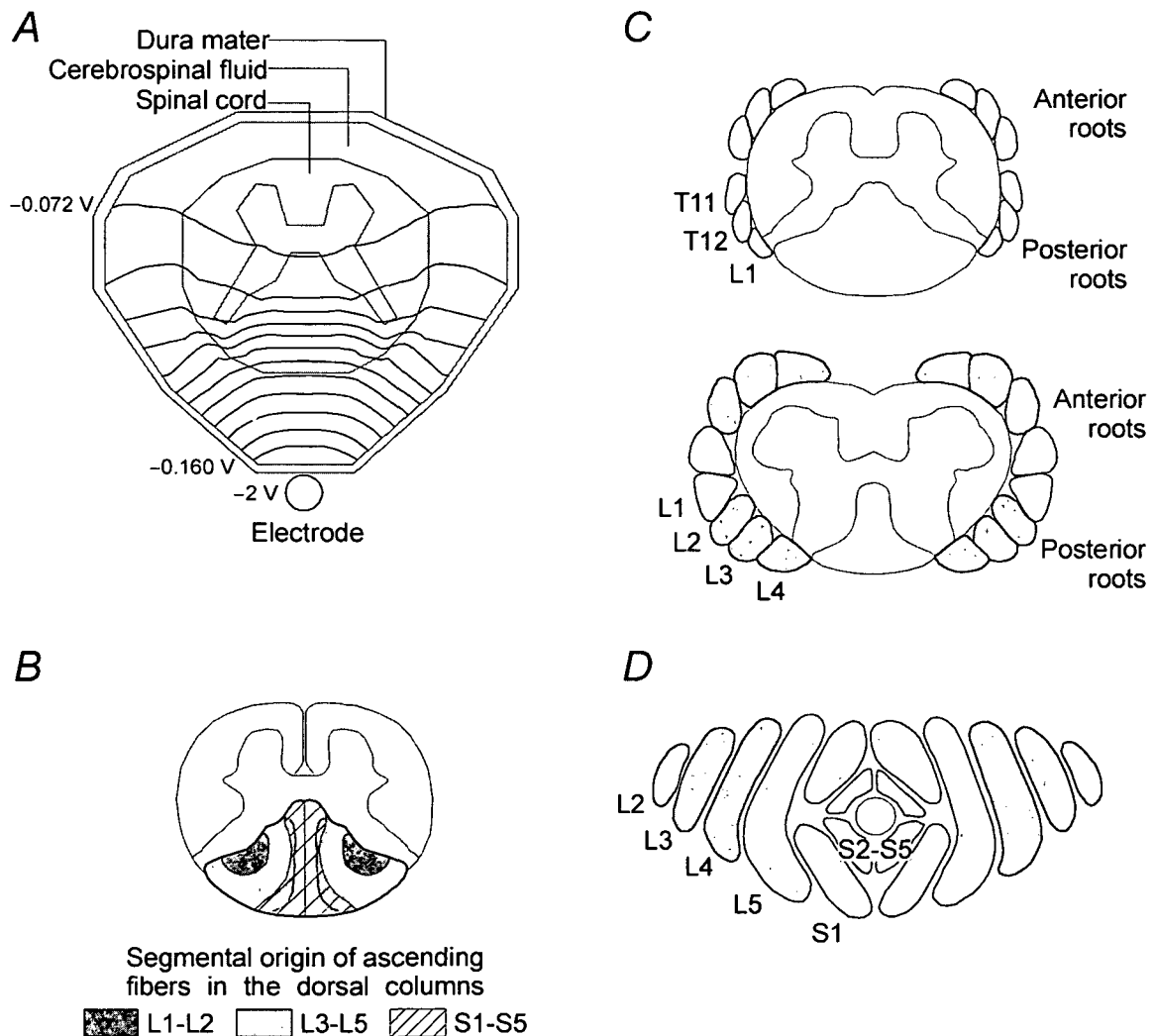


Figure 2.5 Upper lumbar cord stimulation (computer model), topography of posterior columns, and cross-sectional anatomy of spinal roots (drawing)

A, transverse potential distribution at the level of the cathode, generated by a bipolar electrode with a potential difference of 4 V between the two active contacts ($-2/+2\text{ V}$). Isopotential lines between -0.072 V and -0.160 V are presented in 0.008 V increments. The compartments surrounding the dura which were included in the computer model are not shown. *B*, cross-section of a human L1 cord segment outlining the topographic relationships between long ascending axon branches of different segmental origins in the posterior columns (adapted from Smith & Deacon, 1984). *C*, schematic diagrams of cross-sections of spinal cord and nerve roots at the L1 (top) and lower L4 segmental levels and (*D*) at the level of the conus medullaris (adapted from Wall *et al.* 1990).

Fig. 2.5*B* maps the organization of dorsal column fibers at the L1 cord level based on their segmental origins. A certain degree of segmental lamination is present, but with partial overlapping of fibers from adjacent segments. The medial positions of the dorsal columns

are occupied by fibers arising from the most caudal posterior root fibers, whereas fibers originating from more rostral levels join laterally. At a given spinal cord level ascending projections of posterior root fibers of segments corresponding to that level and caudal levels are present in the dorsal columns.

By comparing Fig. 2.5A with 2.5B, the isopotential lines turn out to be rather perpendicular to the segmental organization in the dorsal columns. Consequently, a large set of dorsal column fibers of different sacral and lumbar origins are exposed to a given voltage value (isopotential line) in a non-selective way. Stimulation of dorsal column fibers of specific segmental origins – which is essential for a segmental-selective recruitment of lower limb muscles – would require the presence of factors at the cathode level that result in different excitation thresholds for dorsal column fibers of different segmental origins. Such discrete differences, however, do not exist at lumbar cord levels (see *Muscle responses to epidural lumbosacral cord stimulation are initiated in the posterior roots* in the Discussion).

Lumbosacral segments have long spinal roots that follow rostrocaudal trajectories on the way to their appropriate intervertebral exit levels. These long spinal roots are immersed in the well-conducting cerebrospinal fluid and form a peripheral rim around the lumbosacral cord. Figure 2.5C shows a schematic representation of the cross-sectional anatomy of the spinal cord and roots at the L1 (upper figure) and lower L4 segmental levels (adapted from Wall *et al.* 1990). The multifascicular anterior and posterior roots are organized in separate root layers. At a given segmental level only afferents of segments corresponding to that level and of adjacent rostral segments are present in the posterior roots. Different posterior root layers are organized in a rather posteromedial-anterolateral direction, with the roots of the most rostral segments lying laterally. At the L1 segmental level the spinal cord is flanked only by the T11, T12 and L1 nerve roots. Roots of more rostral segments have already exited the dural sac. At the lower L4-level the cord is surrounded from the first through the fourth lumbar nerve roots. Most of the circumference of the cord is covered by the roots.

The cerebrospinal fluid has the highest electrical conductivity of the relevant anatomic structures surrounding the epidural electrode. Fig. 2.5A demonstrates that the isopotential lines in the cerebrospinal fluid are almost perpendicular to the borders of this layer. In a transverse section, in the dorsal cerebrospinal fluid the current spreads anterolaterally perpendicular to the isopotential lines. (Note that the main direction of the current is longitudinally towards the anode). The current density is highest in the cerebrospinal fluid in the vicinity of the electrode and decreases with increasing anterolateral distance from the electrode. Due to the quite lateral positions and entry points of upper lumbar posterior roots into the cord (upper part of Fig. 2.5C), thresholds for posterior root stimulation can be expected to be lower at more caudal spinal cord levels where the posterior roots are located more dorsomedially (lower part of Fig. 2.5C).

More caudally the spinal cord diminishes in size and the nerve roots are the predominate neural structures. The topographic relationship between the roots of different segments at the lower L1-vertebral level is depicted in Fig. 2.5D (Wall *et al.* 1990). All afferent fibers innervating the lower limb muscles pass the level of the shown cross-section, some belonging to cord segments situated several centimeters rostral to that level. The posterior and anterior roots of the L2–L5 segments have come together and form organized posteroanterior layers. Roots of more caudal segments are located medially and encircle the terminal spinal cord. Interpretations derived from Fig. 2.5A cannot be directly applied at these levels. However, the geometrical and electrical situation is quite simple and thus

allows qualitative conclusions. Considering that all fibers passing the level of the cross-section have trajectories mainly oriented in rostrocaudal direction, different thresholds will be predominantly determined by different cathode-fiber distances (for a given fiber size). S1-posterior root fibers can be expected to have lowest thresholds, while L4, L3, and L2 roots, situated at progressively increasing anterolateral distances from a dorsomedially positioned cathode, respectively, will be recruited only at higher stimulus strengths.

Stimulation of neuronal structures distant from the cathode level

Fig. 2.6A shows the computed electric potential distribution within the dural sac generated by a bipolar electrode in a midsagittal plane and also in a transverse plane at the level of the rostral contact. The potential difference between the two contacts is 1 V (± 0.5 V). The generated potential distribution reflects the high electrical conductivity in rostrocaudal direction of the structures contained in the dural sac. This is due to the high conductivity of the cerebrospinal fluid and its elongated geometry, and due to the anisotropic spinal white matter which has an approximately 7–8 times higher conductivity in axial than in transverse direction.

Fig. 2.6B illustrates the extensive spread of the cathodal field, which is represented by an arbitrary isopotential line (-0.1 V), in caudal direction in a midsagittal plane. The caudal contact is operated as a cathode, the cathode level corresponds to the average group 1 level of Fig. 2.2. The stimulation amplitude is increased from 5 V to 10 V. The segments L2–L4 are displayed in dark gray, L5–S2 in light gray. At an amplitude of 5 V, the isopotential line penetrates only a small portion of the spinal cord in the proximity of the cathode. In caudal direction the isopotential line ranges to the center level of the L2-cord segment in the displayed standard geometry – and covers the associated posterior roots. By increasing the strength to 10 V, additional caudal cord segments and posterior roots are exposed to the given potential value (or to more negative potential values). The isopotential line ranges down to L4-segmental level.

Fig. 2.6C shows a schematic representation of the geometrical relations of the lumbosacral cord and the trajectories of the L1, L3, and L5 posterior roots. The figure is to make obvious that posterior root fibers of different segments enter the spinal cord at levels that are spatially separated in rostrocaudal direction. Comparison of Fig. 2.6B with 2.6C implies the possibility of a segmental-selective recruitment of posterior roots from a rostral cathode position, given by the extent of the current spread in caudal direction.

DISCUSSION

In the present study we consider which neural structures were directly activated by epidural lumbar cord stimulation that gave rise to the described muscle responses. To address this question we combined information on real patient data with calculated electric potential distributions and consolidated knowledge about patterns of segmental organization of the posterior columns and roots. Our computer model is based on well established volume-conductive properties of the spinal cord and its surrounding structures (Coburn & Sin, 1985; Holsheimer, 1998; Rattay *et al.* 2000). Similar qualitative results of spatial distributions of macroscopic fields generated by epidural electrodes could also be obtained from much simpler models involving concentric cylinders with different electric

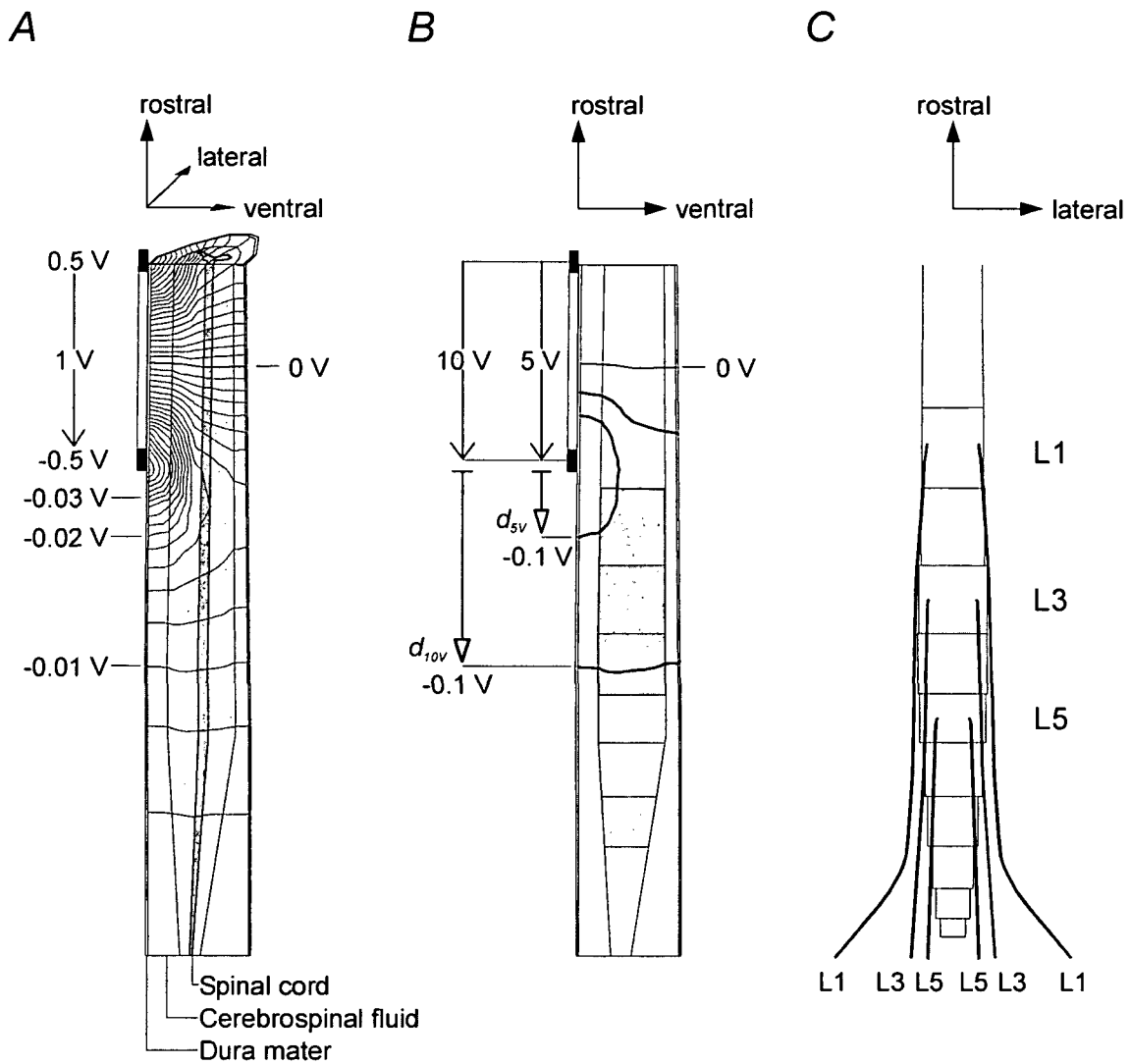


Figure 2.6 Potential distribution in a midsagittal plane (computer model) and dorsal root trajectories (drawing)

A, computed potential distribution within the dural sac in midsagittal and transversal plane generated by a bipolar electrode with 1 V potential difference between the two contacts. *B*, by increasing the stimulation amplitude, the cathodal field represented by an isopotential line of arbitrary strength (-0.1 V) penetrates more and more cord segments. The cord segments L2–L4 and L5–S2 are indicated by dark and light gray areas, respectively. *C*, sketch of the L1, L3, and L5 dorsal root trajectories (back view).

conductivities, the center one being a poorly conducting, anisotropic compartment representing the spinal cord, surrounded by a well conducting cerebrospinal fluid compartment and outer compartments with higher electric resistivities (Holsheimer, 2002).

At any instant a neuron has some threshold, which external electrical excitation must exceed to initiate an action potential. This threshold value is determined by the electric conductivity of the anatomic structure in which the nerve is situated and the nerve trajectory and orientation with respect to the stimulating electrode. In addition, the threshold is related to the electrode-neuron distance and inversely related to the nerve fiber diameter. The epidural electrode can, in principle, affect any neural structures within the spinal cord and

spinal roots if the stimulus amplitude is high enough. However, since applicable stimulation strengths are limited (by intensities which cause discomfort to the subject or by the maximum output of the pulse generator) the large diameter axons within the posterior roots and their axonal branches in the posterior columns are the primary potential targets of stimulation for a dorsomedially positioned epidural electrode. Direct activation of motoneurons and thereby bypassing the spinal cord can be ruled out because this could not account for the complex and patterned EMG responses to sustained stimulation with constant parameters (Figs. 2.3 and 2.4A). Moreover, the analysis of CMAPs induced by pairs of stimuli of equal strength delivered to the posterior structures of the lumbosacral cord at different intervals demonstrated maximum absolute refractory periods of the responses of up to 47.5–62.5 ms (Minassian *et al.* 2004). In contrast, motor responses follow frequencies of up to 100 Hz when elicited by ventral epidural spinal cord stimulation that most probably activates alpha-motoneurons within the ventral roots or in the ventral horn (Struijk *et al.* 1993a; also see Dimitrijevic, 1983). It was shown to be unlikely for epidural spinal cord stimulation with dorsal electrode placement that neural structures other than fibers within the posterior roots or superficial posterior columns are directly activated (Holsheimer, 2002) or contribute to muscle activation (Hunter & Ashby, 1994). Therefore we will first discuss whether low-frequency stimulation (2.2 Hz) of posterior roots or columns can explain the segmental-selective effect of the stimulation and the EMG features of the responses as described in the present study. We will then expand our discussion on the origin and nature of the more complex stimulus-evoked responses at higher frequencies.

Muscle responses to epidural lumbosacral cord stimulation are initiated in the posterior roots

The EMG signals associated with the twitch responses to stimulation at 2.2 Hz and 1–10 V were stimulus coupled and of short latency (Figure 2.1, Table 2.2), equal to about half the latencies of phasic stretch reflexes of the respective muscle groups. At constant stimulation strength, the EMG shapes of successively elicited CMAPs remained constant. When stimulation strength was increased above the threshold level of a given muscle, additional motor units were recruited. The corresponding superimposing EMG responses overlapped in time with the CMAP elicited at lower strength. The resultant signal mainly demonstrated an increase in amplitude and only minor variation in shape or duration. No additional EMG phases of later latencies were generated.

In Figure 2.2 we demonstrated different recruitment orders of the L2–L4 innervated quadriceps and the L5–S2 innervated triceps surae muscles depending on the rostrocaudal cathode position of the stimulating electrode array with respect to spinal cord segments. In Fig. 2.5 we compared the distribution of calculated isopotential lines of the generated electric field with the topography of ascending fibers of different segmental origins. We explained that posterior column fibers from different thigh and leg muscles are non-selectively exposed to a given voltage value (compare Fig. 2.5A with B). This implies that activation of posterior column fibers with given diameter and trajectory hardly depends on the mediolateral position of the fibers (Struijk *et al.* 1992). Therefore, segmental-selective recruitment of muscle groups according to the groups 1 and 2 (Fig. 2.2) as a result of posterior column stimulation would only be possible if there are factors other than the cathode-fiber distance which determine different thresholds of fibers of different segments at a given cathode level. Feirabend *et al.* (2002) recently described in a morphometric study that at the T10/T11 cord levels the fibers in the lateral superficial posterior columns are

only 1–5% larger in diameter than those located medially. The fact that a relevant difference in size could not be demonstrated is significant because lateral and medial fiber groups are associated with different muscles (Fig. 2.5B). Feirabend *et al.* (2002) suggested that any possible differences between the stimulation thresholds of large longitudinal fibers in the median and lateral posterior columns could be related to the presence or absence of collaterals at the stimulation site (see also Struijk *et al.* 1992). However, collaterals are issued by the ascending axon branches within the posterior columns throughout the rostrocaudal levels at which the electrodes were placed in our subjects. For fibers of group Ia afferents from primary muscle spindle endings, some of these collaterals project to motoneurons and interneurons at the segmental level where the group Ia axons enter the cord via the posterior roots and some at the levels of adjacent segments. Others project to Clarke's columns, their most caudal part in man being at the L2 segmental level (Davidoff, 1989). It can be assumed that discrete differences in the factors determining the excitation thresholds of the ascending posterior column fibers of different lower limb muscles do not exist within the extent of the lumbar cord segments. Consequently, the effect of posterior column stimulation can be expected to be general rather than localized to afferent structures of any specific segmental origins. This conclusion is supported by the findings of Hunter & Ashby (1994) who demonstrated that epidural stimulation of the posterior columns at thoracic cord levels resulted in non-selective facilitation of motoneurons innervating thigh and leg muscles. Figure 2.2 further showed that excitation thresholds of muscle responses in the lower limbs increased in accordance with the caudorostral distance of the cathode from the L1 vertebral level. Feirabend *et al.* (2002) revealed that there is no significant caudorostral tapering of large posterior column fibers within the extent of a few cord segments in the human spinal cord. Stimulation of these fibers would therefore not explain the increasing thresholds associated with increasingly rostral cathode positions. The most rostral cathode levels to induce the CMAPs as described in the present study at maximum pulse intensity (10 V) were at T10/T11 vertebral levels for quadriceps and T11/T12 for triceps surae. By contrast, Guru *et al.* (1987) and Hunter & Ashby (1994) reported recruitment of thigh and leg muscles by epidural stimulation with cathodes located over the dorsum of the thoracic cord at positions as rostral as the T8–T10 vertebral levels. At these cathode levels the cord segments and corresponding roots supplying the lower limbs and particularly the calf muscles are located well below the cathode. Guru *et al.* (1987) and Hunter & Ashby (1994) attributed this muscle activity to antidromic activation of the rostral projections of primary afferents in the posterior columns that have collaterals to motoneurons. The latencies reported in their studies were generally about 6–12 ms longer than those of the comparable muscles compiled in our Table 2.2.

We conclude that the CMAPs elicited by lumbosacral cord stimulation are not related to posterior column fiber activation. Thereby, our results do not contradict the results of Guru *et al.* (1987) and Hunter & Ashby (1994). The differences of the effects of stimulation are most probably due to the different subject profiles, electrode setups and the different geometrical characteristics of the spinal cord and roots anatomy at thoracic and lumbosacral levels. The subjects included in the two studies cited above had electrodes implanted for the treatment of pain and had volitional control over the lower limb muscles. In the subjects of the present study, the lumbosacral cord was functionally completely divided from brain control. Moreover, in the studies of Guru *et al.* (1987) and Hunter & Ashby (1994) four different electrode set-ups were utilized, in most cases a fine wire cathode with an uninsulated tip was placed in the posterior epidural space and a larger disc anode at the anterior abdominal wall or embedded in the paraspinal muscles. In such an electrode set-up,

the surface area of the disc anode is much larger than the wire tip contact. This results in a smaller current density and less voltage drop near the anode. A larger portion of the total stimulation voltage is therefore available under the cathode, hence a stronger stimulating effect of this electrode design in the vicinity of the cathode. There are also significant differences of the anatomy between the thoracic and the lumbosacral spinal cord. Because of the disparity in length between the spinal cord and vertebral column, the spinal roots from lumbar and sacral segments have much longer distances to travel prior to reaching their respective foramina of exit. Whereas cervical and upper thoracic roots are situated nearly perpendicular to the cord, lower thoracic, lumbar, and sacral ones enter and leave the cord at increasingly more oblique angles. Most part of the circumference of the lower lumbar and sacral cord is covered by spinal roots (Wall *et al.* 1990). For epidural stimulation, thresholds of fibers within the lumbosacral cord will presumably be increased due to this poorly conducting "root-layer". Finally, the entry points of lower lumbar and sacral posterior roots into the spinal cord are situated more medially than of more rostral ones and are thus nearer to a dorsomedially positioned cathode (Fig. 2.5C). At the level of the conus medullaris some posterior roots are closer to a dorsomedially positioned cathode than the posterior column (Fig 2.5D), which is in contrast to thoracic cord levels. The diameters of posterior root fibers, which are larger than that of corresponding posterior column fibers at any segmental level, add to their lower excitation thresholds (Ishizuka *et al.* 1979; Struijk *et al.* 1998; Holsheimer, 2002).

Further indication that stimulation of posterior column fibers is non segmental-selective comes from the application of spinal cord stimulation in chronic pain control based on reports on paresthesia distributions of patients with intact sensory functions. In this situation, medially placed electrodes elicit a widespread distribution of paresthesiae in body areas at the spinal level of stimulation and far caudally to it. This may occur even at the perception threshold (He *et al.* 1994). This widespread distribution of paresthesiae is attributed to activation of the posterior columns (Barolat *et al.* 1993). In the posterior columns at any spinal level dermatomes corresponding to that level and to more caudal levels are represented by ascending projections of cutaneous afferents. To some extent, they have similar trajectories and topographic organization as axonal branches of group Ia fibers in the posterior columns (Davidoff, 1989). The recruitment of these afferent structures turns out to be non segmental-selective even if the voltage is gradually increased in 0.1-V or 0.25-V intervals (He *et al.* 1994) – which is an approach with higher accuracy than in our study.

Beside neurophysiological studies carried out in parallel to clinical programs, computer modeling of epidural spinal cord stimulation is another method appropriate for obtaining a better knowledge of the immediately evoked electrophysiological phenomena (Coburn 1980; Holsheimer 1998). Theoretical studies of the effect of epidural stimulation on posterior roots have shown that geometric and electric factors result in "hot spots" (low-threshold sites) for extracellular electrical excitation at the sites where posterior root fibers enter the spinal cord (Coburn, 1985; Struijk *et al.* 1993; Rattay *et al.* 2000). These low-threshold sites are created by a sudden change of the generated potential distribution along the afferent fibers – i.e. of the extracellular potential – at the interface between spinal rootlet and cord owing to the different electrical conductances of the cerebrospinal fluid and the spinal cord (Geddes & Baker, 1967; Holsheimer, 2002). The bend of the posterior root fibers as they enter the cord additionally contributes to the inhomogeneity of the extracellular potential. These low-threshold sites were also recognized by studies of diagnostic methods involving lumbosacral nerve root stimulation (Troni *et al.* 1996).

We therefore suggest that the muscle responses to epidural stimulation of the posterior lumbar cord are initiated in the posterior roots, since posterior column fiber stimulation could not explain the motor effects described in the present study. Lumbosacral posterior root fibers entering the cord at the level of the cathode or up to about 2 cm caudally (calculated maximum effective range of the applied bipolar electrode at 10 V, see Rattay *et al.* 2000) can be recruited at their hot spots where the fibers enter the spinal cord. If the cathode is located at L2–L4 segmental levels, the posterior roots containing afferents of the lower limbs can be recruited in a segmental-selective way at their hot spots. At threshold stimulation strength, the largest posterior root fibers will be activated at the level of the cathode (L2–L4). Increasing the stimulation strength will not only recruit additional posterior root fibers at the cathode level, but also posterior roots of the more caudal segments L5 and S1 at the hot spots due to current spread in this direction. This mechanism can explain the segmental selective muscle activation for cathode positions corresponding to the levels of group 2 of Fig. 2.2 (consider also Fig. 2.1B). For cathode positions rostral to the L2 cord level (group 1 of Fig. 2.2), CMAPs can still be induced in the L2–L4 innervated thigh muscles. However the current spread in caudal direction is not sufficient to activate even more caudally situated posterior roots (compare with Fig. 2.6B). These structures are beyond the effective caudal range of the used bipolar electrode. Note that even the L2–L4 innervated quadriceps is recruited at quite high thresholds by group 1-positioned cathodes. This is supported by the very lateral sites of the entry points of the posterior roots into the spinal cord at these levels (Fig. 2.5C).

For caudally located cathodes at levels of the conus medullaris, lumbosacral posterior root fibers which enter the cord rostrally to the cathode will be excited at the level of the cathode (Rattay *et al.* 2000), where their trajectories are primarily oriented in rostrocaudal direction. Lumbosacral segments have long spinal roots of up to 16 cm length (Sunderland, 1976; Lang, 1984b) to reach their appropriate intervertebral exit levels. Due to the high electric conductivity of the cerebrospinal fluid surrounding the roots and the proximity of the descending root trajectories to the posterior border of the dura mater, and thus to the epidural electrode, posterior root fibers that enter the cord well rostrally to the cathode can be recruited at the level of the cathode. At lower L1 vertebral levels, all segments with afferent fibers coming from the lower limb muscles are represented by posterior root fibers and are organized in layers in a posteromedial-anterolateral direction (Fig. 2.5D and 2.6C, see also Wall *et al.* 1990). Due to an evidently greater distance of the L2–L4 posterior roots than of the S1 and L5 ones to a dorsomedially positioned cathode, it is plausible that stimulation of these structures can explain the reversed recruitment order of group 4 in comparison with group 2.

Since stimulation with a cathode at group 2-position resulted in lower thresholds of L2–L4 posterior roots and at group 4-position in lower L5–S2 thresholds, there must be some rostrocaudal cathode position between these two different cathode levels, where thresholds of posterior roots of the adjacent segments L3–L4 and L5–S1 are about equal. These cases constitute the group 3 in Fig. 2.2. Naturally, accurate threshold identification would reveal minor differences in thresholds also in these cases.

Posterior Roots Muscle Reflex Responses

We have presented evidence that the posterior roots are the input structures which led to the CMAPs elicited at 2.2 Hz. Feline (Lloyd, 1943) and human (Magladery *et al.* 1951) studies

showed that electrically induced afferent volleys via the lowest-threshold fibers of the posterior roots caused monosynaptic reflex discharge of motoneurons. Since the fibers with the largest diameter have the lowest thresholds, the direct effects to the motoneurons are mediated by group-Ia fibers from primary muscle spindle endings. Magladery *et al.* (1951) demonstrated that activation of only a portion of the low-threshold afferent fibers was sufficient to produce a massive synchronous reflex outflow through the anterior roots. Lloyd (1943) showed that monosynaptic group-Ia reflex discharges almost reached their full value even with considerably submaximal posterior root volleys. Major intensification of later, multineuron-arc discharges occurred only after the stage of maximum monosynaptic discharge had been reached. This stage was not reached in our study due to the limited stimulation strengths. The central latencies of pure cutaneous nerve-anterior root reflex discharges are about 2 ms longer (Lloyd, 1943). These discharges are irregular and last longer than monosynaptic group-Ia reflex discharges. The CMAPs elicited at 2.2 Hz as described in our results showed mainly increased amplitudes at suprathreshold strengths, while no other later EMG phases were built up.

We infer that the twitch responses elicited in the present study by epidural stimulation at 2.2 Hz were predominantly due to activation of large group-Ia fibers within the posterior roots with subsequent recruitment of motoneurons through monosynaptic connections in the spinal cord. This mechanism can explain the short and constant latencies of the registered muscle responses (Fig. 2.1, Table 2.2). The responses elicited at 2.2 Hz are indirect and are reflexes in origin. They are the physiological equivalents of the H-reflexes of the corresponding muscles. Instead of being elicited by electrical stimulation of low-threshold afferents in mixed peripheral nerves the reflexes induced by epidural stimulation are initiated in the posterior roots. It has been previously demonstrated in able-bodied adult individuals that the soleus H-reflex can be evoked by percutaneous electrical stimulation (Zhu *et al.* 1998) of the proximal S1 nerve root or by needle electrodes inserted into epidural space at cauda equina levels (Ertekin *et al.* 1996). Troni *et al.* (1996) reported that soleus H-reflexes can be elicited by high-voltage percutaneous stimulation at different rostrocaudal levels over the lumbar vertebral column. They suggested that posterior roots were activated by the stimulation procedure precisely at the points where they enter the spinal cord. It was also reported that by stimulation of the lumbosacral roots and the cauda equina responses of muscles other than of the soleus can be obtained (Maertens de Noordhout *et al.* 1988; Ertekin *et al.* 1996).

We conclude that the CMAPs elicited at 2.2 Hz as described in our study are reflex responses arising from a dominating input via large afferents within the posterior roots. We hereinafter refer to this type of stimulus-evoked muscle activity as Posterior Roots Muscle Reflex Responses (PRMRRs). Afferents other than group I primary afferents seem not to contribute to the reflex responses at 2.2 Hz stimulation.

Differences between Posterior Roots Muscle Reflex Responses and the H-reflex

Posterior root stimulation at lumbosacral cord levels is quite different from that of a peripheral nerve trunk. The posterior sensory roots are anatomically isolated from the anteriorly located motoneurons. The spinal cord, due to its lower electric conductivity, acts like a barrier reducing the current flow in ventral direction. Therefore, dorsal epidural spinal cord stimulation can activate posterior root fibers selectively and more completely without stimulating motoneurons (Struijk *et al.* 1993a; Rattay *et al.* 2000). This makes

strong reflex responses possible which are not reduced or blocked by electrically elicited and antidromically propagated action potentials in the α -motoneurons. Similar results can be achieved by percutaneous electrical stimulation applied to the dorsolumbar vertebral column. Troni *et al.* (1996) reported greater amplitudes of the soleus H-reflex to percutaneous stimulation of the lumbosacral roots as opposed to popliteal fossa stimulation. The authors attributed the finding of less occluded H-reflexes to the anatomical situation allowing activation of the Ia fibers in the posterior roots with smaller involvement of the motor fibers.

By stimulating the tibial nerve to elicit the soleus H-reflex, the evoked afferent volley is transmitted predominantly to a single cord segment. An epidural electrode placed at lumbosacral cord levels is in close range to posterior root fibers of different segmental origins. While a segmental-selective excitation is possible to a certain degree at low stimulation strengths, large afferents of probably all cord segments with motoneurons innervating the lower limb muscles can be activated at moderate strengths of 3–6 V for cathode positions corresponding to groups 4, 3 and 2 positions of Fig. 2.2. Thereby, afferent volleys are delivered highly synchronized bilaterally to several lumbar and upper sacral cord segments. As a crucial difference to peripheral nerve stimulation, the epidural stimulation of the posterior roots could not elicit reflex responses in a single muscle group, because each posterior root contains afferents from more than one muscle. In the present study, the recruitment of quadriceps was always accompanied by adductor-activity. For rostral cathodes (group 1 and 2 positions) the hamstrings threshold was related to the one of quadriceps, while for more caudal positions (group 4) hamstrings had generally the same threshold as triceps surae (see also Murg *et al.* 2000).

We have discussed that the reflex responses to epidural stimulation at 2.2 Hz were initiated in group Ia primary spindle afferents within the posterior roots. While there were no indications that fibers of other afferents for example, Ib afferents from Golgi tendon organs, group II secondary muscle afferents or cutaneous afferents contributed to the twitch responses to 2.2 Hz stimulation, this does not mean that some of these afferents were not activated by the stimulation.

Thresholds for eliciting paresthesiae in individuals with intact sensory functions by stimulating cutaneous afferents in the posterior columns and roots with epidural electrodes implanted for pain control applications are quite low. He *et al.* (1994) reported an average perception threshold of 1.69 V for medially placed epidural electrodes at T11–T12 vertebral levels and stimulation at a rate of 50 Hz. The lowest average threshold voltage for eliciting muscle responses to 2.2 Hz stimulation in the present study was 2.5 V for caudally located cathodes (triceps surae, group 4), the highest were 4.5 V for the most rostral cathode positions (lumbar paraspinal trunk muscles, group 1). However, direct comparison of the threshold values is difficult due to the different subject profiles and stimulation procedures of the different studies. Moreover, different electrode types were used, namely percutaneously inserted leads with cylindrical electrode design in our case, in contrast to surgical lead models with plate electrodes and insulated dorsal surfaces in the study of chronic pain management. Unlike plate electrodes with insulated backing, percutaneous electrode designs with circumferentially exposed electrode contacts allow some current to pass laterally and dorsally. Therefore, it can be expected that less current is available for spinal cord and posterior root stimulation making higher stimulation voltages necessary.

It should be considered that the thresholds for eliciting CMAPs reported by us are higher than the actual thresholds for group Ia afferents. First, the threshold voltages V_{th} obtained

by retrospectively analyzing muscle twitch data were whole-numbered. The actual thresholds are in the range between $V_{th} - 1$ Volt and V_{th} . This was confirmed by a case where thresholds had been identified with higher accuracy (subject 4). There the lowest threshold for eliciting CMAPs was as low as 0.5 V in the triceps surae muscle for a cathode located at group 4 levels. Secondly, the threshold for initiating action potentials in group Ia afferents might be lower than the stimulation strength needed to evoke an afferent volley sufficiently to result in a muscle activity which can be identified with surface electrodes.

All things considered, it is still plausible to assume that some afferents with smaller diameters than those of group I like cutaneous fibers were also stimulated directly in our subjects (Holsheimer, 2002). When repetitively stimulated at higher frequencies some of these afferents within the posterior roots might contribute to the motor output by transsynaptically recruiting central spinal structures (see below).

Posterior Roots Muscle Reflex Responses to trains of stimuli at higher frequencies

We have provided evidence that the directly, electrically stimulated structures at 2.2 Hz are axons within the posterior roots. We propose that the posterior roots were also the input structures at higher stimulation frequencies resulting in the more complex motor output patterns and step-like EMG activity as presented in Figs. 2.3 and 2.4A (see also Dimitrijevic *et al.* 1998; Minassian *et al.* 2004). Our notion is that the patterned EMG amplitude modulations are due to an integration of central PRMRR components at particular stimulation frequencies. This is achieved due to the special nature of the continuous tonic input and the connectivity of the activated large afferents with inherent spinal networks involved in gating the flow of sensory information in the spinal cord and in generating the basic locomotor rhythm. The hypothesis of activation of intraspinal structures by synaptically evoked depolarization affected by incoming afferent volleys is in contrast to the direct electrical stimulation of spinal neural circuits by the non-specific field. The latter mechanism would probably activate a highly unnatural admixture of circuits subserving many different, potentially competing functions, resulting in poorly controlled and inefficient patterns of muscle activation.

Hultborn *et al.* (1998) have emphasized that different reflex pathways have direct access to, or may even be part of, the central pattern generator (CPG) for locomotion in the cat. There are also human studies which indicate that sensory afferents interact with central pattern generating networks. Gurfinkel *et al.* (1998) used tonic peripheral afferent stimulation to elicit involuntary stepping in able-bodied individuals. They found that continuous lower limb muscle vibration gave rise to involuntary locomotion-like stepping movements in suspended legs and suggested that the non-specific afferent input induced by vibration activated central structures governing stepping movements. Herman (2002) reported that epidural stimulation of the lumbar cord can augment locomotor capabilities in an incomplete spinal cord injured individual. The author suggested that the stimulation appeared to provide modulation or amplification of neural circuits responsible for locomotion rhythm generation by segmental afferent input. It is worth mentioning that in this study of Herman (2002) electrodes were inserted into the epidural space over the lumbar spinal enlargement on either side of the spinal cord, each electrode placed 1–2 mm off the mid-line. Thereby the lateral location of the epidural electrodes provides a preferential stimulation of the ipsilateral posterior root fibers (Struijk *et al.* 1993b; Struijk *et al.* 1998). Furthermore Herman (2002) applied stimulation at amplitudes above sensory but

below motor threshold. At these rather low stimulus strengths direct activation of small spinal interneurons is unlikely.

Large diameter axons which are the proposed directly stimulated structures in the present study, can easily follow the applied frequencies of up to 25–50 Hz, the range effective to elicit stepping-like movements. Furthermore, we demonstrated that the components of the different patterned tonic (Fig. 2.3A) and rhythmic (Fig. 2.3B) EMG activity were single CMAPs. The burst-style phases during epidurally evoked stepping-like movements consisted of stimulus-triggered, separate CMAPs that were subject to well-defined amplitude modulations resulting in burst-like envelopes of the EMG activity. The CMAPs elicited at higher frequencies and during induced movements had common EMG features with the ones evoked at 2.2 Hz (Fig. 2.1), namely similar EMG potential duration, attainable amplitudes and generally, also the same constant latencies. Under certain conditions and only during burst-like phases of induced alternating flexion/extension movements, however, the CMAP latencies can be prolonged for about 10 ms as well (Minassian *et al.* 2001a,b; Minassian *et al.* 2002; Minassian *et al.* 2004). Note that this was not the case for the example presented in Fig. 2.3B. Finally, Fig. 2.4 demonstrated that the muscle recruitment properties of stimulation with 25 Hz and 50 Hz were quite similar as for 2.2 Hz stimulation. Even stimulation with frequencies effective to induce alternating flexion/extension movements in the lower limbs showed the segmental-selective muscle recruitment (Fig. 2.4A). We have provided evidence that this segmental-selectivity indicates that the stimulus-evoked muscle activity was initiated in the posterior roots. There was no single case of the studied recruitment orders at higher frequencies showing differences from the characteristic posterior root contribution. Thus, there was no data supporting that at higher frequencies structures which were immediately activated by epidural stimulation other than the posterior root fibers contributed to the initiation of the observed muscle activity. Provided that the cathode position and stimulation frequency were optimal to induce stepping-like movement (upper lumbar segmental level and 25–50 Hz), the threshold voltage for initiating stepping-like movements was never below the level sufficient to elicit twitch responses in quadriceps as well as in triceps sure at 2.2 Hz (Minassian *et al.* 2004). All studied main lower limb muscle groups were recruited by the gradually increased stimulation strength before rhythmic activity could be initiated (Fig. 2.4A). This implies that the activation of PRMRRs in the main thigh and leg muscles and thus the recruitment of lumbar and upper sacral posterior roots was an essential condition for initiation of stepping-like movements.

We suggest that the more complex, potentially functional movements of the paralyzed lower limbs induced by repetitive epidural stimulation are initiated within the posterior roots. The tonic input via the posterior roots is delivered bilaterally to several lumbar and upper sacral cord segments simultaneously. Spinal interneurons which normally receive continuous descending input from higher motor centers are deprived of supraspinal influence in the model of the lumbosacral cord completely isolated from descending control. The overall level of activity of these spinal neural circuits is now set by an evenly distributed tonic input coming from periphery. We speculate that besides exerting facilitation of motoneuron pools, the continuous stimulation organizes lumbar spinal interneurons by temporarily combining them into functional units representing different levels of muscle synergies, parts of movements, or even more integrated motor behavior.

Significance of the results

In animal preparations it is possible to identify posterior roots after surgical opening of the spinal canal and to stimulate these neural structures electrically in order to study PRMRRs initiated in axons with different diameters and with different projections to motoneurons and neuronal networks in the spinal cord. The same possibility also exists in humans during surgical intervention of the cord when attempting to control intractable neurogenic pain or spasticity (Gybels & Sweet, 1989; Abbott *et al.* 1989).

Nevertheless, in this study we have shown that it is possible to selectively stimulate posterior roots without opening the spinal canal but by taking advantage of an electrode which had been percutaneously inserted into the posterior epidural space.

By implanting an array of electrodes above the complex anatomical structure of the posterior roots of the lumbosacral cord, it is possible to stimulate large diameter myelinated axons close to their entries into the corresponding segments of the spinal cord. When applying low frequency stimulation of 2.2 Hz we have demonstrated characteristic features of shortest spinal reflex responses of different lower limb muscle groups, similar to the H-reflex responses but of shorter latency time due to reduced afferent reflex path.

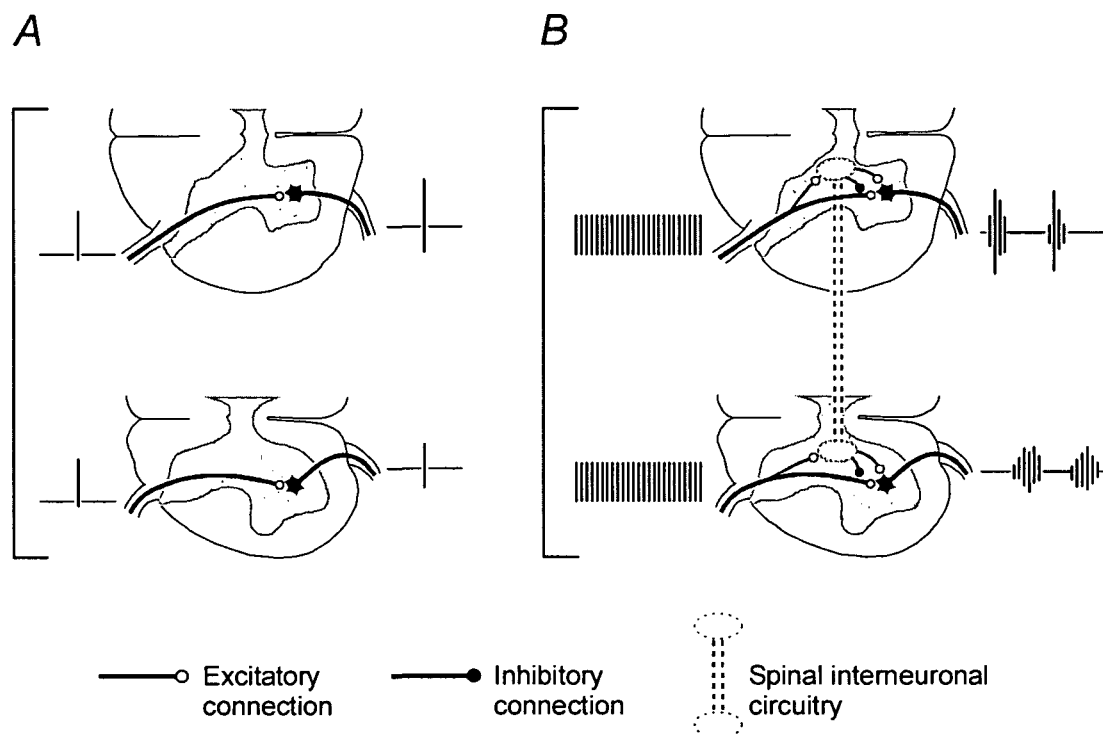


Figure 2.7. Speculative scheme of neural structures activated by epidural spinal cord stimulation

Neural path diagrams are shown in cross-sections at two lumbar segmental levels. *A*, single pulse (2.2 Hz-) stimulation activates segmental primary sensory axons and affects monosynaptic excitatory action on homonymous motoneurons. *B*, same afferent structures repetitively stimulated at higher frequencies activate lumbar neuronal circuits that modulate the afferent flow through monosynaptic pathways by putatively presynaptic inhibitory mechanism and control motoneuronal discharge by excitatory oligosynaptic pathways. Sustained stimuli at 25–50 Hz organize the lumbar spinal interneurons by temporarily combining them into locomotor centers that project over several segments and coordinate the neural activity.

This selective stimulation of the posterior roots and elicitation of PRMRRs should be considered as the product of the unique anatomical conditions of the terminal portion of the lumbosacral cord which determines the resultant electrical field characteristics of the bipolar stimulation from epidural space and its effect on excitable structures. When the biophysical complexity of the generated electrical fields is applied to the known biophysical posterior root characteristics, it is possible to adjust conditions for recording electrophysiological features of PRMRRs in humans.

Another significance of the presented results is the effect of PRMRR modifications by increasing the rate of stimulation from 2.2 Hz (Fig. 2.7A) up to 50 Hz (Fig. 2.7B). At the higher stimulation frequencies, shortest latency spinal reflex responses incorporate additional spinal cord structures resulting in the modulation of PRMRR amplitudes as well as extending the latency beyond the monosynaptic one, thereby establishing oligosynaptic spinal reflex responses. This finding was present when all lumbar and upper sacral segments have been stimulated simultaneously and under such circumstances even functional motor outputs of sustained extension or alternating stepping-like lower limb movements have been established. In other words epidural stimulation of the posterior structures of the lumbosacral cord can be set up to elicit motor reflex responses of muscle groups innervated by corresponding spinal cord segment, or to simultaneously stimulate all posterior root segments of the lumbar and upper sacral cord in order to study more complex sensory-motor organization activity of spinal cord networks. Functional movements of the paralyzed lower limbs can be generated by afferent input in humans after accidental spinal cord injury and complete removal of the brain motor control. This finding permits a new approach to studies of the processing capabilities of the human lumbar cord networks and how such capabilities depend on sensory input codes.

REFERENCES

- Abbott R, Forem SL & Johann M (1989). Selective posterior rhizotomy for the treatment of spasticity: a review. *Childs Nerv Syst* **5**, 337-346.
- Barolat G, Myklebust JB & Wenninger W (1988). Effects of spinal cord stimulation on spasticity and spasms secondary to myelopathy. *Appl Neurophysiol* **51**, 29-44.
- Barolat G, Massaro F, He J, Zeme S & Ketcik B (1993). Mapping of sensory responses to epidural stimulation of the intraspinal neural structures in man. *J Neurosurg* **78**, 233-239.
- Beric A (1988). Stability of lumbosacral somatosensory evoked potentials in a long-term follow-up. *Muscle Nerve* **11**, 621-626.
- Coburn B (1980). Electrical stimulation of the spinal cord: two-dimensional finite element analysis with particular reference to epidural electrodes. *Med Biol Eng Comput* **18**, 573-584.
- Coburn B & Sin WK (1985). A theoretical study of epidural electrical stimulation of the spinal cord--Part I: Finite element analysis of stimulus fields. *IEEE Trans Biomed Eng* **32**, 971-977.
- Davidoff RA (1989). The dorsal columns. *Neurology* **39**, 1377-1385.
- Dimitrijevic MR (1983). Neurophysiological evaluation and epidural stimulation in chronic spinal cord injury patients. In *Spinal Cord Reconstruction*, ed. Reier PJ, Bunge RP & Kao CC, pp. 465-473. Raven Press, New York.
- Dimitrijevic MR, Gerasimenko Y & Pinter MM (1998). Evidence for a spinal central pattern generator in humans. In *Neural Mechanisms for Generating Locomotor Activity*. *Ann N Y Acad Sci Vol. 860*, ed. Kiehn O, Harris-Warrik RM, Jordan LM, Hultborn H & Kudo N, pp. 360-376. New York Academy of Sciences, New York.
- Ertekin C, Mungan B & Uludag B (1996). Sacral cord conduction time of the soleus H-reflex. *J Clin Neurophysiol* **13**, 77-83.
- Feirabend HK, Choufoer H, Ploeger S, Holsheimer J & van Gool JD (2002). Morphometry of human superficial dorsal and dorsolateral column fibers: significance to spinal cord stimulation. *Brain* **125**, 1137-1149.
- Geddes LA & Baker LE (1967). The specific resistance of biological material—a compendium of data for the biomedical engineer and physiologist. *Med Biol Eng* **5**, 271-293.
- Gurfinkel VS, Levik YS, Kazennikov OV & Selionov VA (1998). Locomotor-like movements evoked by leg muscle vibration in humans. *Eur J Neurosci* **10**, 1608-1612.
- Guru K, Mailis A, Ashby P & Vanderlinden G (1987). Postsynaptic potentials in motoneurons caused by spinal cord stimulation in humans. *Electroencephalogr Clin Neurophysiol* **66**, 275-280.
- Gybels JM & Sweet WH (1989). *Neurosurgical treatment of persistent pain*. Karger, Basel.
- He J, Barolat G, Holsheimer J & Struijk JJ (1994). Perception threshold and electrode position for spinal cord stimulation. *Pain* **59**, 55-63.

- Herman R, He J, D'Luzansky S, Willis W & Dilli S (2002). Spinal cord stimulation facilitates functional walking in a chronic, incomplete spinal cord injured. *Spinal Cord* **40**, 65-68.
- Holsheimer J (1998). Computer modeling of spinal cord stimulation and its contribution to therapeutic efficacy. *Spinal Cord* **36**, 531-540.
- Holsheimer J (2002). Which neuronal elements are activated directly by spinal cord stimulation. *Neuromodulation* **5**, 25-31.
- Hultborn H, Conway BA, Gossard JP, Brownstone R, Fedirchuk B, Schomburg ED, Enriquez-Denton M & Perreault MC (1998). How do we approach the locomotor network in the mammalian spinal cord? In *Neural Mechanisms for Generating Locomotor Activity. Ann N Y Acad Sci Vol. 860*, ed. Kiehn O, Harris-Warrick RM, Jordan LM, Hultborn H & Kudo N, pp. 70-82. New York Academy of Sciences, New York.
- Hunter JP & Ashby P (1994). Segmental effects of epidural spinal cord stimulation in humans. *J Physiol* **474**, 407-419.
- Ishizuka N, Mannen H, Hongo T & Sasaki S (1979). Trajectory of group Ia afferent fibers stained with horseradish peroxidase in the lumbosacral spinal cord of the cat: three dimensional reconstructions from serial sections. *J Comp Neurol* **186**, 189-211.
- Jilge B, Minassian K, Rattay F, Pinter MM, Gerstenbrand F, Binder H & Dimitrijevic MR (2004). Initiating extension of the lower limbs in subjects with complete spinal cord injury by epidural lumbar cord stimulation. *Exp Brain Res* **154**, 308-326.
- Lang J (1984a). Morphologie und funktionelle Anatomie der Lendenwirbelsäule und des benachbarten Nervensystems - 1. Rückenmark. In *Neuroorthopädie 2 - Lendenwirbelsäulenerkrankungen mit Beteiligung des Nervensystems*, ed. Hohmann D, Kügelgen B, Liebig K & Schirmer M, pp. 3-9. Springer, Berlin.
- Lang J (1984b). Morphologie und funktionelle Anatomie der Lendenwirbelsäule und des benachbarten Nervensystems - 2. Fila radicularia - Cauda equina. In *Neuroorthopädie 2 - Lendenwirbelsäulenerkrankungen mit Beteiligung des Nervensystems*, ed. Hohmann D, Kügelgen B, Liebig K & Schirmer M, pp. 9-11. Springer, Berlin.
- Lehmkuhl D, Dimitrijevic MR & Renouf F (1984). Electrophysiological characteristics of lumbosacral evoked potentials in patients with established spinal cord injury. *Electroencephalogr Clin Neurophysiol* **59**, 142-155.
- Lloyd DPC (1943). Reflex action in relation to pattern and peripheral source of afferent stimulation. *J Neurophysiol* **16**, 111-120.
- Magladery JW, Porter WE, Park AM & Teasdall RD (1951). Electrophysiological studies of nerve and reflex activity in normal man. *Bull John Hopkins Hosp* **88**, 499-519.
- Maertens de Noordhout A, Rothwell JC, Thompson PD, Day BL & Marsden CD (1988). Percutaneous electrical stimulation of lumbosacral roots in man. *J Neurol Neurosurg Psychiatry* **51**, 174-181.
- Minassian K, Rattay F & Dimitrijevic MR (2001a). Features of the reflex responses of the human lumbar cord isolated from the brain but during externally controlled locomotor activity. *Proceedings of the World Congress on Neuroinformatics. Vienna, Austria; Part II*, pp 267-268.

- Minassian K, Rattay F, Pinter MM, Murg M, Binder H, Sherwood A & Dimitrijevic MR (2001*b*). Effective spinal cord stimulation (SCS) train for evoking stepping locomotor movement of paralyzed human lower limbs due to SCI elicits a late response additionally to the early monosynaptic response. *Soc Neurosci Abstr*; 27: Program No. 935.12.
- Minassian K, Jilge B, Rattay F, Pinter MM, Gerstenbrand F, Binder H & Dimitrijevic MR (2002). Effective spinal cord stimulation (SCS) for evoking stepping movement of paralyzed human lower limbs: study of posterior root muscle reflex responses. *Proceedings of the 7th Annual Conference of the IFESS*. Ljubljana, Slovenia, pp167-169.
- Minassian K, Jilge B, Rattay F, Pinter MM, Binder H, Gerstenbrand F & Dimitrijevic MR (2004). Stepping-like movements in humans with complete spinal cord injury induced by epidural stimulation of the lumbar cord: Electromyographic study of compound muscle action potentials. *Spinal Cord* May 4 [Epub ahead of print].
- Murg M, Binder H & Dimitrijevic MR (2000). Epidural electric stimulation of posterior structures of the human lumbar spinal cord: 1. muscle twitches - a functional method to define the site of stimulation. *Spinal Cord* 38, 394-402.
- Panjabi MM, Takata K, Goel V, Federico D, Oxland T, Duranceau J & Krag M (1991). Thoracic human vertebrae. Quantitative three-dimensional anatomy. *Spine* 16, 888-901.
- Panjabi MM, Goel V, Oxland T, Takata K, Duranceau J, Krag M & Price M (1992). Human lumbar vertebrae. Quantitative three-dimensional anatomy. *Spine* 17, 299-306.
- Pinter MM, Gerstenbrand F & Dimitrijevic MR (2000). Epidural electrical stimulation of posterior structures of the human lumbosacral cord: 3. Control of spasticity. *Spinal Cord* 38, 524-531.
- Rattay F, Minassian K & Dimitrijevic MR (2000). Epidural electrical stimulation of posterior structures of the human lumbosacral cord: 2. quantitative analysis by computer modeling. *Spinal Cord* 38, 473-489.
- Saifuddin A, Burnett SJ & White J (1998). The variation of position of the conus medullaris in an adult population. A magnetic resonance imaging study. *Spine* 23, 1452-1456.
- Shealy CN, Mortimer JT & Reswick JB (1967). Electrical inhibition of pain by stimulation of the dorsal columns: preliminary clinical report. *Anesth Analg* 46, 489-491.
- Sherwood AM, McKay WB & Dimitrijevic MR (1996). Motor control after spinal cord injury: Assessment using surface EMG. *Muscle Nerve* 19, 966-979.
- Smith MC & Deacon P (1984). Topographical anatomy of the posterior columns of the spinal cord in man. The long ascending fibers. *Brain* 107, 671-698.
- Struijk JJ, Holsheimer J, van der Heide GG & Boom HB (1992). Recruitment of dorsal columns fibers in spinal cord stimulation: Influence of collateral branching. *IEEE Trans Biomed Eng* 39, 903-912.
- Struijk JJ, Holsheimer J & Boom HB (1993*a*). Excitation of dorsal root fibers in spinal cord stimulation: A theoretical study. *IEEE Trans Biomed Eng* 40, 632-639.
- Struijk JJ, Holsheimer J, Barolat G, He J & Boom HBK (1993*b*). Paresthesia thresholds in spinal cord stimulation: a comparison of theoretical results with clinical data. *IEEE Trans Rehabil Eng* 1, 101-108.

Struijk JJ, Holsheimer J, Spincemaille GH, Gielen FL & Hoekema R (1998). Theoretical performance and clinical evaluation of transverse tripolar spinal cord stimulation. *IEEE Trans Rehabil Eng* **6**, 277-285.

Sunderland S (1976). Avulsion of nerve roots. In *Handbook of Clinical Neurology*, ed. Vinken PJ & Bruyn GW, pp. 396-435. North Holland, Amsterdam.

Troni W, Bianco C, Moja MC & Dotta M (1996). Improved methodology for lumbosacral nerve root stimulation. *Muscle Nerve* **19**, 595-604.

Wall EJ, Cohen MS, Abitbol JJ & Garfin SR (1990). Organization of intrathecal nerve roots at the level of the conus medullaris. *J Bone Joint Surg* **72**, 1495-1499.

Waltz JM (1998). Chronic stimulation for motor disorders. In *Textbook for Stereotactic and Functional Neurosurgery*, ed. Gildenberg PL & Tasker RR, pp. 1087-1099. McGraw-Hill, New York.

Zhu Y, Starr A, Haldeman S, Chu JK & Sugerman RA (1998). Soleus H-reflex to S1 nerve root stimulation. *Electroencephalogr Clin Neurophysiol* **109**, 10-14.

Chapter 3

Stepping-like movements in humans with complete spinal cord injury induced by epidural stimulation of the lumbar cord: Electromyographic study of compound muscle action potentials

Summary

It has been previously demonstrated that sustained non-patterned electrical stimulation of the posterior lumbar spinal cord from the epidural space can induce stepping-like movements in subjects with chronic, complete spinal cord injury. In the present paper we explore physiologically related components of electromyographic (EMG) recordings during the induced stepping-like activity. The aim is to obtain a better understanding of how the intrinsic organization of human spinal networks is controlled by external stimulation.

The study is based on the assessment of epidural stimulation to control spasticity by simultaneous recordings of the EMG activity of quadriceps, hamstrings, tibialis anterior and triceps surae. We examined induced muscle responses to stimulation frequencies of 2.2–50 Hz in ten subjects classified as having a motor complete spinal cord injury (ASIA A and B). We evaluated stimulus-triggered time windows 50 ms in length from the original EMG traces. Stimulus-evoked compound muscle action potentials (CMAPs) were analyzed with reference to latency, amplitude, and shape. Epidural stimulation of the posterior lumbosacral cord recruited lower limb muscles in a segmental-selective way, which was characteristic for posterior root stimulation.

Stimulation at 2.2 Hz elicited stimulus-coupled CMAPs of short latency which were approximately half that of phasic stretch reflex latencies for the respective muscle groups. EMG-amplitudes were stimulus-strength dependent. Stimulation at 5–15 and 25–50 Hz elicited sustained tonic and rhythmic activity, respectively, and initiated lower limb extension or stepping-like movements representing different levels of muscle synergies. All EMG responses, even during burst-style phases, were composed of separate stimulus-triggered CMAPs with characteristic amplitude modulations. During burst-style phases, a significant increase of CMAP latencies by about 10 ms was observed.

We conclude, that the muscle activity evoked by epidural lumbar cord stimulation as described in the present study was initiated within the posterior roots. These Posterior Roots Muscle Reflex Responses (PRMRRs) to 2.2 Hz stimulation were routed through monosynaptic pathways. Sustained stimulation at 5–50 Hz engaged central spinal PRMRR components. We propose that repeated volleys delivered to the lumbar cord via the posterior roots can effectively modify the central state of spinal circuits by temporarily combining them into functional units, generating integrated motor behavior of sustained extension and rhythmic flexion/extension movements. This study opens the possibility for developing neuroprostheses for activation of inherent spinal networks involved in

generating functional synergistic movements using a single electrode implanted in a localized and stable region.

INTRODUCTION

There is definite evidence that the spinal cord of lower vertebrates has autonomous capabilities to produce basic coordinated patterns of locomotion, whether in swimming of fish or walking of terrestrial animals in the absence of input from higher levels of the central nervous system or from peripheral feedback (Grillner, 1981; Rossignol, 1996). The existence of spinal stepping generators in humans is more difficult to demonstrate and evidence is, by necessity, indirect (Illis, 1995). Bussel and colleagues discussed that some elements of the spinal circuitry on which the generation of stepping rhythms relies in lower vertebrates also exist in man (Roby-Brami & Bussel, 1987; Bussel *et al.* 1996). Calancie and colleagues (1994) investigated involuntary stepping-like movements in a subject with chronic incomplete spinal cord injury (SCI). They concluded that the automatic movement patterns were affected by a preserved but extremely limited supraspinal facilitation and an abnormal afferent inflow from the subject's hip, where they found evidence of pathology. Gurfinkel and colleagues (1998) used tonic peripheral afferent stimulation to elicit involuntary stepping in non-paraplegic individuals. They found that continuous lower limb muscle vibration gave rise to involuntary locomotion-like movements in suspended legs and suggested that the non-specific afferent input induced by vibration activated central structures governing stepping movements.

When epidural spinal cord stimulation became a clinical method to control severe spasticity in chronic spinal cord injured individuals (Dimitrijevic *et al.* 1986 *a,b*; Barolat *et al.* 1995; Pinter *et al.* 2000), it provided a neurophysiological technique to deliver tonic input to the human spinal cord deprived of supraspinal influence, and to examine locomotor capabilities of the lumbar cord (Rosenfeld *et al.* 1995; Gerasimenko *et al.* 1995).

In a clinical program of restorative neurology we evaluated the optimal site and parameters of spinal cord stimulation (SCS) for control of spasticity and thereby applied stimulation strengths from 1–10V at frequencies from 2.2–100 Hz and tested different contact combinations of an epidurally placed electrode array (Pinter *et al.* 2000). In the course of the evaluation procedure we discovered that the electrical stimulation of the posterior structures of the lumbar spinal cord could initiate and maintain rhythmic stepping-like flexion/extension movements of the subject's paralyzed limbs. To illustrate our findings in this initial study, we chose recorded electromyographic (EMG) activity of agonist-antagonist muscles of thigh and leg that lasted for 30 s without changes in the rhythmical patterns (Dimitrijevic *et al.* 1998*a*).

In the present paper we investigate the nature of these responses. We sought to reveal whether the EMG patterns recorded during induced stepping-like activity could be decomposed into physiologically related components. To this end we extended the time scales of the analyzed EMG traces and examined stimulus-triggered time windows of 50 ms length. Responses to 2.2 Hz stimulation and pairs of stimuli were evaluated to identify which directly stimulated neural structures should be considered as inputs resulting in the recorded EMG activity. Responses to trains of electrical stimuli of 5–50 Hz were examined to learn how different pulse frequencies cause lumbar cord neurons to shape different types of sustained tonic or patterned rhythmical motor output.

We provide evidence that the flexion/extension movements evoked by epidural lumbar cord stimulation are initiated by immediate stimulation of the posterior roots. It will be demonstrated that during the different induced EMG-patterns and even during burst-style phases each pulse within the stimulus train triggered a separate compound muscle action potential (CMAP). The electrophysiological characteristics of these Posterior Roots Muscle Reflex Responses (PRMRRs) will be described.

We propose that lumbar interneuronal systems can respond to particular repetition rates of tonic afferent input by temporarily combining into functional networks, which modulate the transmitting pathways and amplitudes of the PRMRRs and thereby generate flexion/extension movements.

MATERIAL AND METHODS

Subjects

The retrospective analyses performed in this study are based on data collected while routinely conducting a clinical protocol for the evaluation of the optimal site and parameters of epidural spinal cord stimulation for spasticity control in subjects who were resistant to other treatment modalities. The effect of stimulation had been assessed by EMG recordings of muscle activity in the lower limbs. For the present study we selected recordings obtained in ten subjects who were neurologically classified as having a complete spinal cord lesion at the cervical or thoracic level with no motor functions below the lesion (ASIA A or B). Pertinent patient-related data are listed in Table 3.1.

Table 3.1 Demographic and clinical data

Subject No.	Sex	Born in	Accident in	Implantation of electrode in	Type of accident	Level of SCI	ASIA Class.
1	m	1977	1994	1999	Motorbike accident	C6	A
2	m	1973	1995	1998	Car accident	C4	A
3	m	1981	1996	1999	Car accident	C4	A
4	m	1973	1997	1998	Ski accident	C7	B
5	m	1978	1996	1999	Car accident	T10	B
6	f	1978	1994	1996	Car accident	T4	A
7	f	1975	1996	2000	Car accident	T6	A
8	m	1973	1996	1997	Car accident	T4	A
9	f	1965	1996	1998	Car accident	T5	A
10	m	1939	1994	1997	Fall accident	T7	A

At the time of data collection the subjects met the following criteria: (1) They were healthy adults with closed, post-traumatic spinal cord lesions; (2) all patients were in a chronic (more than 1 year post-onset) and stable condition; (3) no antispastic medication was being used; (4) the stretch and cutaneomuscular reflexes were preserved; (5) there was no

voluntary activation of motor units below the level of the lesion as confirmed by brain motor control assessment (Sherwood *et al.* 1996); while (6) surface recorded lumbosacral evoked potentials – used to assess the functions of the posterior structures and gray matter of the spinal cord below the level of the lesion – were present (Lehmkuhl *et al.* 1984; Beric, 1988).

To control their spasticity all subjects had an epidural electrode array implanted at some vertebral level ranging from T10 down to L1 (see “Stimulation and recording setup”). The position of the epidurally placed electrodes relative to the vertebral bodies was obtained from postoperative X-rays. The implantations as well as the clinical protocol to evaluate the optimal stimulation parameters were approved by the local ethics committee. All subjects gave their informed consent.

Stimulation and recording setup

Figure 3.1A illustrates the patient set-up used, according to the clinical protocol, for the evaluation of the optimal stimulation parameters for spasticity control. Stimulation was delivered via a quadripolar electrode array with cylindrical electrode design (PISCES-QUAD electrode, Model 3487A, MEDTRONIC, Minneapolis, MN, USA) placed in the dorsomedial epidural space at vertebral levels ranging from T10 to L1 (left side of Fig. 3.1A). The data analyzed in the present study was recorded when the electrode array was operated as a bipolar electrode, the most rostral and caudal electrode contacts being connected to the positive and negative outputs, respectively, of the implanted pulse generator (ITREL 3, Model 7425, MEDTRONIC). The separation of the two active electrode contacts was 27 mm. The bipolar impedance was generally about 1000 Ω . The stimulus pulses were biphasic and actively charge balanced. The first dominant phase was about rectangular with a width of 210 μ s, the amplitude in the second phase was small and irrelevant to the stimulation process. Thus, stimulation was virtually monophasic and the stimulating effect of the epidural electrode was based on its polarity during the first dominant phase. Cathodal stimulation of spinal neural structures is known to result in lower thresholds than anodal stimulation. For posterior root fibers, calculated thresholds for cathodal excitation are about three times lower than anodal thresholds (Struijk *et al.* 1993; Holsheimer, 2002). Reversing the polarity of the bipolar epidural electrode shifted the effective cathode site to a different rostrocaudal level. Thus, setting the electrode polarity allowed for stimulation of posterior structures of the spinal cord at different segmental levels with a single epidural electrode array – given by the cathode site. The maximum stimulation strength was 10 V.

To verify the effect of spinal cord stimulation, electromyographic activity of quadriceps, hamstring, tibialis anterior, and triceps surae was recorded with silver-silver chloride surface electrodes (right side of Fig. 3.1A). Additional surface electrodes were placed over the lumbar paraspinal trunk muscles. Stimulus artifacts captured by this recording electrode allowed the identification of the onsets of applied voltage pulses. The bipolar surface electrodes were placed centrally over the muscle bellies spaced 3 cm apart and oriented along the long axis of the muscles. The skin was slightly abraded such that an electrode impedance of less than 5 k Ω was reached. The EMG signals were amplified with the Grass 12D-16-OS NEURODATA ACQUISITION SYSTEM (GRASS INSTRUMENTS, Quincy, MA) adjusted to a gain of 2000 over a bandwidth of 30–1000 Hz and digitized at 2048 samples/s/channel using a CODAS ADC system (DATAQ INSTRUMENTS, Akron, OH). The EMG data was analyzed off-line using WINDAQ Waveform Browser playback software (DATAQ INSTRUMENTS).

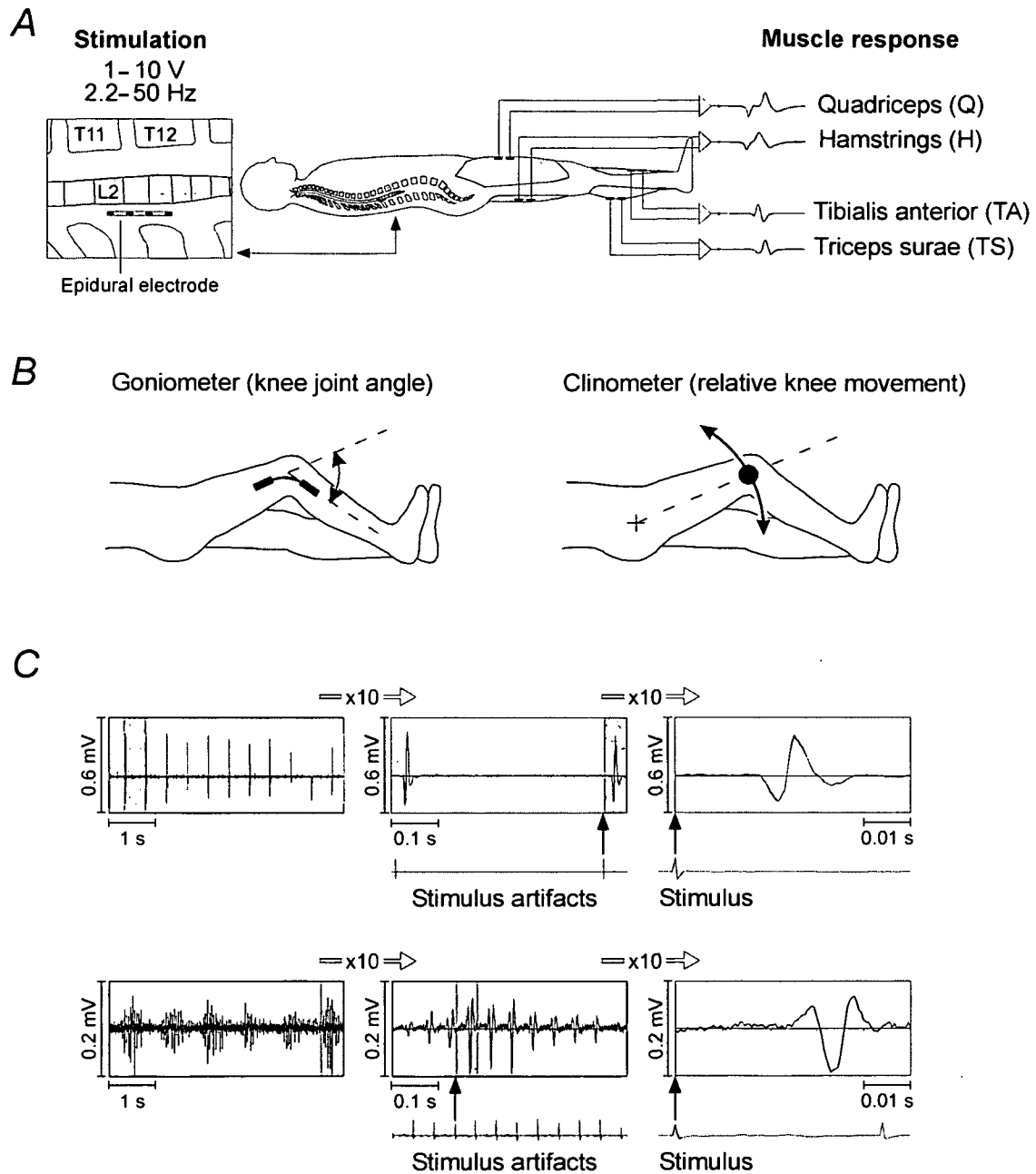


Figure 3.1 Outline of the clinical assessment design and analysis of stimulus-evoked EMG responses

A, all recordings were conducted with the patients in a comfortable supine position. Pairs of surface EMG electrodes were placed over the bellies of the lower limb muscle groups to assess the effects of epidural stimulation. *B*, to monitor relative movements of the lower limbs, goniometers or clinometers were applied bilaterally to the knee. *C*, EMG responses of triceps surae to epidural stimulation at 2.2 Hz (top) and 22 Hz (bottom) displayed with different time scales. Potentials marked by gray backgrounds are shown in extended time scale ($\times 10$) on the right side of the original EMG. 10-second traces of EMG responses are displayed in the left column. In the middle column it is shown that stimulus artifacts (recorded by paraspinal-surface electrodes) allow the identification of the onsets of applied voltage pulses. In the right column EMG potentials of separate responses can be seen. These CMAPs were analyzed for latencies, peak-to-peak amplitudes, and shapes irrespective of the stimulation amplitude or frequency.

One of two different sensor types was used to record knee movement, namely goniometers (Model XM-180, and K100 AMPLIFIER SYSTEM, PENNY & GILES BIOMETRICS LTD.) or electronic clinometers (ACCUSTAR, LUCAS SENSING SYSTEMS, Phoenix, AZ) both attached bilaterally to the knee. The goniometer measured relative changes in the knee joint angle as illustrated in the left side of Fig. 3.1B. The clinometer measured rotations about its axis and thus rotations of the longitudinal axis of the thigh around the hip.

All recordings were conducted with the subjects placed on a comfortable examination table covered with soft sheepskin in a supine position. This configuration allowed flexion/extension movements of the lower limbs to unfold smoothly and minimized friction between the heel and the supporting surface.

Data analysis – Data based on incremental pulse amplitudes

The first set of EMG data had originally been collected to define the rostrocaudal level of the epidural electrode relative to the lumbosacral cord segments based on muscle twitch recruitment patterns (Murg *et al.* 2000). For this purpose a frequency of 2.2 Hz was used, and the stimulation strength was intensified in 1-Volt increments from 1 to 10 V.

In the present study we examined the relationship between the rostrocaudal position of the cathode relative to the spinal cord and the sequence of quadriceps and triceps surae activation. The vertebral cathode level was obtained from X-ray. The estimated, functional segmental level of the cathode was derived from a neurophysiological technique for electrode positioning in subjects with impaired sensory function (Murg *et al.* 2000). Additionally, information on average spatial relations between the cord segments and the vertebral bodies was used (Lang, 1984). The effect of two different rostrocaudal cathode sites were studied in all subjects but subject 4. The electrode array of subject 4 was repositioned a number of times during participation in the clinical program. This allowed comparison of stimulation with six different cathode sites located between the upper third of the T10 and the upper L1 vertebra in a single subject.

The recruitment sequence of quadriceps and triceps surae was given by the whole-numbered threshold voltages for the respective muscles. Only quadriceps and triceps surae were considered in this analysis, because they are muscle groups with separate segmental innervations (L2–L4 vs. L5–S2).

We examined single stimulus-evoked and surface-recorded CMAPs for latencies (quantitatively), peak-to-peak amplitudes, and shapes (qualitatively) of the same data set. The latencies were read off-line from the EMG traces using the playback software and measured as the time between stimulation onset – identified by stimulus artifacts – and the first deflection of the EMG-potential from baseline (Fig. 3.1C, top). Mean latency times based on all subjects were calculated for the threshold stimulus strengths eliciting responses in each muscle group and for the maximum strengths applied.

Data analysis – Data based on incremental pulse frequencies

The second set of EMG data that we analyzed had originally been collected to assess the effect of trains of 5–100 Hz stimuli on spasticity (Pinter *et al.* 2000). These data were used to evaluate the refractory periods of responses to pairs of stimuli delivered at intervals of 200 to 10 ms, based on the first two stimuli of the applied trains.

Furthermore we examined the muscle activity induced by sustained trains of 1–10 V and 5–50 Hz, focusing on the effects of different repetition rates of stimulation on the evoked motor output patterns. To reveal the components of the overall EMG pattern we subsequently enlarged the time scale of the EMG traces. We addressed the question of how far individual responses to single pulses within the applied stimulus train were reflected in the EMG output pattern. Separate successive EMG responses were analyzed for latencies (quantitatively), peak-to-peak amplitudes, and shapes (qualitatively) (Fig. 3.1C, bottom).

RESULTS

Epidurally evoked segmental twitch responses

Electrical stimulation of the lumbosacral cord delivered from the dorsomedial epidural space at 2.2 Hz and 1–10 V gave rise to stimulus-coupled CMAPs in the lower limb muscles. Figure 3.2A shows successively elicited single CMAPs of quadriceps and triceps surae muscles, induced by stimulation with 3–7 V and 2.2 Hz (subject 3). The effective cathode was located at the center level of the T12 vertebral body, the estimated segmental level was L3/L4. Stimulus-triggered time windows of 50 ms in length were extracted from the originally continuous EMG-traces (see also Fig. 3.1C). The left margins of the windows are determined by the onsets of the stimuli. EMG-responses to ten consecutive stimuli are shown for each incremental voltage. In the presented case CMAPs were not induced in the lower limb muscle groups at SCS strengths of 1–2 V. At 3 V CMAPs with short (9.5 ms) and constant latencies were recorded from quadriceps, while triceps surae showed no activity. At 4 V quadriceps showed higher CMAP amplitudes than at 3 V while the latencies remained unchanged. Faint activity was also observed for triceps surae at 4 V, involving latencies of 18.5 ms. At higher stimulation strengths CMAP amplitudes further increased for both muscle groups. The latencies of successive responses remained constant, while no additional components with longer latencies emerged in the EMG-traces at higher stimulus strengths. For a given stimulus strength, amplitudes of successive CMAP showed only minor and unsystematic variations. The demonstrated muscle recruitment sequence was representative for cathodes positioned at the level of the T12 vertebral body.

As shown in Fig. 3.2B, this recruitment pattern was essentially reversed when the effective cathode was located at the lower third of the L1 vertebral body, corresponding to the average position of the conus medullaris. Ten CMAPs are displayed sequentially for incremental stimulus strengths of 4–8 V (subject 5). At the threshold level of 4 V, CMAPs with a latency of 18.5 ms and rather large amplitudes were evoked in triceps surae. The CMAP amplitudes showed progressive increases with increasing stimulus strength until a plateau of EMG activity was reached at 7 V. Weak quadriceps responses with a latency of 10.5 ms was initiated at a strength of 5 V. Quadriceps CMAPs with only moderate amplitudes were evoked even at increased stimulus strength.

Figure 3.2 demonstrates a strong relationship between the rostrocaudal position of the cathode relative to the spinal cord and the sequence of quadriceps and triceps surae activation. In subjects with cathodes located at the T11 vertebral level, rather strong stimulation amplitudes (6–9 V) were needed to elicit CMAPs in the quadriceps muscle, while triceps surae could not be activated even at the maximum strength of 10 V (subjects 4, 6, 9). Note that on average the T11 vertebral level corresponds to the L1 and L2 segmental levels, while the levels L5–S2 are situated well below this rostrocaudal position.

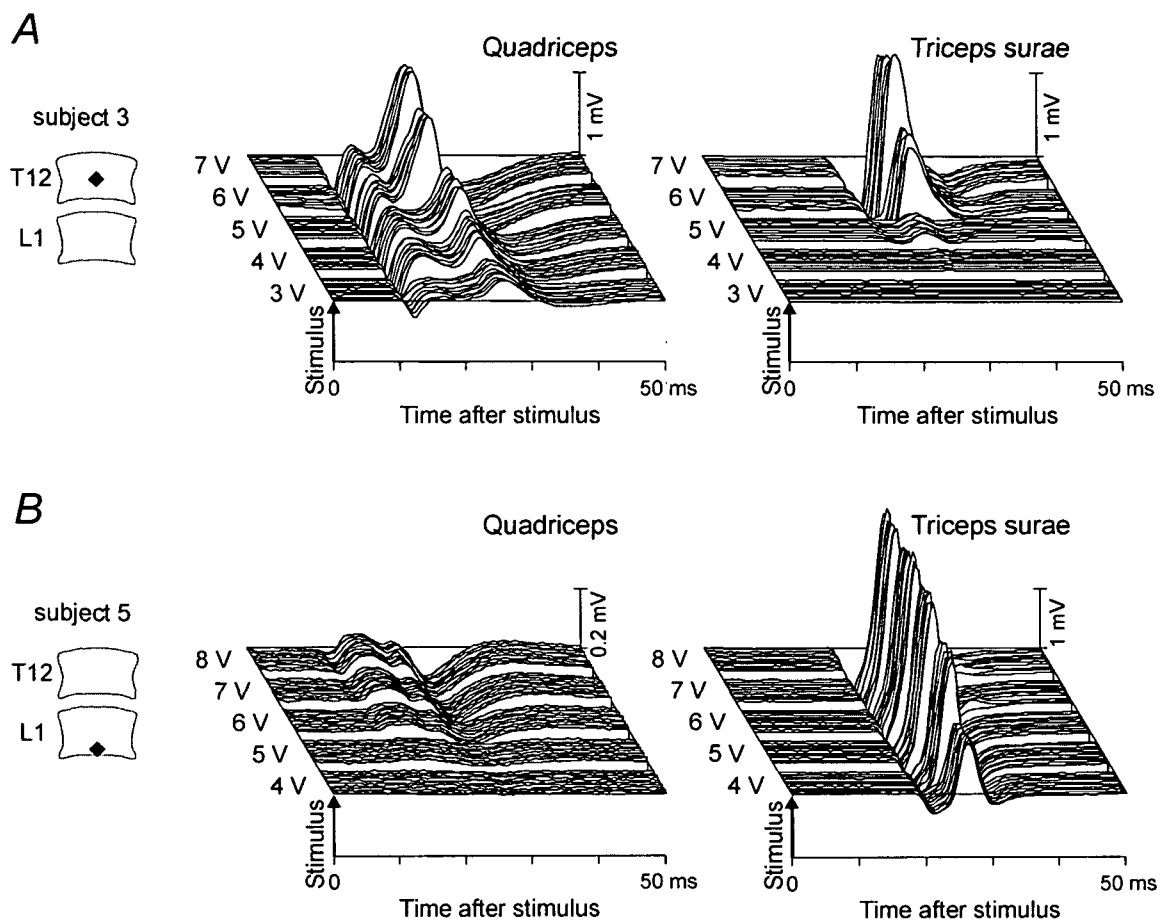


Figure 3.2 EMG responses to 2.2 Hz stimulation

Stimulus-triggered raster presentation of CMAPs induced in quadriceps and triceps surae. The first 50 ms following each stimulus pulse are shown. *A*, the effective cathode was located at the center level of the T12 vertebral body, which approximately corresponds to L3/L4 segmental level (subject 3). The stimulation strength was increased in steps of 1 V. Ten single EMG potentials of successive muscle responses are shown for each incremental voltage (3–7 V). *B*, effective cathode site was at the lower level of the L1 vertebra, corresponding to the level of the conus medullaris (subject 5). Ten stimulus-evoked CMAPs are displayed for each incremental voltage (4–8 V).

The lower third of the T10 vertebral body was the most rostral position from which lower limb muscle responses could be evoked at a stimulation strength of 10 V – in fact solely in the thigh muscles. From the upper third of the T10 vertebral body none of the studied lower limb muscles could be activated with strengths up to 10 V, though the lumbar paraspinal trunk muscles responded at a threshold of 5 V (subject 4).

EMG-data derived from subject 4 during epidural stimulation with considerably different rostrocaudal positions of the effective cathode (see methods) allowed us to reveal any relationship between the segmental cathode level and the response latencies. When the cathode was at the lower third of the T10 vertebral body, CMAPs elicited in quadriceps and hamstrings at threshold level had mean latencies of 9.8 ms and 10.3 ms, respectively. When the cathode was repositioned caudally by 7 cm to the upper L1 vertebral level, the latencies were 9.5 ms and 10.0 ms. Considering that the accuracy of identification of the latencies was 0.25 ms at best, no significant correlation between rostrocaudal cathode position and

response latencies could be demonstrated. Therefore we calculated the average response latencies from the data derived from all subjects irrespective of the positions of their epidurally placed electrodes for quadriceps, hamstrings, tibialis anterior and triceps surae for 2.2 Hz stimulation. The mean latency times for these muscle groups at threshold level and maximum applied stimulation strength (generally 8–10 V) are compiled in Table 3.2 and were about 9–10 ms for the thigh muscles and 16–17 ms for the distal leg muscles. Note that the weak responses induced at threshold stimulation had low CMAP amplitudes and slight onset slopes of the potentials, thus making the precise identification of the onset of the CMAPs difficult. This may account for the longer latencies of muscle responses at threshold level in Table 3.2.

Table 3.2 Mean latencies (ms \pm SD) of CMAPs evoked by 2.2 Hz stimulation based on all subjects at threshold and maximum stimulation strength

	Threshold	Maximum
Q	9.3 \pm 1.6	8.6 \pm 0.9
H	9.9 \pm 1.3	9.3 \pm 0.8
TA	16.4 \pm 2.1	16.1 \pm 1.6
TS	16.7 \pm 1.5	16.3 \pm 1.4

To summarize, 2.2 Hz stimulation of the posterior structures of the lumbosacral cord elicited twitch responses in the lower limb muscles in a segmental-selective way (Fig. 3.2). The EMG signals associated with these responses were stimulus coupled and of short latency (Table 3.2) – approximately half that of the phasic stretch reflexes of the respective muscle groups. Equal-voltage stimuli yielded only negligible variations in CMAP amplitudes and shapes. Thus, successive responses to the stimulus train of a given muscle demonstrated no mutual influence. Responses of a muscle were not influenced by the ongoing activity of responses of the other muscles to the same stimulus pulse. For a given cathode position the CMAP amplitudes elicited at 2.2 Hz were dependent on the stimulus strength.

Stimulation with pairs of stimuli

While equal-voltage stimuli at 2.2 Hz yielded EMG responses with similar amplitudes (Fig. 3.2), different patterns emerged when pulses were applied in close succession. First we analyzed CMAPs induced by pairs of stimuli of equal strength delivered to the posterior structures of the lumbosacral cord at different intervals.

Figure 3.3 shows a representative example of responses to pairs of stimuli with different interstimulus intervals (ISI) derived from the quadriceps muscle (subject 1). Arrows mark the onsets of stimulus pulses. The stimulus strength of the pairs of stimuli was increased in steps of 1 V from threshold level (4 V, top row) to 50% higher voltages (6 V, bottom row). The first stimulus evoked a pronounced CMAP regardless of the interstimulus intervals and can be considered as a control response. At 4 V the second stimulus applied after an interstimulus time of 56 ms only evoked a weak response. The CMAP amplitude of this test response was 7% of the control response magnitude. At the same interstimulus time, but higher strengths of epidural stimulation the second stimulus was capable of inducing a

CMAP with an amplitude nearly as large as the first one. At a stimulus strength of 4 V and an interstimulus interval of 20 ms, the second pulse completely failed to elicit a muscle response, while a second response occurred again when the stimulus voltage was increased.

Thus, the refractory behavior of epidurally evoked muscle responses to pairs of stimuli did not only depend on the interstimulus interval but also on the stimulation strength. At threshold level we found long refractory periods of up to 47.5 ms (subject 1) and even 62.5 ms (subject 3). The shorter the interstimulus intervals were, the lower were the test response magnitudes, with 20 ms being the earliest point for the second stimulus to result in unequivocal CMAPs. At intervals shorter than 20 ms the presence of the final deep positive potential of the first CMAP introduced difficulties in interpreting the decrease in amplitude of the second response.

Figure 3.3 demonstrated that a single stimulus pulse and the corresponding response has long-lasting, stimulus-strength dependent conditioning effects on the excitability of the activated structures.

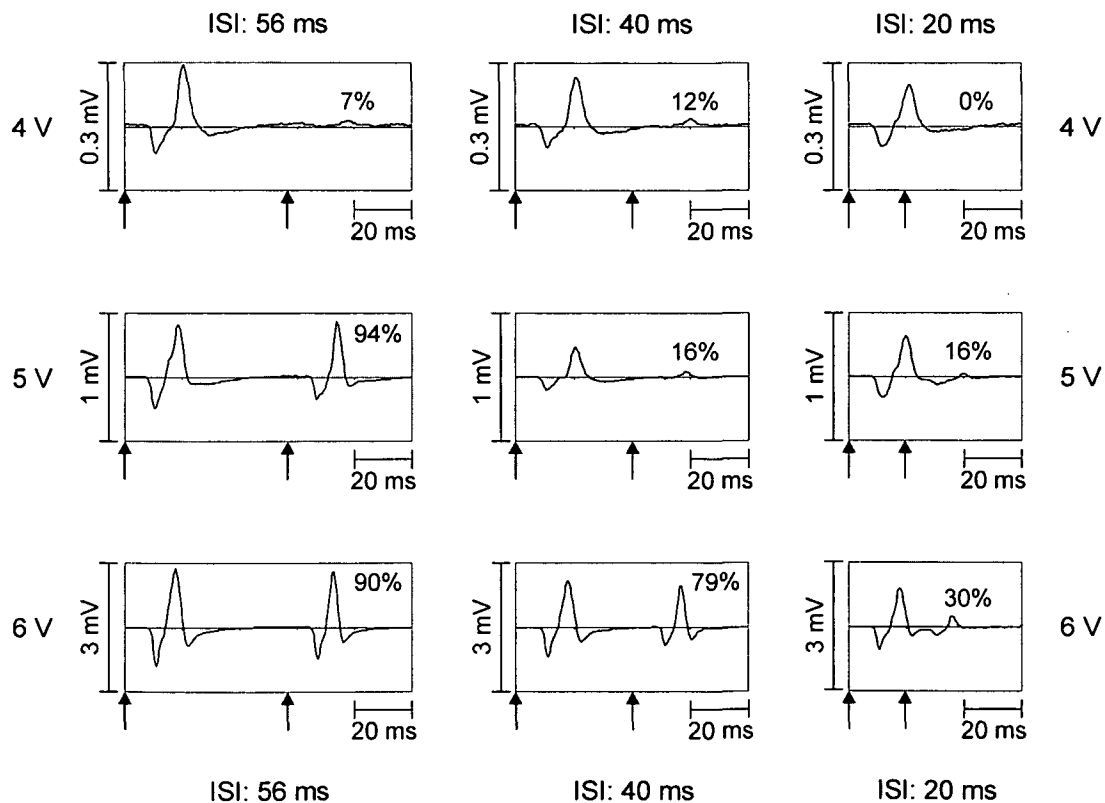


Figure 3.3 EMG potentials of quadriceps (subject 1) induced by pairs of stimuli delivered at different intervals and stimulation strengths

The arrows indicate the onset of each stimulus pulse. Interstimulus intervals (ISI) of 56 ms (18 Hz), 40 ms (25 Hz) and 20 ms (50 Hz) were tested. Stimulation strength was increased from threshold level (4 V) to 150% of the threshold (6 V) in steps of 1 V. The percentage value in each box gives the EMG amplitude of the second response relative to the first response.

Stimulation with trains of stimuli

Figure 3.4A displays EMG recordings and goniometer traces derived from subject 7 during stimulation at 6 Hz (*i*) and 31 Hz (*ii*) without departing from the same sustained and non-patterned mode of input application to the same spinal cord level. Stimulation strength was 10 V, the estimated functional segmental level of the cathode was L3/L4. At the onset of the recordings shown on the left side, the subject's lower extremities had been passively moved to the point of maximum possible flexion, and stimulation was subsequently applied at 6 Hz. The sustained stimulation initiated and maintained an extension movement of the lower limbs. The recruited muscles were visibly contracting briefly, with the tonic EMG output in hamstrings and triceps surae being greater than in their antagonists. During the actual extension movement unfolding from the initially flexed position of the lower limbs the EMG pattern revealed well-defined temporal modulations that were directed toward knee joint stabilization. Thereby the EMG activity in hamstrings progressively decreased while the one in quadriceps increased. When the endpoint of the movement was reached, and the stimulation was sustained, the limbs remained in the extended position, with the muscles visibly contracting. When the electrical stimulation was turned off, the lower limb muscles relaxed immediately.

We studied this finding that epidural stimulation of the human lumbar cord isolated from brain control can induce a sustained extension of the lower extremities in more detail in five of our subjects (subjects 2, 4, 6, 7, 9). Stimulation at 5–15 Hz and 6–10 V applied to the lumbar cord reproducibly elicited the characteristic temporal pattern of EMG-amplitude relations between antagonistic muscles and led to lower limb extension in all five subjects. The induced extension pattern was observed in different trials. The consistency of this finding only depended on application of the appropriate stimulus parameters.

On the right side of the Fig. 3.4A it is demonstrated that by increasing the frequency of the stimulus train to 31 Hz, the previous modulated-tonic EMG activity was replaced by a rhythmical one (*ii*). The EMG recording revealed alternating phases of burst-style activity in the recruited lower limb muscles. While this is not the best example of an induced stepping-like activity (co-activation of TA and TS), both recordings (*i*) and (*ii*) were made during a single session in the same subject without changing the site or strength of stimulation. From this observation it was clear that the spinal cord isolated from supraspinal input was capable of shaping both a motor output with extensor muscles dominating over the flexors and rhythmical reciprocal activation of flexors and extensors in response to sustained stimulation. The stimulation frequency determined which type of induced motor activity was established.

The finding that epidural lumbar cord stimulation can generate stepping-like EMG activity was studied in our pool of subjects. Stepping-like, alternating flexion/extension movements in the lower limbs were repetitively initiated in different recording sessions, which were up to several months apart in a given subject and also in different subjects. Optimal parameter settings were 25–50 Hz and 6–10 V. The cathode site had to provide a dominant stimulation of the upper lumbar cord. Lower thresholds for recruitment of quadriceps than of triceps surae characterized such a location (see Fig. 3.2A). Moreover strengths had to be above the level for eliciting CMAPs in quadriceps as well as triceps surae for a given cathode location. Stimulation commonly induced unilateral stepping-like flexion/extension movements. Similarly, in about 2/3 of all analyzed cases in our subject pool, a unilateral muscle twitch distribution at threshold stimulation level was observed, indicating asymmetric position of the epidural electrode array relative to the spinal cord. Stepping-like

movements of the side associated with the lower thresholds were induced. The contralateral lower limb responded either with tonic activity or with synchronous burst-style co-activations of all studied muscles of this limb.

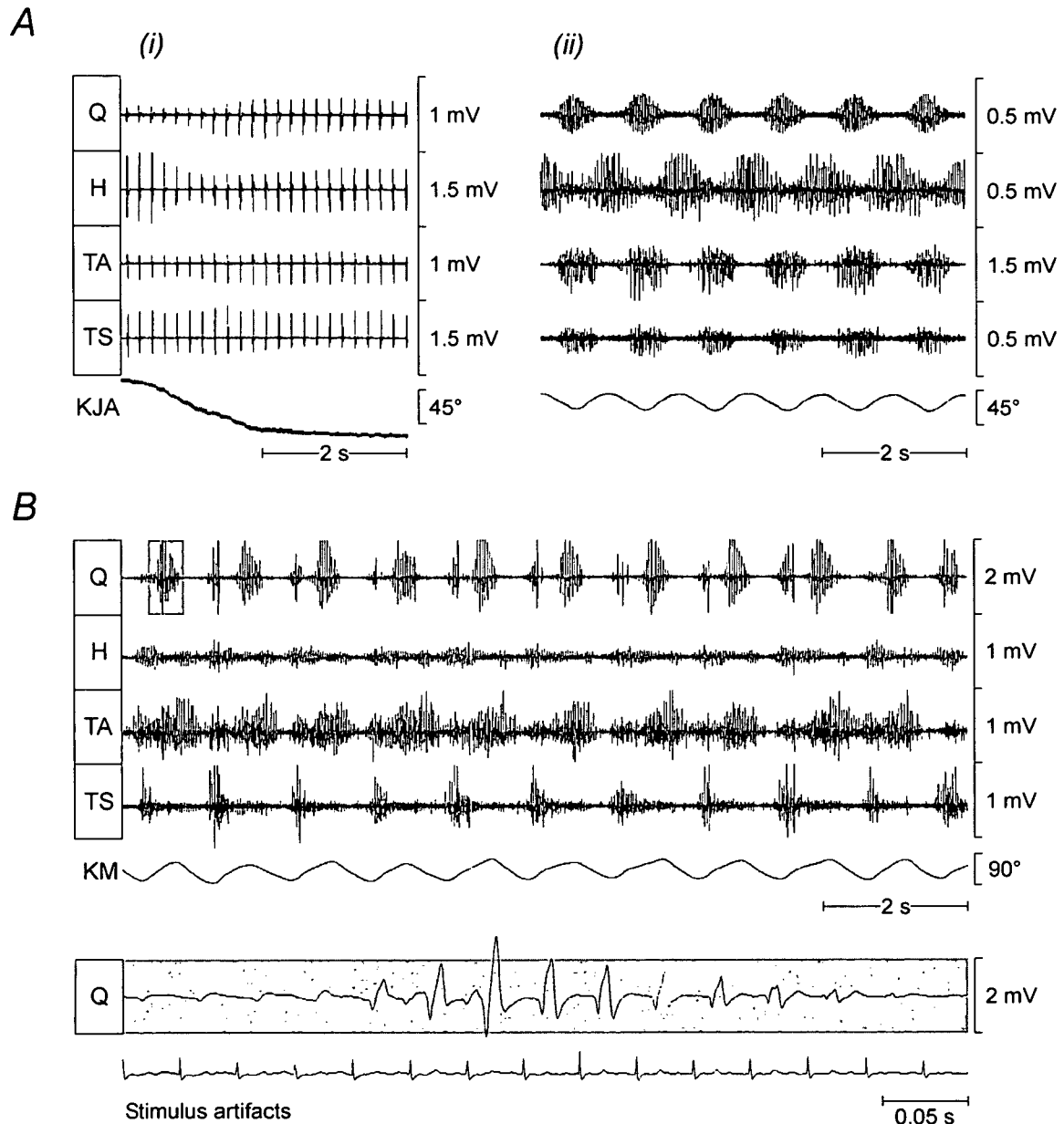


Figure 3.4 EMG responses to trains of stimuli showing characteristic modulations of CMAP-amplitudes

A, EMG recordings from quadriceps (Q), hamstrings (H), tibialis anterior (TA), and triceps surae (TS) during spinal cord stimulation at 6 Hz (*i*) and 31 Hz (*ii*). The goniometer traces (KJA – knee joint angle) illustrate the corresponding induced extension and rhythmical lower limb movements, respectively. The position of the cathode (estimated segmental level: L3/L4) and the stimulation strength (10 V) were left unchanged when switching frequencies. *B*, surface EMG recordings from the right Q, H, TA, and TS; position sensor trace demonstrating flexion/extension movements of the knee (KM). The segmental cathode level was at L4/L5. Stimulation parameters were 9 V and 30 Hz (subject 8). The first burst-style phase of Q marked by gray background is shown in extended time scale on the bottom of the original EMG along with stimulus artifacts captured by electrodes placed over the lumbar paraspinal trunk muscles.

During two seconds of recording shown in Fig. 3.4A(i), twelve separate CMAPs in each muscle were elicited (see the time marker). Thus, a single CMAP was elicited by each stimulus pulse of the 6 Hz-train which induced the characteristic EMG-extension pattern. These consecutively elicited separate CMAPs resulted in the small deflections superimposed on the overall trace of the goniometer recording in Fig. 3.4A(i). Figure 3.4B presents surface EMG recordings from the right quadriceps (Q), hamstrings (H), tibialis anterior (TA), and triceps surae (TS) and position sensor recordings showing knee flexion/extension movements (subject 8). The rostrocaudal cathode site was at the T12/L1 intervertebral level, the functional segmental level about L4/L5. Stimulation parameters were 9 V and 30 Hz. The EMG traces demonstrate alternating phases of burst-style activity in the lower limb flexor and extensor muscles. The corresponding position sensor trace confirms that the induced muscle activity led to actual stepping-like flexion/extension movements of the lower limb. Deflection up indicates flexion and deflection down indicates extension of the lower limb. The range of knee movement was about 65°.

At the bottom of Fig. 3.4B the first of the burst-style phases of quadriceps is displayed in extended time scale along with corresponding stimulus artifacts derived from the paraspinal muscle, which indicate the onsets of the stimulus pulses. It can be clearly seen that each pulse of the stimulus train triggered a single CMAP. Thus, the burst-style phase consisted of stimulus-triggered, separate CMAPs that were subject to well-defined amplitude modulations resulting in a burst-like shape of the EMG activity. Another example of this finding was demonstrated for triceps surae in Fig. 3.1C (bottom figure).

In Fig. 3.5 we compare the EMG features of single CMAPs in response to stimulation with different repetition rates and during different phases of induced rhythmic motor activity. Fig. 3.5A is a stimulus-triggered sequential presentation of CMAPs induced in tibialis anterior by sustained epidural stimulation (subject 1). All CMAPs were recorded during a single session. Stimulation strength was 5 V and constant when frequency was varied. The functional segmental cathode position was L3/L4 and identical in all cases. Ten successive CMAPs are shown for a given repetition rate. Stimulus trains with frequencies of 2.2, 11, and 16 Hz induced tonic EMG activity, whereas at 22 Hz a pattern with slow rhythmical amplitude modulations was evoked. CMAPs elicited at 2.2 Hz had a short, constant latency of 16 ms and rather similar shapes and amplitudes. CMAPs composing the activity in response to a ten times higher frequency of stimulation had a distinctly longer and fairly constant latency of 23 ms. The early negative and positive potential of the CMAPs induced at 2.2 Hz were absent, while additional EMG-components with longer latencies emerged. Analyzing the CMAPs constituting the tonic EMG patterns elicited at 11 Hz and 16 Hz revealed transitional stages between the “short-latency” response to 2.2 Hz stimulation and the “long-latency” response to 22 Hz stimulation. This becomes obvious when ten successively elicited CMAPs were averaged and compared (right side of Fig. 3.5A). By increasing the frequency from 2.2 Hz to 11 Hz, the “short-latency” response decreased in amplitude while small-amplitude late potentials were building up. At 16 Hz the early components of the CMAP were further attenuated and the late components further enhanced. Further decrease of the early components and a dominating contribution of the later ones lead to the CMAP shapes as seen in response to 22 Hz stimulation.

Figure 3.5B displays a continuous EMG of tibialis anterior responses showing three burst-style phases induced by stimulation with 7 V at 28 Hz (trace with corresponding right scale bar). The data is derived from subject 4. The displayed EMG activity is part of a recording of an epidurally induced flexion/extension movement of the lower limb. The burst-style

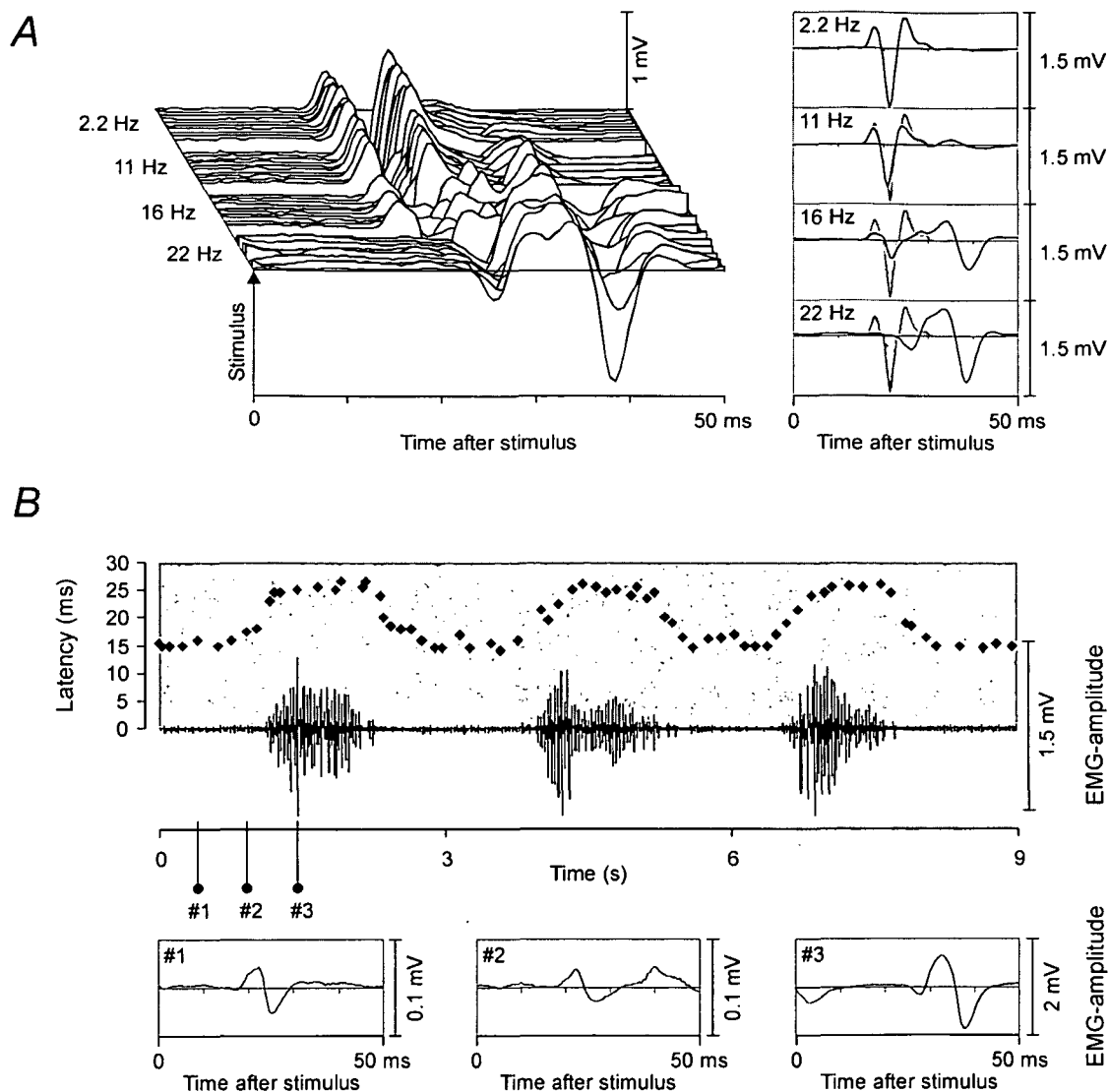


Figure 3.5 Changes of reflex pathways due to increased repetition rates of the sustained stimulation and during induced rhythmic EMG activity

A, Stimulus-triggered sequential presentation of CMAPs induced in tibialis anterior by epidural stimulation at a constant strength of 5 V but different frequencies (subject 1). Cathode position was identical in all cases. Ten single EMG potentials of successive muscle responses are shown for a given stimulation frequency. Averaged responses derived from the respective ten single responses are displayed on the right side of the figure. A template based on the response to 2.2 Hz stimulation is used to indicate changes of the CMAP shape when different frequencies were applied. *B*, Continuous EMG of tibialis anterior responses showing three burst-style phases induced by stimulation with 7 V at 28 Hz along with the latencies of identified separate CMAPs (subject 4). Three single CMAPs evoked before (#1 and #2) and during (#3) the first burst-style phase are displayed in extended time scale at the bottom of the figure.

phases alternated with phases of small amplitude responses allowing the identification of CMAP latencies during the different phases and the transitions between them. The measured latencies are indicated by black diamonds in the figure and are placed in accordance to the times the corresponding CMAPs were initiated (diagram with left scale bar and same abscissa as the EMG trace). The latencies are shown for every third/fourth

single stimulus-evoked CMAP (72 out of 243 successively evoked CMAPs within the displayed 9 s-trace). The missing data points did not differ from the presented relation. While the CMAP latencies were 15–17 ms during the phases with small amplitude responses, they increased significantly to 25–27 ms during the burst-style phases. Thus, CMAP amplitudes as well as latencies were subject to modulations during induced rhythmic activity. Three single EMG responses are presented in extended time scale showing characteristic CMAP shapes during the different phases of the rhythmic EMG activity at the bottom of the figure. The left margins of the 50 ms-time windows indicate when a stimulus was applied. The first CMAP (time marker #1) was elicited between two burst-style phases. It was of small amplitude and had a short latency of 16 ms. The third CMAP (#3) was the one with the largest amplitude during the first burst-style phase, where each pulse of the train elicited a separate CMAP. The displayed CMAP had a latency of 25 ms. Its shape was similar to the tibialis anterior CMAPs in response to 22 Hz depicted in Fig. 3.5A. Because the timeframe covering both the prolonged response latency and the CMAP duration is longer than the interstimulus interval (36 ms), the final negative potentials of the immediately preceding response is seen at the beginning of the time window (covering the first 10 ms). The second CMAP (#2) displayed in extended time scale was elicited between the two time markers #1 and #3 and incorporates both the component of the short latency CMAP and also additional later potentials.

We found that the short-latency CMAP as described in Fig. 3.2 was followed by later EMG components or was even completely replaced by a longer latency CMAP when stimulation frequencies of about 16 Hz or more were used. They were observed consistently when rhythmic EMG activity was induced in the lower extremities. Indeed, in different cases of epidurally evoked rhythmic EMG activity the pattern of CMAP latency prolongation was dissimilar. In some cases only the tibialis anterior muscle showed the longer latency response, in others tibialis anterior and triceps surae, or only the muscle groups functionally acting as flexors showed the longer latency responses. In some cases (subject 7) the stimulus-coupled CMAPs of all recorded lower limb muscles demonstrated prolonged latencies. Analyzing the basis of these differences was beyond the scope of this study. The longer CMAP latencies were prolonged by about 10 ms compared to the CMAPs elicited at 2.2 Hz. An example of a longer latency response induced in the triceps surae muscle was shown in Fig. 3.1C (bottom figure).

To summarize, we have shown that epidural stimulation applied to the same cord segments can evoke two distinct patterns of EMG activity in the lower limb muscles: (i) characteristically modulated tonic EMG activity appropriate to initiate and maintain extension of the lower extremities and (ii) burst-style EMG activity in flexors and extensors that appeared in appropriate sequences for rhythmic flexion and extension movement. Inducing these patterns was a function of different repetition rates of the applied train of electrical stimuli. Decomposing the EMG “interference patterns” into their fundamental physiologically related components was possible by extending the time scales of the analyzed EMG sequences. During the different induced EMG-patterns and even during burst-style phases each pulse within the stimulus train triggered a separate CMAP.

DISCUSSION

Directly stimulated structures which should be considered as inputs resulting in the CMAPs

We have shown that epidural stimulation can evoke different patterns of lower limb muscle activation. Inducing these patterns was a function of different repetition rates of the delivered sustained stimulation. At low frequency of 2.2 Hz amplitudes of stimulus-evoked CMAPs were determined by the stimulus strength. When the lower limbs were passively moved to the point of maximum possible flexion and trains of stimuli were applied at 5–15 Hz, an extension movement was induced and maintained (Jilge *et al.* 2001; Dimitrijevic *et al.* 2002; Jilge *et al.* 2004). Successively elicited CMAPs showed characteristic amplitude modulations with a stronger motor output of the extensor muscles than of the flexors. Stimulation at 25–50 Hz induced alternating burst-style EMG activity in flexors and extensors leading to stepping-like flexion/extension movements. Stimulation at even higher frequencies of 50–100 Hz decreased the muscle tone of the lower limbs (Pinter *et al.* 2000). These patterns could be elicited with a single cathode placed over the upper lumbar segmental levels without changes of position (Fig. 3.4A, (i) and (ii)). Which neural structures have directly been activated by the electrical stimulation resulting in the described muscle activities?

Direct activation of motoneurons – thus bypassing the spinal cord – can be ruled out because this could not account for the specific amplitude modulation of CMAPs during stimulation with constant parameters as presented in the Figs. 3.4 and 3.5. Moreover, CMAPs studied with pairs of stimuli had long refractory periods of up to 62.5 ms. In contrast, direct activation of ventral root motor fibers or motoneurons in the ventral horn follow a stimulus pulse train up to 100 Hz (Dimitrijevic, 1983; Struijk *et al.* 1993).

Due to the dorsomedial position of the epidural electrode the sensory afferents in the dorsal roots and their axonal branches in the dorsal columns are the largest fibers closest to the cathode. These “dorsal root fibers” and “dorsal column fibers” which are part of the same afferent fiber system are the most apparent among the various possible neural targets. Since it is unlikely that neurons or axons other than these are stimulated (Holsheimer, 2002) or contribute to the muscle activation (Hunter & Ashby, 1994), we will discuss if stimulation of dorsal roots or dorsal columns may explain the segmental-selective effect of the stimulation as described in Fig. 3.2. There we demonstrated different recruitment orders of the L2–L4 innervated quadriceps and the L5–S2 innervated triceps surae muscles depending on the rostrocaudal cathode position of the stimulating electrode array. L2–L4 segments had lower stimulation thresholds than L5–S2, when the cathode was at upper lumbar cord levels, while the situation was reversed when the cathode was located at the level of the conus medullaris.

The population of axons within the posterior columns at any spinal level arises from the posterior roots of numerous segments, both rostral and caudal to that level. Thus the effect of posterior column stimulation can be expected to be general rather than localized to afferents of any specific segmental origins. Hunter and Ashby (1994) reported that epidural stimulation of the posterior column at thoracic cord levels resulted in non-selective activation of motoneurons in thigh and leg muscles. Further indication that stimulation of posterior column fibers is not segmentally-selective comes from the application of spinal cord stimulation in chronic pain management basing on reports of the distribution of paresthesiae of patients with intact sensory functions. There, medially placed electrodes

elicit a widespread distribution of paresthesiae in body areas at the spinal level of stimulation and far caudally to it, even at the perception threshold (He *et al.* 1994). The widespread distribution of paresthesiae is attributed to activation of the posterior column fibers (Barolat *et al.* 1993).

The most rostral cathode levels from which CMAPs could still be induced at maximum pulse intensity (10 V) were T10/T11 vertebral levels for quadriceps and T11/T12 for triceps surae. The latencies of the CMAPs were approximately half that of the phasic stretch reflexes of the respective muscle groups (Table 3.2) and did not depend on the rostrocaudal level of the active cathode. Guru and colleagues (1987) and Hunter and Ashby (1994) reported recruitment of thigh and leg muscles by epidural stimulation with cathodes located at positions as rostral as the T8–T10 vertebral levels. At these cathode levels the cord segments and associated roots innervating the lower limbs and particularly the calf muscles are located well below the cathode. The latencies reported in these studies were generally about 6–12 ms longer than those of the comparable muscles compiled in our Table 3.2.

We conclude that the CMAPs described by us are not related to posterior column fiber activation. Thereby, our results do not contradict the findings of Guru *et al.* (1987) and Hunter and Ashby (1994). The differences of the effects of stimulation are most probably due to the different subject profiles, electrode setups and anatomical situation of the spinal cord and roots at the different levels of the epidurally placed electrodes. The subjects included in the above cited studies had spinal cord stimulators implanted for the treatment of pain. They had volitional control over the lower limb muscles. Moreover, four different electrode set-ups were utilized, in most cases a fine wire cathode with an uninsulated tip and a larger disc anode at the anterior abdominal wall or embedded in the paraspinal muscles. In such an electrode set-up, the surface area of the disc anode is much larger than the wire tip contact. This results in a smaller current density and less voltage drop near the anode. A larger portion of the total stimulation voltage is therefore available under the cathode, hence a stronger stimulating effect of this electrode set-up in the vicinity of the cathode. There are also significant differences in the anatomy of the thoracic and the lumbosacral spinal cord. Because of the disparity in length between the spinal cord and vertebral column, the spinal roots from lumbar and sacral segments have a much longer distance to travel prior to reaching their respective foramina of exit. Whereas cervical and upper thoracic rootlets and roots are situated nearly perpendicular to the cord, lower thoracic, lumbar, and sacral ones enter and leave the cord at increasingly more oblique angles. The entry points of lower lumbar and sacral posterior roots into the spinal cord are situated more medially than those of more rostral ones – and are thus nearer to a dorsomedially positioned cathode. Finally, most of the circumference of the lower lumbar and sacral cord is covered by the roots (Wall *et al.* 1990). For epidural stimulation, thresholds of fibers within the lumbosacral cord will presumably be increased due to this poorly conducting “root-layer”.

Geometric and electric factors result in low-threshold sites for electrical stimulation where posterior root fibers enter the spinal cord. These low-threshold sites are created by a sudden change of the generated potential distribution along the afferent fibers at the interface between nerve rootlet and cord owing to the different electrical conductances of the cerebrospinal fluid and the spinal cord (Geddes & Baker, 1967; Holsheimer, 2002). This inhomogeneity is added to by the acute caudal angle of the lumbosacral nerve roots with the bend of the fibers as they enter the cord. The low-threshold sites were predicted by computer simulation (Coburn, 1985; Struijk *et al.* 1993; Rattay *et al.* 2000) and recognized

by clinical studies (Maccabee *et al.* 1996; Troni *et al.* 1996). At these sites posterior root fibers originating caudal to the cathode can have lower thresholds than longitudinal fibers passing the level of the cathode. Naturally, the stimulus has to be applied at a sufficient strength to these structures to reach the threshold of the fiber. This can be achieved due to the high electric conductivity of cerebrospinal fluid and the higher longitudinal than transverse conductivity of the white matter, which allows the current to spread in a rostro-caudal direction. In this way, recruitment of posterior root fibers is not limited to the level of the cathode. Computer simulation of the epidural electrode set-up as used in the present study showed that the largest posterior root fibers entering the cord caudally to the level of the cathode could still be activated by a maximum stimulation voltage of 10 V at a distance up to 2 cm (Rattay *et al.* 2000).

We conclude that the stimulus-evoked CMAPs as described in our study are reflexively elicited by a dominating input via large afferents within the posterior roots. Depending on the relative rostrocaudal position of the effective cathode with respect to a given posterior root fiber we suggest two different sites of the initiation of afferent volleys in the posterior roots. For cathode positions at upper lumbar cord levels, lumbar posterior root fibers entering the cord in the vicinity of the cathode will have lowest thresholds and will be predominantly recruited at their low-threshold sites. Increasing the stimulation intensity will result in stronger afferent volleys to upper lumbar cord segments and a current spread in the caudal direction inducing muscle responses via posterior root recruitment at the low-threshold sites distant from the cathode. This mechanism can explain the exemplary result in Fig. 3.2A, which is characteristic for cathodes at L2–L4 cord levels. For cathode positions at L1 and lower thoracic segmental levels (T11 and T10 vertebral body levels), CMAPs can still be induced in L2–L4 innervated thigh muscles. However the current spread in the caudal direction is not strong enough to activate posterior roots at any greater distance. These structures are beyond the effective caudal range of the applied bipolar electrode.

Lumbosacral posterior root fibers entering the cord more than 2 cm rostral to the cathode will be excited at the level of the cathode (Rattay *et al.* 2000) where their trajectories are mainly oriented in rostrocaudal direction and pass the cathode within a few millimeters. At the level of the conus medullaris, all segments with afferent fibers coming from the lower limb muscles are represented by posterior root fibers and are organized in layers, which are separated in a posteromedial-anterolateral direction (Wall *et al.* 1990). Considering that all posterior root fibers are mainly oriented in same rostrocaudal direction different thresholds will be predominantly determined by different cathode-fiber distances (for a given fiber size). Due to a larger distance of the L2–L4 posterior roots than the S1 and L5 posterior root fibers to a dorsomedially positioned cathode (Wall *et al.* 1990), it is plausible that stimulation of these structures can explain the reversed recruitment order of the characteristic case shown in Fig. 3.2B.

We also propose that the posterior root fibers were the input structures resulting in the more complex motor output patterns at higher stimulation frequencies. First, the directly stimulated long axons within the posterior roots can easily follow the applied frequencies which were effective to induce the sustained extension or rhythmic flexion/extension movements (5–50 Hz). Secondly, stimulation at higher frequencies which induced coordinated flexion/extension movements in the lower limbs also showed the segmentally-selective recruitment of muscle responses as presented in Fig. 3.2. Dimitrijevic and colleagues (1998a) showed surface EMG recordings from stimulus-evoked activity in the

left quadriceps, adductor, hamstrings, tibialis anterior, and triceps surae muscles derived from subject 10 of the present study. The effective cathode of the epidural electrode array was located at an upper lumbar cord level. The stimulation frequency was 25 Hz and constant, while the stimulation strength was progressively increased from 3.5 V to 5 V in 0.5-Volt steps during the continuous recording. At the threshold level of 3.5 V, low-amplitude tonic EMG activity was first induced in the L2–L4 innervated quadriceps and adductor muscles without activating the leg muscles, which required 4.5 V to respond with tonic activity. Another increase in stimulation amplitude to 5 V replaced the tonic EMG activity with rhythmic EMG activity in the recruited lower limb flexor and extensor muscles and initiated flexion/extension movements. We have provided evidence that this segmentally-selective stimulation indicates that the evoked muscle activity was initiated in the posterior roots. Finally, we demonstrated that each single stimulus of the applied train, which induced the characteristic EMG-extension pattern, elicited a single CMAP (Fig. 3.4A(i)). During stimulus-evoked "burst-style" EMG phases each stimulus was followed by a CMAP (Fig. 3.1C, bottom; Fig. 3.4B; Fig. 3.5B, CMAP #3). Shape and duration of these CMAPs were similar to those evoked at 2.2 Hz.

We suggest that the muscle responses to epidural stimulation of the posterior lumbosacral cord disconnected from supraspinal structures are initiated in the posterior roots independently of the applied frequencies of 2.2–50 Hz. We propose that the sustained input via the posterior roots not only affects monosynaptic excitatory action on motoneurons but concomitant activation of spinal interneurons by synaptically evoked depolarization. At particular repetition rates of stimulation these activated populations of spinal interneurons act as functional units which exert defined facilitatory and inhibitory influences on various motoneuron pools (see below).

Epidural stimulation induces Posterior Roots Muscle Reflex Responses

We have demonstrated that the posterior roots are the predominant input structures for the observed twitch responses to 2.2 Hz stimulation. Feline (Lloyd, 1943) and human (Magladery *et al.* 1951) studies showed that electrically induced afferent volleys via the lowest-threshold fibers of the posterior roots secured two-neuron-arc reflex discharges. Considering that the fibers with the largest diameter have the lowest thresholds, the direct action on motoneurons must be due to group-Ia fibers. Furthermore, Lloyd (1943) showed that monosynaptic group-Ia reflex discharges almost reach their full value even with considerably submaximal posterior root volleys. Major intensification of later, multineuron-arc discharges occurs only after the stage of maximum monosynaptic discharge has been reached. The central latencies of pure cutaneous nerve-ventral root reflex discharges are about 2 ms longer (Lloyd, 1943). These discharges are irregular and last longer. The CMAPs as described in our results showed mainly increased amplitudes at suprathreshold strengths, while no other later potentials were built up.

We conclude that the muscle responses elicited in the present study by epidural stimulation at 2.2 Hz were due to activation of large group-Ia primary spindle afferents within the posterior roots with subsequent recruitment of motoneurons through monosynaptic connections in the spinal cord. This mechanism can explain the short and constant latencies of the recorded muscle responses (Fig. 3.2, Table 3.2). Thus the muscle responses at 2.2 Hz are the physiological equivalent of the H-reflex elicited at the peripheral nerve. The essential difference is that the reflex induced by epidural stimulation is initiated at a more proximal site in the posterior roots—hence a short segment of the afferent arc must be

traversed to elicit the reflex. It has been demonstrated previously that the soleus H-reflex can be evoked by electrical stimulation of the S1 nerve root (Ertekin *et al.* 1996; Zhu *et al.* 1998). Troni and colleagues (1996) reported that soleus H and M responses could be elicited by high-voltage percutaneous stimulation at different sites over the lumbar vertebral column. They suggested that posterior and anterior roots were activated by the stimulation procedure precisely at the points where they enter and exit the spinal cord, respectively. Maccabee *et al.* (1996) elicited soleus H and M responses to magnetic stimulation of the cauda equina and observed stable response latencies despite movement of the magnetic coil. They proposed that responses to stimulation occur at fixed low-threshold sites such as the hot spots resulting from the bend of the posterior roots at their entry point into the spinal cord. It was also reported that by stimulation of the lumbosacral roots and the cauda equina responses of lower limb muscles other than of the soleus can be obtained (Maertens de Noordhout *et al.* 1988; Ertekin *et al.* 1996).

We hereinafter refer to this type of reflex responses arising from a dominating input via large afferents within the posterior roots as Posterior Roots Muscle Reflex Responses (PRMRRs). Afferents other than group Ia primary spindle afferents – like Ib afferents from Golgi tendon organs, cutaneous afferents or group II secondary muscle afferents – seem not to contribute to the reflex responses to 2.2 Hz stimulation. This does not mean that some of these afferents are not activated by the stimulation within the posterior roots and the superficial regions of the posterior columns (Holsheimer, 2002). Some of the afferents within the posterior roots with smaller diameters and therefore higher thresholds than group Ia fibers might contribute to shape the motor output when stimulated repetitively at higher frequencies.

Posterior Roots Muscle Reflex Responses and induced central effects

Any single pulse of the applied trains of electrical stimuli can be considered as a test stimulus. Conditioning inputs are then induced by trains of electrical stimuli applied to the cord by the epidural electrode prior to the arbitrarily chosen test stimulus. The EMG features of the elicited test response reveal conditioning effects on the excitability of the PRMRR pathways. Testing the spinal cord circuitries with 2.2 Hz stimulation demonstrated a functional resting state of the spinal interneurons, which receive inputs from the directly stimulated afferents. In this way stimulation at 2.2 Hz established a reflex organization, which routed the afferent impulses through monosynaptic pathways without engaging central components of the “simple” stretch reflex (Clarac *et al.* 2000).

When pairs of stimuli were applied in close succession the second response was influenced by the ongoing activity of the first response (Fig. 3.3). This refractory behavior of pairs of epidurally evoked reflex responses depended on the interval between the applied stimuli and also on the stimulation strength. The stimulus-strength dependent range of the refractory periods of dual PRMRRs (20–62.5 ms) can presumably be ascribed to effects of the first volley activating spinal interneuronal structures and corresponding presynaptic mechanisms involved in the control of the motor output.

Activation of central mechanisms was apparent when sustained trains of 5–100 Hz were used instead of pairs of stimuli. At 25–50 Hz the successively elicited, separate CMAPs were subject to well-defined amplitude modulations resulting in burst-like envelopes of the EMG activity (Fig. 3.1C, bottom; Fig. 3.4A(ii); Fig. 3.4B). The sustained stimulation not

only activated neural structures transmitting the PRMRRs, but also recruited mechanisms involved in a well-coordinated gain control of the PRMRR pathways.

Prolongation of the PRMRR latency was another indication that the sustained epidural stimulation could activate structures other than the components of the two-neuron reflex arc. During tonic activity and during tonic motor output in the form of lower-limb extension induced at 5–15 Hz, PRMRRs with short and constant latencies were elicited like the ones observed during the “resting” spinal central state induced with trains of 2.2 Hz. Thus, the induced tonic activity is composed of stimulus-coupled PRMRRs that are primarily routed through monosynaptic pathways. At higher frequencies and under particular conditions a significant increase of PRMRR latency of about 10 ms was observed (Minassian *et al.* 2001*a,b*; Minassian *et al.* 2002). A prolongation of the central delay of the total reflex latency is the most plausible explanation. We have argued that the CMAPs are initiated at the same proximal sites in the posterior roots independent of the applied frequencies. It is assumed that variations of the afferent and efferent delay of the total CMAP latency with changes of stimulation frequency from 2.2 to 50 Hz are negligible. In Fig. 3.5*A* we have shown that the responses with the longer latency were successively built up with increased stimulation frequencies. At frequencies of 2.2–16 Hz no actual movement of the lower extremity was induced. This finding discards the notion that the latency prolongation was due to changes of geometrical relations between the muscle tissue and the recording surface electrodes during induced movements of the lower limb. Furthermore it is unlikely that the longer latencies were a result of repeated induction of muscle fatigue or refractory periods since it was shown in Fig. 3.5*B*, that prolongation of PRMRR latency was correlated with the burst-style periods during a complex motor output.

We propose that the prolongation of the PRMRR latency was due to an extended integration of central spinal PRMRR components. The epidurally initiated afferent flow was routed through polysynaptic spinal pathways opened only at frequencies higher than 15 Hz and during induced burst-style activity. A concomitant action was the suppression of the monosynaptic component of the PRMRRs during the burst-style phases (Fig. 3.5*B*). We speculate that this is accomplished by recruitment and state-dependent modulations of spinal reflexes, which are nonfunctional during the “resting” state of the lumbar interneuronal circuits. Such modifications of reflex responses have also been shown during normal human locomotion (Zehr & Stein, 1999; Capaday, 2002). Furthermore, feline studies have shown that afferents may mediate their effects on motoneurons via different routes. This is true for large group-I afferents and for smaller high-threshold afferents from muscles, joints and skin such as the “flexor reflex afferents” (FRA) that activate common interneurons (Pearson, 1995; Pearson & Ramirez, 1999; Clarac *et al.* 2000; Hultborn, 2001; McCrea, 2001). Under conditions of intact connections between lumbar cord and brain stem structures, the flow of information into and through the central FRA pathways can be controlled by supraspinal centers (Lundberg, 1979).

Posterior Roots Muscle Reflex Responses and the Lumbar Locomotor Pattern Generator

Epidural stimulation with parameters that induced rhythmic flexion/extension movements of the lower limbs elicited afferent volleys via large diameter fibers within the posterior roots. The stimulated structures are a subset of sensory fibers that are involved in peripheral feedback. During locomotion these sensory fibers transmit phasic input which enter the spinal cord via the posterior roots with spatially and temporally complex patterns. Epidural

stimulation as described in the present study elicited a sustained, tonic non-patterned input that was delivered simultaneously to several lumbar and upper sacral cord segments. Thus, the input was unlike physiological sensory information. We speculate, that – besides exerting facilitation of various motoneuron pools – the input acts as a common drive to spinal interneuronal networks located in the lumbar cord. While coming from periphery, the tonic input of particular frequencies is interpreted as a central command signal due to its code. The sustained stimuli organize lumbar spinal interneurons by temporarily combining them into functional units representing different levels of muscle synergies, parts of movements, or even more integrated motor behavior. The selection and activation of functional units dependent on the repetition rate of tonic input. While at 5–15 Hz extension activity dominates the motor output, at 25–50 Hz the balance of neural activity is shifted to generate a rhythmic motor output. Our notion is that this can be achieved due to the flexibility of operation of spinal interneuronal networks and their multifunctional character (Jankowska, 2001) and due to the connectivity of the activated large diameter sensory neurons with these networks. Hultborn and colleagues (1998) have emphasized that different reflex pathways have direct access to, or may even be part of, the central pattern generator (CPG) for locomotion in the cat. Moreover, Burke and colleagues (2001) stressed, that: “it has been known for some time that a variety of reflexes are modulated in amplitude and even reversed in sign during different phases of the stepping cycle, both in animals and man. Intracellular recordings from motoneurons during fictive locomotion have provided clear evidence that the locomotor CPG exerts powerful control of transmission through reflex pathways as assessed by phasic modulation of synaptic potentials.”

Can we conclude on the basis of the presented findings that the studied model of the human lumbar cord isolated from suprasegmental input by accidental injury has features of a CPG for locomotion? The hallmark for identification of a locomotor CPG within the spinal cord is the production of recognizable and reproducible patterns of rhythmic output in the absence of instructive external drive from higher levels of the central nervous system or from peripheral sensory feedback. So far we have demonstrated that by applying a sustained tonic input to the lumbar cord isolated from supraspinal influence, it is possible to activate and drive interneuronal networks and thereby to initiate stepping-like flexion/extension movements in the paralyzed lower limbs. To stabilize the induced motor activity, additional phasic sensory feedback from the lower limbs associated with the induced stepping-like movements was essential. This was shown in a study on the effects of temporarily reduced peripheral input when locomotor-like movements were evoked by spinal cord stimulation in paraplegics (Dimitrijevic *et al.* 1998b). While the parameters of epidural stimulation were maintained constant, it was observed that the reduced sensory feedback resulted in decreased amplitudes of the EMG activity and increased frequency of the lower limb movement. The phasic input had a timing function in the production of rhythmic movements and additionally augmented the activity of the rhythm-generating spinal circuits. We propose to consider the described capabilities of the human lumbar cord isolated from brain control and tested by repetitively induced PRMRs at 25–50 Hz as evidence for the existence of a Lumbar Locomotor Pattern Generator (LLPG). This LLPG in humans can be activated by sustained, non-patterned trains of electrical stimuli of specific repetition rate applied to the posterior roots of the upper lumbar cord segments.

Significance of the results

Repair of spinal cord injuries is a complex task for contemporary neurosciences and medical practice, and is not yet accomplished, even though the basic science of axon regeneration is making significant progress (Schwab, 2002). There are several experimental treatments for promotion of axonal regeneration in rodent spinal cord injury models but also in these models a full repair of spinal cord injury is not available (Fawcett, 2002).

On the other hand, there has been success in the clinical application of electrical stimulation to intact nerves of paralyzed limbs in order to elicit functional movements in spinal cord injured people (Dimitrijevic *et al.* 1968; Dimitrijevic & Dimitrijevic, 1992). This technique is known as functional electrical stimulation (FES). FES devices with one, two or more stimuli outputs and independent control of electrical parameters are in use in a variety of clinical protocols: in the improvement of trophic conditions of muscles after effects of disuse, suppression of spasticity, correction of single muscle group deficit within patterned, synergistic movements, enhancement of postural and volitional control in incomplete SCI individuals, restoration of externally controlled standing and walking in clinically complete SCI people, and in the restoration of muscle tissue in people with cauda equina lesion (Bajd *et al.* 1989; Kern *et al.* 2002). Working with clinical FES protocols provides opportunity for practicing physicians, clinical neurophysiologists and biomedical engineers to investigate how to use FES for generating force and functional movements in paralyzed muscles and how to apply electrical stimulation to afferents of peripheral nerves in order to modify spinal reflex activity (Dimitrijevic, 1970; Dimitrijevic & Dimitrijevic, 2002).

There is a simultaneous progress in basic research on spinal reflex circuits (McCrea, 2001), organization of inputs to spinal interneuronal populations (Edgley, 2001), flexibility of operation of interneuronal circuits and final common interneuronal pathways (Jankowska, 2001), and on central pattern generators for locomotion (Grillner *et al.* 2001).

We should appreciate these recent findings of basic scientists regarding spinal interneurons when evaluating the present human neurophysiological study of the activation of spinal networks. Populations of spinal interneurons can be organized to act as functional units by tonic afferent input. Spinal interneurons are multifunctional and can be incorporated into different larger networks which exert defined facilitatory and inhibitory influences on various motoneuron pools. This flexibility was also shown in our study. By changing the repetition rate of tonic stimulation a temporarily established pattern generator for stepping-like activity – the LLPG – was promptly converted to a pattern generator for lower limb extension.

The possibility of activating spinal networks involved in generating functional synergistic movements opens a new avenue with great potential for human neurophysiological studies of intrinsic spinal cord functional properties, and may contribute to the development of new methodologies, technologies and clinical practice for restoration of movements in SCI people.

REFERENCES

- Bajd T, Kralj A, Turk R, Benko H & Segal J (1989). Use of functional electrical stimulation in the rehabilitation of patients with incomplete spinal cord injuries. *J Biomed Eng* **11**, 96-102.
- Barolat G, Massaro F, He J, Zeme S & Ketcik B (1993). Mapping of sensory responses to epidural stimulation of the intraspinal neural structures in man. *J Neurosurg* **78**, 233-239.
- Barolat G, Singh-Sahni K, Staas WE, Shatin D, Ketcik B & Allen K (1995). Epidural spinal cord stimulation in the management of spasms in spinal cord injury. A prospective study. *Stereotact Funct Neurosurg* **64**, 153-164.
- Beric A (1988). Stability of lumbosacral somatosensory evoked potentials in a long-term follow-up. *Muscle Nerve* **11**, 621-626.
- Burke RE, Degtyarenko AM & Simon ES (2001). Patterns of locomotor drive to motoneurons and last-order interneurons: clues to the structure of the CPG. *J Neurophysiol* **86**, 447-462.
- Bussel B, Roby-Brami A, Neris OR & Yakovlev A (1996). Evidence for a spinal stepping generator in man. *Paraplegia* **34**, 91-92.
- Calancie B, Needham-Shropshire B, Jacobs P, Willer K, Zych G & Green BA (1994). Involuntary stepping after chronic spinal cord injury. Evidence for a central rhythm generator for locomotion in man. *Brain* **117**, 1143-1159.
- Capaday C (2002). The special nature of human walking and its neural control. *Trends Neurosci* **25**, 370-376.
- Clarac F, Cattaert D & Le Ray D (2000). Central control components of a 'simple' stretch reflex. *Trends Neurosci* **23**, 199-208.
- Coburn B (1985). A theoretical study of epidural electrical stimulation of the spinal cord-Part II: Effects on long myelinated fibers. *IEEE Trans Biomed Eng* **32**, 978-986.
- Dimitrijevic MM, Dimitrijevic MR, Illis LS, Nakajima K, Sharkey PC & Sherwood AM (1986a). Spinal cord stimulation for the control of spasticity in patients with chronic spinal cord injury: I. Clinical observations. *Cent Nerv Syst Trauma* **3**, 129-144.
- Dimitrijevic MM & Dimitrijevic MR (1992). Clinical practice of functional stimulation. In *Spinal Cord Dysfunction, Vol. III: Functional Stimulation*, ed. Illis LS, pp. 168-174. Oxford University Press, USA.
- Dimitrijevic MM & Dimitrijevic MR (2002). Clinical elements for the neuromuscular stimulation and functional electrical stimulation protocols in the practice of neurorehabilitation. *Artif Organs* **26**, 256-259.
- Dimitrijevic MR, Gracanin F, Prevec TS & Trontelj JV (1968). Electronic control of paralysed extremities. *Biomed Eng* **3**, 8-19.
- Dimitrijevic MR (1970). Further advances in use of physiological mechanisms in the external control of human extremities. In *Advances in External Control of Human Extremities*, ed. Gavrilovic MM & Wilson AB, pp 473-486. Yugoslav Committee for Electronics and Automation, Belgrade, Yugoslavia.

Dimitrijevic MR (1983). Neurophysiological evaluation and epidural stimulation in chronic spinal cord injury patients. In *Spinal Cord Reconstruction*, ed. Reier PJ, Bunge RP & Kao CC, pp. 465-473. Raven Press, New York.

Dimitrijevic MR, Illis LS, Nakajima K, Sharkey PC & Sherwood AM (1986b). Spinal cord stimulation for the control of spasticity in patients with chronic spinal cord injury: II. Neurophysiologic observations. *Cent Nerv Syst Trauma* 3, 145-152.

Dimitrijevic MR, Gerasimenko Y & Pinter MM (1998a). Evidence for a spinal central pattern generator in humans. In *Neural Mechanisms for Generating Locomotor Activity. Ann N Y Acad Sci Vol. 860*, ed. Kiehn O, Harris-Warrick RM, Jordan LM, Hultborn H & Kudo N, pp. 360-376. New York Academy of Sciences, New York.

Dimitrijevic MR, Gerasimenko Y & Pinter MM (1998b). Effect of reduced afferent input on lumbar CPG in spinal cord injury subjects. *Soc Neurosci Abstr* 24: Program No. 654.23.

Dimitrijevic MR, Minassian K, Jilge B & Rattay F (2002). Initiation of standing and locomotion like movements in complete SCI subjects "by mimicking" brain stem control of lumbar network with spinal cord stimulation. *Proceedings of the 4th International Symposium on Experimental Spinal Cord Injury Repair and Regeneration*, pp. 25-27, Brescia, Italy.

Edgley SA (2001). Organisation of inputs to spinal interneurone populations. *J Physiol* 533, 51-56.

Ertekin C, Mungan B & Uludag B (1996). Sacral cord conduction time of the soleus H-reflex. *J Clin Neurophysiol* 13, 77-83.

Fawcett J (2002). Repair of spinal cord injuries: where are we, where are we going? *Spinal Cord* 40, 615-623.

Geddes LA & Baker LE (1967). The specific resistance of biological material—a compendium of data for the biomedical engineer and physiologist. *Med Biol Eng* 5, 271-293.

Gerasimenko Y, McKay B, Sherwood A & Dimitrijevic MR (1996). Stepping movements in paraplegic patients induced by spinal cord stimulation. *Soc Neurosci Abstr*; 22: 1372.

Grillner S (1981). Control of locomotion in bipeds, tetrapods, and fish. In: *Handbook of Physiology. The Nervous System. Motor Control*. sect.1, vol. II., ed. Brooks VB pp. 1179-1236. Am Physiol. Soc, Washington, DC.

Grillner S, Wallen P, Hill R, Cangiano L & El Manira A (2001). Ion channels of importance for the locomotor pattern generation in the lamprey brainstem-spinal cord. *J Physiol* 533, 23-30.

Gurfinkel VS, Levik YS, Kazennikov OV & Selionov VA (1998). Locomotor-like movements evoked by leg muscle vibration in humans. *Eur J Neurosci* 10, 1608-1612.

Guru K, Mailis A, Ashby P & Vanderlinden G (1987). Postsynaptic potentials in motoneurons caused by spinal cord stimulation in humans. *Electroencephalogr Clin Neurophysiol* 66, 275-280.

He J, Barolat G, Holsheimer J & Struijk JJ (1994). Perception threshold and electrode position for spinal cord stimulation. *Pain* 59, 55-63.

Holsheimer J (2002). Which neuronal elements are activated directly by spinal cord stimulation. *Neuromodulation* **5**, 25-31.

Hultborn H, Conway BA, Gossard JP, Brownstone R, Fedirchuk B, Schomburg ED, Enriquez-Denton M & Perreault MC (1998). How do we approach the locomotor network in the mammalian spinal cord? In *Neural Mechanisms for Generating Locomotor Activity. Ann N Y Acad Sci Vol. 860*, ed. Kiehn O, Harris-Warrick RM, Jordan LM, Hultborn H & Kudo N, pp. 70-82. New York Academy of Sciences, New York.

Hultborn H (2001). State-dependent modulation of sensory feedback. *J Physiol* **533**, 5-13.

Hunter JP & Ashby P (1994). Segmental effects of epidural spinal cord stimulation in humans. *J Physiol* **474**, 407-419.

Illis LS. Is there a central pattern generator in man (1995)? *Paraplegia* **33**, 239-240.

Jankowska E (2001). Spinal interneuronal systems: identification, multifunctional character and reconfigurations in mammals. *J Physiol* **533**, 31-40.

Jilge B, Minassian K & Dimitrijevic MR (2001). Electrical stimulation of the human lumbar cord can elicit standing parallel extension of paralysed lower limbs after spinal cord injury. *Proceedings of the World Congress on Neuroinformatics Part II*, pp 281-283. Vienna, Austria.

Jilge B, Minassian K, Rattay F, Pinter MM, Gerstenbrand F, Binder H & Dimitrijevic MR (2004). Initiating extension of the lower limbs in subjects with complete spinal cord injury by epidural lumbar cord stimulation. *Exp Brain Res* **154**, 308-326.

Kern H, Hofer C, Modlin M, Forstner C, Raschka-Hogler D, Mayr W & Stohr H (2002). Denervated muscles in humans: limitations and problems of currently used functional electrical stimulation training protocols. *Artif Organs* **26**, 216-218.

Lang J (1984). Morphologie und funktionelle Anatomie der Lendenwirbelsäule und des benachbarten Nervensystems - 1. Rückenmark. In *Neuroorthopädie 2 - Lendenwirbelsäulenerkrankungen mit Beteiligung des Nervensystems*, ed. Hohmann D, Kügelgen B, Liebig K & Schirmer M, pp. 3-9. Springer, Berlin.

Lehmkuhl D, Dimitrijevic MR & Renouf F (1984). Electrophysiological characteristics of lumbosacral evoked potentials in patients with established spinal cord injury. *Electroencephalogr Clin Neurophysiol* **59**, 142-155.

Lloyd DPC (1943). Reflex action in relation to pattern and peripheral source of afferent stimulation. *J Neurophysiol* **16**, 111-120.

Lundberg A. Multisensory control of spinal reflex pathways (1979). *Prog Brain Res* **50**, 11-28.

Maccabee PJ, Lipitz ME, Desudchit T, Golub RW, Nitti VW, Bania JP, Willer JA, Cracco RQ, Cadwell J, Hotson GC, Eberle LP & Amassian VE (1996). A new method using neuromagnetic stimulation to measure conduction time within the cauda equina. *Electroencephalogr Clin Neurophysiol* **101**, 153-166.

Maertens de Noordhout A, Rothwell JC, Thompson PD, Day BL & Marsden CD (1988). Percutaneous electrical stimulation of lumbosacral roots in man. *J Neurol Neurosurg Psychiatry* **51**, 174-181.

- Magladery JW, Porter WE, Park AM & Teasdall RD (1951). Electrophysiological studies of nerve and reflex activity in normal man. *Bull John Hopkins Hosp* **88**, 499-519.
- McCrea DA (2001). Spinal circuitry of sensorimotor control of locomotion. *J Physiol* **533**, 41-50.
- Minassian K, Rattay F & Dimitrijevic MR (2001a). Features of the reflex responses of the human lumbar cord isolated from the brain but during externally controlled locomotor activity. *Proceedings of the World Congress on Neuroinformatics Part II*, pp. 267-268. Vienna, Austria.
- Minassian K, Rattay F, Pinter MM, Murg M, Binder H, Sherwood A & Dimitrijevic MR (2001b). Effective spinal cord stimulation (SCS) train for evoking stepping locomotor movement of paralyzed human lower limbs due to SCI elicits a late response additionally to the early monosynaptic response. *Soc Neurosci Abstr* **27**: Program No. 935.12.
- Minassian K, Gilge B, Rattay F, Pinter MM, Gerstenbrand F, Binder H & Dimitrijevic MR (2002). Effective spinal cord stimulation (SCS) for evoking stepping movement of paralyzed human lower limbs: study of posterior root muscle reflex responses. *Proceedings of the 7th Annual Conference of the IFESS*, pp. 167-169. Ljubljana, Slovenia.
- Murg M, Binder H & Dimitrijevic MR (2000). Epidural electric stimulation of posterior structures of the human lumbar spinal cord: 1. muscle twitches – a functional method to define the site of stimulation. *Spinal Cord* **38**, 394-402.
- Roby-Brami A & Bussel B (1987). Long-latency spinal reflex in man after flexor reflex afferent stimulation. *Brain* **110**, 707-725.
- Pearson KG (1995). Proprioceptive regulation of locomotion. *Curr Opin Neurobiol* **5**, 786-791.
- Pearson KG & Ramirez J-M (1999). Sensory modulation of pattern generating circuits. In *Neurons, Networks and Motor Behavior*, Stein PSG, ed. Grillner S, Selverston AI & Stuart DG. pp. 257-267. MIT Press, Cambridge, USA.
- Pinter MM, Gerstenbrand F & Dimitrijevic MR (2000). Epidural electrical stimulation of posterior structures of the human lumbosacral cord: 3. Control of spasticity. *Spinal Cord* **38**, 524-531.
- Rattay F, Minassian K & Dimitrijevic MR (2000). Epidural electrical stimulation of posterior structures of the human lumbosacral cord: 2. quantitative analysis by computer modeling. *Spinal Cord* **38**, 473-489.
- Rosenfeld JE, McKay WB, Halter JA, Pollo F & Dimitrijevic MR (1995). Evidence of a pattern generator in paralyzed subjects with spinal cord injury during spinal cord stimulation. *Soc Neurosci Abstr*; **21**: 688.
- Rossignol S (1996). Neural control of stereotypic limb movements, In: *Handbook of Physiology. Exercise: Regulation and Integration of Multiple Systems*, ed. Rowell LB & Shepherd JT, pp. 173-216. Am Physiol Soc, Bethesda, MD.
- Schwab ME (2002). Repairing the injured spinal cord. *Science* **295**, 1029-1031.
- Sherwood AM, McKay WB & Dimitrijevic MR (1996). Motor control after spinal cord injury: Assessment using surface EMG. *Muscle Nerve* **19**, 966-979.

Struijk JJ, Holsheimer J & Boom HB (1993). Excitation of dorsal root fibers in spinal cord stimulation: A theoretical study. *IEEE Trans Biomed Eng* **40**, 632-639.

Troni W, Bianco C, Moja MC & Dotta M (1996). Improved methodology for lumbosacral nerve root stimulation. *Muscle Nerve* **19**, 595-604.

Wall EJ, Cohen MS, Abitbol JJ & Garfin SR (1990). Organization of intrathecal nerve roots at the level of the conus medullaris. *J Bone Joint Surg* **72**, 1495-1499.

Zehr EP & Stein RB (1999). What functions do reflexes serve during human locomotion? *Prog Neurobiol* **58**, 185-205.

Zhu Y, Starr A, Haldeman S, Chu JK & Sugerman RA (1998). Soleus H-reflex to S1 nerve root stimulation. *Electroencephalogr Clin Neurophysiol* **109**, 10-14.

Chapter 4

Effect of peripheral afferent and central afferent input to the isolated human lumbar spinal cord

Summary

It has been previously demonstrated that repetitive and regular epidural stimulation of lumbar posterior roots at frequencies of 20–50 Hz can activate the Lumbar Locomotor Pattern Generator (LLPG) and induce stepping-like movements in subjects with chronic, complete spinal cord injury. In these studies, the subjects were lying in a supine position and the lower limbs were weight-supported. Afferent feedback input from load receptors of the lower limbs was minimized. The purpose of this paper is to investigate the interaction between externally induced activity of the LLPG and manually assisted, weight-bearing stepping on a treadmill in paralyzed subjects.

Two subjects with chronic, complete spinal cord injury with epidurally placed electrodes were included in this study. Epidural stimulation with 38 different parameter combinations between 1–10 V and 10–100 Hz was applied, while the same externally controlled maneuver of passive stepping movement was performed. The electromyographic (EMG) activity of the quadriceps, hamstrings, tibialis anterior and triceps surae muscles was simultaneously recorded with surface electrodes.

Peripheral sensory feedback related to assisted treadmill stepping generated EMG bursts which were characterized by low amplitudes and co-activation of muscles. When epidural stimulation was applied, 18 of the 38 studied parameter combinations induced stimulus-related EMG bursts of lower limb muscles during passive treadmill stepping, which were temporally synchronized to specific phases of the step cycle. All effective stimulation parameters were within the range of 20–50 Hz and 6–10 V. Epidural stimulation could enhance and change the patterns of rhythmic EMG activities during passive stepping. The EMG patterns in the paralyzed lower limb muscles induced by mechanical stimulation associated with passive stepping with additional epidural stimulation resembled the patterns of able-bodied subjects.

In conclusion, the LLPG could be activated by epidural stimulation of the lumbar cord in complete spinal cord injured subjects during weight-bearing, manually assisted treadmill stepping. The timing of the rhythmic motor output of the LLPG was not set to some default level, but was matched to specific phases of the manually imposed step cycle. The responsiveness of the spinal circuits to proprioceptive feedback in generating stepping-like motor patterns was significantly enhanced, when stimulation at frequencies of 20–50 Hz was applied. This effect could be achieved immediately as soon as epidural stimulation with the appropriate stimulus parameters was delivered. We conclude that the spinal lumbar networks can integrate and interpret both, the stimulus-evoked tonic input with a “central” code and the proprioceptive feedback input in order to generate effective and functional locomotor patterns. This finding suggests that epidural stimulation of the lumbar cord might

be a useful neuroaugmentative tool to support locomotor training in subjects with spinal cord injury.

INTRODUCTION

It has been previously demonstrated that sustained non-patterned electrical stimulation of the posterior lumbar spinal cord from the epidural space can induce stepping-like alternating flexion and extension movements in subjects with chronic, complete spinal cord injury (Dimitrijevic *et al.* 1998a).

Following studies provided evidence that the stepping-like movements evoked by epidural stimulation were initiated by stimulation of the lumbar posterior roots (Minassian *et al.* 2004a). During the induced burst-style EMG phases each pulse within the train of electrical stimuli elicited a separate compound muscle action potential (CMAP). The electrophysiological characteristics of these Posterior Roots Muscle Reflex Responses (PRMRRs) were described.

PRMRRs in proximal and distal lower limb muscles were shown to depend on the stimulation strength and frequency. The responses could be organized to result in either limb extension or rhythmic alternation of flexion/extension depending on the frequency of the applied stimulation (Jilge *et al.* 2004; Minassian *et al.* 2004b). During induced rhythmic movements, the PRMRRs were modulated with respect to both EMG amplitude and latency. It was proposed that lumbar interneurons can respond to particular repetition rates of tonic afferent input by temporarily combining into the Lumbar Locomotor Pattern Generator (LLPG), which modulates the transmitting pathways and amplitudes of the PRMRRs and thereby generates flexion/extension movements.

The above cited studies were based on EMG recordings of stimulus-evoked muscle responses derived from subjects lying in a supine position. Thus, spinal cord stimulation induced stepping-like movements of the lower limbs without the sensations of weight-bearing, i.e. without or with minimum afferent feedback input from load receptors.

On the other hand, it was shown that reducing phasic sensory feedback from the lower limbs associated with the stepping-like movements had a profound effect on the spinal cord stimulation-induced motor activity (Dimitrijevic *et al.* 1998b). Under constant epidural stimulation conditions, a temporary cuff applied over the thigh muscles to reduce input from large afferents (ischemia) resulted in diminishing amplitudes and increased frequency of the stepping-like movements. The phasic peripheral feedback input had a timing function in the production of rhythmic movements and augmented the activity of the rhythm-generating spinal circuits and the spinal motor pools.

Peripheral sensory input associated with manually assisted stepping over a moving treadmill belt of complete spinal cord injured subjects can generate stepping-like oscillating EMG patterns in the lower limbs (Dietz *et al.* 1995; Dobkin *et al.* 1995). Stretch reflexes are not the sole source of the phasic EMG activity induced in flexors and extensors during manually assisted stepping of the subjects (Harkema *et al.* 1997). An essential contribution of load receptor input to the generation of a locomotor pattern has been recognized in paraplegic patients (Harkema *et al.* 1997, Dietz *et al.* 2002). When assisted air stepping is performed (100% body unloading) EMG activity recorded from paralyzed lower limb muscles is reduced or absent (Dietz *et al.* 2002). Thus, a significant influence of the sensory

feedback input associated with passive weight-bearing stepping could also be expected on the EMG activity induced by epidural stimulation during assisted stepping.

If information on joint angles, displacement and loading of the lower limbs are unavailable to the LLPG, the amplitude and timing of the cyclical motor output can only be set to an arbitrary default level. To generate functional motor patterns, the LLPG has to adapt the efferent output patterns to the specific phases of the step cycle. The purpose of the present paper is to study the effect of electrical epidural stimulation with parameters set to activate the LLPG, with simultaneous assisted treadmill stepping in paraplegic subjects. Particular questions are if the LLPG can be activated during manually imposed treadmill stepping and if the LLPG can process peripheral input associated with manually assisted stepping to generate EMG bursts temporally synchronized to specific phases of the step cycle.

MATERIAL AND METHODS

Subjects

The EMG data of lower limb muscle response patterns which were made available for the present study were derived from two subjects with accidental spinal cord injury. According to the ASIA impairment scale, the subjects were sensory and motor complete (ASIA A). The subjects completed sensory-evoked potentials examinations and brain motor control assessment (BMCA) tests to rule out conductivity between the lower limbs and the brain and any voluntary activation of motor units below the level of the lesion. Stretch and cutaneomuscular reflexes were preserved below the level of spinal cord injury. Patient-related data are listed in Table 4.1.

Table 4.1 Demographic and clinical data

Subject No.	Sex	Born in	Accident in	Implantation of electrode	Type of accident	Level of SCI	ASIA Class.
1	m	1977	1994	1999	Motorbike accident	C6	A
2	f	1978	1994	1996	Car accident	T4	A

Stimulation procedure

EMG activity in the paralyzed lower limb muscles was induced by tonic or phasic stimulation of afferent fibers entering the lumbosacral cord, or by combination of the two stimulus modalities (Fig 4.1A).

Tonic input was delivered by sustained stimulation of the posterior roots of the lumbosacral cord by dorsally placed epidural electrode arrays. The stimulation provided a sustained, non-patterned input at a specific stimulus frequency to several lumbar and upper sacral cord segments simultaneously. For details of the used quadripolar electrode array (PISCES-QUAD electrode, Model 3487A, MEDTRONIC, Minneapolis, MN, USA) and the implanted pulse generator (ITREL 3, Model 7425, MEDTRONIC) see Minassian *et al.* (2004a,b) or Chapters 2 and 3.

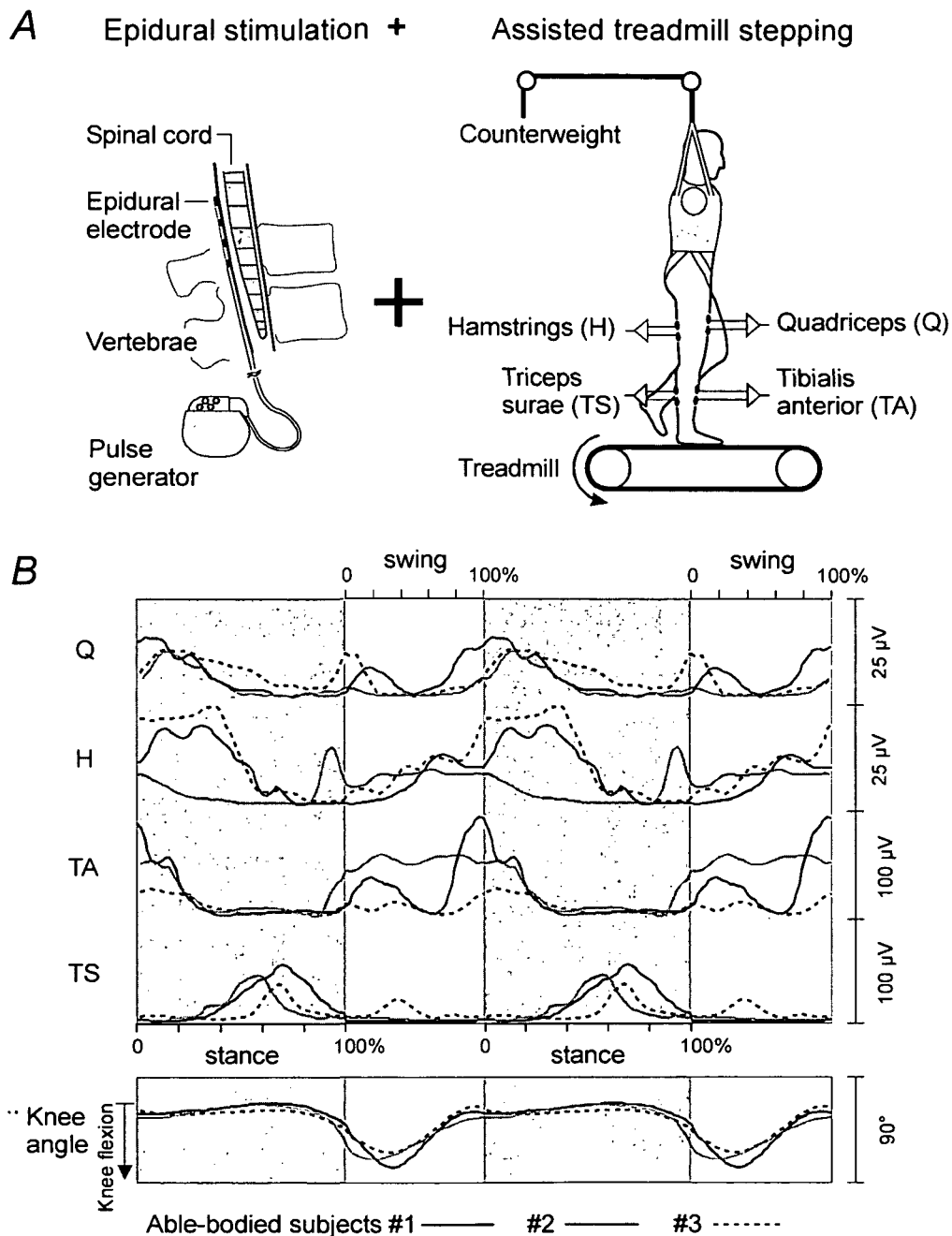


Figure 4.1 Stimulation and recording set-up

A, Tonic stimulation was delivered by an epidural electrode placed in the dorsomedial epidural space at lumbar and upper sacral cord levels. Proprioceptive input to the spinal cord is induced by assisted treadmill stepping with body weight support. Pairs of surface electrodes were placed over the bellies of the lower limb muscles to record the stimulus-induced EMG activity. *B*, Rectified and filtered EMG activity with respect to normalized stance (gray background) and swing phase of three able-bodied subjects during treadmill-stepping. Treadmill speed was 1.2 km/h (0.33 m/s), body weight support was 20 kg. Recording electrodes were placed as in the spinal cord injured subjects.

Three contact combinations of the electrode ("electrode polarity") and thirty-eight stimulation parameter settings between 1–10 V and 10–100 Hz were tested during four recording sessions (Table 4.2). The four independent contacts of the quadripolar lead were

labeled 0, 1, 2, 3, such that contact #0 was at the top and contact #3 at the bottom; 'c' means that the metal case of the implanted pulse generator was used as the indifferent electrode (Table 4.2). One data set was derived from subject 1, and three recordings from subject 2. Table 4.2 also includes information on the site of stimulation based on muscle twitch distribution patterns in supine position (Murg *et al.* 2000).

Table 4.2 Recordings and applied parameter combinations of the epidural electrode

Subject No.	No. of recording	Year of data collection	Electrode polarity	Corresponding muscle twitch thresholds (V)							
				RQ	RH	RTA	RTS	LQ	LH	LTS	LTA
1	1	2003	1+3-	2	2	3	3	3	3	4	4
2	2	1999	c+2-	-	-	-	-	-	-	-	-
			0+3-	5	5	5	5	5	5	5	5
2	3	2000	0+3-	6	4	5	5	6	5	5	5
2	4	2001	0+3-	5	4	4	4	5	4	4	4

Phasic peripheral feedback input was induced by passive, manually assisted stepping on a treadmill with partial body weight support of the subject. The generated afferent volleys are complex and correspond to the phases of passive stepping. This spatially and temporary patterned sensory feedback is similar to the one during normal walking.

Subjects wore a harness connected to an overhead support that provided a vertical constraint on the movement of the torso and reduced vertical ground reaction forces by supporting a portion of the subject's body weight. Two trainers manually facilitated the subjects' lower limbs through the step cycle. The trainers held each stepping limb distal to the patella to facilitate knee flexion during the swing phase, and knee and hip extension during the stance phase. Trainers used their other hand to hold the stepping limb proximal to the ankle during the swing phase to assist with foot lift off and placement. Each spinal cord injured subject passively stepped at a constant treadmill speed (range 0.4–0.8 km/h) and a constant level of harness support (80% of body weight).

Recording procedure

Pairs of recessed, silver-silver chloride surface electrodes were placed 3 cm apart over the midline of the muscle bellies of the quadriceps, hamstrings, tibialis anterior and triceps surae muscles. The skin was prepared by light abrasion to obtain an electrode impedance of less than 5 k Ω for each electrode pair to reduce or eliminate artifacts arising from stretching of the skin and electrode movement.

In subject 1, the EMG channels were amplified using PHOENIX amplifiers (EMS-Handels GmbH, Korneuburg, AUT), with a gain of 4664 over a bandwidth of 10–500 Hz, digitized at 1024 or 2048 Hz per channel. Due to the high gain, EMG signals were cut at ± 536 μ V. Averaged, rectified EMG activity during active treadmill-stepping derived from three able-bodied subjects and recorded with the same set-up as used for subject 1 is displayed in Fig. 4.1B.

In subject 2, the EMG signals were amplified with the Grass 12D-16-OS NEURODATA ACQUISITION SYSTEM (GRASS INSTRUMENTS, Quincy, MA) adjusted to a gain of 2000 over

bandwidth of 30–1000 Hz and digitized at 2048 Hz per channel using a CODAS ADC system (DATAQ INSTRUMENTS, Akron, OH).

A “BMCA event-marker” (a trigger signal) was used to manually mark the stance phases between heel strike and toe-off of one lower limb during assisted treadmill walking. Foot switches or foot pressure sensors were not available.

Data analysis

To find out if the induced EMG bursts were temporally synchronized with the stepping cadence and to illustrate the amount of muscle activity in relation to the phases of the step cycle, the averaged EMG activity versus normalized time was calculated.

The original raw EMG data was rectified. From these data 200 data points were calculated for each stance phase and 100 data points for each swing phase. This was done regardless of the duration of individual stance or swing phases. Thereby each calculated data point represented the muscle activity (integrated EMG) within a time interval of 0.5% of a stance or 1% of a swing phase. After this time normalization, the EMG activity of each stance phase and each swing phase consisted of the same number of data points (200 and 100). This allowed averaging the EMG activity of consecutive stance phases or swing phases.

The EMG activity of 10 stance phases and 10 swing phases was averaged separately. The result was the average muscle activity during the stance and the swing phase versus the percentage of the average stance phase duration and the average swing phase duration, respectively. For the calculations MATLAB 6.1 (THE MATHWORKS, INC., NATIC, MA) was used.

For illustration of the results, the calculated averaged muscle activity during the stance and the swing phase were placed in the order swing-stance-swing-stance to represent two step cycles (Fig. 4.1B).

RESULTS

Effect of spinal cord stimulation on lower limb EMG patterns induced during passive treadmill stepping

Figure 4.2 shows the averaged, rectified EMG activity of the right lower limb muscles with respect to time-normalized stance (marked by gray background) and swing phase. Muscle activity was induced by assisted treadmill walking without (Fig. 4.2A) and with additional epidural stimulation (Fig. 4.2B,C). Data was derived from subject 1. Without epidural stimulation, no activity was induced in quadriceps (Q), while EMG bursts temporally synchronized to the step cycle were induced in hamstrings (H), tibialis anterior (TA), and triceps surae (TS). Triceps surae activity preceded the onset of loading and was active during late swing and the whole stance phase. EMG response of hamstrings and tibialis anterior lagged triceps surae activity for about 10–20% of the swing phase duration and then mainly demonstrated co-activation with triceps surae.

When epidural stimulation was applied at 30 Hz and 6 V during passive treadmill walking (Fig. 4.2B), activity was induced in quadriceps during the whole swing phase. The EMG activity was characterized by components with high amplitudes and low frequency (10 Hz). The EMG burst reached maximum amplitudes at 40% of the swing phase. Hamstrings were mainly active during the swing phase and thus demonstrated a significant change of the

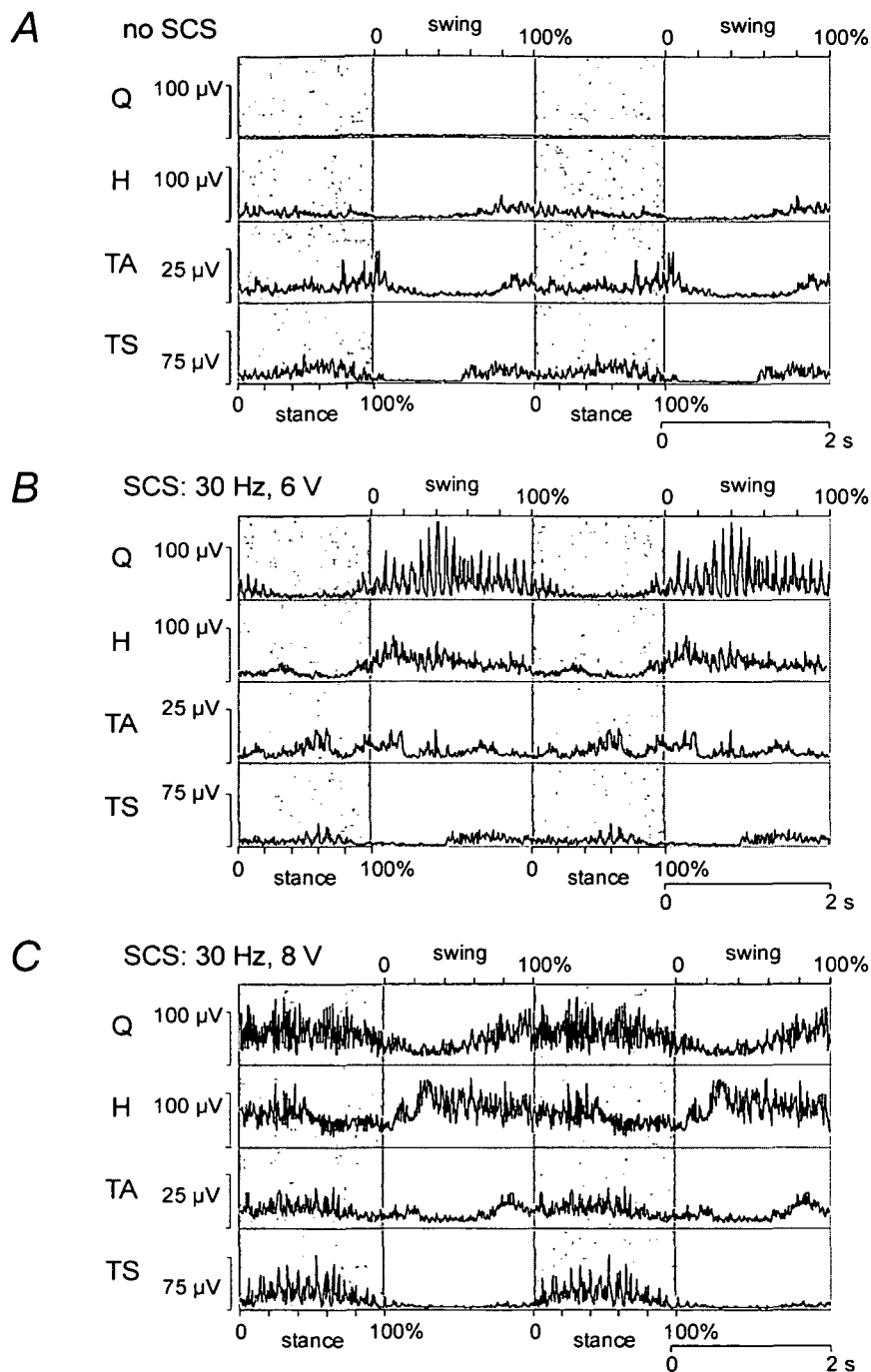


Figure 4.2 Lower limb EMG activity induced by assisted treadmill walking with body weight support (A) and additional spinal cord stimulation (B, C)

Averaged rectified EMG activity relative to normalized step cycle of quadriceps (Q), hamstrings (H), tibialis anterior (TA) and triceps surae (TS) shown for two cycles. Stance phases are marked by gray background. Treadmill speed was 0.8 km/h (0.22 m/s), body weight support was 80%. Data is derived from subject 1.

pattern compared to the trial without stimulation. Tibialis anterior did not show consistent rhythmicity of EMG activity synchronized to any specific phase of the step cycle. There was no apparent change of the triceps surae burst pattern compared to the one recorded during assisted stepping without electrical stimulation.

Increasing the epidural stimulation strength to 8 V at 30 Hz further changed the EMG activation patterns of the paralyzed lower limb muscles (Fig. 4.2C). Quadriceps bursts were prolonged and displayed EMG components evoked at a higher rate than during stimulation with 6 V and 30 Hz. Moreover, the muscle was mainly active during the stance phase and showed a minimum activation between 20 and 40% of the swing phase. During this period of minimum quadriceps activation the hamstrings burst reached highest amplitudes. The EMG burst of triceps surae was primarily present during the stance phase and contained some high-amplitude and low-frequency (10 Hz) components. Tibialis anterior displayed co-activation with triceps surae with some additional components during early and late swing. The EMG patterns in the paralyzed lower limb muscles induced by mechanical stimulation and additional epidural stimulation at 30 Hz and 8 V resembled the patterns recorded in able-bodied subjects (Fig. 4.1B) with the exception of the tibialis anterior activity during the stance phase.

Contributions of mechanical (phasic) and electrical (tonic) stimulation to the induced EMG activities

Figure 4.3 presents the effect of the onset of mechanical stimulation associated with manually assisted treadmill-stepping on the EMG activity of the quadriceps (Q) and triceps surae (TS) muscles under different initial conditions (subject 1). In Fig. 4.3A spinal cord stimulation was off and after the first four seconds of displayed recording the lower limb was manually assisted through the first swing phase. The cyclic mechanical stimulation initiated an EMG burst in triceps surae with a characteristic pattern that was synchronized with the stepping cadence and was consistently preceding the onset of the stance phase (marked by gray background). Passive stepping initially generated some low-amplitude EMG activity in quadriceps without consistent rhythmicity which did not persist more than some step cycles. Before the onset of the recording shown in Fig. 4.3B, epidural stimulation was turned on at 30 Hz and 6 V and was continuously active during the displayed 30 seconds. During supported standing before the first swing was initiated, some low amplitude ($< 30 \mu\text{V}$) CMAPs related to the epidural stimulation were present in quadriceps, while no consistent activation was detected in triceps surae. After completing the first step cycle, amplitudes of the stimulus-related CMAPs in quadriceps increased during the second swing phase. This EMG activity further increased in amplitudes, having burst-like shapes synchronized to the swing phases of the passive stepping. In triceps surae an EMG pattern similar to the one observed in the trial without stimulation was established during the assisted stepping. When epidural stimulation strength was increased to 8 V (Fig. 4.3C) and the lower limbs were not passively moved, each pulse of the 30 Hz-train evoked a single CMAP in the quadriceps muscle with a constant latency of 8 ms. The resulting EMG pattern showed some modulations but without consistent rhythmicity. There was no stimulus-evoked activity recorded in triceps surae. Additional mechanical stimulation associated with assisted stepping had a modulatory effect on the quadriceps activity. The quadriceps EMG activity solely consisted of CMAPs that could be unequivocally related to the electrical stimulation. While the lower limbs were passively moved, the amplitudes of the stimulus-evoked quadriceps-CMAPs during the early stance phases were higher than during supported standing and were attenuated during the swing phases. As in the case of the quadriceps muscle and 6 V-stimulation, 8 V-stimulation induced high-amplitude EMG activity in triceps surae but only in combination with mechanical stimulation. The muscle was solely active during the stance phases.

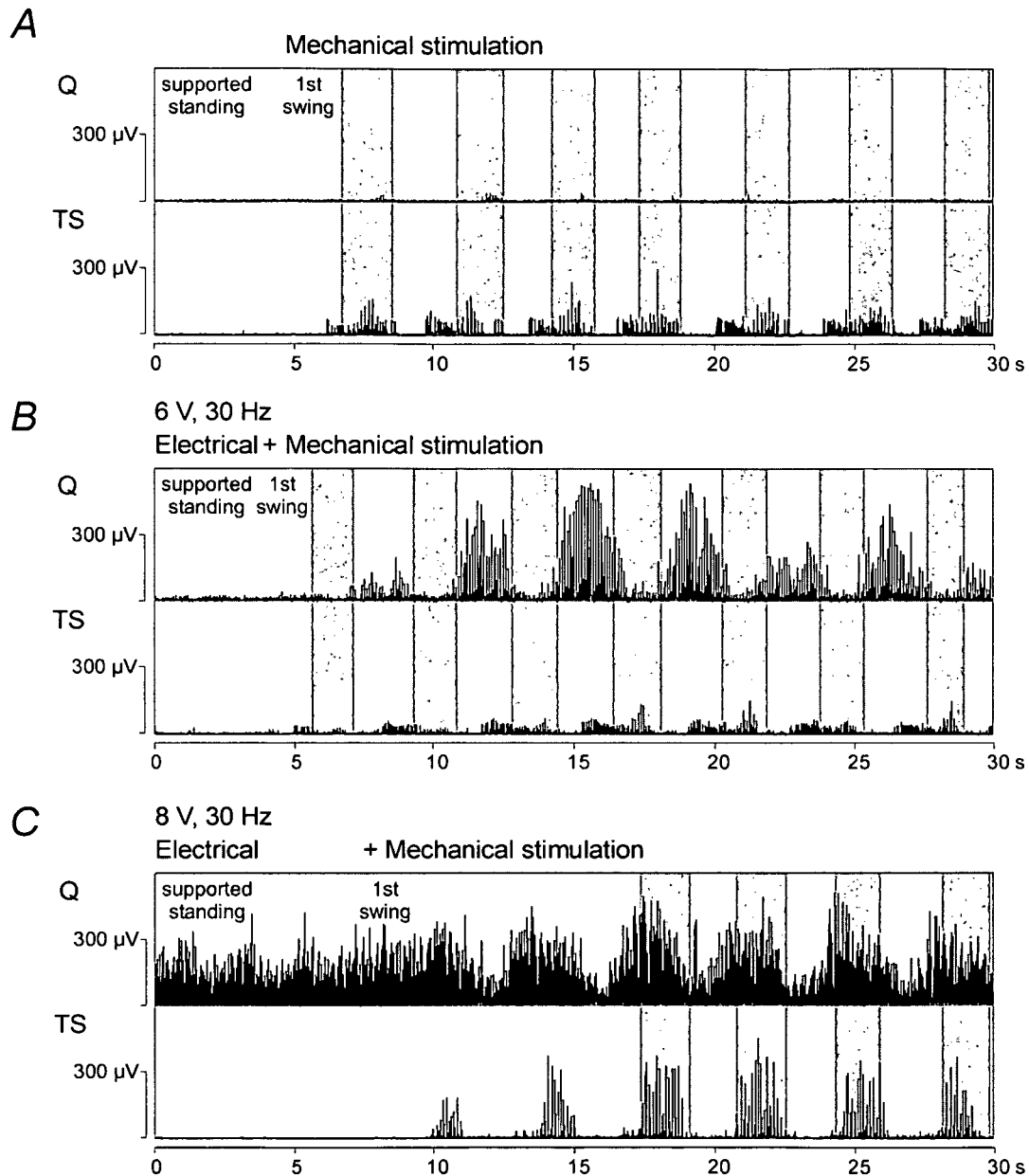


Figure 4.3 Transition from supported standing to passive stepping without (A) and with spinal cord stimulation (B, C)

Continuous rectified EMG activity (1024 samples/s) of quadriceps (Q) and triceps surae (TS) showing the effect of the onset of first manually assisted steps on a treadmill under different initial stimulation conditions. Gray background marks stance phases after a treadmill speed of 0.8 km/h (0.22 m/s) was reached. Data derived from subject 1.

Figure 4.4A demonstrates the enhancing and suppressing effect of mechanical stimulation on the EMG activity of triceps surae (TS) with epidural stimulation continuously active at two different strengths (subject 1). In the top figure, spinal cord stimulation at 8 V and 30 Hz did not initiate an EMG activity before the onset of mechanical stimulation. After the first passive swing of the lower limb, EMG bursts were evoked during the stance phases. The EMG bursts had higher amplitudes than in trials of assisted stepping without epidural stimulation. After the last passive step cycle was performed and a supported standing

position of the subject was established, epidural stimulation was further delivered but was not effective in evoking any activity in triceps surae. In the case illustrated at the bottom of Fig. 4.4A, electrical stimulation was applied at supra-threshold level (10 V, 30 Hz) and continuously elicited high-amplitude EMG responses in triceps surae before the first passive swing was performed. As soon as the lower limb was manually assisted through the first swing phase, epidural stimulation failed to evoke EMG responses during the early swing phases. After the end of passive stepping, epidural stimulation again consistently elicited trains of EMG responses.

In Fig. 4.4B the effect of different strengths of epidural stimulation on the EMG pattern of the evoked quadriceps (Q) activity during passive stepping is outlined (subject 1). Increasing stimulation strength from 6 V to 8 V at 30 Hz significantly changed the timing of the EMG bursts with respect to the phases of the gait cycle. While at 6 V the EMG bursts were induced during the whole swing phase with maximum amplitudes at 40% of the swing phase, at 8 V the muscle showed a maximum activity at the transition from swing to stance and was active during the whole stance phase.

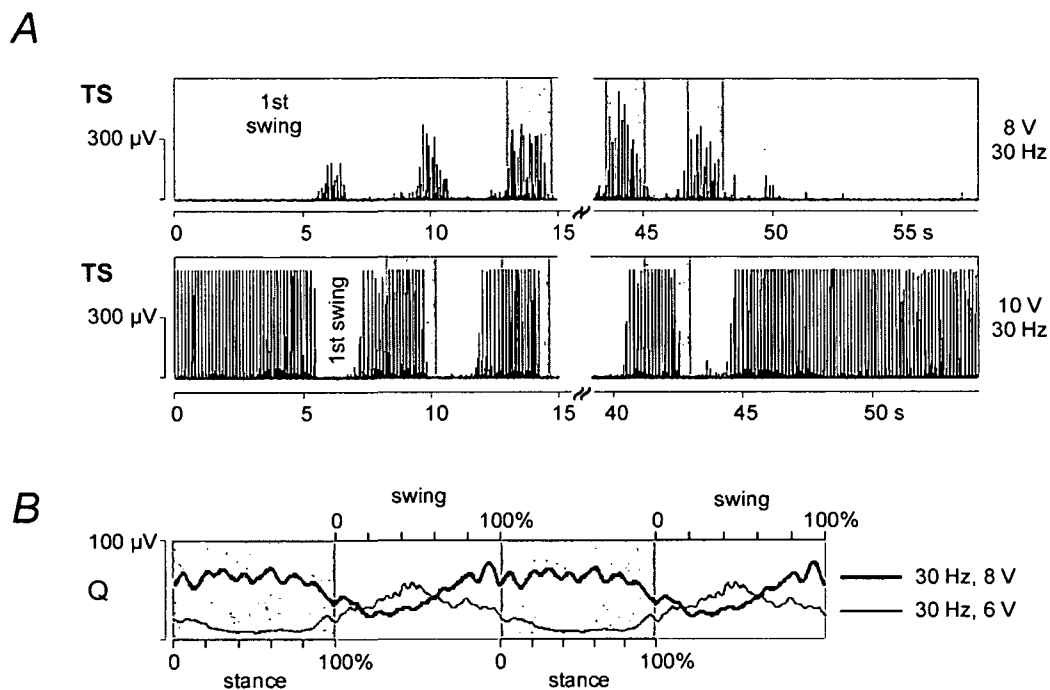


Figure 4.4 Effects of mechanical and electrical stimulation on the EMG patterns during passive treadmill stepping

A, Rectified EMG activity (1024 samples/s) of triceps surae (TS) at the onset and the end of manually assisted treadmill stepping and additional epidural stimulation at 8 V, 30 Hz (top figure) and 10 V, 30 Hz. Stance phases are marked by gray background. EMG signal is cut at $\pm 536 \mu$ V (see *Methods*). *B*, Averaged EMG activity (μ V) with respect to normalized step cycle of the quadriceps (Q) muscle (rectified, low-pass filtered at 5 Hz). Comparison of the effect of 6 V, 30 Hz and 8 V, 30 Hz stimulation, while the same externally controlled maneuver of passive stepping movement is performed.

Figure 4.4 demonstrated the enhancing (Fig 4.4A, top figure) and suppressing (Fig 4.4B, bottom figure) effect of mechanical stimulation in combination with epidural stimulation on the muscle activation pattern during passive treadmill stepping. Furthermore it was shown

that spinal cord stimulation not only induced “test” responses influenced by a dominating conditioning effect of the mechanical stimulation, but could also modulate and change the timing of efferent motor patterns of complete spinal cord injured subjects during manually assisted stepping on a treadmill (Fig 4.4B).

The effect of epidural cathode position on the induced EMG patterns

The optimal cathode levels to initiate stepping-like movements in paralyzed lower limbs, when subjects were lying in a supine position, were identified to be at the L2–L4 segments. In subject 2 the electrode location was more caudal than in subject 1 (see methods). This allowed studying the effect of stimulation with a cathode below the upper lumbar segmental levels. Passive treadmill stepping without epidural stimulation triggered some low-

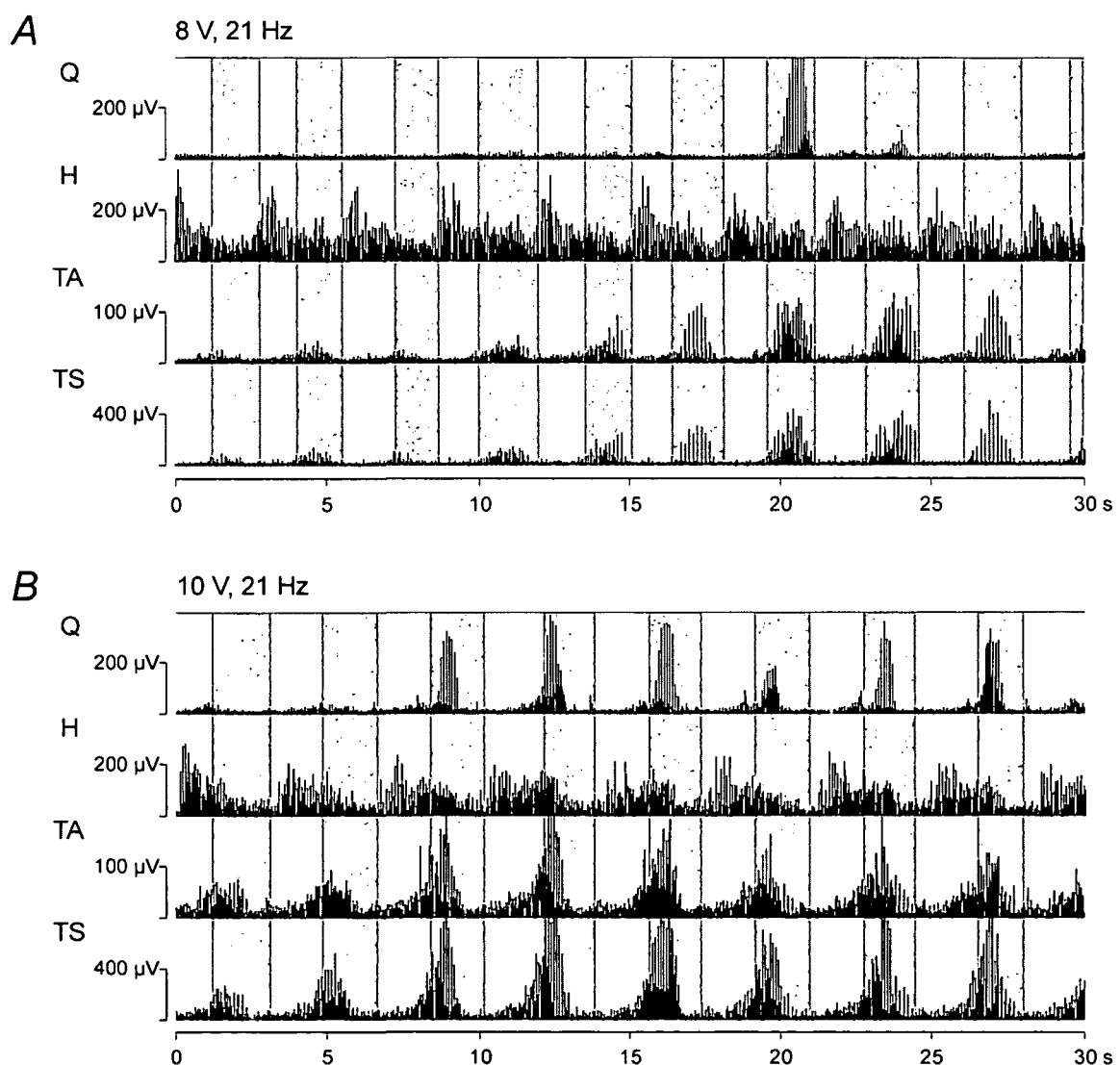


Figure 4.5 Effect of a caudally placed stimulating electrode on the EMG patterns during passive treadmill stepping

Rectified continuous EMG activity (1024 samples/s) of the quadriceps (Q), hamstrings (H), tibialis anterior (TA) and triceps surae (TS) muscles induced by continuous spinal cord stimulation at a constant frequency of 21 Hz and strengths of 8 V (A) and 10 V (B) during passive treadmill stepping displayed for 30 seconds. Treadmill speed was 0.4 km/h (0.11 m/s), body weight support was 80%. Data was derived from subject 2 (recording 3).

amplitude EMG activity mainly in the distal lower limb muscles demonstrating co-activation during the stance phases. Additional spinal cord stimulation at 8 V and 21 Hz (Fig. 4.5A) resulted in EMG bursts in the hamstrings, tibialis anterior and triceps surae muscles temporally synchronized to specific phases of the step cycle. Tibialis anterior and triceps surae showed co-activation during the stance phases (marked by gray background). The corresponding EMG bursts were composed of stimulus-triggered CMAPs with latencies of 16.5 ms. The hamstrings activity consisted of stimulus-evoked CMAPs with latencies of 11 ms and maximum amplitudes during the early swing phases. In the quadriceps muscle only two EMG bursts during the seventh and eighth stance phase of the shown 30 second-trace were evoked. At a stimulation strength of 10 V the EMG amplitudes of the tibialis anterior and triceps surae bursts increased. After the second displayed step cycle, bursts were consistently induced in quadriceps during the early stance phases. The increase in stimulation strength did not enhance the activity in the hamstrings but decreased the amplitude of the induced EMG activity at the transitions from the stance to swing phases.

The recordings derived from subject 2 demonstrated that epidural stimulation during passive treadmill-stepping could induce EMG bursts in the paralyzed lower limb muscles, even if predominantly delivered to cord levels caudal to the L2–L4 segments. However, the burst-style EMG activities did not resemble functional locomotor patterns.

The effect of different frequencies of spinal cord stimulation on the induced EMG patterns

Figure 4.6 shows the effect of “low” stimulation frequencies of 10–30 Hz on the EMG patterns recorded from the quadriceps muscle during manually assisted stepping on a treadmill (subject 2, electrode polarity: c+2–). When spinal cord stimulation was applied with 10 V at 10 Hz without additional mechanical stimulation (supported standing position, first 6 seconds of Fig. 4.6A), stimulus-coupled CMAPs with a constant latency of 9 ms were evoked. Successively elicited CMAPs did not show systematically modulated EMG amplitudes. Mechanical stimulation associated with assisted treadmill walking demonstrated some modulatory effect on the induced EMG activity and increased the amplitudes of the stimulus-evoked CMAPs during the late stance phases. EMG amplitudes of the stimulus-evoked CMAPs decreased when stimulation frequency was increased to 15 Hz (first 6 seconds of Fig. 4.6B). With the onset of mechanical stimulation the EMG amplitudes increased during the late stance and late swing phases. The enhancing effect of the mechanical stimulation which was synchronized with the stepping cadence was more apparent than in the case of 10 Hz-stimulation. Continuous stimulation with 10 V at 30 Hz (Fig. 4.6C) failed to elicit any quadriceps activity when the subject was in a supported standing position. After the first step cycle was carried out passively, a short burst activity was built up during the second stance phase and further increased in amplitude during the following steps. A quasi-stationary condition was reached after the sixth passive step cycle. The short, high-amplitude bursts consisted of frequency-following CMAPs with a latency of 9 ms.

Results of “higher” stimulation frequencies (20–60 Hz) on the induced quadriceps EMG patterns are illustrated in Fig. 4.7 (subject 2, electrode polarity: 0+3–). At a stimulation strength of 10 V, frequencies of 20, 30 and 50 Hz induced EMG bursts during the stance phases of the step cycle. The lowest frequency inducing EMG bursts separated by phases of

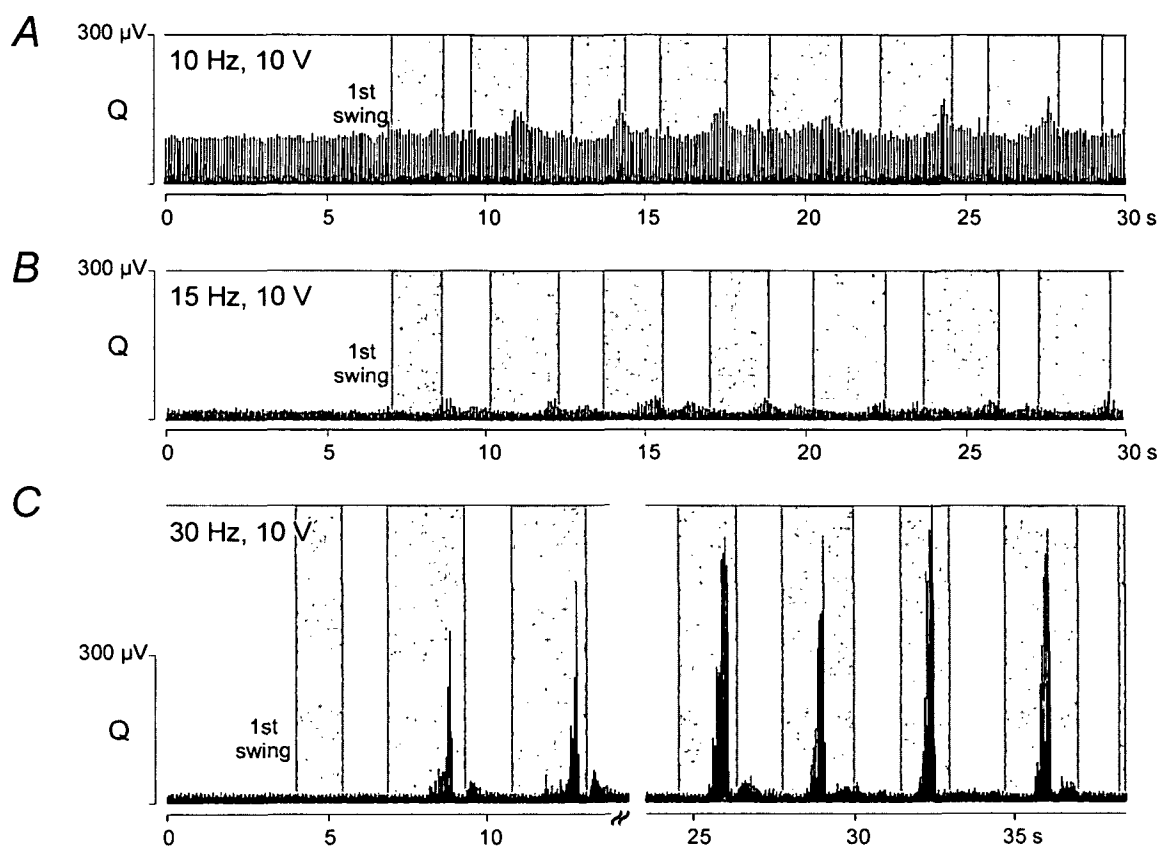


Figure 4.6 Effect of stimulation frequencies of 10–30 Hz on the EMG patterns during passive treadmill stepping

Rectified EMG activity (2048 samples/s) of the left quadriceps muscle induced by mechanical stimulation and additional continuous spinal cord stimulation delivered at a constant strength of 10 V and frequencies of 10, 15 and 30 Hz. At the onset of each displayed trace spinal cord stimulation was on and the subject was in a supported standing position. After some seconds of recording, the lower limb was passively moved through the first step cycle (gray backgrounds mark the stance phases of stepping). Data was derived from subject 2 (recording 2, electrode polarity: c+2–).

inactivity/low activity was 20 Hz. Increasing the frequency to 30 and 50 Hz shifted the EMG burst to the early stance with maximum amplitudes at 20% and 46% of the stance phase, respectively. At 60 Hz epidural stimulation in combination with assisted treadmill stepping did not evoke any systematically modulated EMG activities in the lower limb muscles. This was also the case when frequencies of 80 Hz and 100 Hz were applied at the same strength using the same electrode set-up (not displayed in the figure).

In the subjects 1 and 2, stimulation with 38 different parameter combinations between 1–10 V and 10–100 Hz were applied during four different testing sessions. Eighteen of the combinations induced EMG bursts during passive treadmill stepping, all were within the range of 20–50 Hz and 6–10 V (median: 30 Hz, 10 V, mean: 33.1 Hz, 9 V). The findings were consistent both within and between testing sessions.

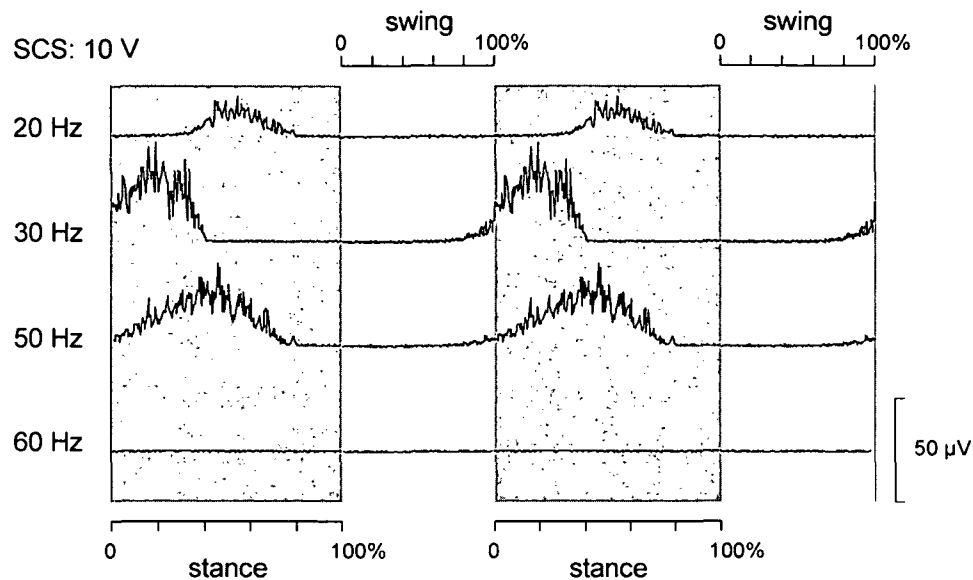


Figure 4.7 Effect of stimulation frequencies of 20–60 Hz on the EMG patterns during passive treadmill stepping

Averaged ($n = 10$ stance and 10 swing phases) rectified EMG activity (μV) with respect to time-normalized stance and swing phase of the step cycle. Stance phases are marked by gray background, the duration of stance and swing phase is displayed with a ratio of 60:40 for all cases. Data is derived from left quadriceps, subject 2 (recording 2, electrode polarity: 0+3–). Stimulation strength was 10 V in the shown cases.

DISCUSSION

Effect of phasic peripheral feedback input to the isolated lumbar cord

Peripheral sensory feedback input to the spinal cord associated with assisted treadmill stepping generated EMG bursts in the paralyzed lower limbs which were characterized by co-activation during the late swing and the whole stance phase (Fig. 4.2A). EMG activity was smallest or even absent in the quadriceps muscle. Thus, proprioceptive feedback input to the isolated spinal cord generated a non-functional EMG burst pattern which was different to the locomotor pattern observed in able-bodied subjects during active treadmill stepping and comparable recording conditions (Fig. 4.1B). Note that the spinal cord injured subjects included in the present study never participated in a locomotor training prior to the recordings.

Effect of tonic input to the lumbar cord generated by spinal cord stimulation

Epidural stimulation applied at strengths above the motor threshold of a given muscle while the subject was in an upright, supported standing position (i.e. without additional proprioceptive input related to passive stepping movements) was not effective in generating EMG bursts in the lower limb muscles (see first seconds of Figs. 4.3C, 4.4A and 4.6). Stimulation at frequencies below 20 Hz (Fig. 4.6A and B) induced a tonic activity consisting of frequency-following CMAPs with short latencies characteristic for monosynaptic Posterior Roots Muscle Reflex Responses (PRMRRs, see Chapter 2;

Minassian *et al.* 2004a). At frequencies between 20–50 Hz and before the onset of passive stepping, modulated tonic EMG patterns were generated in some cases but without consistent rhythmicity or periods of inactivity/low activity (Fig. 4.3C).

On the other hand, rhythmic stepping-like EMG activity could be induced by epidural stimulation in the subjects 1 and 2 when they were lying in a supine position with parameters between 20–50 Hz and 7–10 V (several recordings carried out between 1997 and 1999).

The inefficiency of epidural stimulation to induce stepping-like EMG bursts without additional mechanical stimulation by passive lower limb movements might be due to biophysical and physiological differences resulting from the upright body position of the subject. Since the subjects had subclinically complete spinal cord injuries, any supraspinal influence during the (supported) standing position like additional extrapyramidal control contribution to the excitation of spinal cord motor cell pools can be ruled out.

It is well known in the clinical application of epidural spinal cord stimulation for the control of spasticity that the effect of stimulation depends on the subject's posture. At a given stimulus strength, the effect of stimulation decreases when the subject's position is changed from supine to upright, and from upright to prone position, respectively. The intradural geometry, and primarily the dorsal cerebrospinal fluid layer, strongly influences the effect of epidural spinal cord stimulation (Struijk *et al.* 1993; He *et al.* 1994). The intradural antero-posterior position of the spinal cord, and thus the dorsal cerebrospinal fluid layer-thickness, depends on the subject's posture. The dorsal cerebrospinal fluid layer-thickness is at its minimum when the subject is in a supine position and maximum when the subject is in a prone position (Holsheimer *et al.* 1994). When the subject is upright, the intradural antero-posterior position of the spinal cord is between the situations described by Holsheimer *et al.* (1994). With increasing cerebrospinal fluid layer-thickness, the thresholds for posterior root recruitment increase. Accordingly, during a supported standing position of the subject, the stimulation strength necessary to stimulate lumbar posterior roots sufficiently to activate the Lumbar Locomotor Pattern Generator (LLPG, see Chapter 3; Minassian *et al.* 2004b) might be above the limit (10 V) of the used pulse generator.

Another difference between the supine and supported-standing position of the subjects is the amount of afferent inflow from cutaneous and articular receptors associated with weight-bearing to the spinal cord. During passive standing on the treadmill trainers had one hand on the front of the thigh or knee of the spinal cord injured subject to keep the knee in full extension. Thus, during this supported standing the subject's lower limbs were passively bearing considerable weight (the difference between body weight and body weight support provided by the counterweights). The corresponding sustained proprioceptive input signaling standing could have some suppressive effect on the lumbar spinal interneurons to temporarily combining into locomotor pattern generating networks.

Effect of spinal cord stimulation-evoked tonic input in conjunction with phasic peripheral feedback input to the lumbar cord

When the same externally controlled maneuver of assisted treadmill stepping was performed, very different EMG patterns were induced depending on the frequency of the applied epidural stimulation, namely modulated tonic or burst-type rhythmic activity (Fig. 4.6). When stimulation frequency was increased above 50 Hz, motor output could be even completely suppressed during passive treadmill stepping (Fig. 4.7).

Epidural stimulation applied at frequencies below the range of 20–50 Hz effective to activate the LLPG (Chapter 3; Minassian *et al.* 2004b) could induce a tonic EMG activity during supported standing position. The tonic EMG activity was amplitude-modulated when additional proprioceptive input related to passive stepping was provided to the spinal cord (Figs. 4.6A and B). However, burst-style rhythmic activity could not be induced. It was shown that epidural stimulation with frequencies between 5–15 Hz can set-up an “extension pattern generator”-configuration of the lumbosacral interneuronal networks (Jilge *et al.* 2004), generating a sustained motor output. Once established by the appropriate frequency of stimulation, Figs. 4.6A and B suggest that this set-up of the lumbar internuncial networks cannot be overridden by peripheral phasic feedback input related to passive stepping movements to operate as a locomotor pattern generator.

A mechanism simpler than the contribution of pattern generating spinal networks may account for the amplitude-modulations of the epidurally-evoked tonic EMG activity. In the presented examples in Figs. 4.6A and B the main effect of mechanical stimulation was a periodic augmentation of the tonic quadriceps activity during the late stance phases. During these phases the quadriceps muscle is stretched (imposed knee flexion while the hip is still in an extended position), and the lower limb is loaded. This proprioceptive input to the corresponding lumbar spinal segments may depolarize motoneurons and premotoneuronal spinal structures. These structures would be then closer to threshold and thus more responsive to sustained electrical stimulation during the corresponding phases of the gait cycle. A similar effect was described by Mushahwar and colleagues (2000) in healthy, adult cats. They implanted arrays of microwires in the lumbosacral region of the feline spinal cord to study the quality of lower limb movements that could be elicited from within the active, nonanesthetized spinal cord. The effect of afferent input on stimulus threshold was also described. It was reported that imposed knee flexion increased EMG responses in quadriceps. At a given stimulus intensity of electrical stimulation, EMG responses increased with increasing angular velocities of imposed movement (i.e., the threshold for activating the muscle was reduced). Upon termination of knee flexion, stimulus-evoked EMG activity returned to its pre-stretch levels in the cat.

In Fig. 4.6C, epidural stimulation was applied at 30 Hz while passive stepping movement was performed like in the Figs. 4.6A and B. The modulated tonic EMG activity as induced at frequencies below 20 Hz was replaced by a burst-style rhythmical one at 30 Hz stimulation. This finding indicates that epidural stimulation at appropriate frequencies could facilitate the LLPG set-up of the lumbar internuncial networks. This organization is expressed by generation of rhythmical efferent output.

The stimulation strength and the number of recruited lumbar cord segments determined to what degree the internuncial lumbar cord networks responded to repetitive and regular stimulation at 20–50 Hz by setting up an LLPG organization. The effect of increasing the strength of stimulation at a constant frequency of 30 Hz was demonstrated in the Figs. 4.2 and 4.3. In Fig. 4.3 only quadriceps and triceps surae were considered, since they are the only of the recorded muscle groups with separate segmental innervations (L2–L4 vs. L5–S2). Due to the upper lumbar position of the cathode in subject 1 (see *Methods* and Table 4.2), epidural stimulation predominantly stimulated the segments L2–L4 which were near to the cathode. At 6 V and 30 Hz, epidural stimulation of posterior roots was not strong enough to activate lower limb motor neuron pools during supported standing position (Fig. 4.3B, first 4 seconds of recording). Phasic feedback input related to rhythmic stepping lowered the thresholds of the premotoneuronal spinal structures. During passive stepping,

the 6 V-stimulation induced separate CMAPs in the L2–L4 innervated quadriceps muscle that were subject to well-defined amplitude modulations resulting in burst-like envelopes of the EMG activity (Fig. 4.3B, after the first swing). However, the timing of the burst-style EMG activities was non-functional since they had maximum amplitudes during the swing phases (compare with Fig. 4.1B). The CMAPs composing the burst-style EMG activities in quadriceps were consistently responding at 10 Hz and were not following the stimulation frequency of 30 Hz. (This is in contrast to the findings in supine position, where epidurally-evoked burst-style EMG activities consisted of frequency-following CMAPs, see Minassian *et al.* 2004a,b; Chapters 2 and 3). Due to the cathode position, the current spread in caudal direction was not sufficient at 6 V to activate the more distant posterior roots of the L5 and S1 segments. Consequently, no CMAPs related to the epidural stimulation were detected in triceps surae even during passive treadmill-stepping in the case of 6 V-stimulation. At 8 V and 30 Hz (Fig. 4.3C), a phase shift in the quadriceps activation patterns occurred. The timing of the quadriceps EMG activity was a more functional one. The amplitude-modulated CMAPs composing the burst-style quadriceps activity were elicited with a frequency of 30 Hz and were thus frequency-following. Furthermore, stimulation-related CMAPs were also induced in the triceps surae muscle. These findings suggest that at 6 V the epidural stimulation did not provide strong enough tonic stimuli to sufficiently activate the LLPG. Peripheral feedback input helped to express some features of the LLPG, even when not fully established. The more functional EMG patterns at 8 V indicate that a more complete LLPG set-up was built up by the stronger tonic stimuli.

The importance of a predominant stimulation of upper lumbar cord segments to elicit stepping-like EMG patterns could be deduced from Fig. 4.5. There, epidural stimulation delivered to lower lumbar cord segments during assisted treadmill-walking induced rhythmic EMG activity in the lower limb muscles which mainly co-activated during the stance phases.

Significance of the results

It was shown that subjects with clinically complete spinal cord injuries can generate stepping-like efferent patterns when partially supported over a moving treadmill belt and manually assisted with stepping (Dietz *et al.* 1995; Dobkin *et al.* 1995). These studies were taken as evidence that sensory information associated with weight-bearing passive stepping can activate and coordinate locomotor networks in the spinal cord which can generate stepping-like EMG patterns.

The present study suggests that the peripheral feedback input related to passive treadmill-stepping can make use of pattern generating networks in the isolated lumbar cord to produce rhythmic EMG activities in the lower limb muscles. However, the efficiency of the phasic afferent input in modifying the central state of spinal circuits and to fully develop an LLPG organization was limited. An essential role of the phasic input was that of reinforcing LLPG activities. This could be clearly seen in cases where epidural stimulation was applied at frequencies of 20–50 Hz but at strengths below motor threshold. Another crucial role of peripheral afferent input was a timing function, which was reflected by the temporal synchronization of EMG bursts to specific phases of the step cycle.

Epidural stimulation provided a repetitive, regular input to several lumbar and upper sacral cord segments via the posterior roots to the lumbar spinal cord. While coming from “periphery”, the tonic input at a constant frequency is unlike physiological sensory

feedback information. We speculate that the tonic input of particular frequencies is interpreted by the lumbar interneuronal structures as a central command signal due to its code. This “central” peripheral input was capable of modifying the central state of spinal lumbar networks. At frequencies of 20–50 Hz an LLPG organization could be established. Thereby the responsiveness of the spinal circuits to proprioceptive feedback to generate stepping-like efferent motor patterns was significantly enhanced. This effect could be achieved immediately as soon as the appropriate stimulus parameters were applied.

Originally, evidence has been adduced for the existence of a LLPG in supine individuals (Dimitrijevic *et al.* 1998). With the limited information from periphery to the LLPG, amplitude and timing of the cyclical motor output could only be set to some default level in these studies. The present study provides the significant result, that the LLPG activated by epidural stimulation can adapt its motor output to external demands during passive stepping. The spinal lumbar networks can integrate and interpret the “central” peripheral inputs (provided by epidural stimulation) and the proprioceptive inputs (associated with passive stepping) in order to generate functional locomotor patterns. This also implies that both, the tonic and the phasic afferent inputs – which have very different sources of origin – converge on common components of spinal rhythm-generating networks.

We take the findings of the present study as further evidence that lumbar interneurons can be temporarily incorporated into pattern generating networks for stepping-like activity – the LLPG. The LLPG can be set-up by epidural stimulation even when a massive afferent inflow from various sensory organs in muscles, joints, skin, and connective tissues induced during weight-bearing, manually assisted stepping is delivered to the spinal cord. The internuncial cord network can immediately respond by building up an LLPG circuitry when tonic input at 20–50 Hz is provided to the lumbar cord. To generate and enhance stepping-like EMG activity by solely activating the LLPG with phasic feedback input requires a regular locomotor training for an extended period of time. This might be due to the inappropriate code used to activate the LLPG, i.e. the lack of a tonic component of the mechanical stimulation. Therefore we suggest that sustained electrical stimulation to elicit a multisegmental “central” afferent input to the lumbar spinal cord might be a valuable adjunct to treadmill training in spinal cord injured patients.

REFERENCES

- Dietz V, Colombo G, Jensen L & Baumgartner L (1995). Locomotor capacity of spinal cord in paraplegic patients. *Ann Neurol* **37**, 574-582.
- Dietz V, Muller R & Colombo G (2002). Locomotor activity in spinal man: significance of afferent input from joint and load receptors. *Brain* **125**, 2626-2634.
- Dimitrijevic MR, Gerasimenko Y & Pinter MM (1998a). Evidence for a spinal central pattern generator in humans. In *Neural Mechanisms for Generating Locomotor Activity. Ann N Y Acad Sci Vol. 860*, ed. Kiehn O, Harris-Warrick RM, Jordan LM, Hultborn H & Kudo N, pp. 360-376. New York Academy of Sciences, New York.
- Dimitrijevic MR, Gerasimenko Y & Pinter MM (1998b). Effect of reduced afferent input on lumbar CPG in spinal cord injury subjects. Soc Neurosci Abstr; 24: Program No. 654.23.
- Dobkin BH, Harkema S, Requejo P & Edgerton VR (1995). Modulation of locomotor-like EMG activity in subjects with complete and incomplete spinal cord injury. *J Neurol Rehabil* **9**, 183-190.
- Ferris DP, Gordon KE, Beres-Jones JA & Harkema SJ (2004). Muscle activation during unilateral stepping occurs in the nonstepping limb of humans with clinically complete spinal cord injury. *Spinal Cord* **42**, 14-23.
- Harkema SJ, Hurley SL, Patel UK, Requejo PS, Dobkin BH & Edgerton VR (1997). Human lumbosacral spinal cord interprets loading during stepping. *J Neurophysiol* **77**, 797-811.
- He J, Barolat G, Holsheimer J & Struijk JJ (1994). Perception threshold and electrode position for spinal cord stimulation. *Pain* **59**, 55-63.
- Holsheimer J, den Boer JA, Struijk JJ & Rozeboom AR (1994). MR assessment of the normal position of the spinal cord in the spinal canal. *Am J Neuroradiol* **15**, 951-959.
- Jilge B, Minassian K, Rattay F, Pinter MM, Gerstenbrand F, Binder H & Dimitrijevic MR (2004). Initiating extension of the lower limbs in subjects with complete spinal cord injury by epidural lumbar cord stimulation. *Exp Brain Res* **154**, 308-326.
- Minassian K, Jilge B, Rattay F & Dimitrijevic MR (2004a). Posterior Roots Muscle Reflex Responses elicited by epidural stimulation of the human lumbar cord. *J Physiol*, submitted.
- Minassian K, Jilge B, Rattay F, Pinter MM, Binder H, Gerstenbrand F & Dimitrijevic MR (2004b). Stepping-like movements in humans with complete spinal cord injury induced by epidural stimulation of the lumbar cord: Electromyographic study of compound muscle action potentials. *Spinal Cord* May 4 [Epub ahead of print].
- Murg M, Binder H & Dimitrijevic MR (2000). Epidural electric stimulation of posterior structures of the human lumbar spinal cord: 1. muscle twitches – a functional method to define the site of stimulation. *Spinal Cord* **38**, 394-402.
- Mushahwar VK, Collins DF & Prochazka A (2000). Spinal cord microstimulation generates functional limb movements in chronically implanted cats. *Exp Neurol* **163**, 422-429.
- Struijk JJ, Holsheimer J & Boom HB (1993). Excitation of dorsal root fibers in spinal cord stimulation: A theoretical study. *IEEE Trans Biomed Eng* **40**, 632-639.

Curriculum Vitae

Personal Data

Name Dipl.Ing. Karen Minassian
 Date of Birth 12 April 1974
 Place of Birth Tehran, Iran
 Nationality Austria

Education

Since October 2000 PhD studies at the Vienna University of Technology
 October 1992 – July 2000
 Studies in Technical Physics at the Vienna University of Technology
 1984 – 1992 Secondary School: Bundesrealgymnasium IV, Vienna
 Graduation in June 1992

Internships

June 1998 – July 1998 Internship at the Department of Biomedical Engineering and Physics, Medical University of Vienna
 April 1997 – June 1997 Internship at the Research Department of Hilti, Schaan, Principality of Liechtenstein
 February 1997 – March 1997
 Internship at the Department of Fundamentals and Theory in Electrical Engineering, Vienna University of Technology

Employment Record

Since March 2003 Research associate at the Ludwig Boltzmann Institute for Electrical Stimulation and Physical Rehabilitation, Vienna
 October 2003 – January 2004
 Teaching assistant at the Department for Analysis and Scientific Computing, Vienna University of Technology
 October 2002 – January 2003
 Teaching assistant at the Department for Analysis and Technical Mathematics, Vienna University of Technology
 November 2000 – December 2002
 Research fellow in the project „Neurophysiologische Modellierung der Erregbarkeit der Lokomotionszentren im lumbalen

Rückenmark durch elektrische Stimulation“ (GZ 140.591/4-V/B/9b/2000, Federal Ministry for Transport, Innovation and Technology)

October 2001 – January 2002

Teaching assistant at the Department for Analysis and Technical Mathematics, Vienna University of Technology

List of scientific publications

1. Rattay F & Minassian K (1999). A computer model for the electrical stimulation of the spinal cord. *Med & Biol Eng & Comp* **37**, Suppl. 2: 800-801.
2. Rattay F, Naves Leao R, Minassian K & Markum H (1999). Finite Element Analysis for Electrical Nerve Simulation. Seminarband über Modellbildung und Simulation / MATLAB, Wien: 187-188.
3. Minassian K, Rattay F & Markum H (1999). Modell und Simulation der Rückenmarkstimulation mit implantierten Elektroden. Jahrestagung Österr Physik Ges, Innsbruck: 20.
4. Rattay F, Minassian K & Markum H (1999). The electrical stimulation of the spinal cord: Computer simulation with ANSYS and ACSL. Seminar zu Modellbildung und Simulation, Wien: 65-68.
5. Minassian K, Rattay F & Markum H (2000). The Electrical Stimulation of the Human Spinal Cord: A Computer Model Study. Deutsche Physik Ges.
6. Minassian K, Rattay F & Markum H (2000). The electrical stimulation of the spinal cord: Computer model for electrode positioning. Proc. Poster Session Vol. 3rd Mathmod IMACS Symposium on Math. Modelling: 15.
7. Minassian K, Rattay F & Markum H (2000). 3D Finite Element Approach and Simulation of the Excitation of the Spinal Cord. Jahrestagung Österr Physik Ges, Graz.
8. Rattay F & Minassian K (2000). Excitation of lower spinal cord structures with implanted electrodes: 3D finite element analysis and simulation of neural responses. *Österr Ges Neurowissenschaften-Newsletter* **13**, 27.
9. Minassian K (2000). Excitation of lower spinal cord structures with implanted electrodes: 3D finite element analysis and simulation of neural responses. Diploma Thesis, Vienna University of Technology.
10. Rattay F, Minassian K & Dimitrijevic MR (2000). Epidural electrical stimulation of posterior structures of the human lumbosacral cord: 2. quantitative analysis by computer modeling. *Spinal Cord* **38**, 473-489.
11. Rattay F, Minassian K & Markum H (2001). Simulation of electrical nerve stimulation with ACSL. ARGESIM Report: Modellbildung in der Mechatronik: ACSL, Dymola, ESL: 19-23.
12. Dimitrijevic MR, Minassian K, Murg M, PinterMM, Rattay F, Gerasimenko Y & Binder H (2001). Study of locomotor capabilities induced by spinal cord stimulation (SCS) of the human lumbar cord isolated from the brain control by posttraumatic spinal cord injury (SCI). Soc Neurosci Abstr; 27: Program No. 935.6.
13. Minassian K, Rattay F, Pinter MM, Murg M, Binder H, Sherwood A & Dimitrijevic MR (2001). Effective spinal cord stimulation (SCS) train for evoking stepping locomotor movement of paralyzed human lower limbs due to SCI elicits a late response additionally to the early monosynaptic response. Soc Neurosci Abstr; 27: Program No. 935.12.

14. Minassian K, Rattay F & Dimitrijevic MR (2001). Features of the reflex responses of the human lumbar cord isolated from the brain but during externally controlled locomotor activity. Proceedings of the World Congress on Neuroinformatics, Vienna, Austria; Part I: 55-57.
15. Minassian K, Rattay F & Dimitrijevic MR (2001). Features of the reflex responses of the human lumbar cord isolated from the brain but during externally controlled locomotor activity. Proceedings of the World Congress on Neuroinformatics, Vienna, Austria; Part II: 267-268.
16. Minassian K, Rattay F & Dimitrijevic MR (2001). A computer simulation and electrophysiological methods to identify the primary stimulated spinal cord structures with epidural electrodes. Proceedings of the World Congress on Neuroinformatics, Vienna, Austria; Part II: 284-285.
17. Jilge B, Minassian K, Dimitrijevic MR (2001). Involuntary movements of paralyzed lower limbs and residual brain control below spinal cord injury. Proceedings of the World Congress on Neuroinformatics, Vienna, Austria; Part II: 278-280.
18. Jilge B, Minassian K & Dimitrijevic MR (2001). Electrical stimulation of the human lumbar cord can elicit standing parallel extension of paralysed lower limbs after spinal cord injury. Proceedings of the World Congress on Neuroinformatics, Vienna, Austria; Part II: 281-283.
19. Minassian K, Rattay F, Dimitrijevic MR, Pinter MM, Gerstenbrand F & Binder H (2002). Neurophysiologische Modellierung der Erregbarkeit der Lokomotionszentren im lumbalen Rückenmark durch elektrische Stimulation. 2. Zwischenbericht über das Projekt GZ 140.591/4-V/B/9b/2000.
20. Jilge B, Minassian K, Rattay F & Dimitrijevic MR (2002). Tonic and rhythmic motor units activity of the cord induced by epidural stimulation can alter posterior roots muscle reflex responses. Proceedings of the 7th Annual Conference of the IFESS, Ljubljana, Slovenia: 164-166.
21. Minassian K, Jilge B, Rattay F, Pinter MM, Gerstenbrand F, Binder H & Dimitrijevic MR (2002). Effective spinal cord stimulation (SCS) for evoking stepping movement of paralyzed human lower limbs: study of posterior root muscle reflex responses. Proceedings of the 7th Annual Conference of the IFESS, Ljubljana, Slovenia: 167-169.
22. Dimitrijevic MR, Minassian K, Jilge B & Rattay F (2002). Initiation of standing and locomotion like movements in complete SCI subjects "by mimicking" brain stem control of lumbar network with spinal cord stimulation. Proceedings of the 4th International Symposium on Experimental Spinal Cord Repair and Regeneration, Brescia, Italy: 25-27.
23. Rattay F, Minassian K, Dimitrijevic MR, Pinter MM, Gerstenbrand F & Binder H (2002). Neurophysiologische Modellierung der Erregbarkeit der Lokomotionszentren im lumbalen Rückenmark durch elektrische Stimulation. Endbericht über das Projekt GZ 140.591/4-V/B/9b/2000.
24. Rattay F, Minassian K, Jilge B, Pinter MM, Dimitrijevic MR (2003). EMG analysis of lower limb muscle responses to epidural lumbar cord stimulation. Proceedings of the IEEE EMBS Conference Cancun (Mexico).

25. Rattay F, Resatz S, Lutter P, Minassian K, Gilge B & Dimitrijevic MR (2003). Mechanisms of electrical stimulation with neural prostheses. *Neuromodulation* **6**(1), 42-56.
26. Pinter MM, Minassian K, Gilge B, Rattay F, Binder H, Gerstenbrand F & Dimitrijevic MR (2003). Locomotor movements in complete paraplegic subjects evoked by spinal cord stimulation. *European Journal of Neurology* **10**(s1), 221.
27. Gilge B, Minassian K, Rattay F, Pinter MM, Gerstenbrand F, Binder H & Dimitrijevic MR (2004). Initiating extension of the lower limbs in subjects with complete spinal cord injury by epidural lumbar cord stimulation. *Exp Brain Res* **154**, 308-326.
28. Minassian K, Gilge B, Rattay F, Pinter MM, Binder H, Gerstenbrand F & Dimitrijevic MR (2004) Stepping-like movements in humans with complete spinal cord injury induced by epidural stimulation of the lumbar cord: electromyographic study of compound muscle action potentials. *Spinal Cord* May 4 [Epub ahead of print].
29. Minassian K, Persy I, Rattay F, Binder H, Pinter MM & Dimitrijevic MR (2004). Output induced by manually assisted treadmill stepping of paraplegic individuals can be enhanced by epidural stimulation of the Lumbar Locomotor Pattern Generator. Abstract No. 4770, 34th Annual Meeting of the Society for Neuroscience, San Diego, CA.
30. Dimitrijevic MR, Dimitrijevic MM, Kern H, Minassian K & Rattay F (2004). Electrophysiological characteristics of H-reflexes elicited by percutaneous stimulation of the cauda equina. Abstract No. 4927, 34th Annual Meeting of the Society for Neuroscience, San Diego, CA.

TU

TECHNISCHE UNIVERSITÄT WIEN

DISSERTATION

Modeling of a human spinal pattern generator for locomotion
and its activation by electrical epidural stimulation

ausgeführt zum Zwecke der Erlangung des akademischen Grades eines
Doktors der technischen Wissenschaften unter der Leitung von

Ao. Univ. Prof. DDr. Frank Rattay
E101
Institut für Analysis und Scientific Computing

Eingereicht an der Technischen Universität Wien,
Fakultät für Mathematik und Geoinformation

von

Dipl.-Ing. Karen Minassian
9225637
Blechturmstraße 15–17/3
A-1050 Wien

Wien, im Mai 2004

Karen Minassian

Kurzfassung der Dissertation

Modellierung eines spinalen Mustergenerators für Lokomotion im Menschen und dessen Aktivierung mittels elektrischer, epiduraler Rückenmarksstimulation

Motivation und Ziele der Dissertation

Der erste direkte Hinweis auf die Existenz eines spinalen Mustergenerators für Lokomotion im Menschen gelang 1998 in Patienten mit traumatischen Rückenmarksverletzungen nach Setzen einer epiduralen Rückenmarkselektrode zur Kontrolle der Spastizität. Bei kontinuierlicher, elektrischer Stimulation der posterioren Strukturen des lumbalen Rückenmarks konnten unwillkürliche Schrittbewegungen der unteren Extremitäten ausgelöst werden. Die theoretischen Grundlagen waren zu diesem Zeitpunkt weitgehend unerforscht.

Basierend auf dieser Beobachtung wurde in der vorliegenden Dissertation eine systematische Untersuchung der zugrunde liegenden neuronalen Mechanismen mittels mathematischen Modellen und neurophysiologischen Methoden durchgeführt. Konkrete Ziele waren (i) die Identifizierung der durch die elektrische Rückenmarksstimulation angeregten neuronalen Strukturen zur Auslösung der schrittähnlichen Bewegungen; (ii) Hinweise zu erbringen, dass autonome interneuronale Netzwerke an der Initiierung und Kontrolle der evozierten rhythmischen Bewegung beteiligt sind; (iii) festzustellen, ob das durch elektrische Stimulation aktivierte Lokomotionszentrum im Rückenmark afferentes Feedback ausgelöst durch manuell assistiertes Laufband-Gehen verarbeiten kann, um funktionelle Aktivitätsmuster der Beinmuskeln in paraplegischen Patienten zu generieren.

Methodik

Datensätze von siebzehn Patienten mit traumatischen, kompletten Rückenmarksverletzungen wurden analysiert. Diese Patienten hatten implantierte Elektroden im dorsalen Epiduralraum auf der Höhe zwischen den Wirbelkörpern BWK10–LWK1 zur Behandlung der spinalen Spastizität. Die Wirkung der Stimulation mit verschiedenen Parametern wurde durch die Aufzeichnung der evozierten elektromyographischen (EMG) Aktivität der Beinmuskeln dokumentiert. Diese neurophysiologischen Daten über das Input-Output Verhalten des lumbalen Rückenmarks wurden retrospektiv ausgewertet.

Um die direkte Wirkung der epiduralen Stimulation zu untersuchen, wurden die Rekrutierungsfolgen der Hauptmuskelgruppen der unteren Extremitäten in Abhängigkeit der Kathodenlage der epiduralen Elektrode ermittelt. Die gewonnenen neurophysiologischen Erkenntnisse wurden mit Computersimulationen zur Ermittlung der direkt angeregten neuronalen Strukturen kombiniert.

Um aktivierte zentrale Mechanismen zu studieren, wurden Stimulus-getriggerte Zeitfenster der EMG-Aktivitäten bei kontinuierlich applizierter Stimulation mit 1–10 V und 5–50 Hz analysiert. Es wurden Latenzzeit, Amplitude und Morphologie von EMG-Antworten zu einzelnen Pulsen bei Stimulation mit unterschiedlichen Parametern untersucht.

Der Effekt der elektrischen Rückenmarksstimulation wurde auch in zwei komplett paraplegischen Patienten während manuell assistiertem Laufband-Gehen untersucht.

Ergebnisse

Epidurale 2.2 Hz Stimulation der posterioren Strukturen des Lumbalmarks löste Muskelzuckungen in den unteren Extremitäten aus. Die entsprechenden EMG-Signale (zusammengesetzte Muskelaktionspotentiale) zeigten kurze Latenzzeiten, welche für die verschiedenen Muskelgruppen charakteristisch waren. Die rostrocaudale Lage der Kathode bestimmte die Rekrutierungsfolge der Muskelgruppen und dadurch den segmentalen Ursprung der aktivierten neuronalen Strukturen. Diese Selektivität der Stimulation war ein Hinweis für die direkte Anregung von Hinterwurzelfasern durch die epidurale Elektrode. Computersimulationen bestätigten die Hinterwurzelfasern als unmittelbar angeregte Strukturen, welche zu den induzierten Muskelaktivitäten führten.

Kontinuierliche Stimulation der lumbalen Hinterwurzelfasern mit Frequenzen von 5–15 Hz evozierte eine tonische EMG Aktivität mit charakteristisch modulierten Amplituden in den Beinmuskeln und führte zu einer Extensionsbewegung der Beine.

Direkte elektrische Anregung der gleichen Strukturen mit 25–50 Hz induzierte schrittähnliche Bewegungen mit alternierenden EMG-„bursts“ der Flexoren und Extensoren der Ober- und Unterschenkel. Die Muskelaktionspotentiale, welche die „burst“-Phasen zusammensetzten, zeigten um 10 ms längere Latenzen als jene einfacher Muskelzuckungen.

Bei Applikation elektrischer Rückenmarksstimulation während manuell assistiertem Laufband-Gehen konnten rhythmische, mit dem Gangzyklus synchronisierte EMG Aktivitäten evoziert werden. Alle effektiven Stimulationsparameter lagen im Bereich von 20–50 Hz und 6–10 V.

Schlussfolgerungen

Muskelzuckungen, ausgelöst durch epidurale Stimulation der posterioren Strukturen des Lumbalmarks mit Einzelpulsen, sind monosynaptische Reflexantworten auf Anregung afferenter Axone in den Hinterwurzeln. Diese Muskelantworten wurden als „Posterior Root Muscle Reflex Responses“ (PRMRRs) bezeichnet. Dieselben afferenten Nervenimpulse werden synaptisch an Interneurone im Lumbalmark weitergeleitet, mit denen die Hinterwurzelfasern anatomisch verbunden sind. Bei kontinuierlicher epiduraler Stimulation der lumbalen Hinterwurzeln mit Frequenzen von 5–50 Hz können synaptische und presynaptische Mechanismen aktiviert werden, welche zur Induktion von Extension und schrittähnlichen Bewegungen führen. Die Selektion der funktionellen Wirkung der interneuronalen Strukturen ist frequenzabhängig. Aktivierte spinale Interneurone formen nicht nur das Muster des Motoroutputs, sie leiten die eintreffenden afferenten Impulse über längere, oligosynaptische Pfade und inhibieren die entsprechenden monosynaptischen Bahnen. Die durch epidurale Stimulation mit 25–50 Hz konfigurierten interneuronalen Netzwerke haben Eigenschaften von Mustergeneratoren für Lokomotion und wurden „Lumbar Locomotor Pattern Generator“ (LLPG) genannt. Der LLPG kann durch kontinuierliche elektrische Stimulation während manuell assistierter Laufbandlokomotion aktiviert werden und dabei afferentes Feedback funktionell verarbeiten.

Die Ergebnisse der vorliegenden Dissertation untermauern die empirische Beobachtung der Induktion eines LLPGs durch kontinuierliche Rückenmarksstimulation. Trotz der Einfachheit des äußeren Reizes, ein anhaltender Input durch die Hinterwurzeln mit konstanter Frequenz, wird eine komplexe Muskelaktivierung ausgelöst. Basierend auf den gefundenen Ergebnissen liegt es nahe, die Einbeziehung des LLPG gezielt therapeutisch einzusetzen.

Summary

Modeling of a human spinal pattern generator for locomotion and its activation by electrical epidural stimulation

Motivation and objectives

While evaluating the effect of electrical epidural spinal cord stimulation on spasticity in patients with complete spinal cord injury, it was discovered that the sustained non-patterned stimulation could induce stepping-like lower limb movements. This observation was regarded as evidence for the existence of a spinal locomotor pattern generator in humans. At this early stage the mechanisms underlying the stimulus-evoked stepping-like movements were not clear.

This thesis aimed at studying the capability of the human lumbar spinal cord isolated from brain control to generate stepping-like motor output. Systematic research should establish the existence of a human spinal pattern generator for locomotion by providing further evidence. Particular objectives were (i) to identify the neural structures which are stimulated by the epidural electrode initiating stepping-like movements of the paralyzed lower limbs, (ii) to supply evidence that epidurally evoked stepping-like movement is due to activation of central spinal structures, (iii) to find out if the human spinal pattern generator activated by non-patterned epidural stimulation can process peripheral feedback input related to passive stepping to generate functional electromyographic (EMG) patterns.

Material and Methods

Neurophysiological data on the input-output behavior of the lumbar cord in isolation from supraspinal input but with well-defined input delivered by externally controlled spinal cord stimulation was analyzed. The data was derived from seventeen subjects with complete spinal cord injury. They had implanted electrodes placed in the posterior, epidural space at vertebral levels T10–L1 for the control of spasticity. The effect of stimulation had been assessed by surface EMG recording of induced muscle activity in the lower limbs.

To examine the direct effect of spinal cord stimulation, muscle twitch distribution patterns of the lower limbs with respect to the cathode site of the epidural electrode were evaluated. The results were combined with computer simulations of epidural spinal cord stimulation to calculate the spatial distributions of the electric fields generated by the electrodes.

To study central effects induced by spinal cord stimulation, EMG responses to stimulation with 1–10 V at 5–50 Hz were analyzed. Stimulus-triggered 50 ms time windows from the original EMG traces were evaluated. Stimulus-evoked compound muscle action potentials (CMAPs) were analyzed with reference to latency, amplitude, and shape.

Epidural stimulation was applied during manually assisted stepping on a treadmill in two paralyzed subjects to consider the capabilities of the spinal locomotor pattern generator to process peripheral feedback input to generate functional motor output.

Results

Epidural stimulation of the human lumbar cord caudal to the complete spinal cord injury level elicited single twitch responses and different patterns of tonic and rhythmic EMG

activity in the lower limb muscles depending on the site, frequency and amplitude of stimulation.

Stimulation at 2.2 Hz induced stimulus-coupled CMAPs of short latency. The recruitment order of quadriceps and triceps surae twitch responses was related to the rostrocaudal position of the cathode with respect to spinal cord segments. This segmental-selectivity of stimulation indicated that the stimulus-evoked muscle activity was initiated in the posterior roots. The comparison of calculated electric potential distributions generated by the epidural electrode with the topographical anatomy of neural target structures provided an independent evidence for the direct stimulation of posterior roots.

Sustained stimulation at 5–15 Hz evoked a tonic EMG activity with characteristic amplitude modulations and could initiate an extension movement of the paralyzed lower limbs.

Stimulation at 25–50 Hz with predominant activation of the L2–L4 posterior roots induced alternating burst-style EMG activity in the lower limb muscles leading to stepping-like movements in supine individuals with complete spinal cord injury. Successive stimulus-evoked CMAPs were subject to well-defined amplitude modulations resulting in burst-like envelopes of the EMG activity. A significant increase of CMAP latencies by about 10 ms during burst-style phases was found.

Epidural stimulation applied during manually assisted, weight-bearing treadmill stepping evoked functional EMG bursts in the paralyzed lower limb muscles, which were temporally synchronized to specific phases of the step cycle. All effective stimulation parameters were within the range of 20–50 Hz and 6–10 V.

Conclusion

Single pulse (2.2 Hz-) stimulation of posterior lumbar cord structures activated large afferent fibers within the posterior roots and recruited motoneurons through monosynaptic connections in the spinal cord. The resulting stimulus-evoked muscle activity was termed Posterior Roots Muscle Reflex Responses (PRMRRs). The same afferent input was synaptically transmitted to spinal interneurons. Sustained stimulation of the posterior roots at higher frequencies activated lumbar neuronal circuits that modulated the afferent flow through monosynaptic pathways by presynaptic inhibitory mechanism and controlled motoneuronal discharge by mono- and oligosynaptic excitatory pathways. The responses could be organized to result in either limb extension or stepping-like movements. Inducing these patterns was a function of different frequencies of the applied train of electrical stimuli. The EMG responses during the rhythmical movements elicited by the sustained, non-patterned stimulation were dynamically modulated with respect to both amplitude and latency. It is proposed to consider the described capabilities of the human lumbar cord isolated from brain control and tested by repetitively induced PRMRRs at 25–50 Hz as evidence for the existence of a Lumbar Locomotor Pattern Generator (LLPG). The LLPG could be activated during weight-bearing, manually assisted treadmill stepping by electrically-evoked tonic input and could integrate and interpret peripheral feedback input in order to generate functional locomotor patterns.

The possibility of activating the human spinal pattern generator for locomotion raises the possibility to partially overcome the loss of supraspinal input in patients with spinal cord injury by appropriate electrical stimulation.

Acknowledgements

I wish to acknowledge the invaluable support of Professor Milan R. Dimitrijevic to the work presented in this thesis. His visionary approach to understanding human motor control has inspired and guided me throughout my work. He motivated me to work to my full potential. Thank you for being a teacher and a mentor.

I am grateful to Professor Frank Rattay for introducing me to the field of neuromathematics and "Brain modeling". Thank you for establishing an environment enabling interdisciplinary research. Your support and supervision accompanied me from the very beginning.

I am also thankful to Dozent Dr. Michaela M. Pinter for her extensive effort to allow neurophysiological studies in humans as part of well-established clinical programs.

Many thanks to Ms. Preinfalk, Ms. Auer, and Ms. Alesch for their excellent technical support.

Table of Contents

Kurzfassung der Dissertation	2
Summary	4
Acknowledgements	6
Table of Contents	7
Abbreviations	10
Chapter 1	
Introduction	11
Background and Motivation	11
An autonomous spinal pattern generator for locomotion in humans?	11
Model and Methodology	13
An approach to conduct human neurosciences	13
The model of the lower spinal cord under the condition of well-defined inputs	15
Surface-EMG as an approach to indicate the function and state of activation of the central nervous system	16
Stimulation-response paradigms	17
Computer modeling	18
Computer modeling – Volume conductor model	20
Computer modeling – Nerve fiber model	23
Design of the thesis	27
References	29
Chapter 2	
Posterior Roots Muscle Reflex Responses elicited by epidural stimulation of the human lumbar cord	33
Summary	33
Introduction	34
Material and methods	34
Subjects	34
Stimulation setup	36
Recording procedure	36
Data analysis – Data based on incremental pulse amplitudes	36
Data analysis – Data based on incremental pulse frequencies	37
Computer simulation of the electric potential distribution	38
Results	38
Muscle responses to single stimuli (2.2 Hz stimulation)	38

Relationships between cathode levels, stimulation amplitudes and activated muscle groups – Stimulation frequency: 2.2 Hz	41
Muscle responses to trains of stimuli	43
Relationships between cathode levels, stimulation amplitudes and activated muscle groups – Stimulation frequencies: 2.2, 25, 50 Hz	45
Stimulation of neuronal structures at the level of the cathode	47
Stimulation of neuronal structures distant from the cathode level	50
Discussion	50
Muscle responses to epidural lumbosacral cord stimulation are initiated in the posterior roots	52
Posterior Roots Muscle Reflex Responses	55
Differences between Posterior Roots Muscle Reflex Responses and the H-reflex	56
Posterior Roots Muscle Reflex Responses to trains of stimuli at higher frequencies	58
Significance of the results	60
References	62
Chapter 3	
Stepping-like movements in humans with complete spinal cord injury induced by epidural stimulation of the lumbar cord: Electromyographic study of compound muscle action potentials	66
Summary	66
Introduction	67
Material and methods	68
Subjects	68
Stimulation and recording setup	69
Data analysis – Data based on incremental pulse amplitudes	71
Data analysis – Data based on incremental pulse frequencies	71
Results	72
Epidurally evoked segmental twitch responses	72
Stimulation with pairs of stimuli	74
Stimulation with trains of stimuli	76
Discussion	81
Directly stimulated structures which should be considered as inputs resulting in the CMAPs	81
Epidural stimulation induces Posterior Roots Muscle Reflex Responses	84
Posterior Roots Muscle Reflex Responses and induced central effects	85
Posterior Roots Muscle Reflex Responses and the Lumbar Locomotor Pattern Generator	86
Significance of the results	88
References	89

Chapter 4

Effect of peripheral afferent and central afferent input to the isolated human lumbar spinal cord	94
Summary	94
Introduction	95
Material and methods	96
Subjects	96
Stimulation procedure	96
Recording procedure	98
Data analysis	99
Results	99
Effect of spinal cord stimulation on lower limb EMG patterns induced during passive treadmill stepping	99
Contributions of mechanical (phasic) and electrical (tonic) stimulation to the induced EMG activities	101
The effect of epidural cathode position on the induced EMG patterns	104
The effect of different frequencies of spinal cord stimulation on the induced EMG patterns	105
Discussion	107
Effect of phasic peripheral feedback input to the isolated lumbar cord	107
Effect of tonic input to the lumbar cord generated by spinal cord stimulation	107
Effect of spinal cord stimulation-evoked tonic input in conjunction with phasic peripheral feedback input to the lumbar cord	108
Significance of the results	110
References	112
<i>Curriculum vitae</i>	113
<i>List of scientific publications</i>	115

Abbreviations

A	adductor
ASIA	American Spinal Cord Injury Association
BMCA	brain motor control assessment
CMAP	compound muscle action potential
CPG	central pattern generator
EMG	electromyography, electromyographic
FES	functional electrical stimulation
H	hamstrings
ISI	interstimulus interval
KJA	knee joint angle
KM	knee movement
L	lumbar
LLPG	Lumbar Locomotor Pattern Generator
Mn	motoneuron
PARA	paraspinal trunk muscles
PRMRR	Posterior Roots Muscle Reflex Response
Q	quadriceps
S	sacral
SCI	spinal cord injury, spinal cord injured
SCS	spinal cord stimulation
T	thoracic
TA	tibialis anterior
TS	triceps surae

Chapter 1

Introduction

Background and Motivation

An autonomous spinal pattern generator for locomotion in humans?

Vertebrate locomotion is characterized by rhythmic activity and the utilization of multiple degrees of freedom, i.e. multiple joints and muscles. Motion is generated by the musculoskeletal system in which torques are created by antagonist muscles at the joints of articulated systems composed of rigid bones. By rhythmically applying forces to the ground, reaction forces are generated which move the body forward. This type of locomotion is in contrast to the propulsion of most manmade machines, which usually rely on few degrees of freedom (e.g. a limited number of powered wheels) and continuous rather than rhythmic actuation. From a technological point of view, vertebrate locomotion is significantly more difficult to control than that of wheeled machines. To generate efficient locomotion, the frequencies, amplitudes, and phases of the signals sent to the multiple muscles must be well coordinated. Complex coordination is required not only between different joints and limbs, but also between antagonist muscles which combine periods of co-activation for modulating the stiffness of the joint and periods of alternation for actuating the joint.

While locomotion is highly complex, animal experiments and recent findings in humans have documented, that it is to some degree an automated movement. Vertebrate locomotion control appears to be organized such that autonomous neural networks in the spinal cord generate the basic rhythmic patterns necessary for locomotion. Higher control centers interact with the spinal circuits for posture control and accurate limb movements. This means that the control signals sent to the spinal cord by supraspinal centers do not need to specify all the details of when and how much the multiple muscles must contract, but rather specify higher level commands such as stop and go signals, speed, and heading of motion.

Autonomous neural circuits which can generate a rhythmic motor output without receiving rhythmic input are called "central pattern generators" (CPGs). The hallmark for identification of a locomotor CPG within the spinal cord is the production of recognizable and reproducible patterns of rhythmic output in the absence of instructive external drive from higher levels of the central nervous system or from peripheral sensory feedback.

Definite evidence for spinal CPGs for locomotion exists in lower mammals. Investigations on animals (rat, rabbit, cat, dog) demonstrated that the lumbar spinal cord harbors a pacemaker capable of inducing locomotor-movements. This pacemaker acts autonomously since it had been separated from suprasegmental and peripheral influences by experimentally induced trauma (Grillner, 1981). The existence of a CPG in primates first remained unclear. Eidelberg and colleagues (1981) reported that in acute and chronic spinal macaque monkeys it was not possible to evoke locomotor movement. On the other hand,

Hultborn and colleagues (Hultborn *et al.* 1993; Fedirchuk *et al.* 1998) demonstrated fictive locomotion in spinal marmoset monkeys.

The existence of a spinal CPG in humans according to the definition originally established in animal preparations (as aforementioned to have the capacity to produce movement in the absence of phasic, movement-related sensory input and in the absence of supraspinal input) is more difficult to demonstrate and evidence is, by necessity, indirect. While it is possible to rule out supraspinal inputs to the lower human spinal cord due to complete spinal cord injuries, peripheral segmental input cannot be completely removed (e.g. by posterior rhizotomy) like in the experimental animal model.

Nevertheless, recent observations in patients with spinal cord lesions suggest that there is an autonomous network in the human spinal cord which has the capacity of generating rhythmic alternating muscle activity similar to that seen during active walking.

Calancie and co-workers (1994) documented an indirect evidence for the existence of a human spinal locomotor pattern generator in an individual with incomplete spinal cord injury and periathritic changes in the hip. This individual exhibited involuntary stepping movements of the lower extremities when he was positioned supine with the hip extended. The strength, rate, and rhythmicity of these movements exceeded those that the subject was able to produce voluntarily. The temporal relationships of the electromyographic (EMG) patterns were consistent both within and between testing sessions. The investigators contended that afferent input to the spinal cord due to active osteoarthritis at the hip was a primary factor allowing the central pattern-generated movement to manifest in this individual with spinal cord injury. Bussel and colleagues discussed that some elements of the spinal circuitry in the acute spinal cat, on which the generation of stepping rhythms relies, also exist in man (Roby-Brami & Bussel, 1987; Bussel *et al.* 1996). Gurfinkel and colleagues (1998) used tonic peripheral afferent stimulation to elicit involuntary stepping in able-bodied individuals. They found that continuous lower limb muscle vibration gave rise to involuntary locomotion-like movements in suspended legs and suggested that the non-specific afferent input induced by vibration activated central structures governing stepping movements. Another approach to generate stepping-like oscillating EMG patterns in the paralyzed lower limbs is manually assisted stepping of complete spinal cord injured subjects over a moving treadmill belt (Dietz *et al.* 1995; Dobkin *et al.* 1995). These findings suggested that pattern generating spinal networks can be activated by means of peripheral afferent feedback from muscles, tendon, cutaneous and articular receptors related to passive stepping.

Dimitrijevic *et al.* (1998) were among the first who provided direct evidence for the presence of a human spinal locomotor pattern generator. They discovered that repetitive and regular electrical stimulation of the posterior structures of the lumbar spinal cord could initiate and maintain rhythmic stepping-like flexion/extension movements of the subject's paralyzed limbs. To illustrate their findings, they chose surface-recorded EMG activity of agonist-antagonist muscles of thigh and leg that lasted for 30 s without changes in the rhythmical patterns (Fig. 1.1). The authors demonstrated that the lumbar cord, isolated from brain control, could respond to a sustained, non-patterned train of stimuli with the generation of rhythmic stepping-like motor output. This result was regarded as evidence for the existence of a spinal locomotor pattern generator in humans, which can generate a rhythmic motor output without receiving rhythmic input with spatially and temporally complex patterns.

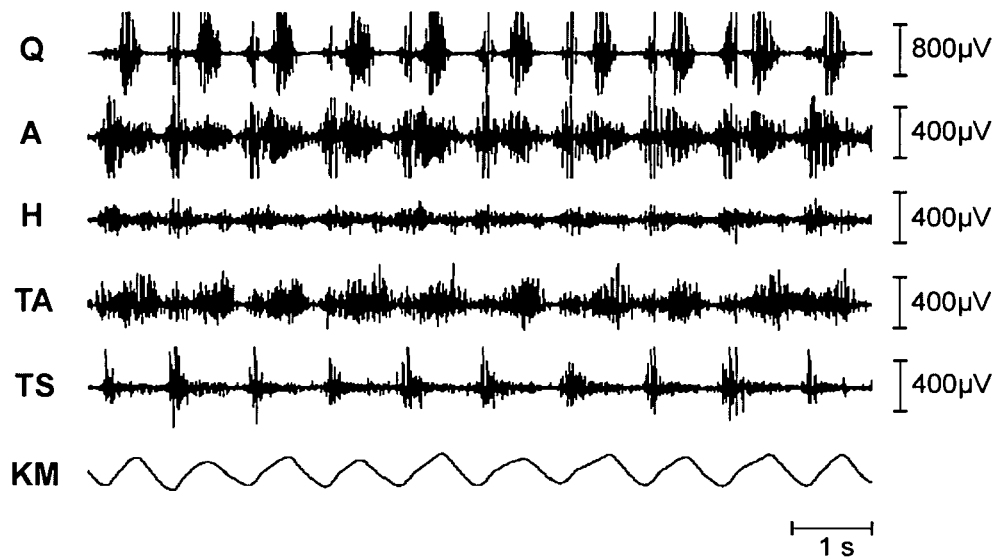


Figure 1.1 Stepping-like modulated EMG activity in response to repetitive and regular epidural lumbar cord stimulation

Surface EMG recordings from the right quadriceps (Q), adductor (A), hamstrings (H), tibialis anterior (TA), and triceps surae (TS) muscles and knee movement (KM, deflection up is flexion, deflection down is extension) in a complete paraplegic. Epidural stimulation was applied over the posterior structures of the L2 cord segment with a train of 30 Hz and stimulus strength of 9 V (Dimitrijevic *et al.* 1998).

At this early stage of Dimitrijevic's initial studies it was not clear which neural structures were stimulated by the electrical epidural stimulation. The mechanisms underlying the stimulus-evoked stepping-like movements were not clear.

The aim of this thesis was to further advance the encouraging findings of Dimitrijevic's pioneering work. Systematic research should establish the existence of a human central pattern generator for locomotion by providing further evidence. The thesis was motivated by the unique opportunity to study human motor control of locomotion on the basis of neurophysiological data. The studied model is the human lumbosacral spinal cord in complete (subclinical) isolation from supraspinal input. Externally controlled spinal cord stimulation provides a well-defined input. A computer model of epidural spinal cord stimulation was applied to identify the directly stimulated neural structures and thus the pathways mediating the activating input to the pattern generating neural circuits. Stimulus-evoked and surface recorded EMG data were analyzed to reveal features of the input-output processing capabilities of the activated spinal neural networks and to investigate the nature of the muscle responses.

Model and Methodology

An approach to conduct human neurosciences


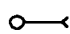
Definite evidence for a CPG in lower mammals was repeatedly demonstrated in acute animal preparations. Thereby, neuronal networks in the spinal cord were completely isolated from sensory input (deafferentation) and separated from suprasegmental influences (spinalization or decerebration) by experimentally induced trauma (transection). The CPG

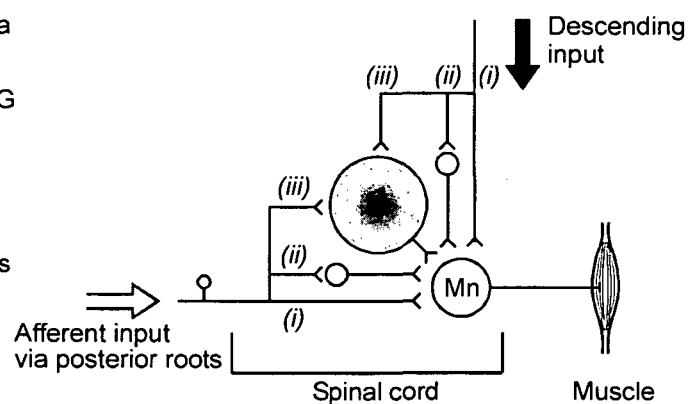
was activated by injection of drugs or application of electrical stimulation. The generated complex coordinated patterns of efferent output were recorded intracellularly from motoneurons during the so-called “fictive locomotion” (Figs. 1.2A and B).

Obviously, this experimental approach is not possible in humans. However, there is the possibility of neurophysiological studies in humans in parallel to well-established clinical programs. Epidural spinal cord stimulation is a clinical method to control severe spasticity in chronic spinal cord injured individuals (Dimitrijevic *et al.* 1986 *a,b*; Barolat *et al.* 1995). In a clinical program of restorative neurology carried out in the Neurological Hospital Maria Theresien Schlössel (Vienna, Austria), the effect of epidural spinal cord stimulation on spasticity of the lower limbs in patients with traumatic spinal cord injury was evaluated. Clinical protocols were conducted to define optimal electrode positions and stimulation parameters, thereby applying stimulation strengths of 1–10 V at frequencies of 2–100 Hz and testing different contact combinations of an epidurally placed electrode array. The effect of stimulation was assessed by surface EMG recordings of lower limb muscle

A

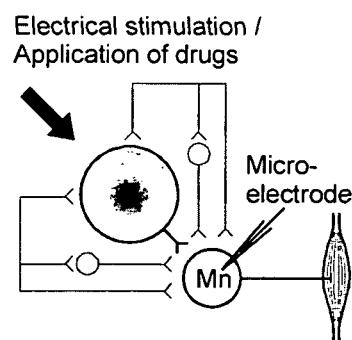
Control of motoneurons (Mn) via
 (i) direct pathways
 (ii) interneurons outside the CPG
 (iii) interneurons capable of
 building-up CPG networks

 CPG / locomotor networks
 Interneurons



B

Animal preparation



C

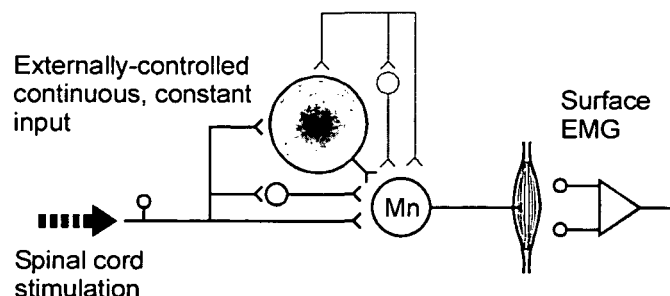
Human lumbar cord model
of the present study

Figure 1.2 Models of the lumbar cord: Schematic drawings of afferent and descending pathways projecting to motoneurons via different pathways

A, Lumbar cord under the influence of (residual) supraspinal input and afferent feedback. B, Experimental animal preparations with the CPG completely isolated from descending and afferent input. Non-functional pathways are displayed gray. C, Model of the human lumbar cord deprived of descending influence and under the condition of well-defined external input.

activity. In a period of six years, more than 1000 recordings were carried out. It was demonstrated that spinal cord stimulation was effective to *suppress* the excitability within particular motor nuclei – and thus reduce spinal spasticity – if the stimulating electrode was located at upper lumbar segmental levels, and the applied stimulus train had an amplitude of 2–7 V at frequencies of 50–100 Hz (Pinter *et al.* 2000). Stimulation at frequencies below 50 Hz *enhanced* the excitability of lumbosacral motor nuclei and *induced* single twitch responses, sustained contractions or even rhythmical activity of the lower limb muscles. These EMG data of stimulus-evoked muscle response patterns was anonymized and made available for the present study. The data analyzed in the present study was derived from subjects with complete spinal cord injuries.

The model of the lower spinal cord under the condition of well-defined inputs

Unlike the studies of animals with deafferentation and complete isolation of the spinal cord from descending input, it is difficult to provide evidence in humans that initiation and maintenance of automated stepping-like activity is due to spinal mechanisms alone. In individuals with incomplete spinal cord injury as well as with clinically complete ones, there is clearly a potential for some influence of remaining supraspinal descending input on the lumbar spinal cord. Furthermore, due to intact sensory input to the spinal cord, some groups of researches proposed simpler mechanisms than the contribution of pattern generating spinal networks to account for stepping-like activity in paralyzed lower limbs. Some researchers initially suggested that rhythmical EMG-activity in lower limb muscles induced during passive treadmill-walking could be due to periodically imposed muscle stretches. Regarding Dimitrijevic's observation, there were even critics considering that repeated induction of fatigue induced by the high frequency stimulation of peripheral nerves might explain the rhythmical activity. The suggestion that stretch reflexes were the sole source of the phasic EMG activity induced in flexors and extensors during manually assisted stepping of paraplegic subjects has meanwhile been discarded (Harkema *et al.* 1997). It is now more and more accepted that sensory information associated with weight-bearing passive stepping can activate and coordinate human spinal locomotor networks. In this thesis evidence will be presented that the epidurally evoked stepping-like activities is due to activation of central spinal structures. Peripheral feedback-input can reinforce the pattern generator activities and has a timing function.

A rather unique approach in this thesis is the attempt to study the locomotor capabilities of the lower spinal cord under the condition of well-defined inputs. All data which was analyzed in this thesis were derived from complete spinal cord injured subjects. Within the clinical program of restorative neurology carried out in the Neurological Hospital Maria Theresien Schlössel, a neurologist examined the subjects' spinal cord functions and assessed their functional status (*clinical* assessment). In addition, non-invasive techniques for the neurophysiological assessment of *sub-clinical* spinal cord functions were applied. The „brain motor control assessment“ (BMCA) protocol was carried out for the examination of residual functional capabilities, i.e., of the degree to which brain influence is preserved below a spinal cord lesion (Sherwood *et al.* 1996). By using this method, a comprehensive multichannel surface EMG recording, it is possible to register objective, quantitative and reproducible data on the altered motor control after an upper motoneuron trauma. The results of the BMCA protocol demonstrate the presence of any trans-lesional brain influence over spinal motor activity and reveal features of motor control that are not apparent in the clinical examination. Furthermore, lumbosacral evoked potentials were used

to assess the functions of the spinal gray matter below the lesion level. They were recorded after tibial nerve stimulation with surface electrodes placed at the S1, L4, L2, and T12 spinous processes referenced to an electrode at T6 (Lehmkuhl, 1984; Beric, 1988).

The results presented in the following chapters were derived from complete spinal cord injured subjects with intact functions of the posterior structures and gray matter of the spinal cord below the lesion level and with preserved stretch and cutaneomuscular reflexes. All results illustrating the successful activation of stepping-like EMG activity and corresponding alternating flexion/extension movements were recorded in subjects with a *sub-clinical* complete spinal cord injury (i.e. no brain influence preserved below the lesion level).

Consequently, actual stepping-like movements were *initiated* under well-defined input conditions to the spinal cord (Fig. 1.2C), namely:

- (i) no supraspinal input
- (ii) minimized and insignificant afferent feedback input (no conditioning by leg movement before the stimulus-evoked movement was initiated) and
- (iii) externally-controlled repetitive and regular input generated by spinal cord stimulation with implanted electrodes.

This is in contrast to the studies of assisted treadmill-stepping of clinically complete spinal cord injured subjects. It was demonstrated there that EMG activity can be generated in response to passive limb movement combined with loading – but there was no *independent stepping*, only *passive leg motion*.

Surface-EMG as an approach to indicate the function and state of activation of the central nervous system

The basis of this thesis was the analysis of surface-recorded electromyographic (sEMG) activities from four main lower limb muscle groups induced under externally-controlled input conditions to the spinal cord. The recording electrodes were placed over the quadriceps (anterior thigh), hamstrings (posterior thigh), tibialis anterior (anterior leg), and triceps surae (posterior leg) muscles. It is important to keep in mind that sEMG were not analyzed to study movement. The sEMG recording was interpreted as a non-invasive technique that provided a measure of central nervous system output to the muscle and as a window to reveal features of the spinal motor control strategies (Fig. 1.2C). Thus, the information contained in the sEMG was investigated to find out how the epidural stimulation affected the circuitries in the spinal cord. Special consideration was given to the EMG activities of the quadriceps and triceps surae muscle groups, because they are the only ones of the recorded muscle groups with separate segmental innervations. Responses in quadriceps and triceps surae were taken as an estimate of the spinal motor neuron pool activity over time of the L2, L3, L4 segments and L5, S1, S2 segments, respectively.

When analyzing the EMG recordings, we assumed that the EMG activity was predominantly related to the epidural stimulation. Motor neuron pool activation by supraspinal input could be ruled out. When the subject was lying in a supine position and no lower limb movements were initiated by the stimulation, afferent feedback input certainly played an insignificant role. When stepping-like movements were induced by the electrical spinal cord stimulation, conditions were set to minimize afferent feedback-input from articular and cutaneous receptors. It was shown that afferent feedback input associated

with “air-stepping” (assisted stepping with the limbs bearing no load) is ineffective to induce rhythmic EMG-activity in the paralyzed lower limbs (Harkema *et al.* 1997, Dietz *et al.* 2002).

Indeed, the analyzed EMG activities consisted of separate compound muscle action potentials (CMAPs) which could unequivocally be related to the stimulus-pulse which had triggered it. EMG potentials of consecutively evoked CMAPs did not interfere with each other when the stimulus frequency did not exceed 30 Hz. The moments when stimulus pulses were applied were indicated by stimulus artifacts recorded by surface electrodes which were placed over the subject’s lower back (paraspinal muscles). Due to the close distance of these paraspinal-electrodes to the epidural electrode, volume-conducted artifacts of the stimulus pulses delivered by the stimulating electrode were picked up by the recording surface electrode. This allowed analyzing stimulus-triggered time windows of the original continuous EMG-recordings, each containing a CMAP. We examined the single surface-recorded CMAPs for latencies (quantitatively), peak-to-peak amplitudes, and shapes (qualitatively). Modulations of the response latency, EMG-amplitude and potential shape of the CMAPs evoked by stimulation with constant parameters could be attributed to activation of premotorneuronal spinal mechanisms that control motoneuronal discharge and the transmission through reflex pathways (see chapters 2 and 3).

Stimulation-response paradigms

When describing the neurophysiological characteristics of motor control in spinal cord injury, two different paradigms can be used as an investigative tool, single stimulus-response and repetitive stimulus-response measurements. Thereby, analyzing the motor responses reveals information about the excitability of the motoneurons, changes in transmission of spinal pathways, and the organization of spinal interneurons into functional circuits. Muscle responses are clinically evoked by muscle stretch delivered manually or by a reflex hammer or vibrator, and through different modalities of electrical stimulation applied to peripheral nerves. Single impulse input to the spinal cord typically produces a single twitch in the muscle corresponding to the stimulated nerve. However, repeated impulses at increasing frequency as would be generated by passive stretch of a muscle or, in the laboratory using strong vibration of the muscle, recruit additional spinal cord internuncial and propriospinal neurons and can build up some regularities in the control of motor output (Kern *et al.* 2004).

Using an electrode which had been percutaneously inserted into the posterior epidural space for the control of severe spasticity, provided a technique to deliver input to the human lumbar cord from a localized and stable region. The advantage of this method is the possibility to

- (i) stimulate different segments in certain isolation with single stimuli
- (ii) continuously and simultaneously stimulate all segments which contain the cell bodies of motoneurons innervating all main lower limb muscles as well as elements of the spinal circuitry involved in generating rhythmic locomotor activity.

Besides recruiting motoneurons, spinal cord stimulation also produces postsynaptic potentials in spinal interneurons. The analysis of the stimulus-responses is based on the concept that the externally applied pulse train could be regarded as conditioning the spinal cord premotorneuronal structures. In parallel, each single pulse within the train is a test

stimulus eliciting an EMG response, which reveals the conditioning effect of the train applied prior to the arbitrarily chosen test stimulus.

Testing the spinal cord circuitries with low frequency stimulation (2 Hz) demonstrated a functional resting state of the spinal interneurons. Due to the long interstimulus interval (0.5 s), a given response is not influenced by the elicited activity of the preceding stimulus. Thus, the effect of 2 Hz-stimulation is similar to the effect of single applied stimulus pulses and can be used to examine the segmental effects of spinal cord stimulation. Particularly, information on the immediately activated structures that generate postsynaptic potentials in lower limb motoneurons can be derived from this “single pulse” stimulation (Murg *et al.* 2000).

Analysis of the responses to the first two stimuli of the applied trains was carried out to describe the refractory behavior of the epidurally evoked muscle responses. Thereby, long-lasting, stimulus-strength dependent conditioning effects of the first stimulus on the excitability of the activated structures is revealed by the second (test) response. The range of the refractory periods and its dependency on stimulation parameters gives further information on the immediately stimulated structures (see chapter 3).

EMG responses to trains of electrical stimuli of 1–10 V and 5–50 Hz were examined to learn how the sustained stimulation causes lumbar cord neurons to shape different types of sustained tonic or patterned rhythmical motor output.

Computer modeling

A central question of the thesis was to identify the directly stimulated neural structures which led to the observed motor effects. Since the directly stimulated pathways are mediating the activating input to the pattern generating neural circuits, recognizing these structures is a precondition for understanding the mechanisms underlying the stepping-like movements activated by electrical epidural stimulation. Their identification is essential to localize the locomotor pattern generating networks within the human spinal cord. Once identified, other methods less invasive than epidural stimulation can target the input structures to the spinal structures for enhancing locomotor capabilities in people with impaired central nervous system functions.

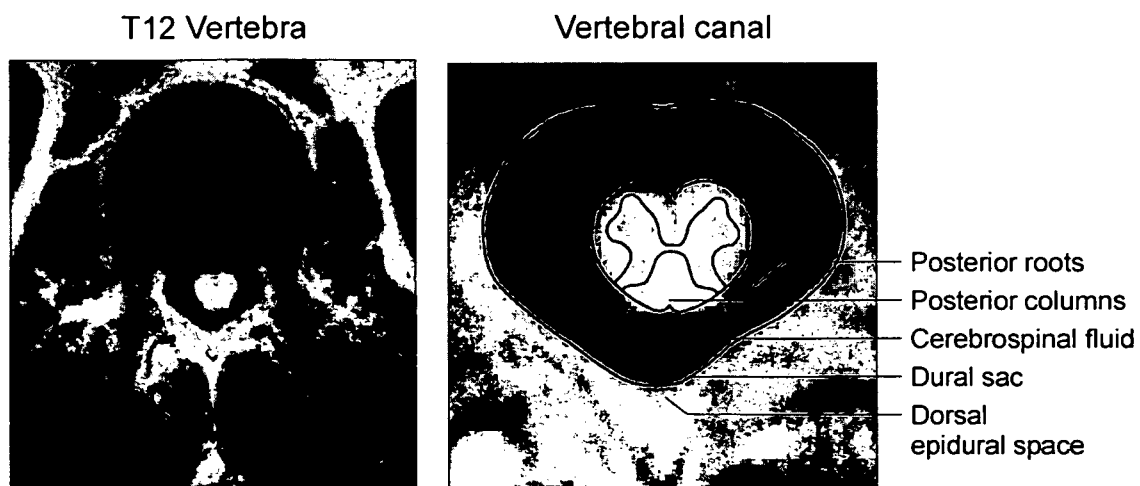


Figure 1.3 Cross-sectional anatomy of the lower spinal cord and its surrounding structures at the level of the twelfth thoracic (T12) vertebra (Bulling *et al.* 1997)

Epidural electrical stimulation is delivered by an array of electrode contacts which is inserted into the epidural space between the inner wall of the spinal canal and the dural sac. The dural sac is a membranous covering containing the spinal cord bathed in cerebrospinal fluid (Fig. 1.3).

In principle, the epidural electrode can directly stimulate any neural structures within the different quadrants of the spinal cord and within the spinal roots if the stimulus amplitude is sufficiently high. Even recruitment of structures dorsal to the epidural space was suggested, such as of small fibers in the ligamentum flavum (North *et al.* 1997).

The immediate effects of spinal cord stimulation are muscle contractions and paresthesiae (felt as tingling sensation on the skin in individuals with intact sensory functions), that are referred to the body parts corresponding to the activated neurons. From the beginning of spinal cord stimulation it has been assumed that primarily the dorsal columns are stimulated, as expressed by the terminology 'Dorsal Column Stimulation' used in many papers. This assumption originally derived from empirical studies based on the main application of epidural spinal cord stimulation, which is chronic pain management. For this application the electrode is placed dorsally in the epidural space, generally between cervical and mid-thoracic vertebral levels. Most work was concentrated in understanding the stimulation of large cutaneous fibers which are the structures initiating paresthesiae, and which were postulated to inhibit spinal cord neurons transmitting noxious information (Melzack & Wall, 1965). Although paresthesiae sometimes starts as segmental sensation, it spreads to dermatomes corresponding with low spinal levels when stimulus amplitude is increased. This widespread distribution of paresthesiae may even occur at the perception threshold (He *et al.* 1994) and can be attributed to activation of the dorsal columns (Barolat *et al.* 1993).

On the other hand, less attention was paid to the mechanisms underlying motor effects, which were regarded as side effects limiting the therapeutic efficacy in pain control stimulation. From previous studies, direct ventral motor root activation (DiMarco *et al.* 1999), direct stimulation of the dorsal columns (Hunter & Ashby, 1994; Regnaud *et al.* 2000), or even of the gray matter seemed a plausible explanation for muscle activation. Initially, rhythmical motor patterns activated by epidural stimulation were attributed to the direct activation of the dorsolateral funiculi (Gerasimenko *et al.* 2000, 2002; Dimitrijevic *et al.* 2001). This hypothesis was influenced by animal experimental work of Kazennikov and colleagues. They showed that stepping movements could be elicited in the decerebrate cat by microstimulation of a particular portion of fibers in the dorsolateral funiculus at the cervical or thoracic level, the so-called "locomotor strip" (see abstract of Kazennikov *et al.* 1983). In the clinical application of epidural stimulation with dorsal electrode placement for control of pain or spasticity, it was repeatedly observed that evoked muscle activity is typically a segmental effect, which, with increasing amplitude, only spreads to adjacent levels. This finding suggested dorsal roots as initiation sites of motor effects (Struijk *et al.* 1993; Murg *et al.* 2000).

A better understanding of this discrepancy of the direct effect of epidural spinal cord stimulation required a better knowledge in the electrical phenomena involved. These phenomena include two main aspects. First, the potential difference between the contacts of the epidural electrode during a stimulation pulse causes ionic current to flow from the anode to the cathode via the intermediate anatomical structures. These structures can be considered as a volume conductor. The resulting three-dimensional distribution of the electric potential and current density are determined by the geometrical relations and

electrical conductivities of the anatomical structures composing the volume conductor. Secondly, the stimulation-induced electrical field causes current to flow across nerve cell membranes, thereby eliciting local depolarization and hyperpolarization of these membranes. If a nerve fiber membrane is sufficiently depolarized, an action potential will be generated that propagates in both orthodromic and antidromic directions. The two separate aspects of the involved electrical phenomena can be represented by a volume conductor model and a nerve fiber model, respectively. Thus, computer modeling was recognized to be an appropriate method to identify the direct effects of epidural stimulation.

Computer modeling –Volume conductor model

The first computer models of spinal cord stimulation were established by Coburn in the late '70s (Coburn, 1980). Since 1986 similar modeling studies were initiated by Holsheimer and colleagues (Holsheimer & Struijk, 1987). Both groups were mainly interested in the mechanism underlying the effect of stimulation for pain control, and to improve the efficiency of spinal cord stimulation, primarily by the design of new epidural electrodes (Struijk & Holsheimer, 1996). Accordingly, the computer models were based on the spinal cord anatomy and geometrical relations at cervical and mid-thoracic vertebral levels. Three-dimensional volume conductor models were defined by prismatically extending a single two-dimensional cross-section of the gray matter, white matter, cerebrospinal fluid, dura mater, epidural fat, vertebral bone, and a surrounding layer. These models are appropriate for these rostral vertebral levels.

The purpose of this thesis was to explore motor effects induced by electrodes placed at low thoracic or first lumbar vertebral levels. Therefore the volume conductor model had to be representative for the terminal spinal cord and had to include the relevant anatomical structures at these levels. The lower spinal cord has a region with enlarged diameter, from which the nerve fibers supply the lower limb muscles. Below this region at the twelfth thoracic vertebral level, the spinal cord tapers to form the conus medullaris and terminates between the first and second lumbar vertebral level. The diameter of the dural sac does not change notably at these vertebral levels. This results in an increasing dorsal thickness of the cerebrospinal fluid layer surrounding the terminal spinal cord. This specific structure of the lower spinal cord required a three-dimensional volume conductor model composed of varying cross-sections (Fig. 1.4).

As indicated, the volume conductor model represents the anatomical structures and related conductivities, and the stimulating electrode contacts. The transverse geometry of the model is based on magnetic resonance images, on an interactive program on the human cross-sectional anatomy ('Visible Human Male', Bulling *et al.* 1997), and on quantitative measurements of the intradural geometry (Wall *et al.* 1990; Holsheimer *et al.* 1994; Kameyama *et al.* 1996). The stylized cross-sections describe the boundaries between gray matter, white matter, cerebrospinal fluid, dura mater, epidural space, vertebral bone, and a surrounding layer.

The first response of a long homogeneous fiber to an electric field is related to the second-order difference of the electric potential ('activating function') along the fiber (Rattay, 1990). Thus, the electric potential along the fiber trajectory has to be computed first. This electric potential is generated during the stimulation pulse of the implanted electrode. In order to obtain the electric potential Φ it is necessary to solve the volume conductor

problem $\nabla \cdot \mathbf{J} = I_V$ subject to specified boundary conditions, where \mathbf{J} is the current density and I_V the current per unit volume defined within the solution domain Ω .

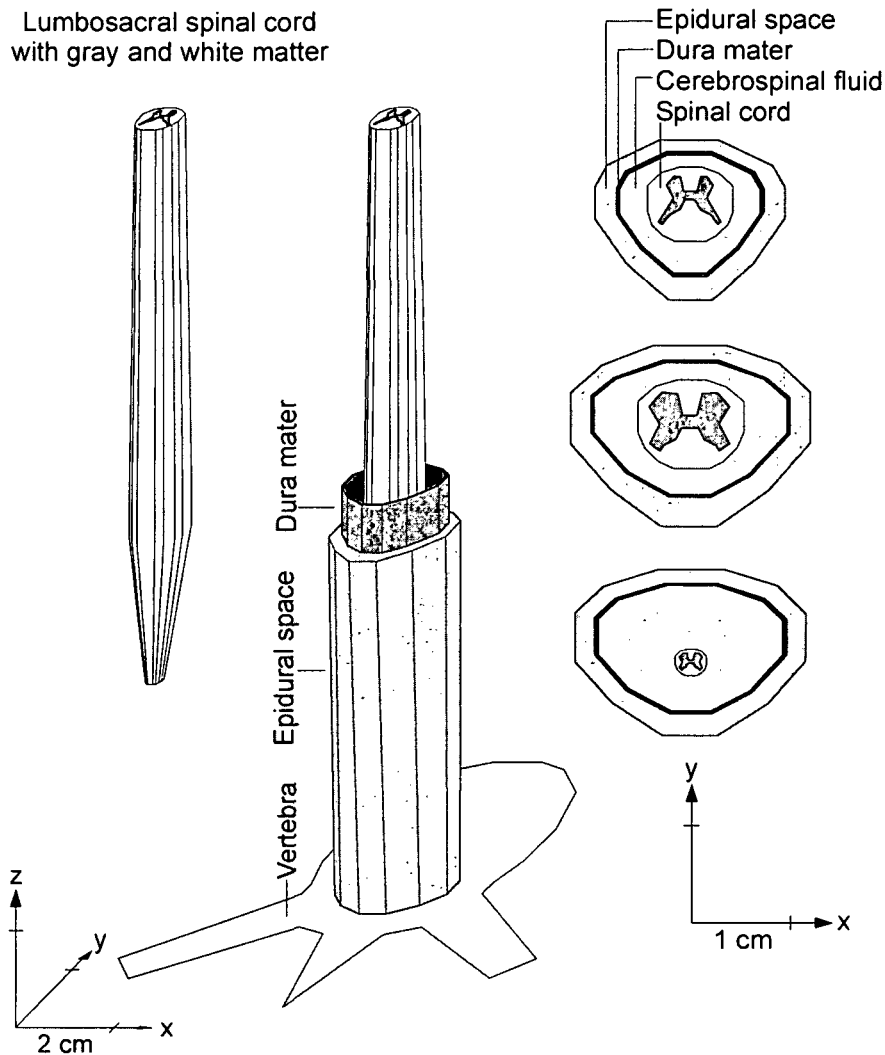


Figure 1.4 Finite-element geometry

Three-dimensional representation of the lumbosacral spinal cord. The geometry of the surrounding compartments (cerebrospinal fluid, dura mater, epidural space and vertebral bone) are only partially displayed. The layer surrounding the vertebrae is not shown. Right side: cross-sections demonstrating the varying geometrical relations within the spinal canal. The y-axis is showing in ventral direction.

With $\mathbf{J} = \sigma \mathbf{E}$ and $\mathbf{E} = -\nabla \Phi$, where \mathbf{E} is the electric field strength and σ is the electrical conductivity tensor, the bioelectric volume conductor can be formulated as the following boundary value problem

$$\nabla \cdot \sigma \nabla \Phi = -I_V \quad \text{in } \Omega. \quad (1.1)$$

Since the imposed current densities are zero ($I_V = 0$, electrodes will be considered as boundary conditions), $\nabla \cdot \mathbf{J} = I_V$ is equivalent to the Laplace equation

$$\nabla \cdot \sigma \nabla \Phi = 0 \quad \text{in } \Omega. \quad (1.2)$$

The original boundary value problem (1.2) can then be replaced with an equivalent integral formulation:

$$\int_{\Omega} (\nabla \cdot \sigma \nabla \Phi) \bar{\Phi} d\Omega = 0 \quad (1.3)$$

where $\bar{\Phi}$ is an arbitrary test function. This equation must hold for all test functions $\bar{\Phi}$. Applying Green's theorem, Eq. (1.3) can be written as

$$\int_{\Omega} \sigma \nabla \Phi \nabla \bar{\Phi} d\Omega - \int_S \sigma \bar{\Phi} \frac{\partial \Phi}{\partial n} dS = 0 \quad (1.4)$$

where S is the boundary of the solution domain Ω . When Dirichlet, $\Phi = \Phi_0$, or Neumann, $\sigma \nabla \Phi \cdot \mathbf{n} = 0$, boundary conditions are specified on S , the weak form of Eq. (1.4) is obtained:

$$\int_{\Omega} \sigma \nabla \Phi \nabla \bar{\Phi} d\Omega = 0. \quad (1.5)$$

The finite element method was applied to turn the continuous problem (1.5) into a discrete formulation. First, the solution domain is discretized into a mesh of finite volume elements which may have various shapes and which are connected via N nodes. Each element represents a part of an anatomical structure and has a constant conductivity.

Furthermore, a finite dimensional subspace V_N is defined. If the basis functions $\Psi_i \in V_N$ are defined as linear piecewise continuous functions that take the value 1 at node points x_i and zero at all other node points, then the function $\bar{\Phi} \in V_N$ can be represented as

$$\bar{\Phi}(x) = \sum_{i=0}^N \alpha_i \Psi_i(x) \quad \alpha_i = \bar{\Phi}(x_i), \quad i = 0, 1, \dots, N \quad (1.6)$$

such that each $\bar{\Phi} \in V_N$ can be written in a unique way as a linear combination of the basis functions $\Psi_i \in V_N$. Now the finite-element approximation of the original boundary value problem can be stated as:

$$\text{Find } \Phi_N \in V_N \text{ such that } \int_{\Omega} \sigma \nabla \Phi_N \nabla \bar{\Phi} d\Omega = 0. \quad (1.7)$$

Furthermore, if $\Phi_N \in V_N$ satisfies problem (1.7), then

$$\int_{\Omega} \sigma \nabla \Phi_N \nabla \Psi_i d\Omega = 0 \quad (1.8)$$

holds. This equation must hold for all (i.e. for a finite number N) basis functions $\Psi_i \in V_N$. Finally, since Φ_N itself can be expressed as the linear combination

$$\Phi_N = \sum_{i=0}^N \xi_i \Psi_i(x) \quad \xi_i = \Phi_N(x_i) \quad (1.9)$$

problem (1.7) can be written as

$$\sum_{i=1}^N \xi_i \int_{\Omega} (\sigma_{ij} \nabla \Psi_i) \nabla \Psi_j d\Omega = 0 \quad j = 0, 1, \dots, N \quad (1.10)$$

Then the finite-element approximation of Eq. (1.2) can equivalently be expressed as a system of N equations with N unknowns ξ_0, \dots, ξ_N , which are the electrostatic potentials at the node points x_i . In matrix form, the preceding system can be written as $A\xi = 0$ where $A = a_{ij}$

has the elements

$$a_{ij} = \int_{\Omega} (\sigma_{ij} \nabla \Psi_i) \nabla \Psi_j \, d\Omega. \quad (1.11)$$

The matrix A contains all geometry and conductivity information of the model. A is symmetric and positive definite and thus is nonsingular and has a unique solution. Since the basis function differs from zero for only a few intervals, A is sparse (only a few of its entries are nonzero). $A\xi = 0$ is subsequently solved for the unknown variable ξ . The finite element software package ANSYS was used to solve this bioelectric volume conductor problem.

The epidural electrode contacts were considered as boundaries with constant voltages (voltage sources, Dirichlet boundary conditions). The electrode had a realistic geometry representing a quadripolar lead with cylindrical, circumferentially exposed electrode contacts (PISCES-QUAD electrode, Model 3487A, MEDTRONIC, Minneapolis, MN, USA). The four independent contacts of the quadripolar lead were labeled 0, 1, 2, 3, such that contact #0 was at the top and contact #3 at the bottom. The epidural electrode was operated as a bipolar electrode with a contact separation of 27 mm. Dirichlet boundary condition of 0.5 Volt was applied to the 0-contact, and -0.5 Volt to the 3-contact. This represented a potential difference of one Volt for the '0+3-' electrode configuration. To obtain the potential distribution along the nerve fiber trajectories for any stimulation voltage strength or the other polarity ('0-3+'), the results calculated by the finite element method were multiplied by the corresponding factor.

The electrical conductivities of the anatomical structures were taken from the compendium by Geddes and Baker (1967). All structures have an isotropic conductivity, except nerve fiber bundles. In the latter structure the conductivity parallel to the constituent fibers exceeds the value in direction normal to these fibers, as is the case for the spinal white matter.

The output of the volume conductor model is the electric potential Φ within the whole, three-dimensional solution domain Ω . To quantitatively calculate the effect of an externally generated electric field on a nerve fiber, the potential distribution computed by the finite element method had to be evaluated along the trajectories of representative target neurons. These voltage profiles then served as the input data V_e (extracellular potential) for the nerve fiber model. Therefore the assumed geometry of the simulated target neurons has an essential influence on the results (Struijk *et al.* 1993). Clinical findings based on the distributions of stimulus-evoked muscle twitches on the lower limb muscle suggested that the predominantly stimulated structures resulting in motor effects were posterior roots of the lumbar spinal cord. Thus, computer modeling was concentrated on these nerve structures. However, there is no anatomical data on posterior root trajectories in humans, which is directly applicable to the computer simulation. Discussions with anatomists, information from anatomical photographs and from Wall *et al.* (1990) and Hasegawa *et al.* (1996) were used to define standard trajectories of the simulated fibers (for details see Minassian, 2000).

Computer modeling – Nerve fiber model

The fundamental unit of information in the nervous system is the action potential. An action potential is an electrical signal that propagates along a nerve fiber from the place of its

generation to the end of the nerve fiber. A neuron consists of three main parts, the soma (the cell body), the dendrites and the axon. From the soma a large number of branching processes called dendrites spread out. Dendrites are specialized for receiving signals from other neurons. The soma also gives rise to a thin and long fiber, called axon. The axon transmits action potentials to other neurons or to muscles. At the end region of an axon called synapse the neuron is in very close contact with other cells and, via the release of chemical substances, the neural information is passed on. The axon consists of a long cylinder of axoplasm, which is surrounded by an electrically excitable membrane. The specific properties of this membrane are the basis for the propagation of action potentials along all nerve fibers. The membrane consists of a lipid bilayer, which contains large protein molecules that penetrate through the membrane. Some of these protein molecules are ion channels. They selectively allow ions and other small hydrophilic molecules to cross the membrane which would otherwise be unable to do so. The ion channels are essential for the generation of action potentials.

The intracellular and the extracellular fluids of the neuron are separated by the membrane. Different ionic concentrations in these fluids cause a voltage gradient across the membrane. When the cell is at rest, the inside potential is about 70 mV lower than the outside. This state is called polarized. During an action potential, the membrane voltage changes from the resting potential of -70 mV up to $+50$ mV. This phase is called depolarization. After reaching the peak value the voltage decreases again to the resting state, commonly with an overshoot to values less than -70 mV being called hyperpolarization.

The neural structures considered in the computer model of epidural spinal cord stimulation were posterior roots of the lumbar cord. Posterior roots at their proximal sites, where the epidural electrodes were placed, contain long axons of sensory neurons, also called dorsal root ganglion cells or sensory afferents. They transmit sensory information to the central nervous system. The somata of the posterior root fibers are contained in the dorsal root ganglia, which are enlargements of the posterior roots at the intervertebral foramen (bony canals formed by two adjacent vertebrae). The main posterior roots containing sensory afferents from the lower limbs are of the spinal cord segments L2–S2. The ganglia of these spinal roots are all situated below the termination of the spinal cord and thus are several centimeters away from the epidural electrodes as positioned in the subjects studied in this thesis. In contrast, the axons within the posterior roots of the segments L2–S2 are in a close distance to the electrode (minimum 3–5 mm). Thus, the nerve model of dorsal root ganglion cells is restricted to a model of a myelinated axon.

In the electrical network model the axon is divided into identical compartments of the length Δx . The first approach is to assume that the myelinated parts of the axon are ideal insulators. Therefore the membrane currents of these internodes are neglected. One compartment per node of Ranvier is considered. The n -th compartment is represented electrically as a single point on the axon's length-coordinate x_n by its mean inside potential $V_{i,n}$, the capacity C_m and the ion current across the membrane $I_{ion,n}$ (Fig. 1.5). The extracellular potential $V_{e,n}$ at the positions x_n is caused by the stimulating electrode current. It is calculated by the finite element method and is the input data for the electrical network model.

Since the spatial axon model is represented by an electrical network where the current efflux of one segment is the current influx for the next, Kirchhoff's law can be used for the n -th compartment to obtain current equations for the capacitive current $I_{C,n}$, the ion current $I_{ion,n}$ and the axonal current $I_{axon,n}$:

$I_{C,n} + I_{ion,n} + I_{axon,n} = 0$ or, in more detail:

$$C_m \frac{d(V_{i,n} - V_{e,n})}{dt} + I_{ion,n} + G_a(V_{i,n} - V_{i,n-1}) + G_a(V_{i,n} - V_{i,n+1}) = 0$$

where C_m and G_a are the membrane capacity and the axonal conductance, respectively.

For a cylindrical axon (Fig. 1.5A), if the membrane currents of the internodes are neglected, C_m , $I_{ion,n}$ and G_a can be substituted by

$$C_m = c_m \pi d L$$

$$I_{ion,n} = i_{ion} \pi d L$$

$$G_a = \frac{\pi d^2}{4 \Delta x \rho_i}$$

where c_m is the membrane capacity per cm^2 , i_{ion} is the ion current density across the membrane and ρ_i is the axoplasmatic resistivity.

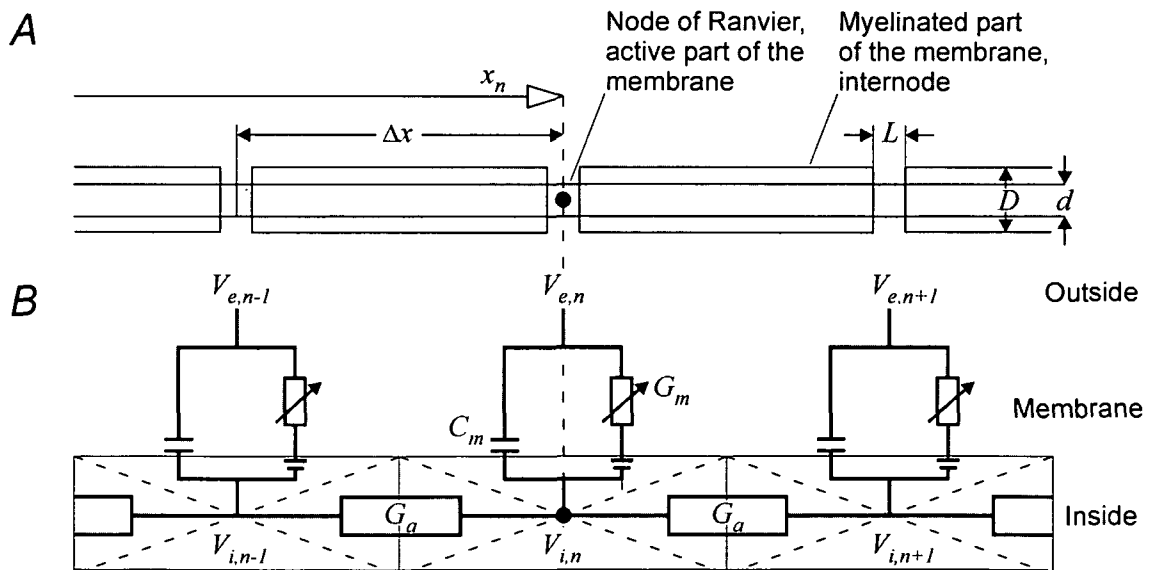


Figure 1.5 Distributed cable network model of myelinated nerve fiber

A, Geometric parameters of a myelinated axon, x_n is the axon's length coordinate. B, Electrical network to simulate the currents in a homogeneous axon with identical, cylindrical compartments of length Δx . Membrane currents are assumed to pass only through the area of active membranes, the internodes are ideal insulators.

Using the reduced membrane potential $V_n = V_{i,n} - V_{e,n} - V_{rest}$, where V_{rest} is the resting membrane potential ($V_{rest} \sim -70\text{mV}$), the following equation will be obtained

$$\frac{dV_n}{dt} = \left[\frac{d\Delta x}{4\rho_i L} \left(\frac{V_{n-1} - 2V_n + V_{n+1}}{\Delta x^2} + \frac{V_{e,n-1} - 2V_{e,n} + V_{e,n+1}}{\Delta x^2} \right) - i_{ion,n} \right] / c_m$$

The influence of an applied electric field on each of the compartments is proportional to the activating function f , which is the second spatial difference quotient of the extracellular potential V_e along the axon (Rattay, 1990):

$$f = \frac{V_{e,n-1} - 2V_{e,n} + V_{e,n+1}}{\Delta x^2}$$

An axon which is in the resting state before an electric field is applied becomes depolarized (stimulated) in regions with $f > 0$ and hyperpolarized in regions with $f < 0$. The origin of an artificially generated action potential is expected in the region where f has its maximum value.

The activating function concept is obvious when derived from the model shown in Fig. 1.5. However, a neuron model of a myelinated axon with additional compartments representing the myelinated parts of the axon (one compartment per internode) was used, because the membrane currents of these parts of the axon can not be neglected completely. Then, the main equation for the n -th compartment is:

$$\frac{dV_n}{dt} = \left[-I_{ion,n} + \frac{V_{n-1} - 2V_n + V_{n+1}}{R_a} + \frac{V_{e,n-1} - 2V_{e,n} + V_{e,n+1}}{R_a} \right] / C_{m,n}$$

where R_a is the axonal resistance, $R_a = l/G_a$ (Fig. 1.6).

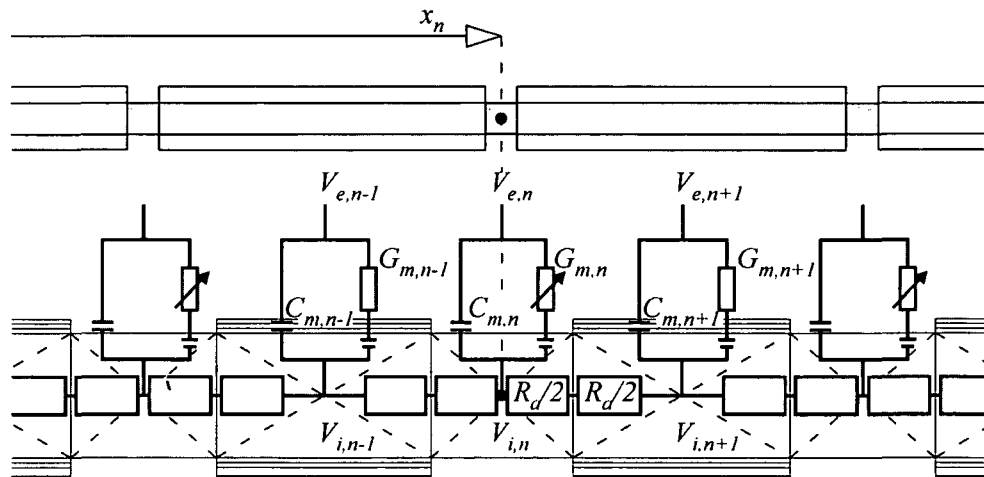


Figure 1.6 Electrical network model of an axon with subunits

Internodes are considered as single compartments with a constant membrane conductance G_m . The active parts of the membrane require an adequate membrane model. The batteries are resulting from differences in ion concentrations between the intracellular and extracellular fluid.

The influence of the extracellular potential can now be described by the generalized activating function f_n :

$$f_n = \left[\frac{V_{e,n-1} - 2V_{e,n} + V_{e,n+1}}{R_a} \right] / C_{m,n}$$

The physical dimension of the generalized activating function f_n is [V/s] or [mV/ms]. Thus, this form of the generalized activating function represents the temporal voltage change in every compartment influenced by the extracellular field.

The internodal compartments are elements with passive membranes and are assumed to have a constant membrane conductance G_m . In these cases $I_{ion,n}$, $C_{m,n}$ and G_m can be substituted by

$$I_{ion,n} = G_m V_n$$

$$G_m = g_m \pi D \Delta x$$

$$C_{m,n} = c_m \pi D \Delta x$$

where c_m is the specific membrane capacity, g_m the specific membrane conductance and $\pi D \Delta x$ the surface of the passive membrane. Note that g_m and c_m are proportional to $1/N$, with N being the number of myelin sheets of the passive membrane.

To describe the membrane kinetics of the nodal compartments, additional differential equations have to be solved to calculate $I_{ion,n}$, the ion current across the membrane at the nodes of Ranvier. The CRRSS (Chiu-Ritchie-Rogart-Stagg-Sweeney) model was used to simulate the nonlinear gating mechanism of the ionic channels in the active parts of the neuron membrane (Sweeney *et al.* 1987). The CRRSS model considers that the potassium current is negligible in mammalian axon membranes and is directly applicable for a temperature of 37°C . An ACSL (Advanced Continuous Simulation Language) program was applied to implement the nerve fiber model and to analyze the excitability of the target fibers. The following standard data for simulation was used: posterior root fiber diameter $D = 22 \mu\text{m}$, $d = 0.64D$, internodal length $\Delta x = 100D$, nodal length $L = 1.5 \mu\text{m}$.

The cable model including ion channel dynamics was applied to identify the thresholds of posterior roots when stimulated by different positioned epidural electrodes (Minassian 2000; Rattay *et al.* 2000). With this expertise, particular emphasis was given to the geometric relations between the calculated isopotential lines and the topographic anatomy of afferent fiber systems in this thesis (chapter 2). This approach is supported by the activating function concept. As aforementioned, the activating function gives a qualitative indication of the effect of an externally applied electric field on a target fiber. The first response of every node and every internode to a stimulus pulse can be estimated with the activating function, which describes the local change of membrane voltage. The activating function uses the extracellular voltage along the neuron as input data, but the complicated ion channel mechanisms are not required in order to find the position of strongest depolarization along a fiber. For a regular myelinated nerve fiber the activating function is related to the second difference quotient of the external potential. When a stimulus pulse is applied to a fiber which has been in resting state before, largest nodal depolarization and thus spike initiation is expected in the region with the highest positive values of the activating function. The value of the activating function is related to the curvature of the extracellular voltage profile along the fiber. For a given stimulus intensity the curvature of the extracellular voltage profile is mostly influenced by the distance to the electrode, the curvature of the fiber and changes of electrical conductivity along the trajectory of the fiber (e.g. the interface between cerebrospinal fluid and white matter at the entry points of the posterior roots into the spinal cord).

Design of the thesis

The following chapters 2–4 are written as independent articles, since they were the outcome of research to be published in peer-reviewed scientific journals.

Chapter 2, Posterior Roots Muscle Reflex Responses elicited by epidural stimulation of the human lumbar cord.

This chapter provides several independent approaches to identify the directly stimulated structures by epidural lumbar cord stimulation leading to single muscle twitches, continuous muscle contractions or alternating flexion/extension movements of the lower limbs. Information on muscle twitch distribution patterns were combined with calculated electric potential distributions and the topographical anatomy of posterior columns and roots. It is concluded that muscle responses to bipolar stimulation from the dorsal epidural space were initiated in large afferent fibers within the posterior roots. It is emphasized that the possibility to selectively elicit these Posterior Roots Muscle Reflex Responses (PRMRRs) is due to the unique anatomical architecture of the terminal spinal cord which determines the resultant electrical field characteristics and its effect on excitable structures. Work from this chapter was also submitted to the *Journal of Physiology*.

Chapter 3, Stepping-like movements in humans with complete spinal cord injury induced by epidural stimulation of the lumbar cord: Electromyographic study of compound muscle action potentials

This chapter provides evidence for the involvement of lumbar interneuronal structures in the generation and control of epidurally induced stepping-like movements. Stimulus-triggered time windows from the original EMG traces were analyzed to reveal features of the intrinsic organization of human spinal networks activated by sustained external stimulation. It is proposed to consider the described processing capabilities of the lumbar cord isolated from brain control and tested by PRMRRs as evidence for the existence of a human Lumbar Locomotor Pattern Generator (LLPG). A shortened version of chapter 3 is published in the journal *Spinal Cord* (Minassian *et al.* 2004a).

Chapter 4, Effect of peripheral afferent and central afferent input to the isolated human lumbar spinal cord

While in the preceding chapters it is demonstrated that sustained stimulation of the posterior roots can activate the LLPG in supine spinal cord injured individuals, the topic of chapter 4 addresses whether the LLPG can be activated during manually assisted treadmill stepping. It is shown that the LLPG activated by a “central” peripheral input (provided by epidural stimulation) can integrate and interpret the proprioceptive input associated with passive stepping to generate functional locomotor patterns. This finding is considered as further evidence that lumbar interneurons can be temporarily incorporated into pattern generating networks for stepping-like activity. The encouraging results of chapter 4 will be presented in the 34th Annual Meeting of the Society for Neuroscience (Minassian *et al.* 2004b).

REFERENCES

- Barolat G, Massaro F, He J, Zeme S & Ketcik B (1993). Mapping of sensory responses to epidural stimulation of the intraspinal neural structures in man. *J Neurosurg* **78**, 233-239.
- Barolat G, Singh-Sahni K, Staas WE, Shatin D, Ketcik B & Allen K (1995). Epidural spinal cord stimulation in the management of spasms in spinal cord injury. A prospective study. *Stereotact Funct Neurosurg* **64**, 153-164.
- Beric A (1988). Stability of lumbosacral somatosensory evoked potentials in a long-term follow-up. *Muscle Nerve* **11**, 621-626.
- Bulling A, Castrop F, Agneskirchner J, Rumitz M, Ovtscharoff W, Wurzinger LJ, Gratzl M (1997). Body Explorer 2.0, An interactive program on the cross-sectional anatomy of the Visible Human Male. Springer Verlag, Heidelberg.
- Bussel B, Roby-Brami A, Neris OR & Yakovlev A (1996). Evidence for a spinal stepping generator in man. *Paraplegia* **34**, 91-92.
- Calancie B, Needham-Shropshire B, Jacobs P, Willer K, Zych G & Green BA (1994). Involuntary stepping after chronic spinal cord injury. Evidence for a central rhythm generator for locomotion in man. *Brain* **117**, 1143-1159.
- Coburn B (1980). Electrical stimulation of the spinal cord: two-dimensional finite element analysis with particular reference to epidural electrodes. *Med Biol Eng Comput* **18**, 573-584.
- Dietz V, Colombo G, Jensen L & Baumgartner L (1995). Locomotor capacity of spinal cord in paraplegic patients. *Ann Neurol* **37**, 574-582.
- Dietz V, Muller R & Colombo G (2002). Locomotor activity in spinal man: significance of afferent input from joint and load receptors. *Brain* **125**, 2626-2634.
- DiMarco AF, Romaniuk JR, Kowalski KE & Supinski G (1999). Pattern of expiratory muscle activation during lower thoracic spinal cord stimulation. *J Appl Physiol* **86**, 1881-1889.
- Dimitrijevic MR, Prevec TS, Sherwood AM (1983) Somatosensory perception and cortical evoked potentials in established paraplegia. *J Neurol Sci* **60**, 253-265
- Dimitrijevic MM, Dimitrijevic MR, Illis LS, Nakajima K, Sharkey PC & Sherwood AM (1986a). Spinal cord stimulation for the control of spasticity in patients with chronic spinal cord injury: I. Clinical observations. *Cent Nerv Syst Trauma* **3**, 129-144.
- Dimitrijevic MR, Illis LS, Nakajima K, Sharkey PC & Sherwood AM (1986b). Spinal cord stimulation for the control of spasticity in patients with chronic spinal cord injury: II. Neurophysiologic observations. *Cent Nerv Syst Trauma* **3**, 145-152.
- Dimitrijevic MR, Gerasimenko Y & Pinter MM (1998). Evidence for a spinal central pattern generator in humans. In *Neural Mechanisms for Generating Locomotor Activity*. *Ann N Y Acad Sci Vol. 860*, ed. Kiehn O, Harris-Warrik RM, Jordan LM, Hultborn H & Kudo N, pp. 360-376. New York Academy of Sciences, New York.
- Dimitrijevic MR, Minassian K, Murg M, PinterMM, Rattay F, Gerasimenko Y & Binder H (2001). Study of locomotor capabilities induced by spinal cord stimulation (SCS) of the

human lumbar cord isolated from the brain control by posttraumatic spinal cord injury (SCI). *Soc Neurosci Abstr*; 27: Program No. 935.6.

Dobkin BH, Harkema S, Requejo P & Edgerton VR (1995). Modulation of locomotor-like EMG activity in subjects with complete and incomplete spinal cord injury. *J Neurol Rehabil* 9, 183-190.

Fedirchuk B, Nielsen J, Petersen N & Hultborn H (1998). Pharmacologically evoked fictive motor patterns in the acutely spinalized marmoset monkey (*Callithrix jacchus*). *Exp Brain Res* 122, 351-361.

Geddes LA & Baker LE (1967). The specific resistance of biological material—a compendium of data for the biomedical engineer and physiologist. *Med Biol Eng* 5, 271-293.

Gerasimenko YP, Dimitrijevic MR, Bussel B, Daniel O, Regnaud JP, Combeaud M, Pinter MM (2000). The mechanisms of central pattern generator activation by means of epidural spinal cord stimulation. *Proceedings of the 5th Annual Conference of the International Functional Electrical Stimulation Society*, pp. 129-131, Aalborg, Denmark.

Gerasimenko YP, Makarovskii AN & Nikitin OA (2002). Control of locomotor activity in humans and animals in the absence of supraspinal influences. *Neurosci Behav Physiol* 32, 417-423.

Grillner S (1981). Control of locomotion in bipeds, tetrapods and fish. In *Handbook of Physiology. The Nervous System. Motor Control. sect. 1, vol. II, part 2*, pp. 1179-1236. Am Physiol Soc, Washington, DC.

Gurfinkel VS, Levik YS, Kazennikov OV & Selionov VA (1998). Locomotor-like movements evoked by leg muscle vibration in humans. *Eur J Neurosci* 10, 1608-1612.

Eidelberg E, Walden JG & Nguyen LH (1981) Locomotor control in macaque monkeys. *Brain* 104, 647-663.

Harkema SJ, Hurley SL, Patel UK, Requejo PS, Dobkin BH & Edgerton VR (1997). Human lumbosacral spinal cord interprets loading during stepping. *J Neurophysiol* 77: 797-811.

Hasegawa T, Mikawa Y & Watanabe R (1996). Morphometric analysis of the lumbosacral nerve roots and dorsal root ganglia by magnetic resonance imaging. *Spine* 21, 1005-1009.

He J, Barolat G, Holsheimer J & Struijk JJ (1994). Perception threshold and electrode position for spinal cord stimulation. *Pain* 59, 55-63.

Holsheimer & Struijk (1987). Electrode combination and specificity in spinal cord stimulation. *Proc. 9th Int Symp 'Advances in external control of human extremities'*, pp. 383-404. Dubrovnik.

Holsheimer J, den Boer JA, Struijk JJ & Rozeboom AR (1994). MR assessment of the normal position of the spinal cord in the spinal canal. *AJNR Am J Neuroradiol* 15, 951-995.

Holsheimer J (1998). Computer modelling of spinal cord stimulation and its contribution to therapeutic efficacy. *Spinal Cord* 36, 531-540.

Holsheimer J (2002). Which neuronal elements are activated directly by spinal cord stimulation. *Neuromodulation* 5, 25-31.

Hultborn H et al. (1993) Evidence of fictive spinal locomotion in the marmoset (*Callithrix jacchus*). *Soc Neurosci Abstr* 19: 539.

Kameyama T, Hashizume Y & Sobue G (1996). Morphologic features of the normal human cadaveric spinal cord. *Spine* 21, 1285-1290.

Kazennikov OV, Shik ML, Yakovleva GV (1983) Stepping elicited by stimulation of the dorsolateral funiculus in the cat spinal cord. *Biull Eksp Biol Med (Bulletin of Experimental Biology and Medicine)* 96, 8-10. [Article in Russian with English abstract]

Kern H, McKay WB, Dimitrijevic MM & Dimitrijevic MR (2004). Motor control in the human spinal cord and the repair of cord function. *Current Pharmaceutical Design* (in press).

Lehmkuhl D, Dimitrijevic MR & Renouf F (1984). Electrophysiological characteristics of lumbosacral evoked potentials in patients with established spinal cord injury. *Electroencephalogr Clin Neurophysiol* 59, 142-155.

Melzack R & Wall PD (1965). Pain mechanisms: a new theory. *Science* 150, 971-979.

Minassian (2000). Excitation of lower spinal cord structures with implanted electrodes: 3D finite element analysis and simulation of neural responses. Diploma Thesis, Vienna University of Technology.

Minassian K, Jilge B, Rattay F, Pinter MM, Binder H, Gerstenbrand F & Dimitrijevic MR (2004a). Stepping-like movements in humans with complete spinal cord injury induced by epidural stimulation of the lumbar cord: Electromyographic study of compound muscle action potentials. *Spinal Cord* May 4 [Epub ahead of print].

Minassian K, Persy I, Rattay F, Binder H, Pinter MM & Dimitrijevic MR (2004b). Output induced by manually assisted treadmill stepping of paraplegic individuals can be enhanced by epidural stimulation of the Lumbar Locomotor Pattern Generator. Abstract No. 4770, 34th Annual Meeting of the Society for Neuroscience, San Diego, CA.

North RB, Lanning A, Hessels R & Cutchis PN (1997). Spinal cord stimulation with percutaneous and plate electrodes: side effects and quantitative comparisons. *Neurosurg Focus* 2(1):ARTICLE.

Pinter MM, Gerstenbrand F & Dimitrijevic MR (2000). Epidural electrical stimulation of posterior structures of the human lumbosacral cord: 3. Control of spasticity. *Spinal Cord* 38, 524-531.

Rattay F (1990). *Electrical Nerve Stimulation: Theory, Experiments and Applications*. Springer, Wien-New York.

Rattay F, Minassian K & Dimitrijevic MR (2000). Epidural electrical stimulation of posterior structures of the human lumbosacral cord: 2. quantitative analysis by computer modeling. *Spinal Cord* 38, 473-489.

Regnaud JP, Daniel O, Combeaud M, Denys P, Remy Neris O, Gerasimenko Y & Busses B (2000). Evidence for a monosynaptic response after low thoracic spinal cord epidural stimulation in paraplegic humans. *Proceedings of the 5th Annual Conference of the International Functional Electrical Stimulation Society*, pp. 171, Aalborg, Denmark.

Roby-Brami A & Bussel B (1987). Long-latency spinal reflex in man after flexor reflex afferent stimulation. *Brain* 110, 707-725.

Sherwood AM, McKay WB & Dimitrijevic MR (1996). Motor control after spinal cord injury: Assessment using surface EMG. *Muscle Nerve* **19**, 966-979.

Struijk JJ, Holsheimer J & Boom HB (1993). Excitation of dorsal root fibers in spinal cord stimulation: A theoretical study. *IEEE Trans Biomed Eng* **40**, 632-639.

Struijk JJ & Holsheimer J (1996). Transverse tripolar spinal cord stimulation: theoretical performance of a dual channel system. *Med Biol Eng Comput* **34**, 273-279.

Sweeney JD, Mortimer JT & Durand D (1987). Modeling of mammalian myelinated nerve for functional neuromuscular electrostimulation. *Proceedings of the IEEE 9th Annual Conference Eng Med Biol Soc*, pp 1577-1578, Boston.

Wall EJ, Cohen MS, Abitbol JJ & Garfin SR (1990). Organization of intrathecal nerve roots at the level of the conus medullaris. *J Bone Joint Surg Am* **72**, 1495-1499.

Chapter 2

Posterior Roots Muscle Reflex Responses elicited by epidural stimulation of the human lumbar cord

Summary

While evaluating the effect of epidural spinal cord stimulation on spasticity of lower limbs in patients with complete spinal cord injury, we found that sustained non-patterned stimulation of posterior lumbar cord structures can induce sustained extension-standing like and alternating stepping-like lower limb movements. In the present paper we identify the stimulated lumbar neural structures which resulted in the evoked muscle activity.

We analyzed surface-recorded electromyographic (EMG) responses of the quadriceps, hamstrings, tibialis anterior, and triceps surae muscles elicited by epidural stimulation of the posterior lumbar cord at 1–10 V and 2.2–50 Hz. Seventeen subjects with motor complete, chronic spinal cord injury at levels rostral to the lumbar cord were included in the study. We examined the relationship between the segmental cathode level of the epidural electrode and the corresponding recruitment order of the quadriceps and triceps surae muscles. We applied a computer model of epidural spinal cord stimulation to calculate the spatial distributions of the electric fields generated by the electrodes. The results were combined with patterns of segmental organization of the posterior columns and roots which are the most obvious targets of stimulation.

We found that EMG signals associated with twitch responses to 2.2 Hz stimulation were stimulus-coupled short-latency compound muscle action potentials (CMAPs). We present evidence that these CMAPs were initiated in large fibers within the posterior roots and refer to this type of stimulus-evoked muscle activity as Posterior Roots Muscle Reflex Responses (PRMRRs). Amplitudes of PRMRRs to 2.2 Hz stimulation were determined by cathode position and stimulus strength. At 5–50 Hz different patterns of tonic and rhythmic EMG activity in the lower limbs were elicited by non-patterned stimulation. The tonic EMG responses as well as the "burst-style" EMG phases during epidurally induced flexion/extension movements consisted of stimulus-triggered CMAPs with similar EMG features as single twitch responses.

We hypothesize that the modulation of PRMRR amplitudes during 5–50 Hz stimulation is due to the fact that in addition to recruitment of motoneurons through monosynaptic connection in the spinal cord the afferent input also produces postsynaptic potentials in spinal interneurons. We argue that at particular higher frequencies the tonic afferent input activates spinal mechanisms that control motoneuronal discharge and the transmission through reflex pathways thereby generating potentially functional lower limb movements.

INTRODUCTION

When a stimulating electrode is placed in the epidural space over the dorsum of the human spinal cord, a variety of neural structures are located in the vicinity of the electrode and are potential sites for direct electrical stimulation. Axons which originate from receptors and free nerve endings in muscles, tendons, joints, and cutaneous and subcutaneous tissues enter the cord via the posterior roots in close proximity to the posterior aspect of the epidural space. Upon entering the spinal cord the axons bifurcate to rostral and caudal branches in the posterior columns, which are close to a midline epidural electrode as well. The immediate effects of epidural electrical stimulation of the spinal cord in humans with intact sensory functions are tingling sensations within the skin (paresthesiae) and muscle contractions that are referred to the body parts corresponding to the activated neurons.

Clinical programs for modifying altered sensations, pain (Shealy *et al.* 1967) or impaired motor control in neurological disorders (Barolat *et al.* 1988; Waltz, 1998) by epidural spinal cord stimulation can provide the possibility of parallel neurophysiological studies to investigate the induced sensory and motor effects.

While evaluating the effect of epidural spinal cord stimulation on spasticity of lower limbs in patients with complete, long-standing spinal cord injury we found that the sustained non-patterned stimulation of posterior lumbar cord structures could induce stepping-like alternating flexion and extension movements (Dimitrijevic *et al.* 1998). We advanced these studies of the locomotor capabilities of the human lumbar cord and examined the mechanisms activated by epidural stimulation which resulted in stepping-like movements in subjects with motor complete spinal cord injury (Minassian *et al.* 2004). Furthermore we provided evidence that epidural stimulation of posterior lumbar cord structures can initiate and retain lower limb extension in paraplegic subjects (Jilge *et al.* 2004).

The purpose of the present study is to find out which posterior lumbar cord structures were stimulated, inducing motor effects and potentially functional movements of the paralyzed lower limbs and to elucidate what the electrophysiological components of the responses are.

MATERIAL AND METHODS

Subjects

The EMG data of stimulus-evoked muscle response patterns which was made available for the present retrospective study was derived from seventeen patients with long-standing motor complete spinal cord injury (SCI). They had participated in a program of restorative neurology for the control of spasticity with epidural spinal cord stimulation, since they did not have a satisfactory response to other therapeutical modalities. Clinical protocols had been conducted to define optimal electrode positions and stimulation parameters. The effect of stimulation had been assessed by surface EMG recordings of induced muscle activity in the lower limbs.

At the time of data collection all subjects met the following criteria: (1) They were healthy adults with closed, post-traumatic spinal cord lesions; (2) all patients were in a chronic (more than 1 year post-onset) and stable condition; (3) no antispastic medication was being used; (4) the stretch and cutaneomuscular reflexes were preserved; (5) there was no voluntary activation of motor units below the level of the lesion as confirmed by brain

motor control assessment (Sherwood *et al.* 1996); while (6) surface recorded lumbosacral evoked potentials – used to assess the functions of the posterior structures and gray matter of the spinal cord below the level of the lesion – were present (Beric, 1988; Lehmkuhl *et al.* 1984).

To control their spasticity all subjects had an electrode array placed in the dorsomedial epidural space (see "*Stimulation setup*"). The implantation procedure has been described in detail previously (Murg *et al.* 2000). The position of the epidurally placed electrodes relative to the vertebral bodies was obtained from postoperative X-rays. The estimated, functional segmental level of the cathode was derived from a neurophysiological technique for electrode positioning in subjects with impaired sensory function (Murg *et al.* 2000). Additionally, information on average spatial relations between the cord segments and the vertebral bodies was used (Lang, 1984a). The implantations as well as the clinical protocol to evaluate the optimal stimulation parameters were approved by the local ethics committee. All patients gave their informed consent. Pertinent patient-related data are listed in Table 2.1.

Table 2.1 Demographic and clinical data.

Subject No.	Sex	Born in	Accident in	Implantation of electrode in	Type of accident	Level of SCI	ASIA Class.
1	m	1970	1996	1999	Car accident	C6	B
2	m	1977	1994	1999	Motorbike accident	C6	A
3	m	1970	1991	1999	Car accident	T4	A
4	m	1973	1995	1998	Car accident	C4	A
5	m	1981	1996	1999	Car accident	C4	A
6	m	1973	1997	1998	Ski accident	C7	B
7	f	1966	1996	1997	Car accident	T5	A
8	m	1974	1993	2001	Fall accident	T2	A
9	f	1976	1992	1998	Fall accident	T2	B
10	m	1978	1996	1999	Car accident	T10	B
11	f	1978	1994	1996	Car accident	T4	A
12	f	1975	1996	2000	Car accident	T6	A
13	m	1967	1987	2001	Motorbike accident	T5	A
14	f	1965	1996	1998	Car accident	T5	A
15	m	1971	1991	1999	Car accident	C6	B
16	m	1939	1994	1997	Fall accident	T7	A
17	m	1973	1996	1997	Car accident	T4	A

Stimulation setup

Stimulation was delivered via a quadripolar lead with cylindrical electrode design (PISCES-QUAD electrode, Model 3487A, MEDTRONIC, Minneapolis, MN, USA) placed in the dorsomedial epidural space at vertebral levels ranging from T10 to L1. The data analyzed in the present study was recorded when the electrode array was operated as a bipolar electrode, the most rostral and caudal electrode contacts being connected to the positive and negative outputs, respectively, of the implanted pulse generator (ITREL 3, Model 7425, MEDTRONIC). The separation of the active electrode contacts was 27 mm. The bipolar impedance was generally about 1000 Ω . The stimulus pulses were biphasic and actively charge balanced. The first dominant phase was about rectangular with a width of 210 μ s, the amplitude in the much longer second phase was small and irrelevant to the stimulation process but avoided charge accumulation. Thus, stimulation was virtually monophasic and the stimulating effect of the epidural electrode based on its polarity during the first dominant phase, i.e. on the electrode contact which had a negative potential during the first phase. Cathodal stimulation of spinal neural structures results in lower thresholds than anodal stimulation. For posterior root fibers the calculated thresholds for cathodal excitation are about three times lower than anodal thresholds (Struijk *et al.* 1993a; Holsheimer, 2002). Reversing the polarity of the bipolar epidural electrode shifted the effective cathode site to a different rostrocaudal level. Thus, setting the electrode polarity allowed for stimulation of posterior structures of the spinal cord at different segmental levels, determined by the cathode site, with a single epidural electrode array.

Recording procedure

To assess the effect of spinal cord stimulation, stimulus-evoked muscle activity of quadriceps, hamstring, tibialis anterior, and triceps surae were recorded with silver-silver chloride surface electrodes. The bipolar electrodes were placed centrally over the muscle bellies spaced 3 cm apart and oriented along the long axis of the muscles. Additionally, electromyographic activity of the lumbar paraspinal trunk muscles was recorded. The skin was slightly abraded to obtain an electrode impedance below 5 k Ω . The EMG signals were amplified with the Grass 12D-16-OS NEURODATA ACQUISITION SYSTEM (GRASS INSTRUMENTS, Quincy, MA) adjusted to a gain of 2000 over a bandwidth of 30–1000 Hz and digitized at 2048 samples/s/channel using a CODAS ADC system (DATAQ INSTRUMENTS, Akron, OH). All recordings were conducted with the patients in a comfortable supine position. The EMG data was analyzed off-line using WINDAQ Waveform Browser playback software (DATAQ INSTRUMENTS).

Data analysis – Data based on incremental pulse amplitudes

The first set of EMG data had originally been collected to define the rostrocaudal level of the electrode relative to the lumbosacral cord segments based on muscle twitch distribution patterns (Murg *et al.* 2000). For this purpose, a frequency of 2.2 Hz was used, and the stimulation strength was intensified in 1-Volt increments from 1 to 10 V.

We examined single stimulus-evoked and surface-recorded compound muscle action potentials (CMAPs) associated with the twitch responses for latencies (quantitatively), peak-to-peak amplitudes, and shapes (qualitatively) of the same data set. The latencies were read off-line from the EMG traces using the playback software and measured as the time

between stimulation onset – identified by stimulus artifacts – and the first deflection of the EMG potential from baseline. Mean latency times based on all subjects were calculated for the threshold stimulus strengths eliciting responses in each muscle group and for the maximum strengths applied.

Furthermore, the recruitment order of the quadriceps and triceps surae muscles was examined by establishing the threshold voltages at which they responded – i.e. the lowest whole-numbered stimulation voltage inducing an unequivocal EMG activity (about $\pm 10 \mu\text{V}$). To this end, EMG data of the subjects 1–15 were analyzed. Quadriceps and triceps surae were considered in this analysis, because they are the only ones of the recorded muscle groups with separate segmental innervations (L2–L4 vs. L5–S2). For each subject and given electrode array position, data of two different recording sets were examined, where first the most rostral and then the most caudal electrode of the array had been operated as the effective cathode. Four subjects had two epidural electrode arrays positioned at different rostrocaudal levels or had a single one repositioned during participation in the clinical program. Moreover, threshold values for right and left side were frequently different (in 62% of all cases), thus each lower extremity was taken as a separate case. In this way, a total of 76 (19 electrode array positions) \times (2 cathode positions each) \times (2 cases: left and right side) muscle recruitment orders and corresponding threshold voltages were obtained, 75 of the 76 cases could be assigned to one of four distinct groups. In group 1, only the thigh muscles were recruited even with the stimulation strength at its maximum level of 10 V. Group 2 was characterized by a lower threshold for quadriceps than for triceps surae responses. In group 3, quadriceps and triceps surae had the same (whole-numbered) threshold. In group 4, triceps surae responded at lower voltages than quadriceps, i.e. the recruitment order was reversed in comparison with group 2.

The rostrocaudal position of the active cathode was entered into a chart of vertebral body levels that also featured a spinal cord with "standard" spatial relations of the cord segments to the vertebral bodies (adapted from Lang, 1984a) to estimate the geometric segmental level of the cathode. Additional information about relative heights of the vertebral bodies (Panjabi *et al.* 1991; Panjabi *et al.* 1992) and the mean position of the termination of the spinal cord (Saifuddin *et al.* 1998) were also considered in this model. For each of the four groups of subjects with different muscle recruitment patterns, the mean cathode level relative to the spine was established, based on the positions in the chart.

Data analysis – Data based on incremental pulse frequencies

The second set of EMG data that was analyzed had originally been collected to assess the effect of trains of electrical stimuli at 5–100 Hz on spasticity (Pinter *et al.* 2000). The same data was used to examine the motor output patterns induced by sustained trains over a frequency range of 5–50 Hz. To examine the components of the overall EMG pattern the time scale of the EMG traces was subsequently enlarged. This allowed us to address the question of how far individual responses to the single pulses within the applied stimulus train were reflected in the EMG output pattern. Separate successive responses to these pulses were analyzed for characteristic patterns of relative EMG amplitudes.

Again, the data was analyzed for the recruitment order of the quadriceps and triceps surae muscles as was done for 2.2 Hz stimulation. Recruitment properties of stimulation with 2.2 Hz, 25 Hz and 50 Hz were compared in the same subject and for a given cathode position. For this retrospective analysis, data were available from the subjects 1, 2, 5, 7, 10, 12, 13

and 16. The recruitment orders were classified in groups according to the relative threshold voltages at which quadriceps and triceps surae responded to the 2.2 Hz stimulation.

Computer simulation of the electric potential distribution

A computer model was established to learn more about the potential distribution within the spinal cord and its surrounding tissues, focusing on the geometric relations between the calculated isopotential lines and the topographic anatomy of posterior root and posterior column fibers of different segmental origins. This model consisted of 3-dimensional volume conductors representing the spinal cord, cerebrospinal fluid, dura mater, epidural space, vertebral bone, and a compartment surrounding the spine. The potential distribution was determined by the geometry and electric conductivities of the anatomical structures. The finite-element method was applied to calculate the steady-state solutions of this volume conductor problem, which included inhomogeneity, anisotropy and a complex geometry. This finite-element model based on varying cross-sections to represent the lumbosacral spinal cord, including the lumbar enlargement and the lower end of the cord, which tapers to form the conus medullaris. For further details of the volume conductor model to calculate the generated potential distributions see Rattay *et al.* (2000).

RESULTS

Muscle responses to single stimuli (2.2 Hz stimulation)

Electrical stimulation of the lumbosacral cord delivered from the dorsomedial epidural space at 2.2 Hz and 1–10 V elicited twitch responses in the lower limb muscles. Figure 2.1A shows characteristic EMG features associated with these stimulus-evoked responses of the quadriceps (Q), triceps surae (TS) and lumbar paraspinal trunk (PARA) muscles displayed with different time scales. The rostrocaudal position of the active cathode was at the center level of the twelfth thoracic vertebra, the estimated segmental cathode level was L3/L4 (subject 5). Stimulation strength was 5 V. On the left side of Fig. 2.1A, 10-second traces of EMG recordings are displayed. Twenty-two separate responses of quadriceps and triceps surae were elicited within this time. The EMG activity of successive single responses demonstrated only minor variation of the peak-to-peak amplitudes. There was no EMG activity between two consecutive twitch responses. The EMG trace derived from the paraspinal muscles showed more deflections than those from the lower limb muscles. Their origins can be identified in the middle column of Fig. 2.1A, where the last second of the EMG recordings is shown in a time scale extended 10 times. The deflections are artifacts which are superimposed on the recordings of the stimulus-evoked EMG activity of the paraspinal muscle. Due to the close distance of the paraspinal-electrode to the epidural electrode, volume-conducted artifacts of the stimulus pulses are picked up by the recording surface electrode. Three of these stimulus artifacts can be seen within the one-second trace, each followed by single low-amplitude paraspinal EMG response. The prominent potential with long duration between the first two stimulus artifacts is an electrocardiographic activity.

Each pulse within the sustained stimulus train which is identifiable by the stimulus artifacts triggered a single compound muscle action potential (CMAP) in quadriceps and triceps surae. The EMG features of these CMAPs can be seen on the right side of Fig. 2.1A, where

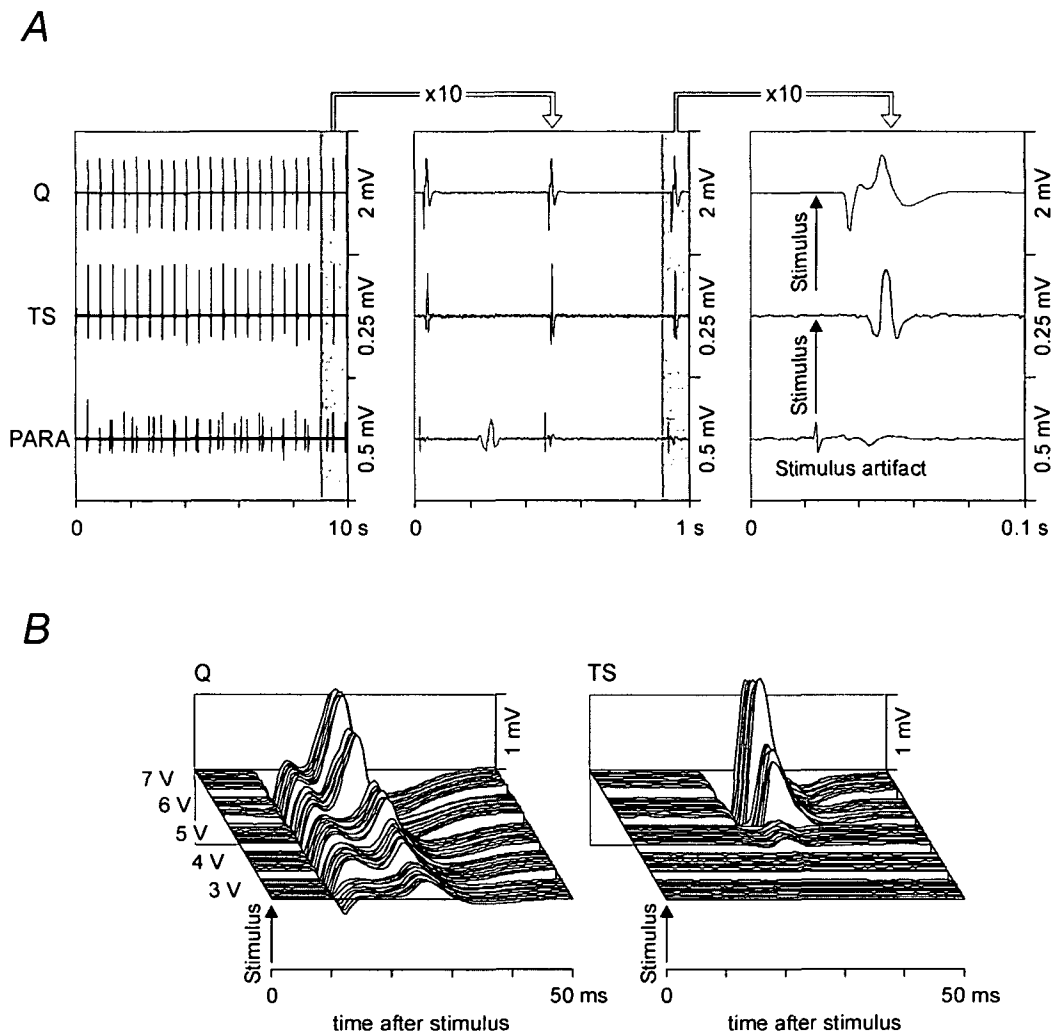


Figure 2.1 EMG responses to 2.2 Hz stimulation

A, EMG responses of the quadriceps (Q), triceps surae (TS) and lumbar paraspinal (PARA) muscles presented with different time scales (subject 5). Stimulus strength was 5 V, cathode was located at the center level of the T12 vertebral body. Stimulus artifacts captured by the paraspinal-surface electrodes allow the identification of the onsets of applied voltage pulses. *B*, stimulus-triggered sequential presentation of EMG potentials induced in the Q and TS. The graph shows the first 50 ms following the onset of each stimulus pulse. Same subject and cathode position as in *A*, but the stimulation strength was increased in steps of 1 V (3–7 V). Ten single EMG potentials of successive twitch responses are shown for each incremental voltage.

the last 100 milliseconds of the original recording are shown. The latency times of the different muscle groups were rather short. The quadriceps twitch had a latency of 9.5 ms, the more distal triceps surae muscle responded with a latency of 18.5 ms.

Figure 2.1*B* compares single surface recorded CMAPs of quadriceps and triceps surae muscles induced by stimuli at 3–7 V and 2.2 Hz in the same subject as in Fig. 2.1*A* (same cathode position). The figure is a stimulus-triggered sequential presentation of successively elicited CMAPs in which the original continuous EMG traces are shown as time windows of 50 ms that are arranged behind each other (compare with right side of Fig. 2.1*A*). The left

margins of the windows indicate the onsets of the stimuli. CMAPs associated with ten single twitch responses are shown for each incremental voltage. In the presented case, muscle responses could not be elicited in the lower limbs at 1–2 V. At 3 V, single CMAPs with short (9.5 ms) and constant latencies were recorded in quadriceps, while triceps surae showed no activity. At 4 V, quadriceps CMAPs had higher amplitudes than at 3 V while the latencies remained unchanged. Faint activity was also observed in triceps surae at 4 V, involving latencies of 18.5 ms. At higher stimulation strengths, EMG amplitudes of the twitch responses further increased for both muscle groups. The results shown in Fig. 2.1 are representative for subjects with cathodes positioned at T12 vertebral body level.

The latencies of successive responses remained constant in both muscle groups, while no additional EMG components with longer latencies or later potential-peaks emerged at higher stimulus strengths. In each subject and for a given muscle group, latency times were rather invariable regardless of stimulus strength and site. The mean latency times for quadriceps, hamstrings, tibialis anterior and triceps surae at threshold level and maximum applied stimulation strength (generally 8–10 V) are compiled in Table 2.2. They were about 10 ms for the thigh muscles and 17 ms for the leg muscles. Note that the weak responses induced at threshold stimulation had low CMAP amplitudes and slight onset slopes of the potentials, thus making the precise identification of the onset of the CMAPs difficult. This may partially account for the longer latencies of muscle responses at threshold level in Table 2.2.

Table 2.2 Mean latencies (ms \pm SD) of CMAPs evoked by 2.2 Hz stimulation based on all subjects at threshold and maximum stimulation strength

	Threshold	Maximum
Q	9.7 \pm 1.7	9.3 \pm 1.2
H	10.2 \pm 1.6	9.7 \pm 1.1
TA	16.8 \pm 1.6	16.6 \pm 1.1
TS	17.1 \pm 1.4	16.9 \pm 0.9

Consecutive CMAPs to continuous stimulation of the same strength and at 2.2 Hz exhibited essentially identical potential shapes. The shape of the EMG responses of a given muscle group was alike in different subjects. The CMAPs showed mainly increased amplitudes at suprathreshold strengths, with only minor changes of the EMG shape.

To summarize, the EMG signals associated with the twitch responses elicited by 2.2 Hz stimulation were separate, stimulus coupled CMAPs with short latency. Equal-voltage stimuli yielded only negligible variations in CMAP amplitudes and shapes. Thus, a given response demonstrated no influence on following responses to the stimulus train. For a given cathode position the CMAP amplitudes were governed by the stimulus strength. The effect of 2.2 Hz stimulation was like the effect of single applied stimulus pulses.

Relationships between cathode levels, stimulation amplitudes and activated muscle groups – Stimulation frequency: 2.2 Hz

Figure 2.2A illustrates the four different groups of muscle recruitment patterns as described in Methods under "*Data analysis – Data based on incremental pulse amplitudes*". The left margins of the black bars of the vertical-bar diagrams indicate the mean threshold voltages eliciting quadriceps (Q) and triceps surae (TS) responses at 2.2 Hz in the subjects 1–15. In group 1, quadriceps had a rather high mean threshold of 7.9 V, while triceps surae could not be recruited at stimulus strengths up to 10 V. In this group the lumbar paraspinal trunk muscles responded to the stimulation on average at 4.5 V and thus demonstrated lower response thresholds than the lower limb muscles. In group 2, the mean threshold of quadriceps was lower than of triceps surae responses (3.9 V vs. 5.9 V). Thus, similarly to group 1, stimulation was selective to a certain degree, i.e. it was possible to activate quadriceps without activating triceps surae, which required an additional increase of 51% of the stimulus strength to respond. In group 3, the whole-numbered thresholds of quadriceps and triceps surae were rather low and identical (mean 3.0 V). In group 4, triceps surae responded at lower voltages than quadriceps (2.5 V vs. 3.4 V), i.e. the recruitment order was reversed in comparison with group 2 and activation of triceps surae without eliciting quadriceps twitch responses was possible.

Note that the limited accuracy of our methodology to identify thresholds by increasing the stimulus strength in 1 Volt-steps may partially account for the "non-selective" effect of stimulation in group 3. However, stimulation was also selective to a certain degree in this group as reflected by the EMG amplitudes of the muscle responses at threshold level: in 44% of the cases classified as group 3, the mean ratio of quadriceps and triceps surae amplitudes was 33:1, in the remaining cases the ratio was 1:12. Thus, two subgroups within group 3 could be revealed, one related more to group 2, the other more to group 4.

Figure 2.2B shows the cathode levels of the four groups with respect to the vertebral body levels T10 to L1. First, the total distribution of rostrocaudal cathode positions in the subjects 1–15 is indicated (black diamonds). Then, the mean cathode level (black rectangle), the calculated average distance between the cathode positions and the mean cathode level (shaded rectangle), and the rostrocaudal range (white rectangle) within each group are illustrated.

It turns out that the four different groups – originally defined according to the recruitment order of the L2–L4 innervated quadriceps and the L5–S2 innervated triceps surae muscles – have considerably different rostrocaudal cathode levels. The most rostral cathode positions mainly belonged to the group 1, while responses elicited by the most caudal positions were recruited according to the pattern of group 4.

Mean thresholds of quadriceps responses considerably increased to more than 200% with cathode site in caudorostral direction from the group 2 to the group 1 position. Thresholds of triceps surae activation steadily increased the more rostrally the cathode was located. The lower third of the T10 vertebral body was the most rostral position from which lower limb muscle responses could be evoked at a stimulation strength of 10 V – in fact solely in the thigh muscles. From the upper third of the vertebral body T10 none of the studied lower limb muscles could be activated with strengths up to 10 V (see the cathode position marked by the most rostral black diamond in the chart displayed in Fig. 2.2B). At this rostral level segmental twitch responses could be elicited in the lumbar paraspinal trunk muscles at a moderate threshold of 5 V.

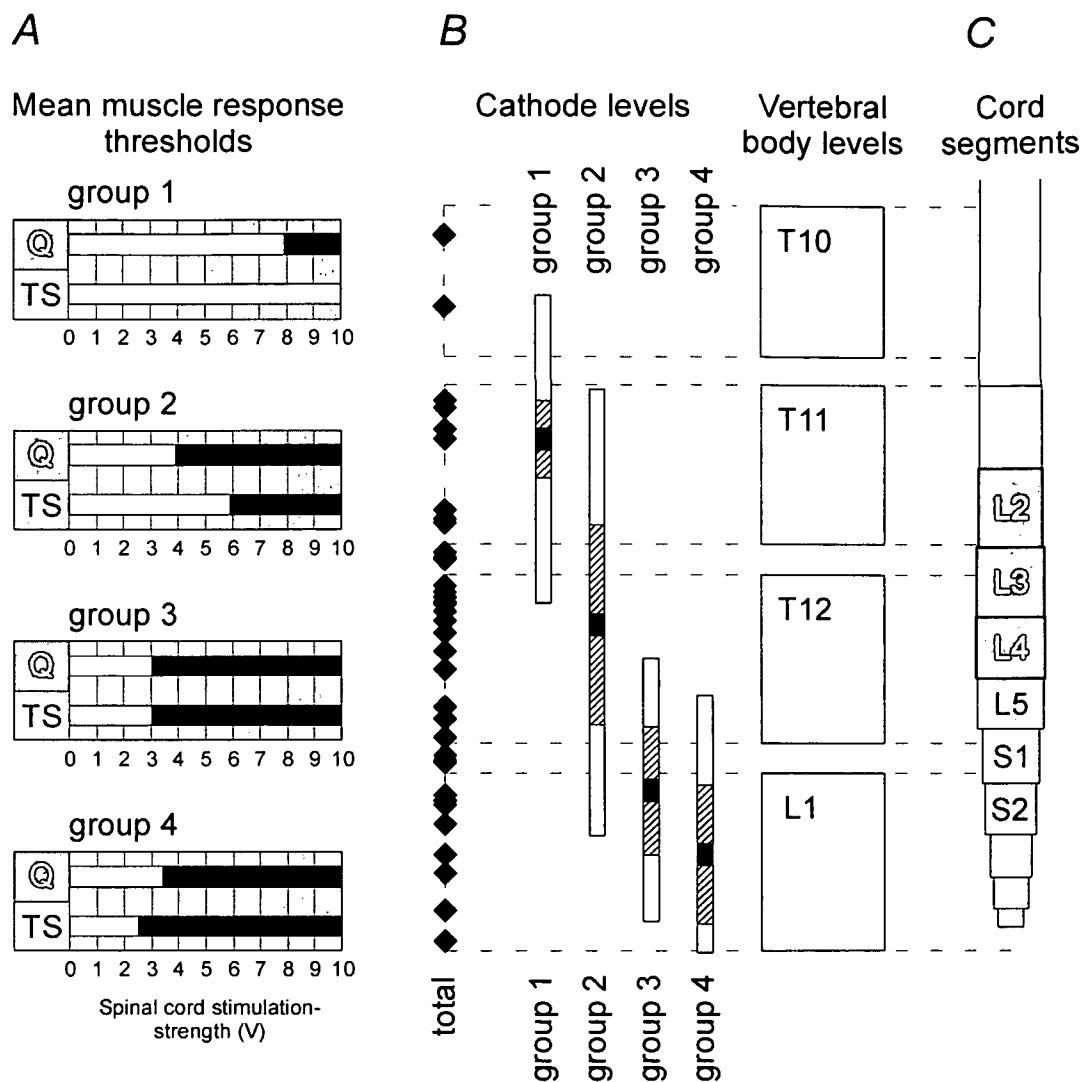


Figure 2.2 Mean response threshold voltages and corresponding cathode positions of quadriceps (Q) and triceps surae (TS) of the subjects 1–15

A, the threshold voltages are indicated by the left margins of the black bars. In group 1, Q was recruited but not TS with strengths up to 10 V ($n = 8$). In group 2, the thresholds were lower for Q than for TS ($n = 47$). In group 3, the whole-numbered thresholds were identical for both muscle groups ($n = 9$). In group 4, they were higher for Q than for TS ($n = 11$). *B*, the total distribution of cathode positions relative to vertebral body levels T10–L1 (black diamonds) are indicated, and for each group the mean cathode level (black rectangle), the averaged distance between the cathode positions and the mean cathode level (shaded rectangle), and the rostrocaudal range (white rectangle) are shown. *C*, spinal cord model adapted from Lang (1984a) showing average segmental lengths and positions relative to the vertebral body levels T10–L1 shown on the left side. The designated segments L2–L4 and L5–S2 provide innervation of Q and TS, respectively.

The lowest whole-numbered threshold of lower extremity muscle responses was 1 V and was found in three subjects (subjects 1, 4, and 8), all with cathodes at L1 vertebral body levels, corresponding to the average position of the conus medullaris. In a single case (subject 4, cathode at the lower third of the vertebral body level L1), muscle twitch

thresholds had been identified by increasing the stimulus strength in 0.1 V-steps. The threshold for eliciting CMAPs in triceps surae was as low as 0.5 V.

Figure 2.2C gives an average model of spatial relations between the spinal cord segments L2–S2 and the rostrocaudal vertebral body levels introduced in Fig. 2.2B. This model can be used to get information about the cathode levels relative to lumbosacral cord segments. The segmental innervations of quadriceps (L2–L4) and triceps surae (L5–S2) are indicated by different shades of gray. Comparison between Figs. 2.2A–C demonstrates the following mean segmental cathode levels for the groups with different muscle recruitment orders – group 1: rostral to L2, group 2: L3/L4, group 3: S1/S2, group 4: caudal to S2.

Figure 2.2 exposes a strong relationship between the rostrocaudal position of the cathode relative to spinal cord segments and the recruitment order of quadriceps and triceps surae twitch responses. The cathode level and the stimulation amplitude determine a segmental-selective recruitment of lower limb muscles.

Muscle responses to trains of stimuli

Figure 2.3A displays 0.5-second traces of induced tonic EMG activity of the antagonistic muscles quadriceps (Q) and hamstrings (H) derived from subject 2. The active cathode was at upper T12 vertebral level (estimated L3/L4 segmental level), stimulation strength was 6 V and left unchanged when switching frequencies from 16 Hz to 22 Hz. At both frequencies, each single pulse of the sustained train of electrical stimuli, marked by black diamonds in the figure, elicited a separate CMAP. Successive stimuli evoked alternately strong and weak responses. At 16 Hz, strong responses occurred simultaneously in Q and H, while increasing the stimulation frequency to 22 Hz changed the pattern of the muscle activity. In this case, each stimulus pulse induced a strong response in one muscle and a weaker one in its antagonist indicating mutual influences of the responses. The CMAP amplitudes were subject to a modulatory influence and were not solely governed by the stimulation strength, like in case of 2.2 Hz stimulation. Moreover, the trains of stimulus-evoked CMAPs of a given muscle had one of only two different characteristic types of EMG shapes.

Mutual influence of responses in different muscle groups could not be observed only in the time base of single responses. Figure 2.3B shows surface EMG recordings from the right quadriceps (Q), hamstrings (H), tibialis anterior (TA) and triceps surae (TS), and position sensor recordings showing knee flexion/extension movements (KM – knee movement). The data were derived from a complete paraplegic (subject 17). The rostrocaudal cathode site was at the T12-L1 intervertebral level, the segmental level was estimated as L4/L5. Stimulation parameters were 9 V and 30 Hz and constant during the continuous recording. The EMG traces demonstrate alternating phases of burst-style activity in the lower limb muscles. The corresponding position sensor trace confirms that the induced muscle activity led to actual flexion/extension movements of the lower limb. Deflection up indicates flexion and deflection down extension of the lower limb, the range of knee movement (rotation of the longitudinal axis of the thigh around the hip) was about 65°.

To identify whether individual responses to single pulses within the applied stimulus train were reflected in the EMG output pattern, the first of the burst-style phases of quadriceps is displayed in extended time scale at the bottom of Fig. 2.3B. Corresponding stimulus artifacts derived from the paraspinal muscle indicate the onset of the stimulus pulses. It can be seen that each pulse of the stimulus train triggered a separate CMAP. Thus, the burst-

style phase consisted of stimulus-triggered CMAPs that were subject to well-defined amplitude modulations resulting in a burst-like shape of the EMG activity.

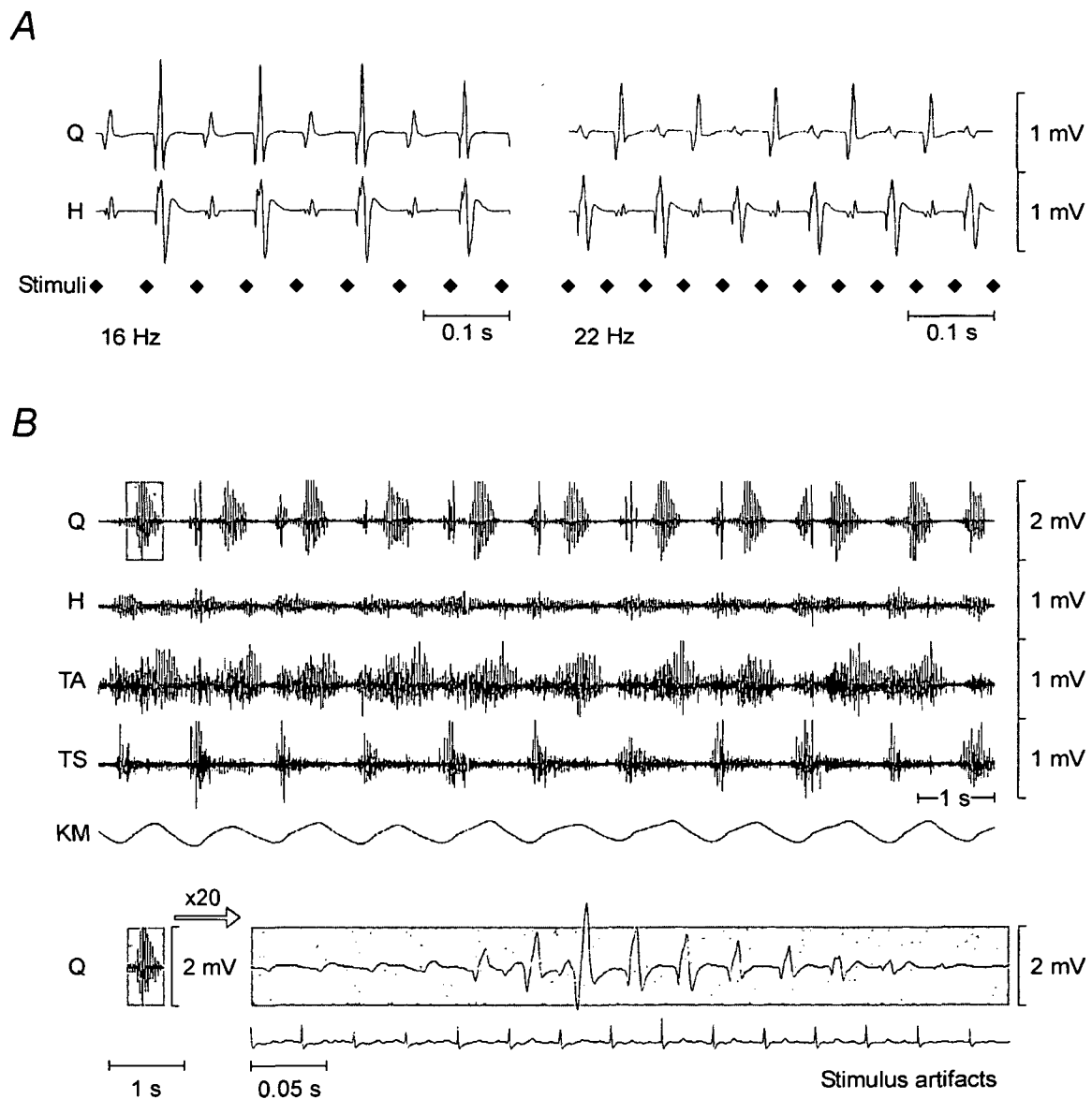


Figure 2.3 EMG responses to trains of stimuli showing modulations of amplitudes

A, 0.5 seconds of induced EMG activity of quadriceps (Q) and hamstrings (H), single pulses of the sustained electrical stimulation (black diamonds). The cathode was at upper T12 vertebral level, stimulation strength was 6 V, and frequency was changed from 16 Hz to 22 Hz (subject 2). *B*, surface EMG recordings from the right quadriceps (Q), hamstrings (H), tibialis anterior (TA), and triceps surae (TS); position sensor traces demonstrating flexion/extension movements of the knee (KM). The cathode was at the T12-L1 intervertebral level. Stimulation parameters were 9 V and 30 Hz (subject 17). The first "burst-style" phase of quadriceps marked by gray background is shown in extended time scale on the bottom of the original EMG. Note that some peaks of the quadriceps activity displayed in the original trace are cut at ± 1 mV.

A discussion of the great variety of responses to epidural stimulation with patterned amplitude modulations is beyond the scope of the present study. Figure 2.3 is to demonstrate that at higher stimulation frequencies the amplitudes of the evoked EMG

responses were not determined solely by the stimulus strength. Applying trains of electrical stimuli with constant parameters to the posterior lumbosacral cord structures at 5–50 Hz yielded well-defined EMG patterns of amplitude modulation in lower limb muscles. Moreover, it turns out that the different tonic, patterned tonic (Fig. 2.3A) and rhythmic EMG activity and even "burst-style" phases (Fig. 2.3B) consist of separate stimulus-triggered CMAPs.

Relationships between cathode levels, stimulation amplitudes and activated muscle groups – Stimulation frequencies: 2.2, 25, 50 Hz

Figure 2.4A displays approximately 16 seconds of surface EMG recordings from the left lower limb muscles along with a recording of a position sensor measuring flexion/extension movements of the knee (subject 16). The effective cathode was located at upper lumbar segmental level. The stimulation frequency was 25 Hz and constant, while the stimulation strength was increased in 0.5-Volt steps during continuous recording. At the threshold level of 3.5 V, low amplitude EMG activity was induced in quadriceps. At 4 V the quadriceps activity increased in amplitude and additionally hamstrings responses of smaller amplitudes were induced. A further increase in stimulation strength to 4.5 V elicited faint activity in the tibialis anterior and triceps surae muscles. The EMG activity of the previously recruited quadriceps muscle decreased, while hamstrings showed approximately reciprocal temporal changes in EMG amplitudes. This is substantially different from the findings derived from EMG data of stimulus-evoked responses at 2.2 Hz, where CMAP amplitudes showed progressive increase with increasing stimulus strength. Another increase in stimulation amplitude to 5 V induced rhythmic EMG activity in the recruited lower limb muscles and flexion/extension movements. The sustained stimulus train at 25 Hz and strengths of 3.5–4.5 V induced a tonic EMG activity consisting of separate, frequency following single EMG responses. Also at 5 V during the phases of burst-style activity, which alternated with phases of inactivity/low activity, each pulse of the stimulus train triggered a single CMAP.

Figure 2.4A demonstrated that once a muscle group was recruited by the epidural stimulation, the EMG amplitudes of the stimulus-evoked CMAPs elicited at 25 Hz were not solely governed by the stimulus strength. However, the muscle recruitment sequence was quite similar to the one at the lower stimulation frequency of 2.2 Hz. The EMG activity displayed in Fig. 2.4A was evoked by an epidural electrode with a cathode located at the T11-T12 intervertebral level, thus similar to the mean rostrocaudal cathode level of the group 2 introduced in Fig. 2.2. It also shows the characteristic muscle recruitment order of group 2. This finding prompted us to perform the same analysis as conducted for Fig. 2.2 for higher stimulation frequencies.

In Fig. 2.4B the recruitment properties of sustained epidural stimulation at 2.2 Hz, 25 Hz and 50 Hz are compared. Less data were available for this analysis than for the one presented in Fig. 2.2. In all available cases the rostrocaudal positions of the effective cathodes were located between the T11-T12 intervertebral level and the lower third of the L1 vertebral body. All cases could be classified into two groups with characteristic recruitment order of the quadriceps and triceps surae muscles for stimulation with 2.2 Hz – group 2' and group 3'. In group 2', quadriceps responded at lower stimulation strengths (mean 3.1 V) than triceps surae (4.5 V). The mean cathode level of group 2' was located more caudally than that of group 2 (Fig. 2.2), since no data were available from subjects with cathodes positioned rostrally to the T11-T12 intervertebral level for this retrospective

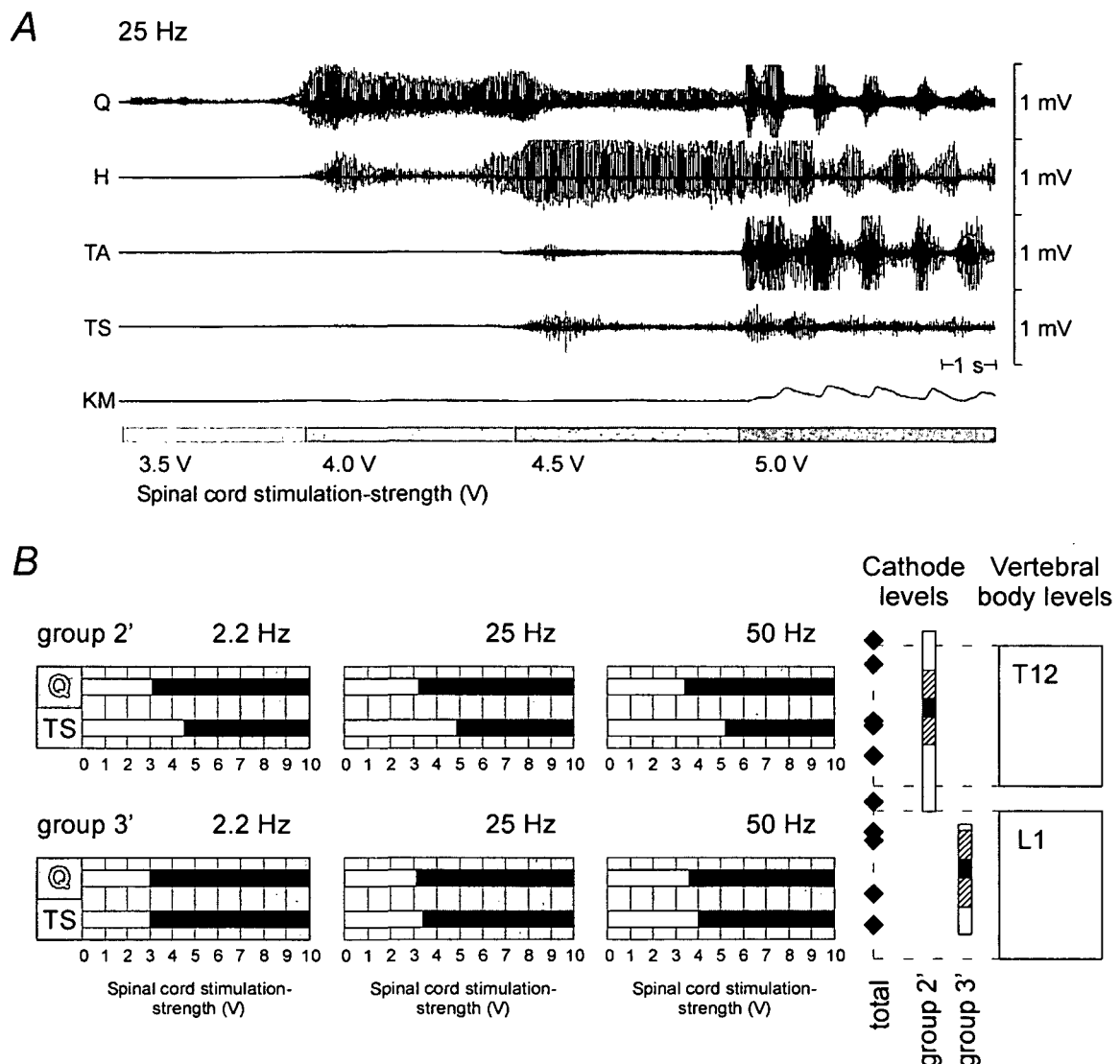


Figure 2.4 Muscle recruitment properties of sustained epidural stimulation

A, continuous surface EMG recordings from the left quadriceps (Q), hamstrings (H), tibialis anterior (TA), and triceps surae (TS); position sensor traces measuring flexion/extension movements of the knee (KM). The cathode was at the T11-T12 intervertebral level. The stimulation frequency was 25 Hz, stimulation strength was intensified in 0.5-Volt increments from 3.5 V to 5 V (subject 16). *B*, mean thresholds of quadriceps (Q) and triceps surae (TS) responses to stimulation frequencies at 2.2, 25 and 50 Hz. Data were derived from subjects 1, 2, 5, 7, 10, 12, 13 and 16. Cases were classified in groups 2' and 3' according to characteristic recruitment orders, the corresponding mean vertebral cathode levels of the two groups are shown on the right side of the figure.

analysis to contribute to the calculated mean value. Increasing the frequency of the sustained stimulation in the same subjects and for the same cathode positions resulted in higher muscle response thresholds for all muscle groups. This was mainly due to the fact that EMG activity generally decreased in amplitude at higher stimulation frequencies. When the EMG activity elicited at the threshold level for stimulation at 2.2 Hz were of low amplitudes, it could frequently not be evoked at all at 25 Hz or 50 Hz, unless the stimulation strength was increased. No single case was found where response thresholds

became lower when stimulation frequency was increased from 2.2 Hz to 25 or 50 Hz. Moreover, rhythmical flexion/extension movements were never induced at stimulation voltages less than the strength required to induce twitch responses in both quadriceps and triceps. The recruitment pattern of this group 2' was independent of the stimulation frequency. The ratios of the quadriceps and triceps surae thresholds were 1:1.45, 1:1.53 and 1:1.53 for stimulation at 2.2 Hz, 25 Hz and 50 Hz, respectively. The same ratio was 1:1.51 for the cases classified as group 2 in Fig. 2.2.

In group 3', quadriceps and triceps surae were recruited at the same stimulus strength (mean 3.0 V) when stimulation frequency was 2.2 Hz. The mean cathode level was somewhat more caudally than for group 3 (Fig. 2.2). As in the case for group 2', thresholds increased at stimulation frequencies of 25 Hz and 50 Hz. The ratios of the quadriceps and triceps surae thresholds were 1:1 at 2.2 Hz and 1:1.10 and 1:1.11 for stimulation at 25 Hz and 50 Hz, respectively.

In summary, epidural stimulation could elicit muscle activity in response to frequencies of 2.2, 25, and 50 Hz. At 25 and 50 Hz, CMAP amplitudes of induced activity did not increase systematically with increasing stimulus strengths as was seen in case of 2.2 Hz stimulation. The thresholds for initiation of muscle activity at 25 and 50 Hz were higher than for evoking single twitch responses to 2.2 Hz stimulation. Stimulation with higher frequencies and also with parameters which induced coordinated flexion/extension movements in the lower limbs showed the segmental-selective recruitment of muscle responses, as demonstrated for 2.2 Hz stimulation.

Stimulation of neuronal structures at the level of the cathode

Due to the dorsomedial position of the epidural electrode, the sensory afferents in the posterior roots and their axonal branches in the posterior columns are the largest fibers closest to the cathode. These "dorsal root fibers" and "dorsal column fibers" – which are part of the same afferent fiber system – are the most apparent among the various possible neural targets. To address the question whether our findings of segmental-selective muscle activation that depended on the segmental cathode level can be explained by stimulation of posterior root or column fibers, we established a three-dimensional computer model of electric potential distributions in the spinal cord and its surrounding tissues, generated by the epidural electrode. The spatial distributions of calculated fields were then compared with the topographic relationships between fibers of different segmental origins in the posterior roots and columns.

The computed isopotential lines in Fig. 2.5A illustrate how a field generated by a bipolar epidural electrode placed over the upper lumbar cord, penetrates the dorsal columns in a transversal plane at the level of the cathode. The isopotential lines are not circular around the electrode as would be expected in a homogeneous medium. The potential distribution spreads in accordance with the geometry and electric conductivities of the anatomical structures around the electrode. Initially the isopotential lines are rounder, but then become flatter as they enter the dorsal columns as a consequence of the higher electric resistance of the spinal cord compared to the cerebrospinal fluid. In the dorsal columns, the isopotential lines are perpendicular to the median septum. The direction of current flow is perpendicular to the isopotential lines. The current density is inversely proportional to the distance between the isopotential lines and proportional to the conductivity of the medium. The transverse electric conductivity of the white matter is about 20 times lower than that of the

cerebrospinal fluid (Geddes & Baker, 1967; Holsheimer, 2002) and restricts current flow into the spinal cord. Consequently in ventral direction the current density is reduced markedly when entering the dorsal columns.

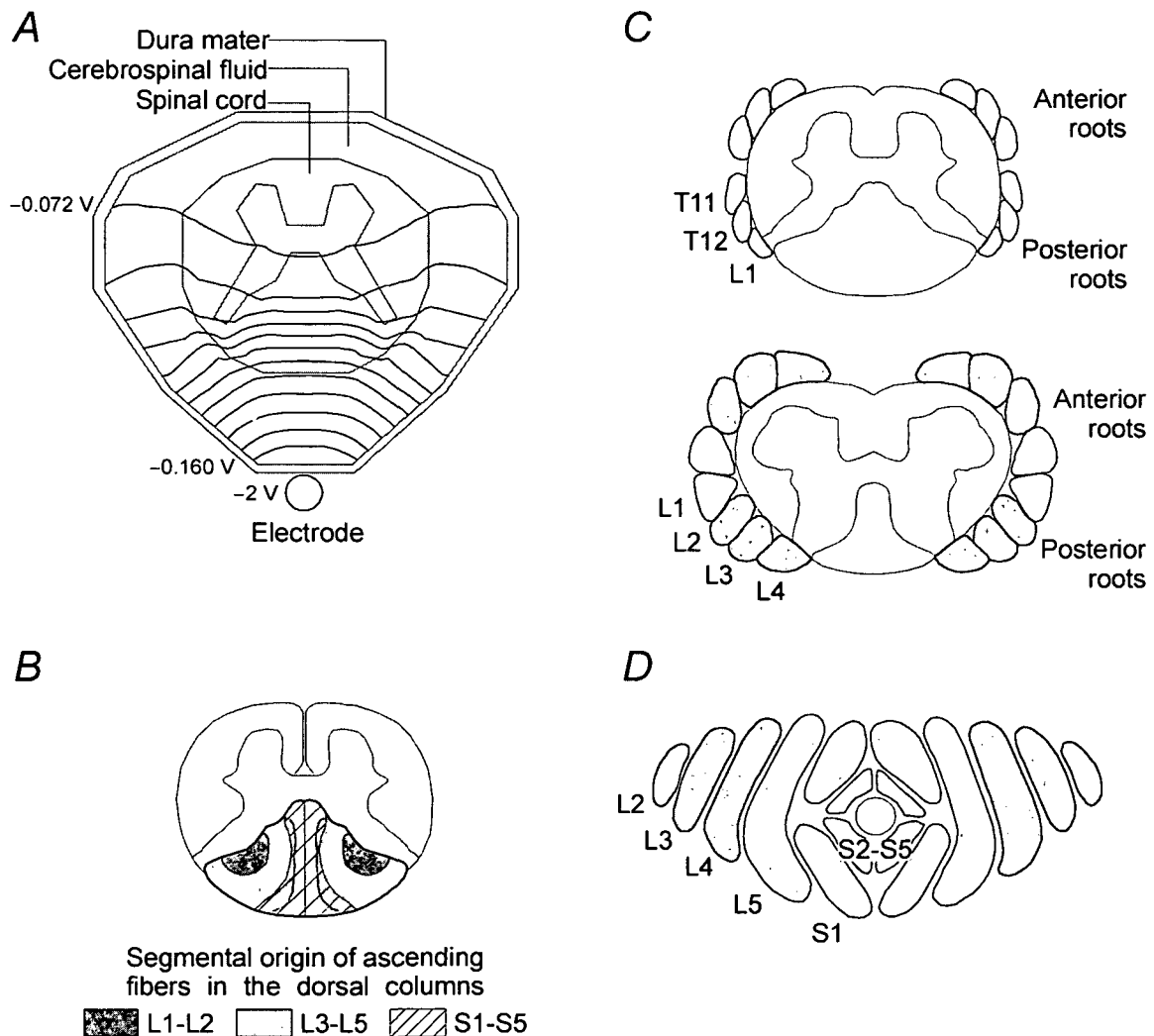


Figure 2.5 Upper lumbar cord stimulation (computer model), topography of posterior columns, and cross-sectional anatomy of spinal roots (drawing)

A, transverse potential distribution at the level of the cathode, generated by a bipolar electrode with a potential difference of 4 V between the two active contacts ($-2/+2\text{ V}$). Isopotential lines between -0.072 V and -0.160 V are presented in 0.008 V increments. The compartments surrounding the dura which were included in the computer model are not shown. *B*, cross-section of a human L1 cord segment outlining the topographic relationships between long ascending axon branches of different segmental origins in the posterior columns (adapted from Smith & Deacon, 1984). *C*, schematic diagrams of cross-sections of spinal cord and nerve roots at the L1 (top) and lower L4 segmental levels and (*D*) at the level of the conus medullaris (adapted from Wall *et al.* 1990).

Fig. 2.5*B* maps the organization of dorsal column fibers at the L1 cord level based on their segmental origins. A certain degree of segmental lamination is present, but with partial overlapping of fibers from adjacent segments. The medial positions of the dorsal columns

are occupied by fibers arising from the most caudal posterior root fibers, whereas fibers originating from more rostral levels join laterally. At a given spinal cord level ascending projections of posterior root fibers of segments corresponding to that level and caudal levels are present in the dorsal columns.

By comparing Fig. 2.5A with 2.5B, the isopotential lines turn out to be rather perpendicular to the segmental organization in the dorsal columns. Consequently, a large set of dorsal column fibers of different sacral and lumbar origins are exposed to a given voltage value (isopotential line) in a non-selective way. Stimulation of dorsal column fibers of specific segmental origins – which is essential for a segmental-selective recruitment of lower limb muscles – would require the presence of factors at the cathode level that result in different excitation thresholds for dorsal column fibers of different segmental origins. Such discrete differences, however, do not exist at lumbar cord levels (see *Muscle responses to epidural lumbosacral cord stimulation are initiated in the posterior roots* in the Discussion).

Lumbosacral segments have long spinal roots that follow rostrocaudal trajectories on the way to their appropriate intervertebral exit levels. These long spinal roots are immersed in the well-conducting cerebrospinal fluid and form a peripheral rim around the lumbosacral cord. Figure 2.5C shows a schematic representation of the cross-sectional anatomy of the spinal cord and roots at the L1 (upper figure) and lower L4 segmental levels (adapted from Wall *et al.* 1990). The multifascicular anterior and posterior roots are organized in separate root layers. At a given segmental level only afferents of segments corresponding to that level and of adjacent rostral segments are present in the posterior roots. Different posterior root layers are organized in a rather posteromedial-anterolateral direction, with the roots of the most rostral segments lying laterally. At the L1 segmental level the spinal cord is flanked only by the T11, T12 and L1 nerve roots. Roots of more rostral segments have already exited the dural sac. At the lower L4-level the cord is surrounded from the first through the fourth lumbar nerve roots. Most of the circumference of the cord is covered by the roots.

The cerebrospinal fluid has the highest electrical conductivity of the relevant anatomic structures surrounding the epidural electrode. Fig. 2.5A demonstrates that the isopotential lines in the cerebrospinal fluid are almost perpendicular to the borders of this layer. In a transverse section, in the dorsal cerebrospinal fluid the current spreads anterolaterally perpendicular to the isopotential lines. (Note that the main direction of the current is longitudinally towards the anode). The current density is highest in the cerebrospinal fluid in the vicinity of the electrode and decreases with increasing anterolateral distance from the electrode. Due to the quite lateral positions and entry points of upper lumbar posterior roots into the cord (upper part of Fig. 2.5C), thresholds for posterior root stimulation can be expected to be lower at more caudal spinal cord levels where the posterior roots are located more dorsomedially (lower part of Fig. 2.5C).

More caudally the spinal cord diminishes in size and the nerve roots are the predominate neural structures. The topographic relationship between the roots of different segments at the lower L1-vertebral level is depicted in Fig. 2.5D (Wall *et al.* 1990). All afferent fibers innervating the lower limb muscles pass the level of the shown cross-section, some belonging to cord segments situated several centimeters rostral to that level. The posterior and anterior roots of the L2–L5 segments have come together and form organized posteroanterior layers. Roots of more caudal segments are located medially and encircle the terminal spinal cord. Interpretations derived from Fig. 2.5A cannot be directly applied at these levels. However, the geometrical and electrical situation is quite simple and thus

allows qualitative conclusions. Considering that all fibers passing the level of the cross-section have trajectories mainly oriented in rostrocaudal direction, different thresholds will be predominantly determined by different cathode-fiber distances (for a given fiber size). S1-posterior root fibers can be expected to have lowest thresholds, while L4, L3, and L2 roots, situated at progressively increasing anterolateral distances from a dorsomedially positioned cathode, respectively, will be recruited only at higher stimulus strengths.

Stimulation of neuronal structures distant from the cathode level

Fig. 2.6A shows the computed electric potential distribution within the dural sac generated by a bipolar electrode in a midsagittal plane and also in a transverse plane at the level of the rostral contact. The potential difference between the two contacts is 1 V (± 0.5 V). The generated potential distribution reflects the high electrical conductivity in rostrocaudal direction of the structures contained in the dural sac. This is due to the high conductivity of the cerebrospinal fluid and its elongated geometry, and due to the anisotropic spinal white matter which has an approximately 7–8 times higher conductivity in axial than in transverse direction.

Fig. 2.6B illustrates the extensive spread of the cathodal field, which is represented by an arbitrary isopotential line (-0.1 V), in caudal direction in a midsagittal plane. The caudal contact is operated as a cathode, the cathode level corresponds to the average group 1 level of Fig. 2.2. The stimulation amplitude is increased from 5 V to 10 V. The segments L2–L4 are displayed in dark gray, L5–S2 in light gray. At an amplitude of 5 V, the isopotential line penetrates only a small portion of the spinal cord in the proximity of the cathode. In caudal direction the isopotential line ranges to the center level of the L2-cord segment in the displayed standard geometry – and covers the associated posterior roots. By increasing the strength to 10 V, additional caudal cord segments and posterior roots are exposed to the given potential value (or to more negative potential values). The isopotential line ranges down to L4-segmental level.

Fig. 2.6C shows a schematic representation of the geometrical relations of the lumbosacral cord and the trajectories of the L1, L3, and L5 posterior roots. The figure is to make obvious that posterior root fibers of different segments enter the spinal cord at levels that are spatially separated in rostrocaudal direction. Comparison of Fig. 2.6B with 2.6C implies the possibility of a segmental-selective recruitment of posterior roots from a rostral cathode position, given by the extent of the current spread in caudal direction.

DISCUSSION

In the present study we consider which neural structures were directly activated by epidural lumbar cord stimulation that gave rise to the described muscle responses. To address this question we combined information on real patient data with calculated electric potential distributions and consolidated knowledge about patterns of segmental organization of the posterior columns and roots. Our computer model is based on well established volume-conductive properties of the spinal cord and its surrounding structures (Coburn & Sin, 1985; Holsheimer, 1998; Rattay *et al.* 2000). Similar qualitative results of spatial distributions of macroscopic fields generated by epidural electrodes could also be obtained from much simpler models involving concentric cylinders with different electric

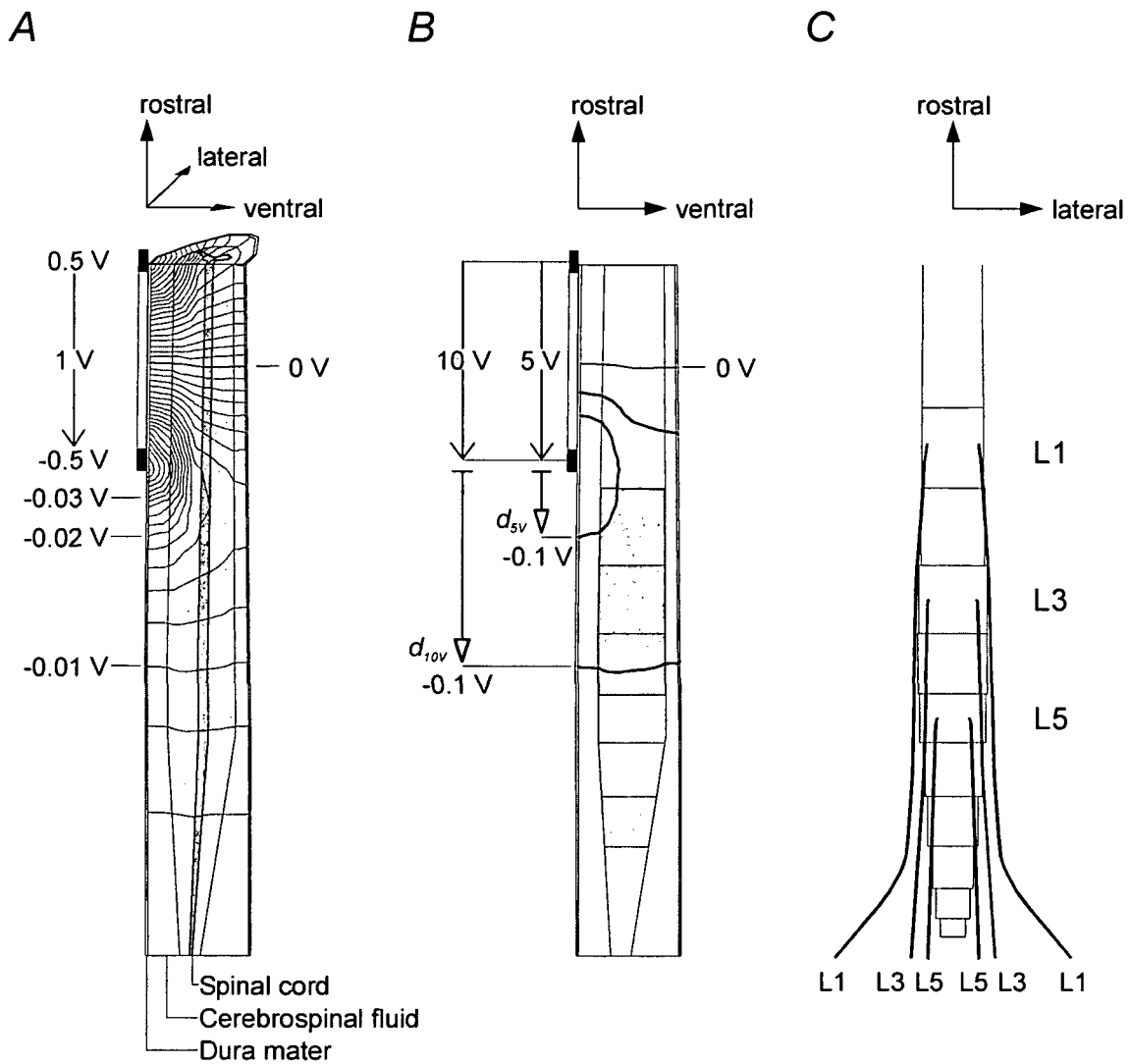


Figure 2.6 Potential distribution in a midsagittal plane (computer model) and dorsal root trajectories (drawing)

A, computed potential distribution within the dural sac in midsagittal and transversal plane generated by a bipolar electrode with 1 V potential difference between the two contacts. *B*, by increasing the stimulation amplitude, the cathodal field represented by an isopotential line of arbitrary strength (-0.1 V) penetrates more and more cord segments. The cord segments L2–L4 and L5–S2 are indicated by dark and light gray areas, respectively. *C*, sketch of the L1, L3, and L5 dorsal root trajectories (back view).

conductivities, the center one being a poorly conducting, anisotropic compartment representing the spinal cord, surrounded by a well conducting cerebrospinal fluid compartment and outer compartments with higher electric resistivities (Holsheimer, 2002).

At any instant a neuron has some threshold, which external electrical excitation must exceed to initiate an action potential. This threshold value is determined by the electric conductivity of the anatomic structure in which the nerve is situated and the nerve trajectory and orientation with respect to the stimulating electrode. In addition, the threshold is related to the electrode-neuron distance and inversely related to the nerve fiber diameter. The epidural electrode can, in principle, affect any neural structures within the spinal cord and

spinal roots if the stimulus amplitude is high enough. However, since applicable stimulation strengths are limited (by intensities which cause discomfort to the subject or by the maximum output of the pulse generator) the large diameter axons within the posterior roots and their axonal branches in the posterior columns are the primary potential targets of stimulation for a dorsomedially positioned epidural electrode. Direct activation of motoneurons and thereby bypassing the spinal cord can be ruled out because this could not account for the complex and patterned EMG responses to sustained stimulation with constant parameters (Figs. 2.3 and 2.4A). Moreover, the analysis of CMAPs induced by pairs of stimuli of equal strength delivered to the posterior structures of the lumbosacral cord at different intervals demonstrated maximum absolute refractory periods of the responses of up to 47.5–62.5 ms (Minassian *et al.* 2004). In contrast, motor responses follow frequencies of up to 100 Hz when elicited by ventral epidural spinal cord stimulation that most probably activates alpha-motoneurons within the ventral roots or in the ventral horn (Struijk *et al.* 1993a; also see Dimitrijevic, 1983). It was shown to be unlikely for epidural spinal cord stimulation with dorsal electrode placement that neural structures other than fibers within the posterior roots or superficial posterior columns are directly activated (Holsheimer, 2002) or contribute to muscle activation (Hunter & Ashby, 1994). Therefore we will first discuss whether low-frequency stimulation (2.2 Hz) of posterior roots or columns can explain the segmental-selective effect of the stimulation and the EMG features of the responses as described in the present study. We will then expand our discussion on the origin and nature of the more complex stimulus-evoked responses at higher frequencies.

Muscle responses to epidural lumbosacral cord stimulation are initiated in the posterior roots

The EMG signals associated with the twitch responses to stimulation at 2.2 Hz and 1–10 V were stimulus coupled and of short latency (Figure 2.1, Table 2.2), equal to about half the latencies of phasic stretch reflexes of the respective muscle groups. At constant stimulation strength, the EMG shapes of successively elicited CMAPs remained constant. When stimulation strength was increased above the threshold level of a given muscle, additional motor units were recruited. The corresponding superimposing EMG responses overlapped in time with the CMAP elicited at lower strength. The resultant signal mainly demonstrated an increase in amplitude and only minor variation in shape or duration. No additional EMG phases of later latencies were generated.

In Figure 2.2 we demonstrated different recruitment orders of the L2–L4 innervated quadriceps and the L5–S2 innervated triceps surae muscles depending on the rostrocaudal cathode position of the stimulating electrode array with respect to spinal cord segments. In Fig. 2.5 we compared the distribution of calculated isopotential lines of the generated electric field with the topography of ascending fibers of different segmental origins. We explained that posterior column fibers from different thigh and leg muscles are non-selectively exposed to a given voltage value (compare Fig. 2.5A with B). This implies that activation of posterior column fibers with given diameter and trajectory hardly depends on the mediolateral position of the fibers (Struijk *et al.* 1992). Therefore, segmental-selective recruitment of muscle groups according to the groups 1 and 2 (Fig. 2.2) as a result of posterior column stimulation would only be possible if there are factors other than the cathode-fiber distance which determine different thresholds of fibers of different segments at a given cathode level. Feirabend *et al.* (2002) recently described in a morphometric study that at the T10/T11 cord levels the fibers in the lateral superficial posterior columns are

only 1–5% larger in diameter than those located medially. The fact that a relevant difference in size could not be demonstrated is significant because lateral and medial fiber groups are associated with different muscles (Fig. 2.5B). Feirabend *et al.* (2002) suggested that any possible differences between the stimulation thresholds of large longitudinal fibers in the median and lateral posterior columns could be related to the presence or absence of collaterals at the stimulation site (see also Struijk *et al.* 1992). However, collaterals are issued by the ascending axon branches within the posterior columns throughout the rostrocaudal levels at which the electrodes were placed in our subjects. For fibers of group Ia afferents from primary muscle spindle endings, some of these collaterals project to motoneurons and interneurons at the segmental level where the group Ia axons enter the cord via the posterior roots and some at the levels of adjacent segments. Others project to Clarke's columns, their most caudal part in man being at the L2 segmental level (Davidoff, 1989). It can be assumed that discrete differences in the factors determining the excitation thresholds of the ascending posterior column fibers of different lower limb muscles do not exist within the extent of the lumbar cord segments. Consequently, the effect of posterior column stimulation can be expected to be general rather than localized to afferent structures of any specific segmental origins. This conclusion is supported by the findings of Hunter & Ashby (1994) who demonstrated that epidural stimulation of the posterior columns at thoracic cord levels resulted in non-selective facilitation of motoneurons innervating thigh and leg muscles. Figure 2.2 further showed that excitation thresholds of muscle responses in the lower limbs increased in accordance with the caudorostral distance of the cathode from the L1 vertebral level. Feirabend *et al.* (2002) revealed that there is no significant caudorostral tapering of large posterior column fibers within the extent of a few cord segments in the human spinal cord. Stimulation of these fibers would therefore not explain the increasing thresholds associated with increasingly rostral cathode positions. The most rostral cathode levels to induce the CMAPs as described in the present study at maximum pulse intensity (10 V) were at T10/T11 vertebral levels for quadriceps and T11/T12 for triceps surae. By contrast, Guru *et al.* (1987) and Hunter & Ashby (1994) reported recruitment of thigh and leg muscles by epidural stimulation with cathodes located over the dorsum of the thoracic cord at positions as rostral as the T8–T10 vertebral levels. At these cathode levels the cord segments and corresponding roots supplying the lower limbs and particularly the calf muscles are located well below the cathode. Guru *et al.* (1987) and Hunter & Ashby (1994) attributed this muscle activity to antidromic activation of the rostral projections of primary afferents in the posterior columns that have collaterals to motoneurons. The latencies reported in their studies were generally about 6–12 ms longer than those of the comparable muscles compiled in our Table 2.2.

We conclude that the CMAPs elicited by lumbosacral cord stimulation are not related to posterior column fiber activation. Thereby, our results do not contradict the results of Guru *et al.* (1987) and Hunter & Ashby (1994). The differences of the effects of stimulation are most probably due to the different subject profiles, electrode setups and the different geometrical characteristics of the spinal cord and roots anatomy at thoracic and lumbosacral levels. The subjects included in the two studies cited above had electrodes implanted for the treatment of pain and had volitional control over the lower limb muscles. In the subjects of the present study, the lumbosacral cord was functionally completely divided from brain control. Moreover, in the studies of Guru *et al.* (1987) and Hunter & Ashby (1994) four different electrode set-ups were utilized, in most cases a fine wire cathode with an uninsulated tip was placed in the posterior epidural space and a larger disc anode at the anterior abdominal wall or embedded in the paraspinal muscles. In such an electrode set-up,

the surface area of the disc anode is much larger than the wire tip contact. This results in a smaller current density and less voltage drop near the anode. A larger portion of the total stimulation voltage is therefore available under the cathode, hence a stronger stimulating effect of this electrode design in the vicinity of the cathode. There are also significant differences of the anatomy between the thoracic and the lumbosacral spinal cord. Because of the disparity in length between the spinal cord and vertebral column, the spinal roots from lumbar and sacral segments have much longer distances to travel prior to reaching their respective foramina of exit. Whereas cervical and upper thoracic roots are situated nearly perpendicular to the cord, lower thoracic, lumbar, and sacral ones enter and leave the cord at increasingly more oblique angles. Most part of the circumference of the lower lumbar and sacral cord is covered by spinal roots (Wall *et al.* 1990). For epidural stimulation, thresholds of fibers within the lumbosacral cord will presumably be increased due to this poorly conducting "root-layer". Finally, the entry points of lower lumbar and sacral posterior roots into the spinal cord are situated more medially than of more rostral ones and are thus nearer to a dorsomedially positioned cathode (Fig. 2.5C). At the level of the conus medullaris some posterior roots are closer to a dorsomedially positioned cathode than the posterior column (Fig 2.5D), which is in contrast to thoracic cord levels. The diameters of posterior root fibers, which are larger than that of corresponding posterior column fibers at any segmental level, add to their lower excitation thresholds (Ishizuka *et al.* 1979; Struijk *et al.* 1998; Holsheimer, 2002).

Further indication that stimulation of posterior column fibers is non segmental-selective comes from the application of spinal cord stimulation in chronic pain control based on reports on paresthesia distributions of patients with intact sensory functions. In this situation, medially placed electrodes elicit a widespread distribution of paresthesiae in body areas at the spinal level of stimulation and far caudally to it. This may occur even at the perception threshold (He *et al.* 1994). This widespread distribution of paresthesiae is attributed to activation of the posterior columns (Barolat *et al.* 1993). In the posterior columns at any spinal level dermatomes corresponding to that level and to more caudal levels are represented by ascending projections of cutaneous afferents. To some extent, they have similar trajectories and topographic organization as axonal branches of group Ia fibers in the posterior columns (Davidoff, 1989). The recruitment of these afferent structures turns out to be non segmental-selective even if the voltage is gradually increased in 0.1-V or 0.25-V intervals (He *et al.* 1994) – which is an approach with higher accuracy than in our study.

Beside neurophysiological studies carried out in parallel to clinical programs, computer modeling of epidural spinal cord stimulation is another method appropriate for obtaining a better knowledge of the immediately evoked electrophysiological phenomena (Coburn 1980; Holsheimer 1998). Theoretical studies of the effect of epidural stimulation on posterior roots have shown that geometric and electric factors result in "hot spots" (low-threshold sites) for extracellular electrical excitation at the sites where posterior root fibers enter the spinal cord (Coburn, 1985; Struijk *et al.* 1993; Rattay *et al.* 2000). These low-threshold sites are created by a sudden change of the generated potential distribution along the afferent fibers – i.e. of the extracellular potential – at the interface between spinal rootlet and cord owing to the different electrical conductances of the cerebrospinal fluid and the spinal cord (Geddes & Baker, 1967; Holsheimer, 2002). The bend of the posterior root fibers as they enter the cord additionally contributes to the inhomogeneity of the extracellular potential. These low-threshold sites were also recognized by studies of diagnostic methods involving lumbosacral nerve root stimulation (Troni *et al.* 1996).

We therefore suggest that the muscle responses to epidural stimulation of the posterior lumbar cord are initiated in the posterior roots, since posterior column fiber stimulation could not explain the motor effects described in the present study. Lumbosacral posterior root fibers entering the cord at the level of the cathode or up to about 2 cm caudally (calculated maximum effective range of the applied bipolar electrode at 10 V, see Rattay *et al.* 2000) can be recruited at their hot spots where the fibers enter the spinal cord. If the cathode is located at L2–L4 segmental levels, the posterior roots containing afferents of the lower limbs can be recruited in a segmental-selective way at their hot spots. At threshold stimulation strength, the largest posterior root fibers will be activated at the level of the cathode (L2–L4). Increasing the stimulation strength will not only recruit additional posterior root fibers at the cathode level, but also posterior roots of the more caudal segments L5 and S1 at the hot spots due to current spread in this direction. This mechanism can explain the segmental selective muscle activation for cathode positions corresponding to the levels of group 2 of Fig. 2.2 (consider also Fig. 2.1B). For cathode positions rostral to the L2 cord level (group 1 of Fig. 2.2), CMAPs can still be induced in the L2–L4 innervated thigh muscles. However the current spread in caudal direction is not sufficient to activate even more caudally situated posterior roots (compare with Fig. 2.6B). These structures are beyond the effective caudal range of the used bipolar electrode. Note that even the L2–L4 innervated quadriceps is recruited at quite high thresholds by group 1-positioned cathodes. This is supported by the very lateral sites of the entry points of the posterior roots into the spinal cord at these levels (Fig. 2.5C).

For caudally located cathodes at levels of the conus medullaris, lumbosacral posterior root fibers which enter the cord rostrally to the cathode will be excited at the level of the cathode (Rattay *et al.* 2000), where their trajectories are primarily oriented in rostrocaudal direction. Lumbosacral segments have long spinal roots of up to 16 cm length (Sunderland, 1976; Lang, 1984b) to reach their appropriate intervertebral exit levels. Due to the high electric conductivity of the cerebrospinal fluid surrounding the roots and the proximity of the descending root trajectories to the posterior border of the dura mater, and thus to the epidural electrode, posterior root fibers that enter the cord well rostrally to the cathode can be recruited at the level of the cathode. At lower L1 vertebral levels, all segments with afferent fibers coming from the lower limb muscles are represented by posterior root fibers and are organized in layers in a posteromedial-anterolateral direction (Fig. 2.5D and 2.6C, see also Wall *et al.* 1990). Due to an evidently greater distance of the L2–L4 posterior roots than of the S1 and L5 ones to a dorsomedially positioned cathode, it is plausible that stimulation of these structures can explain the reversed recruitment order of group 4 in comparison with group 2.

Since stimulation with a cathode at group 2-position resulted in lower thresholds of L2–L4 posterior roots and at group 4-position in lower L5–S2 thresholds, there must be some rostrocaudal cathode position between these two different cathode levels, where thresholds of posterior roots of the adjacent segments L3–L4 and L5–S1 are about equal. These cases constitute the group 3 in Fig. 2.2. Naturally, accurate threshold identification would reveal minor differences in thresholds also in these cases.

Posterior Roots Muscle Reflex Responses

We have presented evidence that the posterior roots are the input structures which led to the CMAPs elicited at 2.2 Hz. Feline (Lloyd, 1943) and human (Magladery *et al.* 1951) studies

showed that electrically induced afferent volleys via the lowest-threshold fibers of the posterior roots caused monosynaptic reflex discharge of motoneurons. Since the fibers with the largest diameter have the lowest thresholds, the direct effects to the motoneurons are mediated by group-Ia fibers from primary muscle spindle endings. Magladery *et al.* (1951) demonstrated that activation of only a portion of the low-threshold afferent fibers was sufficient to produce a massive synchronous reflex outflow through the anterior roots. Lloyd (1943) showed that monosynaptic group-Ia reflex discharges almost reached their full value even with considerably submaximal posterior root volleys. Major intensification of later, multineuron-arc discharges occurred only after the stage of maximum monosynaptic discharge had been reached. This stage was not reached in our study due to the limited stimulation strengths. The central latencies of pure cutaneous nerve-anterior root reflex discharges are about 2 ms longer (Lloyd, 1943). These discharges are irregular and last longer than monosynaptic group-Ia reflex discharges. The CMAPs elicited at 2.2 Hz as described in our results showed mainly increased amplitudes at suprathreshold strengths, while no other later EMG phases were built up.

We infer that the twitch responses elicited in the present study by epidural stimulation at 2.2 Hz were predominantly due to activation of large group-Ia fibers within the posterior roots with subsequent recruitment of motoneurons through monosynaptic connections in the spinal cord. This mechanism can explain the short and constant latencies of the registered muscle responses (Fig. 2.1, Table 2.2). The responses elicited at 2.2 Hz are indirect and are reflexes in origin. They are the physiological equivalents of the H-reflexes of the corresponding muscles. Instead of being elicited by electrical stimulation of low-threshold afferents in mixed peripheral nerves the reflexes induced by epidural stimulation are initiated in the posterior roots. It has been previously demonstrated in able-bodied adult individuals that the soleus H-reflex can be evoked by percutaneous electrical stimulation (Zhu *et al.* 1998) of the proximal S1 nerve root or by needle electrodes inserted into epidural space at cauda equina levels (Ertekin *et al.* 1996). Troni *et al.* (1996) reported that soleus H-reflexes can be elicited by high-voltage percutaneous stimulation at different rostrocaudal levels over the lumbar vertebral column. They suggested that posterior roots were activated by the stimulation procedure precisely at the points where they enter the spinal cord. It was also reported that by stimulation of the lumbosacral roots and the cauda equina responses of muscles other than of the soleus can be obtained (Maertens de Noordhout *et al.* 1988; Ertekin *et al.* 1996).

We conclude that the CMAPs elicited at 2.2 Hz as described in our study are reflex responses arising from a dominating input via large afferents within the posterior roots. We hereinafter refer to this type of stimulus-evoked muscle activity as Posterior Roots Muscle Reflex Responses (PRMRRs). Afferents other than group I primary afferents seem not to contribute to the reflex responses at 2.2 Hz stimulation.

Differences between Posterior Roots Muscle Reflex Responses and the H-reflex

Posterior root stimulation at lumbosacral cord levels is quite different from that of a peripheral nerve trunk. The posterior sensory roots are anatomically isolated from the anteriorly located motoneurons. The spinal cord, due to its lower electric conductivity, acts like a barrier reducing the current flow in ventral direction. Therefore, dorsal epidural spinal cord stimulation can activate posterior root fibers selectively and more completely without stimulating motoneurons (Struijk *et al.* 1993a; Rattay *et al.* 2000). This makes

strong reflex responses possible which are not reduced or blocked by electrically elicited and antidromically propagated action potentials in the α -motoneurons. Similar results can be achieved by percutaneous electrical stimulation applied to the dorsolumbar vertebral column. Troni *et al.* (1996) reported greater amplitudes of the soleus H-reflex to percutaneous stimulation of the lumbosacral roots as opposed to popliteal fossa stimulation. The authors attributed the finding of less occluded H-reflexes to the anatomical situation allowing activation of the Ia fibers in the posterior roots with smaller involvement of the motor fibers.

By stimulating the tibial nerve to elicit the soleus H-reflex, the evoked afferent volley is transmitted predominantly to a single cord segment. An epidural electrode placed at lumbosacral cord levels is in close range to posterior root fibers of different segmental origins. While a segmental-selective excitation is possible to a certain degree at low stimulation strengths, large afferents of probably all cord segments with motoneurons innervating the lower limb muscles can be activated at moderate strengths of 3–6 V for cathode positions corresponding to groups 4, 3 and 2 positions of Fig. 2.2. Thereby, afferent volleys are delivered highly synchronized bilaterally to several lumbar and upper sacral cord segments. As a crucial difference to peripheral nerve stimulation, the epidural stimulation of the posterior roots could not elicit reflex responses in a single muscle group, because each posterior root contains afferents from more than one muscle. In the present study, the recruitment of quadriceps was always accompanied by adductor-activity. For rostral cathodes (group 1 and 2 positions) the hamstrings threshold was related to the one of quadriceps, while for more caudal positions (group 4) hamstrings had generally the same threshold as triceps surae (see also Murg *et al.* 2000).

We have discussed that the reflex responses to epidural stimulation at 2.2 Hz were initiated in group Ia primary spindle afferents within the posterior roots. While there were no indications that fibers of other afferents for example, Ib afferents from Golgi tendon organs, group II secondary muscle afferents or cutaneous afferents contributed to the twitch responses to 2.2 Hz stimulation, this does not mean that some of these afferents were not activated by the stimulation.

Thresholds for eliciting paresthesiae in individuals with intact sensory functions by stimulating cutaneous afferents in the posterior columns and roots with epidural electrodes implanted for pain control applications are quite low. He *et al.* (1994) reported an average perception threshold of 1.69 V for medially placed epidural electrodes at T11–T12 vertebral levels and stimulation at a rate of 50 Hz. The lowest average threshold voltage for eliciting muscle responses to 2.2 Hz stimulation in the present study was 2.5 V for caudally located cathodes (triceps surae, group 4), the highest were 4.5 V for the most rostral cathode positions (lumbar paraspinal trunk muscles, group 1). However, direct comparison of the threshold values is difficult due to the different subject profiles and stimulation procedures of the different studies. Moreover, different electrode types were used, namely percutaneously inserted leads with cylindrical electrode design in our case, in contrast to surgical lead models with plate electrodes and insulated dorsal surfaces in the study of chronic pain management. Unlike plate electrodes with insulated backing, percutaneous electrode designs with circumferentially exposed electrode contacts allow some current to pass laterally and dorsally. Therefore, it can be expected that less current is available for spinal cord and posterior root stimulation making higher stimulation voltages necessary.

It should be considered that the thresholds for eliciting CMAPs reported by us are higher than the actual thresholds for group Ia afferents. First, the threshold voltages V_{th} obtained

by retrospectively analyzing muscle twitch data were whole-numbered. The actual thresholds are in the range between $V_{th} - 1$ Volt and V_{th} . This was confirmed by a case where thresholds had been identified with higher accuracy (subject 4). There the lowest threshold for eliciting CMAPs was as low as 0.5 V in the triceps surae muscle for a cathode located at group 4 levels. Secondly, the threshold for initiating action potentials in group Ia afferents might be lower than the stimulation strength needed to evoke an afferent volley sufficiently to result in a muscle activity which can be identified with surface electrodes.

All things considered, it is still plausible to assume that some afferents with smaller diameters than those of group I like cutaneous fibers were also stimulated directly in our subjects (Holsheimer, 2002). When repetitively stimulated at higher frequencies some of these afferents within the posterior roots might contribute to the motor output by transsynaptically recruiting central spinal structures (see below).

Posterior Roots Muscle Reflex Responses to trains of stimuli at higher frequencies

We have provided evidence that the directly, electrically stimulated structures at 2.2 Hz are axons within the posterior roots. We propose that the posterior roots were also the input structures at higher stimulation frequencies resulting in the more complex motor output patterns and step-like EMG activity as presented in Figs. 2.3 and 2.4A (see also Dimitrijevic *et al.* 1998; Minassian *et al.* 2004). Our notion is that the patterned EMG amplitude modulations are due to an integration of central PRMRR components at particular stimulation frequencies. This is achieved due to the special nature of the continuous tonic input and the connectivity of the activated large afferents with inherent spinal networks involved in gating the flow of sensory information in the spinal cord and in generating the basic locomotor rhythm. The hypothesis of activation of intraspinal structures by synaptically evoked depolarization affected by incoming afferent volleys is in contrast to the direct electrical stimulation of spinal neural circuits by the non-specific field. The latter mechanism would probably activate a highly unnatural admixture of circuits subserving many different, potentially competing functions, resulting in poorly controlled and inefficient patterns of muscle activation.

Hultborn *et al.* (1998) have emphasized that different reflex pathways have direct access to, or may even be part of, the central pattern generator (CPG) for locomotion in the cat. There are also human studies which indicate that sensory afferents interact with central pattern generating networks. Gurfinkel *et al.* (1998) used tonic peripheral afferent stimulation to elicit involuntary stepping in able-bodied individuals. They found that continuous lower limb muscle vibration gave rise to involuntary locomotion-like stepping movements in suspended legs and suggested that the non-specific afferent input induced by vibration activated central structures governing stepping movements. Herman (2002) reported that epidural stimulation of the lumbar cord can augment locomotor capabilities in an incomplete spinal cord injured individual. The author suggested that the stimulation appeared to provide modulation or amplification of neural circuits responsible for locomotion rhythm generation by segmental afferent input. It is worth mentioning that in this study of Herman (2002) electrodes were inserted into the epidural space over the lumbar spinal enlargement on either side of the spinal cord, each electrode placed 1–2 mm off the mid-line. Thereby the lateral location of the epidural electrodes provides a preferential stimulation of the ipsilateral posterior root fibers (Struijk *et al.* 1993b; Struijk *et al.* 1998). Furthermore Herman (2002) applied stimulation at amplitudes above sensory but

below motor threshold. At these rather low stimulus strengths direct activation of small spinal interneurons is unlikely.

Large diameter axons which are the proposed directly stimulated structures in the present study, can easily follow the applied frequencies of up to 25–50 Hz, the range effective to elicit stepping-like movements. Furthermore, we demonstrated that the components of the different patterned tonic (Fig. 2.3A) and rhythmic (Fig. 2.3B) EMG activity were single CMAPs. The burst-style phases during epidurally evoked stepping-like movements consisted of stimulus-triggered, separate CMAPs that were subject to well-defined amplitude modulations resulting in burst-like envelopes of the EMG activity. The CMAPs elicited at higher frequencies and during induced movements had common EMG features with the ones evoked at 2.2 Hz (Fig. 2.1), namely similar EMG potential duration, attainable amplitudes and generally, also the same constant latencies. Under certain conditions and only during burst-like phases of induced alternating flexion/extension movements, however, the CMAP latencies can be prolonged for about 10 ms as well (Minassian *et al.* 2001a,b; Minassian *et al.* 2002; Minassian *et al.* 2004). Note that this was not the case for the example presented in Fig. 2.3B. Finally, Fig. 2.4 demonstrated that the muscle recruitment properties of stimulation with 25 Hz and 50 Hz were quite similar as for 2.2 Hz stimulation. Even stimulation with frequencies effective to induce alternating flexion/extension movements in the lower limbs showed the segmental-selective muscle recruitment (Fig. 2.4A). We have provided evidence that this segmental-selectivity indicates that the stimulus-evoked muscle activity was initiated in the posterior roots. There was no single case of the studied recruitment orders at higher frequencies showing differences from the characteristic posterior root contribution. Thus, there was no data supporting that at higher frequencies structures which were immediately activated by epidural stimulation other than the posterior root fibers contributed to the initiation of the observed muscle activity. Provided that the cathode position and stimulation frequency were optimal to induce stepping-like movement (upper lumbar segmental level and 25–50 Hz), the threshold voltage for initiating stepping-like movements was never below the level sufficient to elicit twitch responses in quadriceps as well as in triceps sure at 2.2 Hz (Minassian *et al.* 2004). All studied main lower limb muscle groups were recruited by the gradually increased stimulation strength before rhythmic activity could be initiated (Fig. 2.4A). This implies that the activation of PRMRRs in the main thigh and leg muscles and thus the recruitment of lumbar and upper sacral posterior roots was an essential condition for initiation of stepping-like movements.

We suggest that the more complex, potentially functional movements of the paralyzed lower limbs induced by repetitive epidural stimulation are initiated within the posterior roots. The tonic input via the posterior roots is delivered bilaterally to several lumbar and upper sacral cord segments simultaneously. Spinal interneurons which normally receive continuous descending input from higher motor centers are deprived of supraspinal influence in the model of the lumbosacral cord completely isolated from descending control. The overall level of activity of these spinal neural circuits is now set by an evenly distributed tonic input coming from periphery. We speculate that besides exerting facilitation of motoneuron pools, the continuous stimulation organizes lumbar spinal interneurons by temporarily combining them into functional units representing different levels of muscle synergies, parts of movements, or even more integrated motor behavior.

Significance of the results

In animal preparations it is possible to identify posterior roots after surgical opening of the spinal canal and to stimulate these neural structures electrically in order to study PRMRRs initiated in axons with different diameters and with different projections to motoneurons and neuronal networks in the spinal cord. The same possibility also exists in humans during surgical intervention of the cord when attempting to control intractable neurogenic pain or spasticity (Gybels & Sweet, 1989; Abbott *et al.* 1989).

Nevertheless, in this study we have shown that it is possible to selectively stimulate posterior roots without opening the spinal canal but by taking advantage of an electrode which had been percutaneously inserted into the posterior epidural space.

By implanting an array of electrodes above the complex anatomical structure of the posterior roots of the lumbosacral cord, it is possible to stimulate large diameter myelinated axons close to their entries into the corresponding segments of the spinal cord. When applying low frequency stimulation of 2.2 Hz we have demonstrated characteristic features of shortest spinal reflex responses of different lower limb muscle groups, similar to the H-reflex responses but of shorter latency time due to reduced afferent reflex path.

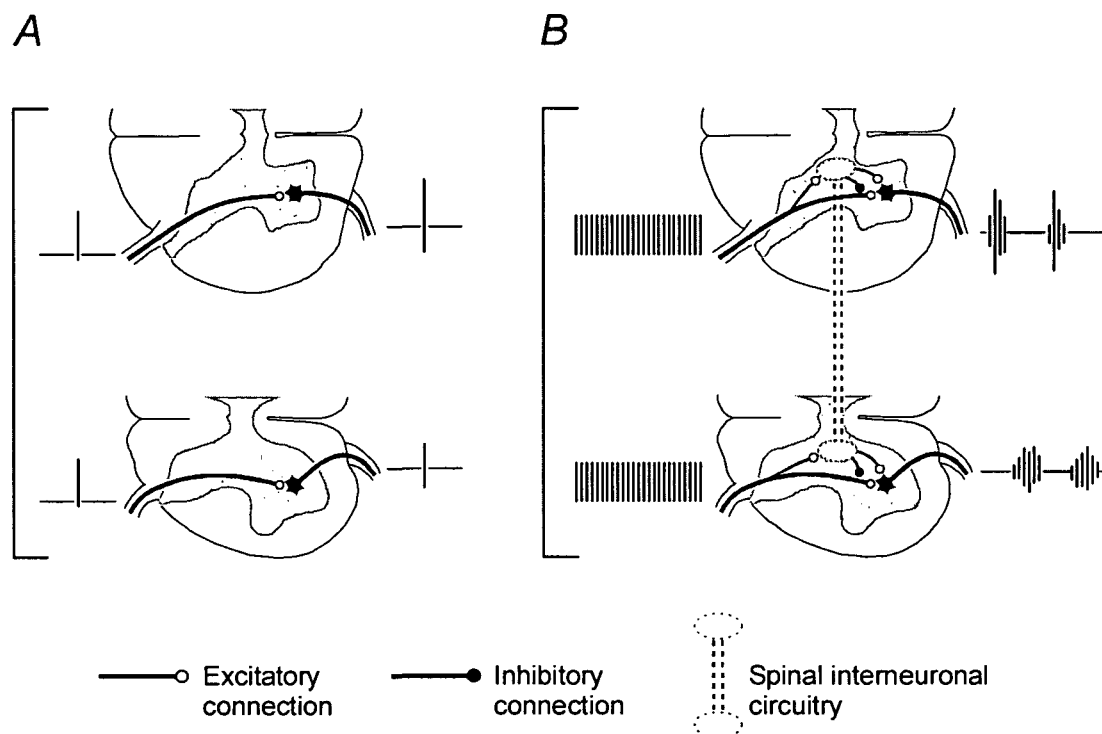


Figure 2.7. Speculative scheme of neural structures activated by epidural spinal cord stimulation

Neural path diagrams are shown in cross-sections at two lumbar segmental levels. *A*, single pulse (2.2 Hz-) stimulation activates segmental primary sensory axons and affects monosynaptic excitatory action on homonymous motoneurons. *B*, same afferent structures repetitively stimulated at higher frequencies activate lumbar neuronal circuits that modulate the afferent flow through monosynaptic pathways by putatively presynaptic inhibitory mechanism and control motoneuronal discharge by excitatory oligosynaptic pathways. Sustained stimuli at 25–50 Hz organize the lumbar spinal interneurons by temporarily combining them into locomotor centers that project over several segments and coordinate the neural activity.

This selective stimulation of the posterior roots and elicitation of PRMRRs should be considered as the product of the unique anatomical conditions of the terminal portion of the lumbosacral cord which determines the resultant electrical field characteristics of the bipolar stimulation from epidural space and its effect on excitable structures. When the biophysical complexity of the generated electrical fields is applied to the known biophysical posterior root characteristics, it is possible to adjust conditions for recording electrophysiological features of PRMRRs in humans.

Another significance of the presented results is the effect of PRMRR modifications by increasing the rate of stimulation from 2.2 Hz (Fig. 2.7A) up to 50 Hz (Fig. 2.7B). At the higher stimulation frequencies, shortest latency spinal reflex responses incorporate additional spinal cord structures resulting in the modulation of PRMRR amplitudes as well as extending the latency beyond the monosynaptic one, thereby establishing oligosynaptic spinal reflex responses. This finding was present when all lumbar and upper sacral segments have been stimulated simultaneously and under such circumstances even functional motor outputs of sustained extension or alternating stepping-like lower limb movements have been established. In other words epidural stimulation of the posterior structures of the lumbosacral cord can be set up to elicit motor reflex responses of muscle groups innervated by corresponding spinal cord segment, or to simultaneously stimulate all posterior root segments of the lumbar and upper sacral cord in order to study more complex sensory-motor organization activity of spinal cord networks. Functional movements of the paralyzed lower limbs can be generated by afferent input in humans after accidental spinal cord injury and complete removal of the brain motor control. This finding permits a new approach to studies of the processing capabilities of the human lumbar cord networks and how such capabilities depend on sensory input codes.

REFERENCES

- Abbott R, Forem SL & Johann M (1989). Selective posterior rhizotomy for the treatment of spasticity: a review. *Childs Nerv Syst* **5**, 337-346.
- Barolat G, Myklebust JB & Wenninger W (1988). Effects of spinal cord stimulation on spasticity and spasms secondary to myelopathy. *Appl Neurophysiol* **51**, 29-44.
- Barolat G, Massaro F, He J, Zeme S & Ketcik B (1993). Mapping of sensory responses to epidural stimulation of the intraspinal neural structures in man. *J Neurosurg* **78**, 233-239.
- Beric A (1988). Stability of lumbosacral somatosensory evoked potentials in a long-term follow-up. *Muscle Nerve* **11**, 621-626.
- Coburn B (1980). Electrical stimulation of the spinal cord: two-dimensional finite element analysis with particular reference to epidural electrodes. *Med Biol Eng Comput* **18**, 573-584.
- Coburn B & Sin WK (1985). A theoretical study of epidural electrical stimulation of the spinal cord--Part I: Finite element analysis of stimulus fields. *IEEE Trans Biomed Eng* **32**, 971-977.
- Davidoff RA (1989). The dorsal columns. *Neurology* **39**, 1377-1385.
- Dimitrijevic MR (1983). Neurophysiological evaluation and epidural stimulation in chronic spinal cord injury patients. In *Spinal Cord Reconstruction*, ed. Reier PJ, Bunge RP & Kao CC, pp. 465-473. Raven Press, New York.
- Dimitrijevic MR, Gerasimenko Y & Pinter MM (1998). Evidence for a spinal central pattern generator in humans. In *Neural Mechanisms for Generating Locomotor Activity*. *Ann N Y Acad Sci Vol. 860*, ed. Kiehn O, Harris-Warrik RM, Jordan LM, Hultborn H & Kudo N, pp. 360-376. New York Academy of Sciences, New York.
- Ertekin C, Mungan B & Uludag B (1996). Sacral cord conduction time of the soleus H-reflex. *J Clin Neurophysiol* **13**, 77-83.
- Feirabend HK, Choufoer H, Ploeger S, Holsheimer J & van Gool JD (2002). Morphometry of human superficial dorsal and dorsolateral column fibers: significance to spinal cord stimulation. *Brain* **125**, 1137-1149.
- Geddes LA & Baker LE (1967). The specific resistance of biological material—a compendium of data for the biomedical engineer and physiologist. *Med Biol Eng* **5**, 271-293.
- Gurfinkel VS, Levik YS, Kazennikov OV & Selionov VA (1998). Locomotor-like movements evoked by leg muscle vibration in humans. *Eur J Neurosci* **10**, 1608-1612.
- Guru K, Mailis A, Ashby P & Vanderlinden G (1987). Postsynaptic potentials in motoneurons caused by spinal cord stimulation in humans. *Electroencephalogr Clin Neurophysiol* **66**, 275-280.
- Gybels JM & Sweet WH (1989). *Neurosurgical treatment of persistent pain*. Karger, Basel.
- He J, Barolat G, Holsheimer J & Struijk JJ (1994). Perception threshold and electrode position for spinal cord stimulation. *Pain* **59**, 55-63.

- Herman R, He J, D'Luzansky S, Willis W & Dilli S (2002). Spinal cord stimulation facilitates functional walking in a chronic, incomplete spinal cord injured. *Spinal Cord* **40**, 65-68.
- Holsheimer J (1998). Computer modeling of spinal cord stimulation and its contribution to therapeutic efficacy. *Spinal Cord* **36**, 531-540.
- Holsheimer J (2002). Which neuronal elements are activated directly by spinal cord stimulation. *Neuromodulation* **5**, 25-31.
- Hultborn H, Conway BA, Gossard JP, Brownstone R, Fedirchuk B, Schomburg ED, Enriquez-Denton M & Perreault MC (1998). How do we approach the locomotor network in the mammalian spinal cord? In *Neural Mechanisms for Generating Locomotor Activity. Ann N Y Acad Sci Vol. 860*, ed. Kiehn O, Harris-Warrick RM, Jordan LM, Hultborn H & Kudo N, pp. 70-82. New York Academy of Sciences, New York.
- Hunter JP & Ashby P (1994). Segmental effects of epidural spinal cord stimulation in humans. *J Physiol* **474**, 407-419.
- Ishizuka N, Mannen H, Hongo T & Sasaki S (1979). Trajectory of group Ia afferent fibers stained with horseradish peroxidase in the lumbosacral spinal cord of the cat: three dimensional reconstructions from serial sections. *J Comp Neurol* **186**, 189-211.
- Jilge B, Minassian K, Rattay F, Pinter MM, Gerstenbrand F, Binder H & Dimitrijevic MR (2004). Initiating extension of the lower limbs in subjects with complete spinal cord injury by epidural lumbar cord stimulation. *Exp Brain Res* **154**, 308-326.
- Lang J (1984a). Morphologie und funktionelle Anatomie der Lendenwirbelsäule und des benachbarten Nervensystems - 1. Rückenmark. In *Neuroorthopädie 2 - Lendenwirbelsäulenerkrankungen mit Beteiligung des Nervensystems*, ed. Hohmann D, Kügelgen B, Liebig K & Schirmer M, pp. 3-9. Springer, Berlin.
- Lang J (1984b). Morphologie und funktionelle Anatomie der Lendenwirbelsäule und des benachbarten Nervensystems - 2. Fila radicularia - Cauda equina. In *Neuroorthopädie 2 - Lendenwirbelsäulenerkrankungen mit Beteiligung des Nervensystems*, ed. Hohmann D, Kügelgen B, Liebig K & Schirmer M, pp. 9-11. Springer, Berlin.
- Lehmkuhl D, Dimitrijevic MR & Renouf F (1984). Electrophysiological characteristics of lumbosacral evoked potentials in patients with established spinal cord injury. *Electroencephalogr Clin Neurophysiol* **59**, 142-155.
- Lloyd DPC (1943). Reflex action in relation to pattern and peripheral source of afferent stimulation. *J Neurophysiol* **16**, 111-120.
- Magladery JW, Porter WE, Park AM & Teasdall RD (1951). Electrophysiological studies of nerve and reflex activity in normal man. *Bull John Hopkins Hosp* **88**, 499-519.
- Maertens de Noordhout A, Rothwell JC, Thompson PD, Day BL & Marsden CD (1988). Percutaneous electrical stimulation of lumbosacral roots in man. *J Neurol Neurosurg Psychiatry* **51**, 174-181.
- Minassian K, Rattay F & Dimitrijevic MR (2001a). Features of the reflex responses of the human lumbar cord isolated from the brain but during externally controlled locomotor activity. *Proceedings of the World Congress on Neuroinformatics. Vienna, Austria; Part II*, pp 267-268.

- Minassian K, Rattay F, Pinter MM, Murg M, Binder H, Sherwood A & Dimitrijevic MR (2001*b*). Effective spinal cord stimulation (SCS) train for evoking stepping locomotor movement of paralyzed human lower limbs due to SCI elicits a late response additionally to the early monosynaptic response. *Soc Neurosci Abstr*; 27: Program No. 935.12.
- Minassian K, Jilge B, Rattay F, Pinter MM, Gerstenbrand F, Binder H & Dimitrijevic MR (2002). Effective spinal cord stimulation (SCS) for evoking stepping movement of paralyzed human lower limbs: study of posterior root muscle reflex responses. *Proceedings of the 7th Annual Conference of the IFEES*. Ljubljana, Slovenia, pp167-169.
- Minassian K, Jilge B, Rattay F, Pinter MM, Binder H, Gerstenbrand F & Dimitrijevic MR (2004). Stepping-like movements in humans with complete spinal cord injury induced by epidural stimulation of the lumbar cord: Electromyographic study of compound muscle action potentials. *Spinal Cord* May 4 [Epub ahead of print].
- Murg M, Binder H & Dimitrijevic MR (2000). Epidural electric stimulation of posterior structures of the human lumbar spinal cord: 1. muscle twitches - a functional method to define the site of stimulation. *Spinal Cord* 38, 394-402.
- Panjabi MM, Takata K, Goel V, Federico D, Oxland T, Duranceau J & Krag M (1991). Thoracic human vertebrae. Quantitative three-dimensional anatomy. *Spine* 16, 888-901.
- Panjabi MM, Goel V, Oxland T, Takata K, Duranceau J, Krag M & Price M (1992). Human lumbar vertebrae. Quantitative three-dimensional anatomy. *Spine* 17, 299-306.
- Pinter MM, Gerstenbrand F & Dimitrijevic MR (2000). Epidural electrical stimulation of posterior structures of the human lumbosacral cord: 3. Control of spasticity. *Spinal Cord* 38, 524-531.
- Rattay F, Minassian K & Dimitrijevic MR (2000). Epidural electrical stimulation of posterior structures of the human lumbosacral cord: 2. quantitative analysis by computer modeling. *Spinal Cord* 38, 473-489.
- Saifuddin A, Burnett SJ & White J (1998). The variation of position of the conus medullaris in an adult population. A magnetic resonance imaging study. *Spine* 23, 1452-1456.
- Shealy CN, Mortimer JT & Reswick JB (1967). Electrical inhibition of pain by stimulation of the dorsal columns: preliminary clinical report. *Anesth Analg* 46, 489-491.
- Sherwood AM, McKay WB & Dimitrijevic MR (1996). Motor control after spinal cord injury: Assessment using surface EMG. *Muscle Nerve* 19, 966-979.
- Smith MC & Deacon P (1984). Topographical anatomy of the posterior columns of the spinal cord in man. The long ascending fibers. *Brain* 107, 671-698.
- Struijk JJ, Holsheimer J, van der Heide GG & Boom HB (1992). Recruitment of dorsal columns fibers in spinal cord stimulation: Influence of collateral branching. *IEEE Trans Biomed Eng* 39, 903-912.
- Struijk JJ, Holsheimer J & Boom HB (1993*a*). Excitation of dorsal root fibers in spinal cord stimulation: A theoretical study. *IEEE Trans Biomed Eng* 40, 632-639.
- Struijk JJ, Holsheimer J, Barolat G, He J & Boom HBK (1993*b*). Paresthesia thresholds in spinal cord stimulation: a comparison of theoretical results with clinical data. *IEEE Trans Rehabil Eng* 1, 101-108.

Struijk JJ, Holsheimer J, Spincemaille GH, Gielen FL & Hoekema R (1998). Theoretical performance and clinical evaluation of transverse tripolar spinal cord stimulation. *IEEE Trans Rehabil Eng* **6**, 277-285.

Sunderland S (1976). Avulsion of nerve roots. In *Handbook of Clinical Neurology*, ed. Vinken PJ & Bruyn GW, pp. 396-435. North Holland, Amsterdam.

Troni W, Bianco C, Moja MC & Dotta M (1996). Improved methodology for lumbosacral nerve root stimulation. *Muscle Nerve* **19**, 595-604.

Wall EJ, Cohen MS, Abitbol JJ & Garfin SR (1990). Organization of intrathecal nerve roots at the level of the conus medullaris. *J Bone Joint Surg* **72**, 1495-1499.

Waltz JM (1998). Chronic stimulation for motor disorders. In *Textbook for Stereotactic and Functional Neurosurgery*, ed. Gildenberg PL & Tasker RR, pp. 1087-1099. McGraw-Hill, New York.

Zhu Y, Starr A, Haldeman S, Chu JK & Sugerman RA (1998). Soleus H-reflex to S1 nerve root stimulation. *Electroencephalogr Clin Neurophysiol* **109**, 10-14.

Chapter 3

Stepping-like movements in humans with complete spinal cord injury induced by epidural stimulation of the lumbar cord: Electromyographic study of compound muscle action potentials

Summary

It has been previously demonstrated that sustained non-patterned electrical stimulation of the posterior lumbar spinal cord from the epidural space can induce stepping-like movements in subjects with chronic, complete spinal cord injury. In the present paper we explore physiologically related components of electromyographic (EMG) recordings during the induced stepping-like activity. The aim is to obtain a better understanding of how the intrinsic organization of human spinal networks is controlled by external stimulation.

The study is based on the assessment of epidural stimulation to control spasticity by simultaneous recordings of the EMG activity of quadriceps, hamstrings, tibialis anterior and triceps surae. We examined induced muscle responses to stimulation frequencies of 2.2–50 Hz in ten subjects classified as having a motor complete spinal cord injury (ASIA A and B). We evaluated stimulus-triggered time windows 50 ms in length from the original EMG traces. Stimulus-evoked compound muscle action potentials (CMAPs) were analyzed with reference to latency, amplitude, and shape. Epidural stimulation of the posterior lumbosacral cord recruited lower limb muscles in a segmental-selective way, which was characteristic for posterior root stimulation.

Stimulation at 2.2 Hz elicited stimulus-coupled CMAPs of short latency which were approximately half that of phasic stretch reflex latencies for the respective muscle groups. EMG-amplitudes were stimulus-strength dependent. Stimulation at 5–15 and 25–50 Hz elicited sustained tonic and rhythmic activity, respectively, and initiated lower limb extension or stepping-like movements representing different levels of muscle synergies. All EMG responses, even during burst-style phases, were composed of separate stimulus-triggered CMAPs with characteristic amplitude modulations. During burst-style phases, a significant increase of CMAP latencies by about 10 ms was observed.

We conclude, that the muscle activity evoked by epidural lumbar cord stimulation as described in the present study was initiated within the posterior roots. These Posterior Roots Muscle Reflex Responses (PRMRRs) to 2.2 Hz stimulation were routed through monosynaptic pathways. Sustained stimulation at 5–50 Hz engaged central spinal PRMRR components. We propose that repeated volleys delivered to the lumbar cord via the posterior roots can effectively modify the central state of spinal circuits by temporarily combining them into functional units, generating integrated motor behavior of sustained extension and rhythmic flexion/extension movements. This study opens the possibility for developing neuroprostheses for activation of inherent spinal networks involved in

generating functional synergistic movements using a single electrode implanted in a localized and stable region.

INTRODUCTION

There is definite evidence that the spinal cord of lower vertebrates has autonomous capabilities to produce basic coordinated patterns of locomotion, whether in swimming of fish or walking of terrestrial animals in the absence of input from higher levels of the central nervous system or from peripheral feedback (Grillner, 1981; Rossignol, 1996). The existence of spinal stepping generators in humans is more difficult to demonstrate and evidence is, by necessity, indirect (Illis, 1995). Bussel and colleagues discussed that some elements of the spinal circuitry on which the generation of stepping rhythms relies in lower vertebrates also exist in man (Roby-Brami & Bussel, 1987; Bussel *et al.* 1996). Calancie and colleagues (1994) investigated involuntary stepping-like movements in a subject with chronic incomplete spinal cord injury (SCI). They concluded that the automatic movement patterns were affected by a preserved but extremely limited supraspinal facilitation and an abnormal afferent inflow from the subject's hip, where they found evidence of pathology. Gurfinkel and colleagues (1998) used tonic peripheral afferent stimulation to elicit involuntary stepping in non-paraplegic individuals. They found that continuous lower limb muscle vibration gave rise to involuntary locomotion-like movements in suspended legs and suggested that the non-specific afferent input induced by vibration activated central structures governing stepping movements.

When epidural spinal cord stimulation became a clinical method to control severe spasticity in chronic spinal cord injured individuals (Dimitrijevic *et al.* 1986 *a,b*; Barolat *et al.* 1995; Pinter *et al.* 2000), it provided a neurophysiological technique to deliver tonic input to the human spinal cord deprived of supraspinal influence, and to examine locomotor capabilities of the lumbar cord (Rosenfeld *et al.* 1995; Gerasimenko *et al.* 1995).

In a clinical program of restorative neurology we evaluated the optimal site and parameters of spinal cord stimulation (SCS) for control of spasticity and thereby applied stimulation strengths from 1–10V at frequencies from 2.2–100 Hz and tested different contact combinations of an epidurally placed electrode array (Pinter *et al.* 2000). In the course of the evaluation procedure we discovered that the electrical stimulation of the posterior structures of the lumbar spinal cord could initiate and maintain rhythmic stepping-like flexion/extension movements of the subject's paralyzed limbs. To illustrate our findings in this initial study, we chose recorded electromyographic (EMG) activity of agonist-antagonist muscles of thigh and leg that lasted for 30 s without changes in the rhythmical patterns (Dimitrijevic *et al.* 1998*a*).

In the present paper we investigate the nature of these responses. We sought to reveal whether the EMG patterns recorded during induced stepping-like activity could be decomposed into physiologically related components. To this end we extended the time scales of the analyzed EMG traces and examined stimulus-triggered time windows of 50 ms length. Responses to 2.2 Hz stimulation and pairs of stimuli were evaluated to identify which directly stimulated neural structures should be considered as inputs resulting in the recorded EMG activity. Responses to trains of electrical stimuli of 5–50 Hz were examined to learn how different pulse frequencies cause lumbar cord neurons to shape different types of sustained tonic or patterned rhythmical motor output.

We provide evidence that the flexion/extension movements evoked by epidural lumbar cord stimulation are initiated by immediate stimulation of the posterior roots. It will be demonstrated that during the different induced EMG-patterns and even during burst-style phases each pulse within the stimulus train triggered a separate compound muscle action potential (CMAP). The electrophysiological characteristics of these Posterior Roots Muscle Reflex Responses (PRMRRs) will be described.

We propose that lumbar interneuronal systems can respond to particular repetition rates of tonic afferent input by temporarily combining into functional networks, which modulate the transmitting pathways and amplitudes of the PRMRRs and thereby generate flexion/extension movements.

MATERIAL AND METHODS

Subjects

The retrospective analyses performed in this study are based on data collected while routinely conducting a clinical protocol for the evaluation of the optimal site and parameters of epidural spinal cord stimulation for spasticity control in subjects who were resistant to other treatment modalities. The effect of stimulation had been assessed by EMG recordings of muscle activity in the lower limbs. For the present study we selected recordings obtained in ten subjects who were neurologically classified as having a complete spinal cord lesion at the cervical or thoracic level with no motor functions below the lesion (ASIA A or B). Pertinent patient-related data are listed in Table 3.1.

Table 3.1 Demographic and clinical data

Subject No.	Sex	Born in	Accident in	Implantation of electrode in	Type of accident	Level of SCI	ASIA Class.
1	m	1977	1994	1999	Motorbike accident	C6	A
2	m	1973	1995	1998	Car accident	C4	A
3	m	1981	1996	1999	Car accident	C4	A
4	m	1973	1997	1998	Ski accident	C7	B
5	m	1978	1996	1999	Car accident	T10	B
6	f	1978	1994	1996	Car accident	T4	A
7	f	1975	1996	2000	Car accident	T6	A
8	m	1973	1996	1997	Car accident	T4	A
9	f	1965	1996	1998	Car accident	T5	A
10	m	1939	1994	1997	Fall accident	T7	A

At the time of data collection the subjects met the following criteria: (1) They were healthy adults with closed, post-traumatic spinal cord lesions; (2) all patients were in a chronic (more than 1 year post-onset) and stable condition; (3) no antispastic medication was being used; (4) the stretch and cutaneomuscular reflexes were preserved; (5) there was no

voluntary activation of motor units below the level of the lesion as confirmed by brain motor control assessment (Sherwood *et al.* 1996); while (6) surface recorded lumbosacral evoked potentials – used to assess the functions of the posterior structures and gray matter of the spinal cord below the level of the lesion – were present (Lehmkuhl *et al.* 1984; Beric, 1988).

To control their spasticity all subjects had an epidural electrode array implanted at some vertebral level ranging from T10 down to L1 (see “Stimulation and recording setup”). The position of the epidurally placed electrodes relative to the vertebral bodies was obtained from postoperative X-rays. The implantations as well as the clinical protocol to evaluate the optimal stimulation parameters were approved by the local ethics committee. All subjects gave their informed consent.

Stimulation and recording setup

Figure 3.1A illustrates the patient set-up used, according to the clinical protocol, for the evaluation of the optimal stimulation parameters for spasticity control. Stimulation was delivered via a quadripolar electrode array with cylindrical electrode design (PISCES-QUAD electrode, Model 3487A, MEDTRONIC, Minneapolis, MN, USA) placed in the dorsomedial epidural space at vertebral levels ranging from T10 to L1 (left side of Fig. 3.1A). The data analyzed in the present study was recorded when the electrode array was operated as a bipolar electrode, the most rostral and caudal electrode contacts being connected to the positive and negative outputs, respectively, of the implanted pulse generator (ITREL 3, Model 7425, MEDTRONIC). The separation of the two active electrode contacts was 27 mm. The bipolar impedance was generally about 1000 Ω . The stimulus pulses were biphasic and actively charge balanced. The first dominant phase was about rectangular with a width of 210 μ s, the amplitude in the second phase was small and irrelevant to the stimulation process. Thus, stimulation was virtually monophasic and the stimulating effect of the epidural electrode was based on its polarity during the first dominant phase. Cathodal stimulation of spinal neural structures is known to result in lower thresholds than anodal stimulation. For posterior root fibers, calculated thresholds for cathodal excitation are about three times lower than anodal thresholds (Struijk *et al.* 1993; Holsheimer, 2002). Reversing the polarity of the bipolar epidural electrode shifted the effective cathode site to a different rostrocaudal level. Thus, setting the electrode polarity allowed for stimulation of posterior structures of the spinal cord at different segmental levels with a single epidural electrode array – given by the cathode site. The maximum stimulation strength was 10 V.

To verify the effect of spinal cord stimulation, electromyographic activity of quadriceps, hamstring, tibialis anterior, and triceps surae was recorded with silver-silver chloride surface electrodes (right side of Fig. 3.1A). Additional surface electrodes were placed over the lumbar paraspinal trunk muscles. Stimulus artifacts captured by this recording electrode allowed the identification of the onsets of applied voltage pulses. The bipolar surface electrodes were placed centrally over the muscle bellies spaced 3 cm apart and oriented along the long axis of the muscles. The skin was slightly abraded such that an electrode impedance of less than 5 k Ω was reached. The EMG signals were amplified with the Grass 12D-16-OS NEURODATA ACQUISITION SYSTEM (GRASS INSTRUMENTS, Quincy, MA) adjusted to a gain of 2000 over a bandwidth of 30–1000 Hz and digitized at 2048 samples/s/channel using a CODAS ADC system (DATAQ INSTRUMENTS, Akron, OH). The EMG data was analyzed off-line using WINDAQ Waveform Browser playback software (DATAQ INSTRUMENTS).

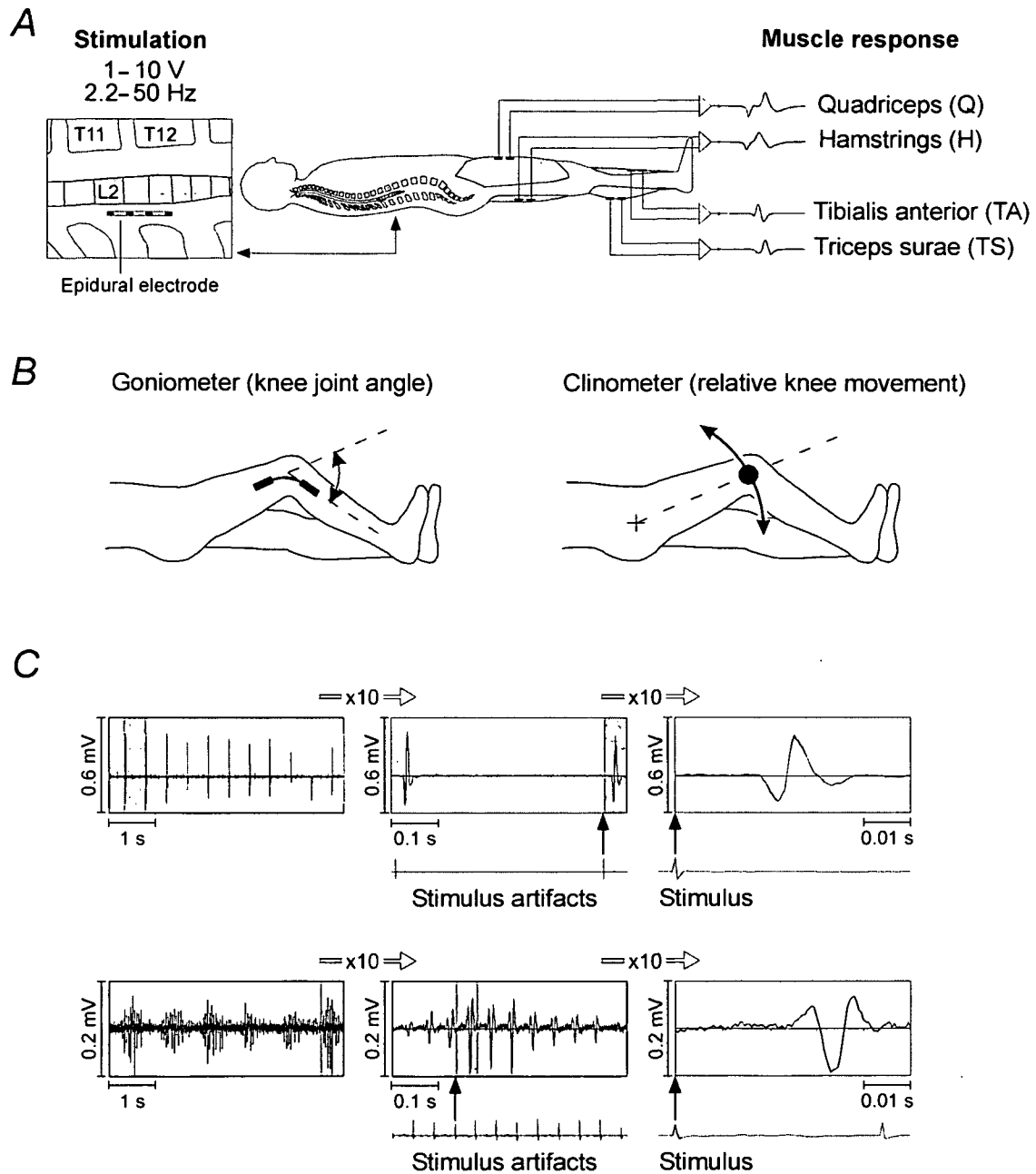


Figure 3.1 Outline of the clinical assessment design and analysis of stimulus-evoked EMG responses

A, all recordings were conducted with the patients in a comfortable supine position. Pairs of surface EMG electrodes were placed over the bellies of the lower limb muscle groups to assess the effects of epidural stimulation. *B*, to monitor relative movements of the lower limbs, goniometers or clinometers were applied bilaterally to the knee. *C*, EMG responses of triceps surae to epidural stimulation at 2.2 Hz (top) and 22 Hz (bottom) displayed with different time scales. Potentials marked by gray backgrounds are shown in extended time scale ($\times 10$) on the right side of the original EMG. 10-second traces of EMG responses are displayed in the left column. In the middle column it is shown that stimulus artifacts (recorded by paraspinal-surface electrodes) allow the identification of the onsets of applied voltage pulses. In the right column EMG potentials of separate responses can be seen. These CMAPs were analyzed for latencies, peak-to-peak amplitudes, and shapes irrespective of the stimulation amplitude or frequency.

One of two different sensor types was used to record knee movement, namely goniometers (Model XM-180, and K100 AMPLIFIER SYSTEM, PENNY & GILES BIOMETRICS LTD.) or electronic clinometers (ACCUSTAR, LUCAS SENSING SYSTEMS, Phoenix, AZ) both attached bilaterally to the knee. The goniometer measured relative changes in the knee joint angle as illustrated in the left side of Fig. 3.1B. The clinometer measured rotations about its axis and thus rotations of the longitudinal axis of the thigh around the hip.

All recordings were conducted with the subjects placed on a comfortable examination table covered with soft sheepskin in a supine position. This configuration allowed flexion/extension movements of the lower limbs to unfold smoothly and minimized friction between the heel and the supporting surface.

Data analysis – Data based on incremental pulse amplitudes

The first set of EMG data had originally been collected to define the rostrocaudal level of the epidural electrode relative to the lumbosacral cord segments based on muscle twitch recruitment patterns (Murg *et al.* 2000). For this purpose a frequency of 2.2 Hz was used, and the stimulation strength was intensified in 1-Volt increments from 1 to 10 V.

In the present study we examined the relationship between the rostrocaudal position of the cathode relative to the spinal cord and the sequence of quadriceps and triceps surae activation. The vertebral cathode level was obtained from X-ray. The estimated, functional segmental level of the cathode was derived from a neurophysiological technique for electrode positioning in subjects with impaired sensory function (Murg *et al.* 2000). Additionally, information on average spatial relations between the cord segments and the vertebral bodies was used (Lang, 1984). The effect of two different rostrocaudal cathode sites were studied in all subjects but subject 4. The electrode array of subject 4 was repositioned a number of times during participation in the clinical program. This allowed comparison of stimulation with six different cathode sites located between the upper third of the T10 and the upper L1 vertebra in a single subject.

The recruitment sequence of quadriceps and triceps surae was given by the whole-numbered threshold voltages for the respective muscles. Only quadriceps and triceps surae were considered in this analysis, because they are muscle groups with separate segmental innervations (L2–L4 vs. L5–S2).

We examined single stimulus-evoked and surface-recorded CMAPs for latencies (quantitatively), peak-to-peak amplitudes, and shapes (qualitatively) of the same data set. The latencies were read off-line from the EMG traces using the playback software and measured as the time between stimulation onset – identified by stimulus artifacts – and the first deflection of the EMG-potential from baseline (Fig. 3.1C, top). Mean latency times based on all subjects were calculated for the threshold stimulus strengths eliciting responses in each muscle group and for the maximum strengths applied.

Data analysis – Data based on incremental pulse frequencies

The second set of EMG data that we analyzed had originally been collected to assess the effect of trains of 5–100 Hz stimuli on spasticity (Pinter *et al.* 2000). These data were used to evaluate the refractory periods of responses to pairs of stimuli delivered at intervals of 200 to 10 ms, based on the first two stimuli of the applied trains.

Furthermore we examined the muscle activity induced by sustained trains of 1–10 V and 5–50 Hz, focusing on the effects of different repetition rates of stimulation on the evoked motor output patterns. To reveal the components of the overall EMG pattern we subsequently enlarged the time scale of the EMG traces. We addressed the question of how far individual responses to single pulses within the applied stimulus train were reflected in the EMG output pattern. Separate successive EMG responses were analyzed for latencies (quantitatively), peak-to-peak amplitudes, and shapes (qualitatively) (Fig. 3.1C, bottom).

RESULTS

Epidurally evoked segmental twitch responses

Electrical stimulation of the lumbosacral cord delivered from the dorsomedial epidural space at 2.2 Hz and 1–10 V gave rise to stimulus-coupled CMAPs in the lower limb muscles. Figure 3.2A shows successively elicited single CMAPs of quadriceps and triceps surae muscles, induced by stimulation with 3–7 V and 2.2 Hz (subject 3). The effective cathode was located at the center level of the T12 vertebral body, the estimated segmental level was L3/L4. Stimulus-triggered time windows of 50 ms in length were extracted from the originally continuous EMG-traces (see also Fig. 3.1C). The left margins of the windows are determined by the onsets of the stimuli. EMG-responses to ten consecutive stimuli are shown for each incremental voltage. In the presented case CMAPs were not induced in the lower limb muscle groups at SCS strengths of 1–2 V. At 3 V CMAPs with short (9.5 ms) and constant latencies were recorded from quadriceps, while triceps surae showed no activity. At 4 V quadriceps showed higher CMAP amplitudes than at 3 V while the latencies remained unchanged. Faint activity was also observed for triceps surae at 4 V, involving latencies of 18.5 ms. At higher stimulation strengths CMAP amplitudes further increased for both muscle groups. The latencies of successive responses remained constant, while no additional components with longer latencies emerged in the EMG-traces at higher stimulus strengths. For a given stimulus strength, amplitudes of successive CMAP showed only minor and unsystematic variations. The demonstrated muscle recruitment sequence was representative for cathodes positioned at the level of the T12 vertebral body.

As shown in Fig. 3.2B, this recruitment pattern was essentially reversed when the effective cathode was located at the lower third of the L1 vertebral body, corresponding to the average position of the conus medullaris. Ten CMAPs are displayed sequentially for incremental stimulus strengths of 4–8 V (subject 5). At the threshold level of 4 V, CMAPs with a latency of 18.5 ms and rather large amplitudes were evoked in triceps surae. The CMAP amplitudes showed progressive increases with increasing stimulus strength until a plateau of EMG activity was reached at 7 V. Weak quadriceps responses with a latency of 10.5 ms was initiated at a strength of 5 V. Quadriceps CMAPs with only moderate amplitudes were evoked even at increased stimulus strength.

Figure 3.2 demonstrates a strong relationship between the rostrocaudal position of the cathode relative to the spinal cord and the sequence of quadriceps and triceps surae activation. In subjects with cathodes located at the T11 vertebral level, rather strong stimulation amplitudes (6–9 V) were needed to elicit CMAPs in the quadriceps muscle, while triceps surae could not be activated even at the maximum strength of 10 V (subjects 4, 6, 9). Note that on average the T11 vertebral level corresponds to the L1 and L2 segmental levels, while the levels L5–S2 are situated well below this rostrocaudal position.

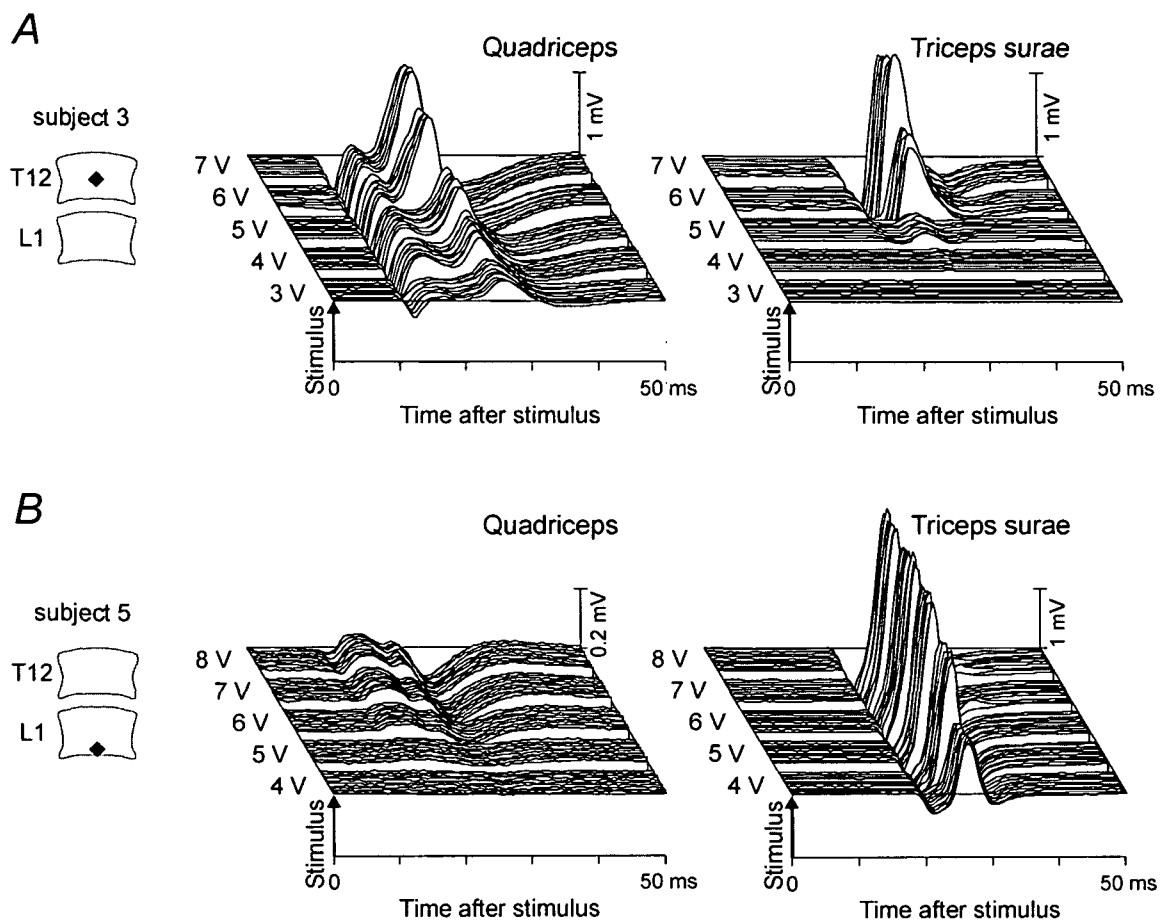


Figure 3.2 EMG responses to 2.2 Hz stimulation

Stimulus-triggered raster presentation of CMAPs induced in quadriceps and triceps surae. The first 50 ms following each stimulus pulse are shown. *A*, the effective cathode was located at the center level of the T12 vertebral body, which approximately corresponds to L3/L4 segmental level (subject 3). The stimulation strength was increased in steps of 1 V. Ten single EMG potentials of successive muscle responses are shown for each incremental voltage (3–7 V). *B*, effective cathode site was at the lower level of the L1 vertebra, corresponding to the level of the conus medullaris (subject 5). Ten stimulus-evoked CMAPs are displayed for each incremental voltage (4–8 V).

The lower third of the T10 vertebral body was the most rostral position from which lower limb muscle responses could be evoked at a stimulation strength of 10 V – in fact solely in the thigh muscles. From the upper third of the T10 vertebral body none of the studied lower limb muscles could be activated with strengths up to 10 V, though the lumbar paraspinal trunk muscles responded at a threshold of 5 V (subject 4).

EMG-data derived from subject 4 during epidural stimulation with considerably different rostrocaudal positions of the effective cathode (see methods) allowed us to reveal any relationship between the segmental cathode level and the response latencies. When the cathode was at the lower third of the T10 vertebral body, CMAPs elicited in quadriceps and hamstrings at threshold level had mean latencies of 9.8 ms and 10.3 ms, respectively. When the cathode was repositioned caudally by 7 cm to the upper L1 vertebral level, the latencies were 9.5 ms and 10.0 ms. Considering that the accuracy of identification of the latencies was 0.25 ms at best, no significant correlation between rostrocaudal cathode position and

response latencies could be demonstrated. Therefore we calculated the average response latencies from the data derived from all subjects irrespective of the positions of their epidurally placed electrodes for quadriceps, hamstrings, tibialis anterior and triceps surae for 2.2 Hz stimulation. The mean latency times for these muscle groups at threshold level and maximum applied stimulation strength (generally 8–10 V) are compiled in Table 3.2 and were about 9–10 ms for the thigh muscles and 16–17 ms for the distal leg muscles. Note that the weak responses induced at threshold stimulation had low CMAP amplitudes and slight onset slopes of the potentials, thus making the precise identification of the onset of the CMAPs difficult. This may account for the longer latencies of muscle responses at threshold level in Table 3.2.

Table 3.2 Mean latencies (ms \pm SD) of CMAPs evoked by 2.2 Hz stimulation based on all subjects at threshold and maximum stimulation strength

	Threshold	Maximum
Q	9.3 \pm 1.6	8.6 \pm 0.9
H	9.9 \pm 1.3	9.3 \pm 0.8
TA	16.4 \pm 2.1	16.1 \pm 1.6
TS	16.7 \pm 1.5	16.3 \pm 1.4

To summarize, 2.2 Hz stimulation of the posterior structures of the lumbosacral cord elicited twitch responses in the lower limb muscles in a segmental-selective way (Fig. 3.2). The EMG signals associated with these responses were stimulus coupled and of short latency (Table 3.2) – approximately half that of the phasic stretch reflexes of the respective muscle groups. Equal-voltage stimuli yielded only negligible variations in CMAP amplitudes and shapes. Thus, successive responses to the stimulus train of a given muscle demonstrated no mutual influence. Responses of a muscle were not influenced by the ongoing activity of responses of the other muscles to the same stimulus pulse. For a given cathode position the CMAP amplitudes elicited at 2.2 Hz were dependent on the stimulus strength.

Stimulation with pairs of stimuli

While equal-voltage stimuli at 2.2 Hz yielded EMG responses with similar amplitudes (Fig. 3.2), different patterns emerged when pulses were applied in close succession. First we analyzed CMAPs induced by pairs of stimuli of equal strength delivered to the posterior structures of the lumbosacral cord at different intervals.

Figure 3.3 shows a representative example of responses to pairs of stimuli with different interstimulus intervals (ISI) derived from the quadriceps muscle (subject 1). Arrows mark the onsets of stimulus pulses. The stimulus strength of the pairs of stimuli was increased in steps of 1 V from threshold level (4 V, top row) to 50% higher voltages (6 V, bottom row). The first stimulus evoked a pronounced CMAP regardless of the interstimulus intervals and can be considered as a control response. At 4 V the second stimulus applied after an interstimulus time of 56 ms only evoked a weak response. The CMAP amplitude of this test response was 7% of the control response magnitude. At the same interstimulus time, but higher strengths of epidural stimulation the second stimulus was capable of inducing a

CMAP with an amplitude nearly as large as the first one. At a stimulus strength of 4 V and an interstimulus interval of 20 ms, the second pulse completely failed to elicit a muscle response, while a second response occurred again when the stimulus voltage was increased.

Thus, the refractory behavior of epidurally evoked muscle responses to pairs of stimuli did not only depend on the interstimulus interval but also on the stimulation strength. At threshold level we found long refractory periods of up to 47.5 ms (subject 1) and even 62.5 ms (subject 3). The shorter the interstimulus intervals were, the lower were the test response magnitudes, with 20 ms being the earliest point for the second stimulus to result in unequivocal CMAPs. At intervals shorter than 20 ms the presence of the final deep positive potential of the first CMAP introduced difficulties in interpreting the decrease in amplitude of the second response.

Figure 3.3 demonstrated that a single stimulus pulse and the corresponding response has long-lasting, stimulus-strength dependent conditioning effects on the excitability of the activated structures.

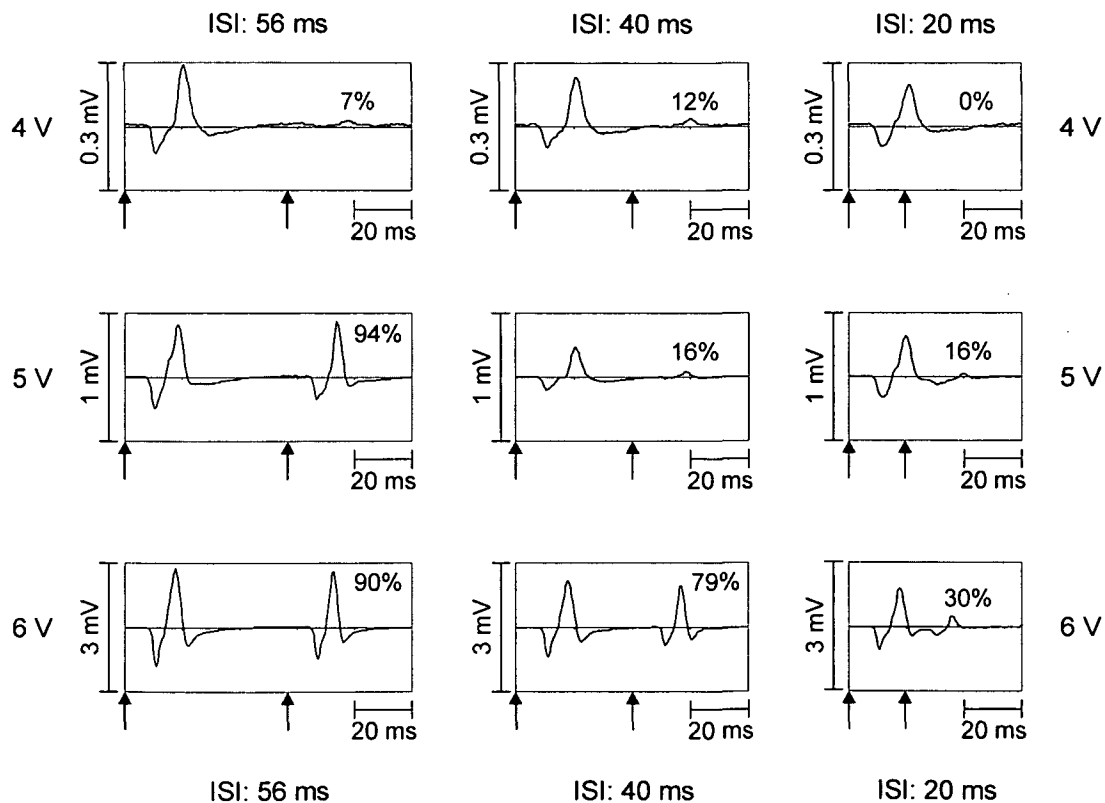


Figure 3.3 EMG potentials of quadriceps (subject 1) induced by pairs of stimuli delivered at different intervals and stimulation strengths

The arrows indicate the onset of each stimulus pulse. Interstimulus intervals (ISI) of 56 ms (18 Hz), 40 ms (25 Hz) and 20 ms (50 Hz) were tested. Stimulation strength was increased from threshold level (4 V) to 150% of the threshold (6 V) in steps of 1 V. The percentage value in each box gives the EMG amplitude of the second response relative to the first response.

Stimulation with trains of stimuli

Figure 3.4*A* displays EMG recordings and goniometer traces derived from subject 7 during stimulation at 6 Hz (*i*) and 31 Hz (*ii*) without departing from the same sustained and non-patterned mode of input application to the same spinal cord level. Stimulation strength was 10 V, the estimated functional segmental level of the cathode was L3/L4. At the onset of the recordings shown on the left side, the subject's lower extremities had been passively moved to the point of maximum possible flexion, and stimulation was subsequently applied at 6 Hz. The sustained stimulation initiated and maintained an extension movement of the lower limbs. The recruited muscles were visibly contracting briefly, with the tonic EMG output in hamstrings and triceps surae being greater than in their antagonists. During the actual extension movement unfolding from the initially flexed position of the lower limbs the EMG pattern revealed well-defined temporal modulations that were directed toward knee joint stabilization. Thereby the EMG activity in hamstrings progressively decreased while the one in quadriceps increased. When the endpoint of the movement was reached, and the stimulation was sustained, the limbs remained in the extended position, with the muscles visibly contracting. When the electrical stimulation was turned off, the lower limb muscles relaxed immediately.

We studied this finding that epidural stimulation of the human lumbar cord isolated from brain control can induce a sustained extension of the lower extremities in more detail in five of our subjects (subjects 2, 4, 6, 7, 9). Stimulation at 5–15 Hz and 6–10 V applied to the lumbar cord reproducibly elicited the characteristic temporal pattern of EMG-amplitude relations between antagonistic muscles and led to lower limb extension in all five subjects. The induced extension pattern was observed in different trials. The consistency of this finding only depended on application of the appropriate stimulus parameters.

On the right side of the Fig. 3.4*A* it is demonstrated that by increasing the frequency of the stimulus train to 31 Hz, the previous modulated-tonic EMG activity was replaced by a rhythmical one (*ii*). The EMG recording revealed alternating phases of burst-style activity in the recruited lower limb muscles. While this is not the best example of an induced stepping-like activity (co-activation of TA and TS), both recordings (*i*) and (*ii*) were made during a single session in the same subject without changing the site or strength of stimulation. From this observation it was clear that the spinal cord isolated from supraspinal input was capable of shaping both a motor output with extensor muscles dominating over the flexors and rhythmical reciprocal activation of flexors and extensors in response to sustained stimulation. The stimulation frequency determined which type of induced motor activity was established.

The finding that epidural lumbar cord stimulation can generate stepping-like EMG activity was studied in our pool of subjects. Stepping-like, alternating flexion/extension movements in the lower limbs were repetitively initiated in different recording sessions, which were up to several months apart in a given subject and also in different subjects. Optimal parameter settings were 25–50 Hz and 6–10 V. The cathode site had to provide a dominant stimulation of the upper lumbar cord. Lower thresholds for recruitment of quadriceps than of triceps surae characterized such a location (see Fig. 3.2*A*). Moreover strengths had to be above the level for eliciting CMAPs in quadriceps as well as triceps surae for a given cathode location. Stimulation commonly induced unilateral stepping-like flexion/extension movements. Similarly, in about 2/3 of all analyzed cases in our subject pool, a unilateral muscle twitch distribution at threshold stimulation level was observed, indicating asymmetric position of the epidural electrode array relative to the spinal cord. Stepping-like

movements of the side associated with the lower thresholds were induced. The contralateral lower limb responded either with tonic activity or with synchronous burst-style co-activations of all studied muscles of this limb.

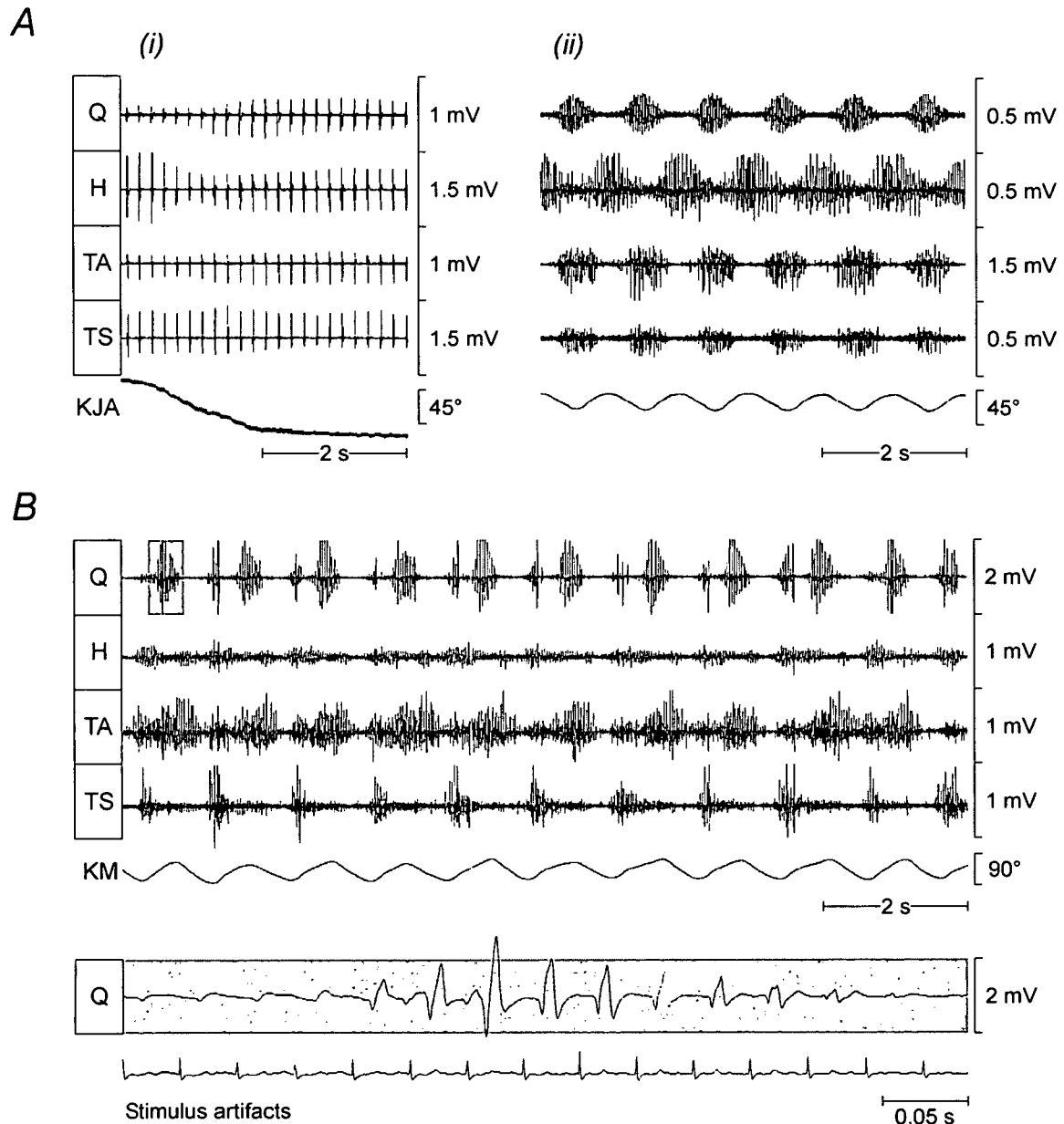


Figure 3.4 EMG responses to trains of stimuli showing characteristic modulations of CMAP-amplitudes

A, EMG recordings from quadriceps (Q), hamstrings (H), tibialis anterior (TA), and triceps surae (TS) during spinal cord stimulation at 6 Hz (*i*) and 31 Hz (*ii*). The goniometer traces (KJA – knee joint angle) illustrate the corresponding induced extension and rhythmical lower limb movements, respectively. The position of the cathode (estimated segmental level: L3/L4) and the stimulation strength (10 V) were left unchanged when switching frequencies. *B*, surface EMG recordings from the right Q, H, TA, and TS; position sensor trace demonstrating flexion/extension movements of the knee (KM). The segmental cathode level was at L4/L5. Stimulation parameters were 9 V and 30 Hz (subject 8). The first burst-style phase of Q marked by gray background is shown in extended time scale on the bottom of the original EMG along with stimulus artifacts captured by electrodes placed over the lumbar paraspinal trunk muscles.

During two seconds of recording shown in Fig. 3.4A(i), twelve separate CMAPs in each muscle were elicited (see the time marker). Thus, a single CMAP was elicited by each stimulus pulse of the 6 Hz-train which induced the characteristic EMG-extension pattern. These consecutively elicited separate CMAPs resulted in the small deflections superimposed on the overall trace of the goniometer recording in Fig. 3.4A(i). Figure 3.4B presents surface EMG recordings from the right quadriceps (Q), hamstrings (H), tibialis anterior (TA), and triceps surae (TS) and position sensor recordings showing knee flexion/extension movements (subject 8). The rostrocaudal cathode site was at the T12/L1 intervertebral level, the functional segmental level about L4/L5. Stimulation parameters were 9 V and 30 Hz. The EMG traces demonstrate alternating phases of burst-style activity in the lower limb flexor and extensor muscles. The corresponding position sensor trace confirms that the induced muscle activity led to actual stepping-like flexion/extension movements of the lower limb. Deflection up indicates flexion and deflection down indicates extension of the lower limb. The range of knee movement was about 65°.

At the bottom of Fig. 3.4B the first of the burst-style phases of quadriceps is displayed in extended time scale along with corresponding stimulus artifacts derived from the paraspinal muscle, which indicate the onsets of the stimulus pulses. It can be clearly seen that each pulse of the stimulus train triggered a single CMAP. Thus, the burst-style phase consisted of stimulus-triggered, separate CMAPs that were subject to well-defined amplitude modulations resulting in a burst-like shape of the EMG activity. Another example of this finding was demonstrated for triceps surae in Fig. 3.1C (bottom figure).

In Fig. 3.5 we compare the EMG features of single CMAPs in response to stimulation with different repetition rates and during different phases of induced rhythmic motor activity. Fig. 3.5A is a stimulus-triggered sequential presentation of CMAPs induced in tibialis anterior by sustained epidural stimulation (subject 1). All CMAPs were recorded during a single session. Stimulation strength was 5 V and constant when frequency was varied. The functional segmental cathode position was L3/L4 and identical in all cases. Ten successive CMAPs are shown for a given repetition rate. Stimulus trains with frequencies of 2.2, 11, and 16 Hz induced tonic EMG activity, whereas at 22 Hz a pattern with slow rhythmical amplitude modulations was evoked. CMAPs elicited at 2.2 Hz had a short, constant latency of 16 ms and rather similar shapes and amplitudes. CMAPs composing the activity in response to a ten times higher frequency of stimulation had a distinctly longer and fairly constant latency of 23 ms. The early negative and positive potential of the CMAPs induced at 2.2 Hz were absent, while additional EMG-components with longer latencies emerged. Analyzing the CMAPs constituting the tonic EMG patterns elicited at 11 Hz and 16 Hz revealed transitional stages between the “short-latency” response to 2.2 Hz stimulation and the “long-latency” response to 22 Hz stimulation. This becomes obvious when ten successively elicited CMAPs were averaged and compared (right side of Fig. 3.5A). By increasing the frequency from 2.2 Hz to 11 Hz, the “short-latency” response decreased in amplitude while small-amplitude late potentials were building up. At 16 Hz the early components of the CMAP were further attenuated and the late components further enhanced. Further decrease of the early components and a dominating contribution of the later ones lead to the CMAP shapes as seen in response to 22 Hz stimulation.

Figure 3.5B displays a continuous EMG of tibialis anterior responses showing three burst-style phases induced by stimulation with 7 V at 28 Hz (trace with corresponding right scale bar). The data is derived from subject 4. The displayed EMG activity is part of a recording of an epidurally induced flexion/extension movement of the lower limb. The burst-style

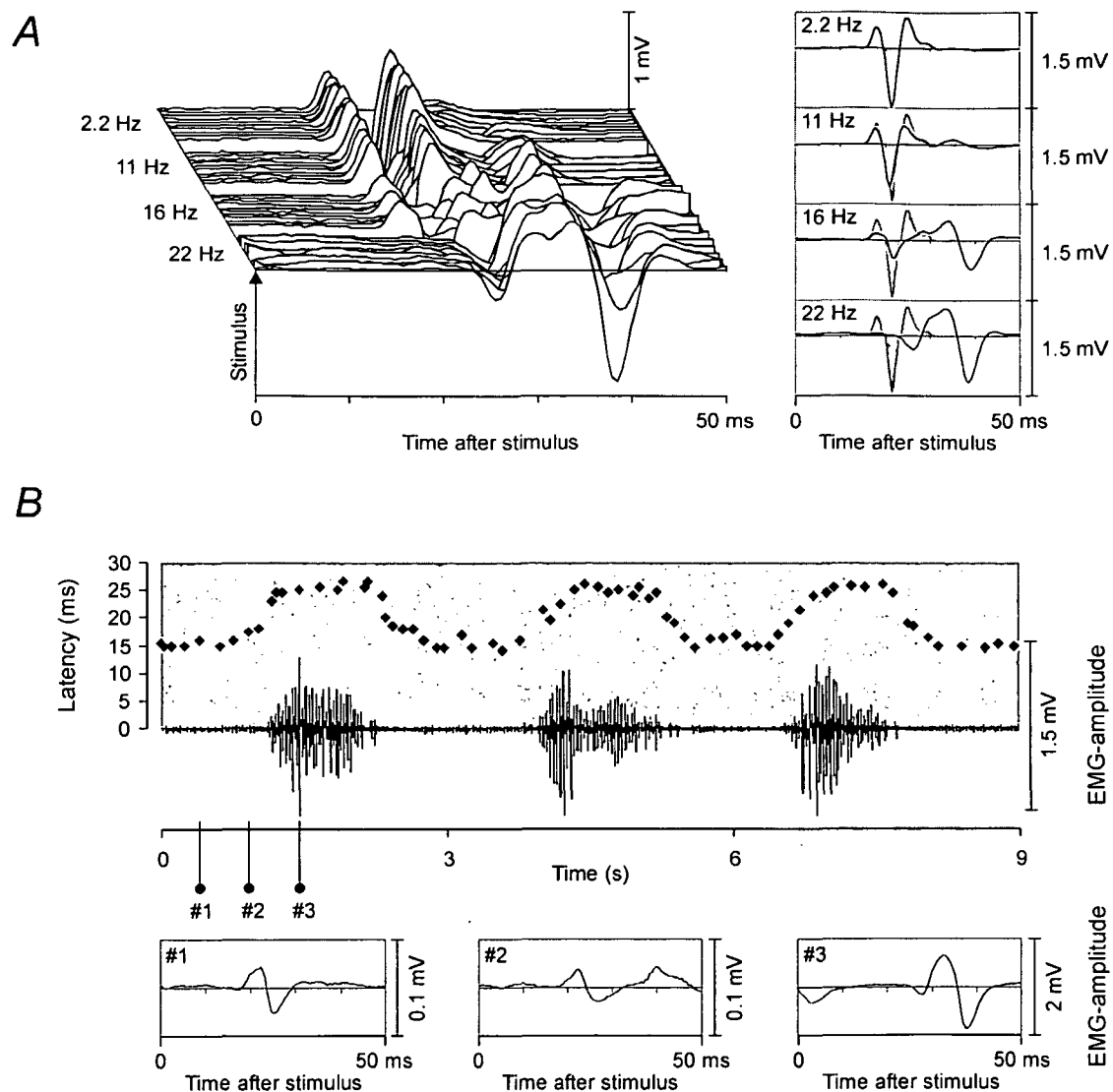


Figure 3.5 Changes of reflex pathways due to increased repetition rates of the sustained stimulation and during induced rhythmic EMG activity

A, Stimulus-triggered sequential presentation of CMAPs induced in tibialis anterior by epidural stimulation at a constant strength of 5 V but different frequencies (subject 1). Cathode position was identical in all cases. Ten single EMG potentials of successive muscle responses are shown for a given stimulation frequency. Averaged responses derived from the respective ten single responses are displayed on the right side of the figure. A template based on the response to 2.2 Hz stimulation is used to indicate changes of the CMAP shape when different frequencies were applied. *B*, Continuous EMG of tibialis anterior responses showing three burst-style phases induced by stimulation with 7 V at 28 Hz along with the latencies of identified separate CMAPs (subject 4). Three single CMAPs evoked before (#1 and #2) and during (#3) the first burst-style phase are displayed in extended time scale at the bottom of the figure.

phases alternated with phases of small amplitude responses allowing the identification of CMAP latencies during the different phases and the transitions between them. The measured latencies are indicated by black diamonds in the figure and are placed in accordance to the times the corresponding CMAPs were initiated (diagram with left scale bar and same abscissa as the EMG trace). The latencies are shown for every third/fourth

single stimulus-evoked CMAP (72 out of 243 successively evoked CMAPs within the displayed 9 s-trace). The missing data points did not differ from the presented relation. While the CMAP latencies were 15–17 ms during the phases with small amplitude responses, they increased significantly to 25–27 ms during the burst-style phases. Thus, CMAP amplitudes as well as latencies were subject to modulations during induced rhythmic activity. Three single EMG responses are presented in extended time scale showing characteristic CMAP shapes during the different phases of the rhythmic EMG activity at the bottom of the figure. The left margins of the 50 ms-time windows indicate when a stimulus was applied. The first CMAP (time marker #1) was elicited between two burst-style phases. It was of small amplitude and had a short latency of 16 ms. The third CMAP (#3) was the one with the largest amplitude during the first burst-style phase, where each pulse of the train elicited a separate CMAP. The displayed CMAP had a latency of 25 ms. Its shape was similar to the tibialis anterior CMAPs in response to 22 Hz depicted in Fig. 3.5A. Because the timeframe covering both the prolonged response latency and the CMAP duration is longer than the interstimulus interval (36 ms), the final negative potentials of the immediately preceding response is seen at the beginning of the time window (covering the first 10 ms). The second CMAP (#2) displayed in extended time scale was elicited between the two time markers #1 and #3 and incorporates both the component of the short latency CMAP and also additional later potentials.

We found that the short-latency CMAP as described in Fig. 3.2 was followed by later EMG components or was even completely replaced by a longer latency CMAP when stimulation frequencies of about 16 Hz or more were used. They were observed consistently when rhythmic EMG activity was induced in the lower extremities. Indeed, in different cases of epidurally evoked rhythmic EMG activity the pattern of CMAP latency prolongation was dissimilar. In some cases only the tibialis anterior muscle showed the longer latency response, in others tibialis anterior and triceps surae, or only the muscle groups functionally acting as flexors showed the longer latency responses. In some cases (subject 7) the stimulus-coupled CMAPs of all recorded lower limb muscles demonstrated prolonged latencies. Analyzing the basis of these differences was beyond the scope of this study. The longer CMAP latencies were prolonged by about 10 ms compared to the CMAPs elicited at 2.2 Hz. An example of a longer latency response induced in the triceps surae muscle was shown in Fig. 3.1C (bottom figure).

To summarize, we have shown that epidural stimulation applied to the same cord segments can evoke two distinct patterns of EMG activity in the lower limb muscles: (i) characteristically modulated tonic EMG activity appropriate to initiate and maintain extension of the lower extremities and (ii) burst-style EMG activity in flexors and extensors that appeared in appropriate sequences for rhythmic flexion and extension movement. Inducing these patterns was a function of different repetition rates of the applied train of electrical stimuli. Decomposing the EMG “interference patterns” into their fundamental physiologically related components was possible by extending the time scales of the analyzed EMG sequences. During the different induced EMG-patterns and even during burst-style phases each pulse within the stimulus train triggered a separate CMAP.

DISCUSSION

Directly stimulated structures which should be considered as inputs resulting in the CMAPs

We have shown that epidural stimulation can evoke different patterns of lower limb muscle activation. Inducing these patterns was a function of different repetition rates of the delivered sustained stimulation. At low frequency of 2.2 Hz amplitudes of stimulus-evoked CMAPs were determined by the stimulus strength. When the lower limbs were passively moved to the point of maximum possible flexion and trains of stimuli were applied at 5–15 Hz, an extension movement was induced and maintained (Jilge *et al.* 2001; Dimitrijevic *et al.* 2002; Jilge *et al.* 2004). Successively elicited CMAPs showed characteristic amplitude modulations with a stronger motor output of the extensor muscles than of the flexors. Stimulation at 25–50 Hz induced alternating burst-style EMG activity in flexors and extensors leading to stepping-like flexion/extension movements. Stimulation at even higher frequencies of 50–100 Hz decreased the muscle tone of the lower limbs (Pinter *et al.* 2000). These patterns could be elicited with a single cathode placed over the upper lumbar segmental levels without changes of position (Fig. 3.4A, (i) and (ii)). Which neural structures have directly been activated by the electrical stimulation resulting in the described muscle activities?

Direct activation of motoneurons – thus bypassing the spinal cord – can be ruled out because this could not account for the specific amplitude modulation of CMAPs during stimulation with constant parameters as presented in the Figs. 3.4 and 3.5. Moreover, CMAPs studied with pairs of stimuli had long refractory periods of up to 62.5 ms. In contrast, direct activation of ventral root motor fibers or motoneurons in the ventral horn follow a stimulus pulse train up to 100 Hz (Dimitrijevic, 1983; Struijk *et al.* 1993).

Due to the dorsomedial position of the epidural electrode the sensory afferents in the dorsal roots and their axonal branches in the dorsal columns are the largest fibers closest to the cathode. These “dorsal root fibers” and “dorsal column fibers” which are part of the same afferent fiber system are the most apparent among the various possible neural targets. Since it is unlikely that neurons or axons other than these are stimulated (Holsheimer, 2002) or contribute to the muscle activation (Hunter & Ashby, 1994), we will discuss if stimulation of dorsal roots or dorsal columns may explain the segmental-selective effect of the stimulation as described in Fig. 3.2. There we demonstrated different recruitment orders of the L2–L4 innervated quadriceps and the L5–S2 innervated triceps surae muscles depending on the rostrocaudal cathode position of the stimulating electrode array. L2–L4 segments had lower stimulation thresholds than L5–S2, when the cathode was at upper lumbar cord levels, while the situation was reversed when the cathode was located at the level of the conus medullaris.

The population of axons within the posterior columns at any spinal level arises from the posterior roots of numerous segments, both rostral and caudal to that level. Thus the effect of posterior column stimulation can be expected to be general rather than localized to afferents of any specific segmental origins. Hunter and Ashby (1994) reported that epidural stimulation of the posterior column at thoracic cord levels resulted in non-selective activation of motoneurons in thigh and leg muscles. Further indication that stimulation of posterior column fibers is not segmentally-selective comes from the application of spinal cord stimulation in chronic pain management basing on reports of the distribution of paresthesiae of patients with intact sensory functions. There, medially placed electrodes

elicit a widespread distribution of paresthesiae in body areas at the spinal level of stimulation and far caudally to it, even at the perception threshold (He *et al.* 1994). The widespread distribution of paresthesiae is attributed to activation of the posterior column fibers (Barolat *et al.* 1993).

The most rostral cathode levels from which CMAPs could still be induced at maximum pulse intensity (10 V) were T10/T11 vertebral levels for quadriceps and T11/T12 for triceps surae. The latencies of the CMAPs were approximately half that of the phasic stretch reflexes of the respective muscle groups (Table 3.2) and did not depend on the rostrocaudal level of the active cathode. Guru and colleagues (1987) and Hunter and Ashby (1994) reported recruitment of thigh and leg muscles by epidural stimulation with cathodes located at positions as rostral as the T8–T10 vertebral levels. At these cathode levels the cord segments and associated roots innervating the lower limbs and particularly the calf muscles are located well below the cathode. The latencies reported in these studies were generally about 6–12 ms longer than those of the comparable muscles compiled in our Table 3.2.

We conclude that the CMAPs described by us are not related to posterior column fiber activation. Thereby, our results do not contradict the findings of Guru *et al.* (1987) and Hunter and Ashby (1994). The differences of the effects of stimulation are most probably due to the different subject profiles, electrode setups and anatomical situation of the spinal cord and roots at the different levels of the epidurally placed electrodes. The subjects included in the above cited studies had spinal cord stimulators implanted for the treatment of pain. They had volitional control over the lower limb muscles. Moreover, four different electrode set-ups were utilized, in most cases a fine wire cathode with an uninsulated tip and a larger disc anode at the anterior abdominal wall or embedded in the paraspinal muscles. In such an electrode set-up, the surface area of the disc anode is much larger than the wire tip contact. This results in a smaller current density and less voltage drop near the anode. A larger portion of the total stimulation voltage is therefore available under the cathode, hence a stronger stimulating effect of this electrode set-up in the vicinity of the cathode. There are also significant differences in the anatomy of the thoracic and the lumbosacral spinal cord. Because of the disparity in length between the spinal cord and vertebral column, the spinal roots from lumbar and sacral segments have a much longer distance to travel prior to reaching their respective foramina of exit. Whereas cervical and upper thoracic rootlets and roots are situated nearly perpendicular to the cord, lower thoracic, lumbar, and sacral ones enter and leave the cord at increasingly more oblique angles. The entry points of lower lumbar and sacral posterior roots into the spinal cord are situated more medially than those of more rostral ones – and are thus nearer to a dorsomedially positioned cathode. Finally, most of the circumference of the lower lumbar and sacral cord is covered by the roots (Wall *et al.* 1990). For epidural stimulation, thresholds of fibers within the lumbosacral cord will presumably be increased due to this poorly conducting “root-layer”.

Geometric and electric factors result in low-threshold sites for electrical stimulation where posterior root fibers enter the spinal cord. These low-threshold sites are created by a sudden change of the generated potential distribution along the afferent fibers at the interface between nerve rootlet and cord owing to the different electrical conductances of the cerebrospinal fluid and the spinal cord (Geddes & Baker, 1967; Holsheimer, 2002). This inhomogeneity is added to by the acute caudal angle of the lumbosacral nerve roots with the bend of the fibers as they enter the cord. The low-threshold sites were predicted by computer simulation (Coburn, 1985; Struijk *et al.* 1993; Rattay *et al.* 2000) and recognized

by clinical studies (Maccabee *et al.* 1996; Troni *et al.* 1996). At these sites posterior root fibers originating caudal to the cathode can have lower thresholds than longitudinal fibers passing the level of the cathode. Naturally, the stimulus has to be applied at a sufficient strength to these structures to reach the threshold of the fiber. This can be achieved due to the high electric conductivity of cerebrospinal fluid and the higher longitudinal than transverse conductivity of the white matter, which allows the current to spread in a rostro-caudal direction. In this way, recruitment of posterior root fibers is not limited to the level of the cathode. Computer simulation of the epidural electrode set-up as used in the present study showed that the largest posterior root fibers entering the cord caudally to the level of the cathode could still be activated by a maximum stimulation voltage of 10 V at a distance up to 2 cm (Rattay *et al.* 2000).

We conclude that the stimulus-evoked CMAPs as described in our study are reflexively elicited by a dominating input via large afferents within the posterior roots. Depending on the relative rostrocaudal position of the effective cathode with respect to a given posterior root fiber we suggest two different sites of the initiation of afferent volleys in the posterior roots. For cathode positions at upper lumbar cord levels, lumbar posterior root fibers entering the cord in the vicinity of the cathode will have lowest thresholds and will be predominantly recruited at their low-threshold sites. Increasing the stimulation intensity will result in stronger afferent volleys to upper lumbar cord segments and a current spread in the caudal direction inducing muscle responses via posterior root recruitment at the low-threshold sites distant from the cathode. This mechanism can explain the exemplary result in Fig. 3.2A, which is characteristic for cathodes at L2–L4 cord levels. For cathode positions at L1 and lower thoracic segmental levels (T11 and T10 vertebral body levels), CMAPs can still be induced in L2–L4 innervated thigh muscles. However the current spread in the caudal direction is not strong enough to activate posterior roots at any greater distance. These structures are beyond the effective caudal range of the applied bipolar electrode.

Lumbosacral posterior root fibers entering the cord more than 2 cm rostral to the cathode will be excited at the level of the cathode (Rattay *et al.* 2000) where their trajectories are mainly oriented in rostrocaudal direction and pass the cathode within a few millimeters. At the level of the conus medullaris, all segments with afferent fibers coming from the lower limb muscles are represented by posterior root fibers and are organized in layers, which are separated in a posteromedial-anterolateral direction (Wall *et al.* 1990). Considering that all posterior root fibers are mainly oriented in same rostrocaudal direction different thresholds will be predominantly determined by different cathode-fiber distances (for a given fiber size). Due to a larger distance of the L2–L4 posterior roots than the S1 and L5 posterior root fibers to a dorsomedially positioned cathode (Wall *et al.* 1990), it is plausible that stimulation of these structures can explain the reversed recruitment order of the characteristic case shown in Fig. 3.2B.

We also propose that the posterior root fibers were the input structures resulting in the more complex motor output patterns at higher stimulation frequencies. First, the directly stimulated long axons within the posterior roots can easily follow the applied frequencies which were effective to induce the sustained extension or rhythmic flexion/extension movements (5–50 Hz). Secondly, stimulation at higher frequencies which induced coordinated flexion/extension movements in the lower limbs also showed the segmentally-selective recruitment of muscle responses as presented in Fig. 3.2. Dimitrijevic and colleagues (1998a) showed surface EMG recordings from stimulus-evoked activity in the

left quadriceps, adductor, hamstrings, tibialis anterior, and triceps surae muscles derived from subject 10 of the present study. The effective cathode of the epidural electrode array was located at an upper lumbar cord level. The stimulation frequency was 25 Hz and constant, while the stimulation strength was progressively increased from 3.5 V to 5 V in 0.5-Volt steps during the continuous recording. At the threshold level of 3.5 V, low-amplitude tonic EMG activity was first induced in the L2–L4 innervated quadriceps and adductor muscles without activating the leg muscles, which required 4.5 V to respond with tonic activity. Another increase in stimulation amplitude to 5 V replaced the tonic EMG activity with rhythmic EMG activity in the recruited lower limb flexor and extensor muscles and initiated flexion/extension movements. We have provided evidence that this segmentally-selective stimulation indicates that the evoked muscle activity was initiated in the posterior roots. Finally, we demonstrated that each single stimulus of the applied train, which induced the characteristic EMG-extension pattern, elicited a single CMAP (Fig. 3.4A(i)). During stimulus-evoked "burst-style" EMG phases each stimulus was followed by a CMAP (Fig. 3.1C, bottom; Fig. 3.4B; Fig. 3.5B, CMAP #3). Shape and duration of these CMAPs were similar to those evoked at 2.2 Hz.

We suggest that the muscle responses to epidural stimulation of the posterior lumbosacral cord disconnected from supraspinal structures are initiated in the posterior roots independently of the applied frequencies of 2.2–50 Hz. We propose that the sustained input via the posterior roots not only affects monosynaptic excitatory action on motoneurons but concomitant activation of spinal interneurons by synaptically evoked depolarization. At particular repetition rates of stimulation these activated populations of spinal interneurons act as functional units which exert defined facilitatory and inhibitory influences on various motoneuron pools (see below).

Epidural stimulation induces Posterior Roots Muscle Reflex Responses

We have demonstrated that the posterior roots are the predominant input structures for the observed twitch responses to 2.2 Hz stimulation. Feline (Lloyd, 1943) and human (Magladery *et al.* 1951) studies showed that electrically induced afferent volleys via the lowest-threshold fibers of the posterior roots secured two-neuron-arc reflex discharges. Considering that the fibers with the largest diameter have the lowest thresholds, the direct action on motoneurons must be due to group-Ia fibers. Furthermore, Lloyd (1943) showed that monosynaptic group-Ia reflex discharges almost reach their full value even with considerably submaximal posterior root volleys. Major intensification of later, multineuron-arc discharges occurs only after the stage of maximum monosynaptic discharge has been reached. The central latencies of pure cutaneous nerve-ventral root reflex discharges are about 2 ms longer (Lloyd, 1943). These discharges are irregular and last longer. The CMAPs as described in our results showed mainly increased amplitudes at suprathreshold strengths, while no other later potentials were built up.

We conclude that the muscle responses elicited in the present study by epidural stimulation at 2.2 Hz were due to activation of large group-Ia primary spindle afferents within the posterior roots with subsequent recruitment of motoneurons through monosynaptic connections in the spinal cord. This mechanism can explain the short and constant latencies of the recorded muscle responses (Fig. 3.2, Table 3.2). Thus the muscle responses at 2.2 Hz are the physiological equivalent of the H-reflex elicited at the peripheral nerve. The essential difference is that the reflex induced by epidural stimulation is initiated at a more proximal site in the posterior roots—hence a short segment of the afferent arc must be

traversed to elicit the reflex. It has been demonstrated previously that the soleus H-reflex can be evoked by electrical stimulation of the S1 nerve root (Ertekin *et al.* 1996; Zhu *et al.* 1998). Troni and colleagues (1996) reported that soleus H and M responses could be elicited by high-voltage percutaneous stimulation at different sites over the lumbar vertebral column. They suggested that posterior and anterior roots were activated by the stimulation procedure precisely at the points where they enter and exit the spinal cord, respectively. Maccabee *et al.* (1996) elicited soleus H and M responses to magnetic stimulation of the cauda equina and observed stable response latencies despite movement of the magnetic coil. They proposed that responses to stimulation occur at fixed low-threshold sites such as the hot spots resulting from the bend of the posterior roots at their entry point into the spinal cord. It was also reported that by stimulation of the lumbosacral roots and the cauda equina responses of lower limb muscles other than of the soleus can be obtained (Maertens de Noordhout *et al.* 1988; Ertekin *et al.* 1996).

We hereinafter refer to this type of reflex responses arising from a dominating input via large afferents within the posterior roots as Posterior Roots Muscle Reflex Responses (PRMRRs). Afferents other than group Ia primary spindle afferents – like Ib afferents from Golgi tendon organs, cutaneous afferents or group II secondary muscle afferents – seem not to contribute to the reflex responses to 2.2 Hz stimulation. This does not mean that some of these afferents are not activated by the stimulation within the posterior roots and the superficial regions of the posterior columns (Holsheimer, 2002). Some of the afferents within the posterior roots with smaller diameters and therefore higher thresholds than group Ia fibers might contribute to shape the motor output when stimulated repetitively at higher frequencies.

Posterior Roots Muscle Reflex Responses and induced central effects

Any single pulse of the applied trains of electrical stimuli can be considered as a test stimulus. Conditioning inputs are then induced by trains of electrical stimuli applied to the cord by the epidural electrode prior to the arbitrarily chosen test stimulus. The EMG features of the elicited test response reveal conditioning effects on the excitability of the PRMRR pathways. Testing the spinal cord circuitries with 2.2 Hz stimulation demonstrated a functional resting state of the spinal interneurons, which receive inputs from the directly stimulated afferents. In this way stimulation at 2.2 Hz established a reflex organization, which routed the afferent impulses through monosynaptic pathways without engaging central components of the “simple” stretch reflex (Clarac *et al.* 2000).

When pairs of stimuli were applied in close succession the second response was influenced by the ongoing activity of the first response (Fig. 3.3). This refractory behavior of pairs of epidurally evoked reflex responses depended on the interval between the applied stimuli and also on the stimulation strength. The stimulus-strength dependent range of the refractory periods of dual PRMRRs (20–62.5 ms) can presumably be ascribed to effects of the first volley activating spinal interneuronal structures and corresponding presynaptic mechanisms involved in the control of the motor output.

Activation of central mechanisms was apparent when sustained trains of 5–100 Hz were used instead of pairs of stimuli. At 25–50 Hz the successively elicited, separate CMAPs were subject to well-defined amplitude modulations resulting in burst-like envelopes of the EMG activity (Fig. 3.1C, bottom; Fig. 3.4A(ii); Fig. 3.4B). The sustained stimulation not

only activated neural structures transmitting the PRMRRs, but also recruited mechanisms involved in a well-coordinated gain control of the PRMRR pathways.

Prolongation of the PRMRR latency was another indication that the sustained epidural stimulation could activate structures other than the components of the two-neuron reflex arc. During tonic activity and during tonic motor output in the form of lower-limb extension induced at 5–15 Hz, PRMRRs with short and constant latencies were elicited like the ones observed during the “resting” spinal central state induced with trains of 2.2 Hz. Thus, the induced tonic activity is composed of stimulus-coupled PRMRRs that are primarily routed through monosynaptic pathways. At higher frequencies and under particular conditions a significant increase of PRMRR latency of about 10 ms was observed (Minassian *et al.* 2001*a,b*; Minassian *et al.* 2002). A prolongation of the central delay of the total reflex latency is the most plausible explanation. We have argued that the CMAPs are initiated at the same proximal sites in the posterior roots independent of the applied frequencies. It is assumed that variations of the afferent and efferent delay of the total CMAP latency with changes of stimulation frequency from 2.2 to 50 Hz are negligible. In Fig. 3.5*A* we have shown that the responses with the longer latency were successively built up with increased stimulation frequencies. At frequencies of 2.2–16 Hz no actual movement of the lower extremity was induced. This finding discards the notion that the latency prolongation was due to changes of geometrical relations between the muscle tissue and the recording surface electrodes during induced movements of the lower limb. Furthermore it is unlikely that the longer latencies were a result of repeated induction of muscle fatigue or refractory periods since it was shown in Fig. 3.5*B*, that prolongation of PRMRR latency was correlated with the burst-style periods during a complex motor output.

We propose that the prolongation of the PRMRR latency was due to an extended integration of central spinal PRMRR components. The epidurally initiated afferent flow was routed through polysynaptic spinal pathways opened only at frequencies higher than 15 Hz and during induced burst-style activity. A concomitant action was the suppression of the monosynaptic component of the PRMRRs during the burst-style phases (Fig. 3.5*B*). We speculate that this is accomplished by recruitment and state-dependent modulations of spinal reflexes, which are nonfunctional during the “resting” state of the lumbar interneuronal circuits. Such modifications of reflex responses have also been shown during normal human locomotion (Zehr & Stein, 1999; Capaday, 2002). Furthermore, feline studies have shown that afferents may mediate their effects on motoneurons via different routes. This is true for large group-I afferents and for smaller high-threshold afferents from muscles, joints and skin such as the “flexor reflex afferents” (FRA) that activate common interneurons (Pearson, 1995; Pearson & Ramirez, 1999; Clarac *et al.* 2000; Hultborn, 2001; McCrea, 2001). Under conditions of intact connections between lumbar cord and brain stem structures, the flow of information into and through the central FRA pathways can be controlled by supraspinal centers (Lundberg, 1979).

Posterior Roots Muscle Reflex Responses and the Lumbar Locomotor Pattern Generator

Epidural stimulation with parameters that induced rhythmic flexion/extension movements of the lower limbs elicited afferent volleys via large diameter fibers within the posterior roots. The stimulated structures are a subset of sensory fibers that are involved in peripheral feedback. During locomotion these sensory fibers transmit phasic input which enter the spinal cord via the posterior roots with spatially and temporally complex patterns. Epidural

stimulation as described in the present study elicited a sustained, tonic non-patterned input that was delivered simultaneously to several lumbar and upper sacral cord segments. Thus, the input was unlike physiological sensory information. We speculate, that – besides exerting facilitation of various motoneuron pools – the input acts as a common drive to spinal interneuronal networks located in the lumbar cord. While coming from periphery, the tonic input of particular frequencies is interpreted as a central command signal due to its code. The sustained stimuli organize lumbar spinal interneurons by temporarily combining them into functional units representing different levels of muscle synergies, parts of movements, or even more integrated motor behavior. The selection and activation of functional units dependent on the repetition rate of tonic input. While at 5–15 Hz extension activity dominates the motor output, at 25–50 Hz the balance of neural activity is shifted to generate a rhythmic motor output. Our notion is that this can be achieved due to the flexibility of operation of spinal interneuronal networks and their multifunctional character (Jankowska, 2001) and due to the connectivity of the activated large diameter sensory neurons with these networks. Hultborn and colleagues (1998) have emphasized that different reflex pathways have direct access to, or may even be part of, the central pattern generator (CPG) for locomotion in the cat. Moreover, Burke and colleagues (2001) stressed, that: “it has been known for some time that a variety of reflexes are modulated in amplitude and even reversed in sign during different phases of the stepping cycle, both in animals and man. Intracellular recordings from motoneurons during fictive locomotion have provided clear evidence that the locomotor CPG exerts powerful control of transmission through reflex pathways as assessed by phasic modulation of synaptic potentials.”

Can we conclude on the basis of the presented findings that the studied model of the human lumbar cord isolated from suprasegmental input by accidental injury has features of a CPG for locomotion? The hallmark for identification of a locomotor CPG within the spinal cord is the production of recognizable and reproducible patterns of rhythmic output in the absence of instructive external drive from higher levels of the central nervous system or from peripheral sensory feedback. So far we have demonstrated that by applying a sustained tonic input to the lumbar cord isolated from supraspinal influence, it is possible to activate and drive interneuronal networks and thereby to initiate stepping-like flexion/extension movements in the paralyzed lower limbs. To stabilize the induced motor activity, additional phasic sensory feedback from the lower limbs associated with the induced stepping-like movements was essential. This was shown in a study on the effects of temporarily reduced peripheral input when locomotor-like movements were evoked by spinal cord stimulation in paraplegics (Dimitrijevic *et al.* 1998b). While the parameters of epidural stimulation were maintained constant, it was observed that the reduced sensory feedback resulted in decreased amplitudes of the EMG activity and increased frequency of the lower limb movement. The phasic input had a timing function in the production of rhythmic movements and additionally augmented the activity of the rhythm-generating spinal circuits. We propose to consider the described capabilities of the human lumbar cord isolated from brain control and tested by repetitively induced PRMRs at 25–50 Hz as evidence for the existence of a Lumbar Locomotor Pattern Generator (LLPG). This LLPG in humans can be activated by sustained, non-patterned trains of electrical stimuli of specific repetition rate applied to the posterior roots of the upper lumbar cord segments.

Significance of the results

Repair of spinal cord injuries is a complex task for contemporary neurosciences and medical practice, and is not yet accomplished, even though the basic science of axon regeneration is making significant progress (Schwab, 2002). There are several experimental treatments for promotion of axonal regeneration in rodent spinal cord injury models but also in these models a full repair of spinal cord injury is not available (Fawcett, 2002).

On the other hand, there has been success in the clinical application of electrical stimulation to intact nerves of paralyzed limbs in order to elicit functional movements in spinal cord injured people (Dimitrijevic *et al.* 1968; Dimitrijevic & Dimitrijevic, 1992). This technique is known as functional electrical stimulation (FES). FES devices with one, two or more stimuli outputs and independent control of electrical parameters are in use in a variety of clinical protocols: in the improvement of trophic conditions of muscles after effects of disuse, suppression of spasticity, correction of single muscle group deficit within patterned, synergistic movements, enhancement of postural and volitional control in incomplete SCI individuals, restoration of externally controlled standing and walking in clinically complete SCI people, and in the restoration of muscle tissue in people with cauda equina lesion (Bajd *et al.* 1989; Kern *et al.* 2002). Working with clinical FES protocols provides opportunity for practicing physicians, clinical neurophysiologists and biomedical engineers to investigate how to use FES for generating force and functional movements in paralyzed muscles and how to apply electrical stimulation to afferents of peripheral nerves in order to modify spinal reflex activity (Dimitrijevic, 1970; Dimitrijevic & Dimitrijevic, 2002).

There is a simultaneous progress in basic research on spinal reflex circuits (McCrea, 2001), organization of inputs to spinal interneuronal populations (Edgley, 2001), flexibility of operation of interneuronal circuits and final common interneuronal pathways (Jankowska, 2001), and on central pattern generators for locomotion (Grillner *et al.* 2001).

We should appreciate these recent findings of basic scientists regarding spinal interneurons when evaluating the present human neurophysiological study of the activation of spinal networks. Populations of spinal interneurons can be organized to act as functional units by tonic afferent input. Spinal interneurons are multifunctional and can be incorporated into different larger networks which exert defined facilitatory and inhibitory influences on various motoneuron pools. This flexibility was also shown in our study. By changing the repetition rate of tonic stimulation a temporarily established pattern generator for stepping-like activity – the LLPG – was promptly converted to a pattern generator for lower limb extension.

The possibility of activating spinal networks involved in generating functional synergistic movements opens a new avenue with great potential for human neurophysiological studies of intrinsic spinal cord functional properties, and may contribute to the development of new methodologies, technologies and clinical practice for restoration of movements in SCI people.

REFERENCES

- Bajd T, Kralj A, Turk R, Benko H & Segal J (1989). Use of functional electrical stimulation in the rehabilitation of patients with incomplete spinal cord injuries. *J Biomed Eng* **11**, 96-102.
- Barolat G, Massaro F, He J, Zeme S & Ketcik B (1993). Mapping of sensory responses to epidural stimulation of the intraspinal neural structures in man. *J Neurosurg* **78**, 233-239.
- Barolat G, Singh-Sahni K, Staas WE, Shatin D, Ketcik B & Allen K (1995). Epidural spinal cord stimulation in the management of spasms in spinal cord injury. A prospective study. *Stereotact Funct Neurosurg* **64**, 153-164.
- Beric A (1988). Stability of lumbosacral somatosensory evoked potentials in a long-term follow-up. *Muscle Nerve* **11**, 621-626.
- Burke RE, Degtyarenko AM & Simon ES (2001). Patterns of locomotor drive to motoneurons and last-order interneurons: clues to the structure of the CPG. *J Neurophysiol* **86**, 447-462.
- Bussel B, Roby-Brami A, Neris OR & Yakovlev A (1996). Evidence for a spinal stepping generator in man. *Paraplegia* **34**, 91-92.
- Calancie B, Needham-Shropshire B, Jacobs P, Willer K, Zych G & Green BA (1994). Involuntary stepping after chronic spinal cord injury. Evidence for a central rhythm generator for locomotion in man. *Brain* **117**, 1143-1159.
- Capaday C (2002). The special nature of human walking and its neural control. *Trends Neurosci* **25**, 370-376.
- Clarac F, Cattaert D & Le Ray D (2000). Central control components of a 'simple' stretch reflex. *Trends Neurosci* **23**, 199-208.
- Coburn B (1985). A theoretical study of epidural electrical stimulation of the spinal cord-Part II: Effects on long myelinated fibers. *IEEE Trans Biomed Eng* **32**, 978-986.
- Dimitrijevic MM, Dimitrijevic MR, Illis LS, Nakajima K, Sharkey PC & Sherwood AM (1986a). Spinal cord stimulation for the control of spasticity in patients with chronic spinal cord injury: I. Clinical observations. *Cent Nerv Syst Trauma* **3**, 129-144.
- Dimitrijevic MM & Dimitrijevic MR (1992). Clinical practice of functional stimulation. In *Spinal Cord Dysfunction, Vol. III: Functional Stimulation*, ed. Illis LS, pp. 168-174. Oxford University Press, USA.
- Dimitrijevic MM & Dimitrijevic MR (2002). Clinical elements for the neuromuscular stimulation and functional electrical stimulation protocols in the practice of neurorehabilitation. *Artif Organs* **26**, 256-259.
- Dimitrijevic MR, Gracanin F, Prevec TS & Trontelj JV (1968). Electronic control of paralysed extremities. *Biomed Eng* **3**, 8-19.
- Dimitrijevic MR (1970). Further advances in use of physiological mechanisms in the external control of human extremities. In *Advances in External Control of Human Extremities*, ed. Gavrilovic MM & Wilson AB, pp 473-486. Yugoslav Committee for Electronics and Automation, Belgrade, Yugoslavia.

Dimitrijevic MR (1983). Neurophysiological evaluation and epidural stimulation in chronic spinal cord injury patients. In *Spinal Cord Reconstruction*, ed. Reier PJ, Bunge RP & Kao CC, pp. 465-473. Raven Press, New York.

Dimitrijevic MR, Illis LS, Nakajima K, Sharkey PC & Sherwood AM (1986b). Spinal cord stimulation for the control of spasticity in patients with chronic spinal cord injury: II. Neurophysiologic observations. *Cent Nerv Syst Trauma* 3, 145-152.

Dimitrijevic MR, Gerasimenko Y & Pinter MM (1998a). Evidence for a spinal central pattern generator in humans. In *Neural Mechanisms for Generating Locomotor Activity. Ann N Y Acad Sci Vol. 860*, ed. Kiehn O, Harris-Warrick RM, Jordan LM, Hultborn H & Kudo N, pp. 360-376. New York Academy of Sciences, New York.

Dimitrijevic MR, Gerasimenko Y & Pinter MM (1998b). Effect of reduced afferent input on lumbar CPG in spinal cord injury subjects. *Soc Neurosci Abstr* 24: Program No. 654.23.

Dimitrijevic MR, Minassian K, Gilge B & Rattay F (2002). Initiation of standing and locomotion like movements in complete SCI subjects "by mimicking" brain stem control of lumbar network with spinal cord stimulation. *Proceedings of the 4th International Symposium on Experimental Spinal Cord Injury Repair and Regeneration*, pp. 25-27, Brescia, Italy.

Edgley SA (2001). Organisation of inputs to spinal interneurone populations. *J Physiol* 533, 51-56.

Ertekin C, Mungan B & Uludag B (1996). Sacral cord conduction time of the soleus H-reflex. *J Clin Neurophysiol* 13, 77-83.

Fawcett J (2002). Repair of spinal cord injuries: where are we, where are we going? *Spinal Cord* 40, 615-623.

Geddes LA & Baker LE (1967). The specific resistance of biological material—a compendium of data for the biomedical engineer and physiologist. *Med Biol Eng* 5, 271-293.

Gerasimenko Y, McKay B, Sherwood A & Dimitrijevic MR (1996). Stepping movements in paraplegic patients induced by spinal cord stimulation. *Soc Neurosci Abstr*; 22: 1372.

Grillner S (1981). Control of locomotion in bipeds, tetrapods, and fish. In: *Handbook of Physiology. The Nervous System. Motor Control*. sect.1, vol. II., ed. Brooks VB pp. 1179-1236. Am Physiol. Soc, Washington, DC.

Grillner S, Wallen P, Hill R, Cangiano L & El Manira A (2001). Ion channels of importance for the locomotor pattern generation in the lamprey brainstem-spinal cord. *J Physiol* 533, 23-30.

Gurfinkel VS, Levik YS, Kazennikov OV & Selionov VA (1998). Locomotor-like movements evoked by leg muscle vibration in humans. *Eur J Neurosci* 10, 1608-1612.

Guru K, Mailis A, Ashby P & Vanderlinden G (1987). Postsynaptic potentials in motoneurons caused by spinal cord stimulation in humans. *Electroencephalogr Clin Neurophysiol* 66, 275-280.

He J, Barolat G, Holsheimer J & Struijk JJ (1994). Perception threshold and electrode position for spinal cord stimulation. *Pain* 59, 55-63.

Holsheimer J (2002). Which neuronal elements are activated directly by spinal cord stimulation. *Neuromodulation* **5**, 25-31.

Hultborn H, Conway BA, Gossard JP, Brownstone R, Fedirchuk B, Schomburg ED, Enriquez-Denton M & Perreault MC (1998). How do we approach the locomotor network in the mammalian spinal cord? In *Neural Mechanisms for Generating Locomotor Activity. Ann N Y Acad Sci Vol. 860*, ed. Kiehn O, Harris-Warrick RM, Jordan LM, Hultborn H & Kudo N, pp. 70-82. New York Academy of Sciences, New York.

Hultborn H (2001). State-dependent modulation of sensory feedback. *J Physiol* **533**, 5-13.

Hunter JP & Ashby P (1994). Segmental effects of epidural spinal cord stimulation in humans. *J Physiol* **474**, 407-419.

Illis LS. Is there a central pattern generator in man (1995)? *Paraplegia* **33**, 239-240.

Jankowska E (2001). Spinal interneuronal systems: identification, multifunctional character and reconfigurations in mammals. *J Physiol* **533**, 31-40.

Jilge B, Minassian K & Dimitrijevic MR (2001). Electrical stimulation of the human lumbar cord can elicit standing parallel extension of paralysed lower limbs after spinal cord injury. *Proceedings of the World Congress on Neuroinformatics Part II*, pp 281-283. Vienna, Austria.

Jilge B, Minassian K, Rattay F, Pinter MM, Gerstenbrand F, Binder H & Dimitrijevic MR (2004). Initiating extension of the lower limbs in subjects with complete spinal cord injury by epidural lumbar cord stimulation. *Exp Brain Res* **154**, 308-326.

Kern H, Hofer C, Modlin M, Forstner C, Raschka-Hogler D, Mayr W & Stohr H (2002). Denervated muscles in humans: limitations and problems of currently used functional electrical stimulation training protocols. *Artif Organs* **26**, 216-218.

Lang J (1984). Morphologie und funktionelle Anatomie der Lendenwirbelsäule und des benachbarten Nervensystems - 1. Rückenmark. In *Neuroorthopädie 2 - Lendenwirbelsäulenerkrankungen mit Beteiligung des Nervensystems*, ed. Hohmann D, Kügelgen B, Liebig K & Schirmer M, pp. 3-9. Springer, Berlin.

Lehmkuhl D, Dimitrijevic MR & Renouf F (1984). Electrophysiological characteristics of lumbosacral evoked potentials in patients with established spinal cord injury. *Electroencephalogr Clin Neurophysiol* **59**, 142-155.

Lloyd DPC (1943). Reflex action in relation to pattern and peripheral source of afferent stimulation. *J Neurophysiol* **16**, 111-120.

Lundberg A. Multisensory control of spinal reflex pathways (1979). *Prog Brain Res* **50**, 11-28.

Maccabee PJ, Lipitz ME, Desudchit T, Golub RW, Nitti VW, Bania JP, Willer JA, Cracco RQ, Cadwell J, Hotson GC, Eberle LP & Amassian VE (1996). A new method using neuromagnetic stimulation to measure conduction time within the cauda equina. *Electroencephalogr Clin Neurophysiol* **101**, 153-166.

Maertens de Noordhout A, Rothwell JC, Thompson PD, Day BL & Marsden CD (1988). Percutaneous electrical stimulation of lumbosacral roots in man. *J Neurol Neurosurg Psychiatry* **51**, 174-181.

- Magladery JW, Porter WE, Park AM & Teasdall RD (1951). Electrophysiological studies of nerve and reflex activity in normal man. *Bull John Hopkins Hosp* **88**, 499-519.
- McCrea DA (2001). Spinal circuitry of sensorimotor control of locomotion. *J Physiol* **533**, 41-50.
- Minassian K, Rattay F & Dimitrijevic MR (2001a). Features of the reflex responses of the human lumbar cord isolated from the brain but during externally controlled locomotor activity. *Proceedings of the World Congress on Neuroinformatics Part II*, pp. 267-268. Vienna, Austria.
- Minassian K, Rattay F, Pinter MM, Murg M, Binder H, Sherwood A & Dimitrijevic MR (2001b). Effective spinal cord stimulation (SCS) train for evoking stepping locomotor movement of paralyzed human lower limbs due to SCI elicits a late response additionally to the early monosynaptic response. *Soc Neurosci Abstr* **27**: Program No. 935.12.
- Minassian K, Gilge B, Rattay F, Pinter MM, Gerstenbrand F, Binder H & Dimitrijevic MR (2002). Effective spinal cord stimulation (SCS) for evoking stepping movement of paralyzed human lower limbs: study of posterior root muscle reflex responses. *Proceedings of the 7th Annual Conference of the IFESS*, pp. 167-169. Ljubljana, Slovenia.
- Murg M, Binder H & Dimitrijevic MR (2000). Epidural electric stimulation of posterior structures of the human lumbar spinal cord: 1. muscle twitches – a functional method to define the site of stimulation. *Spinal Cord* **38**, 394-402.
- Roby-Brami A & Bussel B (1987). Long-latency spinal reflex in man after flexor reflex afferent stimulation. *Brain* **110**, 707-725.
- Pearson KG (1995). Proprioceptive regulation of locomotion. *Curr Opin Neurobiol* **5**, 786-791.
- Pearson KG & Ramirez J-M (1999). Sensory modulation of pattern generating circuits. In *Neurons, Networks and Motor Behavior*, Stein PSG, ed. Grillner S, Selverston AI & Stuart DG. pp. 257-267. MIT Press, Cambridge, USA.
- Pinter MM, Gerstenbrand F & Dimitrijevic MR (2000). Epidural electrical stimulation of posterior structures of the human lumbosacral cord: 3. Control of spasticity. *Spinal Cord* **38**, 524-531.
- Rattay F, Minassian K & Dimitrijevic MR (2000). Epidural electrical stimulation of posterior structures of the human lumbosacral cord: 2. quantitative analysis by computer modeling. *Spinal Cord* **38**, 473-489.
- Rosenfeld JE, McKay WB, Halter JA, Pollo F & Dimitrijevic MR (1995). Evidence of a pattern generator in paralyzed subjects with spinal cord injury during spinal cord stimulation. *Soc Neurosci Abstr*; **21**: 688.
- Rossignol S (1996). Neural control of stereotypic limb movements, In: *Handbook of Physiology. Exercise: Regulation and Integration of Multiple Systems*, ed. Rowell LB & Shepherd JT, pp. 173-216. Am Physiol Soc, Bethesda, MD.
- Schwab ME (2002). Repairing the injured spinal cord. *Science* **295**, 1029-1031.
- Sherwood AM, McKay WB & Dimitrijevic MR (1996). Motor control after spinal cord injury: Assessment using surface EMG. *Muscle Nerve* **19**, 966-979.

Struijk JJ, Holsheimer J & Boom HB (1993). Excitation of dorsal root fibers in spinal cord stimulation: A theoretical study. *IEEE Trans Biomed Eng* **40**, 632-639.

Troni W, Bianco C, Moja MC & Dotta M (1996). Improved methodology for lumbosacral nerve root stimulation. *Muscle Nerve* **19**, 595-604.

Wall EJ, Cohen MS, Abitbol JJ & Garfin SR (1990). Organization of intrathecal nerve roots at the level of the conus medullaris. *J Bone Joint Surg* **72**, 1495-1499.

Zehr EP & Stein RB (1999). What functions do reflexes serve during human locomotion? *Prog Neurobiol* **58**, 185-205.

Zhu Y, Starr A, Haldeman S, Chu JK & Sugerman RA (1998). Soleus H-reflex to S1 nerve root stimulation. *Electroencephalogr Clin Neurophysiol* **109**, 10-14.

Chapter 4

Effect of peripheral afferent and central afferent input to the isolated human lumbar spinal cord

Summary

It has been previously demonstrated that repetitive and regular epidural stimulation of lumbar posterior roots at frequencies of 20–50 Hz can activate the Lumbar Locomotor Pattern Generator (LLPG) and induce stepping-like movements in subjects with chronic, complete spinal cord injury. In these studies, the subjects were lying in a supine position and the lower limbs were weight-supported. Afferent feedback input from load receptors of the lower limbs was minimized. The purpose of this paper is to investigate the interaction between externally induced activity of the LLPG and manually assisted, weight-bearing stepping on a treadmill in paralyzed subjects.

Two subjects with chronic, complete spinal cord injury with epidurally placed electrodes were included in this study. Epidural stimulation with 38 different parameter combinations between 1–10 V and 10–100 Hz was applied, while the same externally controlled maneuver of passive stepping movement was performed. The electromyographic (EMG) activity of the quadriceps, hamstrings, tibialis anterior and triceps surae muscles was simultaneously recorded with surface electrodes.

Peripheral sensory feedback related to assisted treadmill stepping generated EMG bursts which were characterized by low amplitudes and co-activation of muscles. When epidural stimulation was applied, 18 of the 38 studied parameter combinations induced stimulus-related EMG bursts of lower limb muscles during passive treadmill stepping, which were temporally synchronized to specific phases of the step cycle. All effective stimulation parameters were within the range of 20–50 Hz and 6–10 V. Epidural stimulation could enhance and change the patterns of rhythmic EMG activities during passive stepping. The EMG patterns in the paralyzed lower limb muscles induced by mechanical stimulation associated with passive stepping with additional epidural stimulation resembled the patterns of able-bodied subjects.

In conclusion, the LLPG could be activated by epidural stimulation of the lumbar cord in complete spinal cord injured subjects during weight-bearing, manually assisted treadmill stepping. The timing of the rhythmic motor output of the LLPG was not set to some default level, but was matched to specific phases of the manually imposed step cycle. The responsiveness of the spinal circuits to proprioceptive feedback in generating stepping-like motor patterns was significantly enhanced, when stimulation at frequencies of 20–50 Hz was applied. This effect could be achieved immediately as soon as epidural stimulation with the appropriate stimulus parameters was delivered. We conclude that the spinal lumbar networks can integrate and interpret both, the stimulus-evoked tonic input with a “central” code and the proprioceptive feedback input in order to generate effective and functional locomotor patterns. This finding suggests that epidural stimulation of the lumbar cord might

be a useful neuroaugmentative tool to support locomotor training in subjects with spinal cord injury.

INTRODUCTION

It has been previously demonstrated that sustained non-patterned electrical stimulation of the posterior lumbar spinal cord from the epidural space can induce stepping-like alternating flexion and extension movements in subjects with chronic, complete spinal cord injury (Dimitrijevic *et al.* 1998a).

Following studies provided evidence that the stepping-like movements evoked by epidural stimulation were initiated by stimulation of the lumbar posterior roots (Minassian *et al.* 2004a). During the induced burst-style EMG phases each pulse within the train of electrical stimuli elicited a separate compound muscle action potential (CMAP). The electrophysiological characteristics of these Posterior Roots Muscle Reflex Responses (PRMRRs) were described.

PRMRRs in proximal and distal lower limb muscles were shown to depend on the stimulation strength and frequency. The responses could be organized to result in either limb extension or rhythmic alternation of flexion/extension depending on the frequency of the applied stimulation (Jilge *et al.* 2004; Minassian *et al.* 2004b). During induced rhythmic movements, the PRMRRs were modulated with respect to both EMG amplitude and latency. It was proposed that lumbar interneurons can respond to particular repetition rates of tonic afferent input by temporarily combining into the Lumbar Locomotor Pattern Generator (LLPG), which modulates the transmitting pathways and amplitudes of the PRMRRs and thereby generates flexion/extension movements.

The above cited studies were based on EMG recordings of stimulus-evoked muscle responses derived from subjects lying in a supine position. Thus, spinal cord stimulation induced stepping-like movements of the lower limbs without the sensations of weight-bearing, i.e. without or with minimum afferent feedback input from load receptors.

On the other hand, it was shown that reducing phasic sensory feedback from the lower limbs associated with the stepping-like movements had a profound effect on the spinal cord stimulation-induced motor activity (Dimitrijevic *et al.* 1998b). Under constant epidural stimulation conditions, a temporary cuff applied over the thigh muscles to reduce input from large afferents (ischemia) resulted in diminishing amplitudes and increased frequency of the stepping-like movements. The phasic peripheral feedback input had a timing function in the production of rhythmic movements and augmented the activity of the rhythm-generating spinal circuits and the spinal motor pools.

Peripheral sensory input associated with manually assisted stepping over a moving treadmill belt of complete spinal cord injured subjects can generate stepping-like oscillating EMG patterns in the lower limbs (Dietz *et al.* 1995; Dobkin *et al.* 1995). Stretch reflexes are not the sole source of the phasic EMG activity induced in flexors and extensors during manually assisted stepping of the subjects (Harkema *et al.* 1997). An essential contribution of load receptor input to the generation of a locomotor pattern has been recognized in paraplegic patients (Harkema *et al.* 1997, Dietz *et al.* 2002). When assisted air stepping is performed (100% body unloading) EMG activity recorded from paralyzed lower limb muscles is reduced or absent (Dietz *et al.* 2002). Thus, a significant influence of the sensory

feedback input associated with passive weight-bearing stepping could also be expected on the EMG activity induced by epidural stimulation during assisted stepping.

If information on joint angles, displacement and loading of the lower limbs are unavailable to the LLPG, the amplitude and timing of the cyclical motor output can only be set to an arbitrary default level. To generate functional motor patterns, the LLPG has to adapt the efferent output patterns to the specific phases of the step cycle. The purpose of the present paper is to study the effect of electrical epidural stimulation with parameters set to activate the LLPG, with simultaneous assisted treadmill stepping in paraplegic subjects. Particular questions are if the LLPG can be activated during manually imposed treadmill stepping and if the LLPG can process peripheral input associated with manually assisted stepping to generate EMG bursts temporally synchronized to specific phases of the step cycle.

MATERIAL AND METHODS

Subjects

The EMG data of lower limb muscle response patterns which were made available for the present study were derived from two subjects with accidental spinal cord injury. According to the ASIA impairment scale, the subjects were sensory and motor complete (ASIA A). The subjects completed sensory-evoked potentials examinations and brain motor control assessment (BMCA) tests to rule out conductivity between the lower limbs and the brain and any voluntary activation of motor units below the level of the lesion. Stretch and cutaneomuscular reflexes were preserved below the level of spinal cord injury. Patient-related data are listed in Table 4.1.

Table 4.1 Demographic and clinical data

Subject No.	Sex	Born in	Accident in	Implantation of electrode	Type of accident	Level of SCI	ASIA Class.
1	m	1977	1994	1999	Motorbike accident	C6	A
2	f	1978	1994	1996	Car accident	T4	A

Stimulation procedure

EMG activity in the paralyzed lower limb muscles was induced by tonic or phasic stimulation of afferent fibers entering the lumbosacral cord, or by combination of the two stimulus modalities (Fig 4.1A).

Tonic input was delivered by sustained stimulation of the posterior roots of the lumbosacral cord by dorsally placed epidural electrode arrays. The stimulation provided a sustained, non-patterned input at a specific stimulus frequency to several lumbar and upper sacral cord segments simultaneously. For details of the used quadripolar electrode array (PISCES-QUAD electrode, Model 3487A, MEDTRONIC, Minneapolis, MN, USA) and the implanted pulse generator (ITREL 3, Model 7425, MEDTRONIC) see Minassian *et al.* (2004a,b) or Chapters 2 and 3.

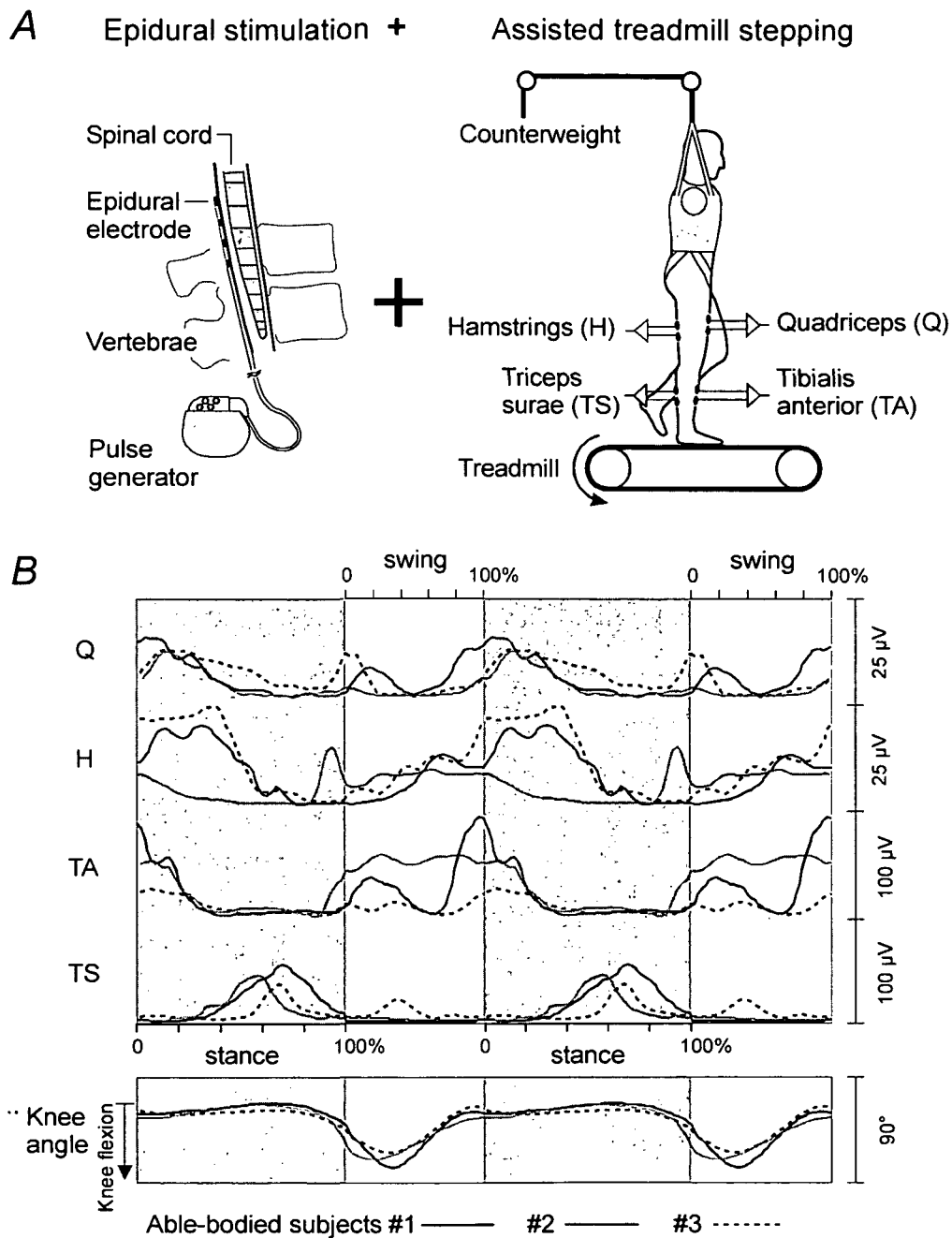


Figure 4.1 Stimulation and recording set-up

A, Tonic stimulation was delivered by an epidural electrode placed in the dorsomedial epidural space at lumbar and upper sacral cord levels. Proprioceptive input to the spinal cord is induced by assisted treadmill stepping with body weight support. Pairs of surface electrodes were placed over the bellies of the lower limb muscles to record the stimulus-induced EMG activity. *B*, Rectified and filtered EMG activity with respect to normalized stance (gray background) and swing phase of three able-bodied subjects during treadmill-stepping. Treadmill speed was 1.2 km/h (0.33 m/s), body weight support was 20 kg. Recording electrodes were placed as in the spinal cord injured subjects.

Three contact combinations of the electrode ("electrode polarity") and thirty-eight stimulation parameter settings between 1–10 V and 10–100 Hz were tested during four recording sessions (Table 4.2). The four independent contacts of the quadripolar lead were

labeled 0, 1, 2, 3, such that contact #0 was at the top and contact #3 at the bottom; 'c' means that the metal case of the implanted pulse generator was used as the indifferent electrode (Table 4.2). One data set was derived from subject 1, and three recordings from subject 2. Table 4.2 also includes information on the site of stimulation based on muscle twitch distribution patterns in supine position (Murg *et al.* 2000).

Table 4.2 Recordings and applied parameter combinations of the epidural electrode

Subject No.	No. of recording	Year of data collection	Electrode polarity	Corresponding muscle twitch thresholds (V)							
				RQ	RH	RTA	RTS	LQ	LH	LTS	LTA
1	1	2003	1+3-	2	2	3	3	3	3	4	4
2	2	1999	c+2-	-	-	-	-	-	-	-	-
			0+3-	5	5	5	5	5	5	5	5
2	3	2000	0+3-	6	4	5	5	6	5	5	5
2	4	2001	0+3-	5	4	4	4	5	4	4	4

Phasic peripheral feedback input was induced by passive, manually assisted stepping on a treadmill with partial body weight support of the subject. The generated afferent volleys are complex and correspond to the phases of passive stepping. This spatially and temporary patterned sensory feedback is similar to the one during normal walking.

Subjects wore a harness connected to an overhead support that provided a vertical constraint on the movement of the torso and reduced vertical ground reaction forces by supporting a portion of the subject's body weight. Two trainers manually facilitated the subjects' lower limbs through the step cycle. The trainers held each stepping limb distal to the patella to facilitate knee flexion during the swing phase, and knee and hip extension during the stance phase. Trainers used their other hand to hold the stepping limb proximal to the ankle during the swing phase to assist with foot lift off and placement. Each spinal cord injured subject passively stepped at a constant treadmill speed (range 0.4–0.8 km/h) and a constant level of harness support (80% of body weight).

Recording procedure

Pairs of recessed, silver-silver chloride surface electrodes were placed 3 cm apart over the midline of the muscle bellies of the quadriceps, hamstrings, tibialis anterior and triceps surae muscles. The skin was prepared by light abrasion to obtain an electrode impedance of less than 5 k Ω for each electrode pair to reduce or eliminate artifacts arising from stretching of the skin and electrode movement.

In subject 1, the EMG channels were amplified using PHOENIX amplifiers (EMS-Handels GmbH, Korneuburg, AUT), with a gain of 4664 over a bandwidth of 10–500 Hz, digitized at 1024 or 2048 Hz per channel. Due to the high gain, EMG signals were cut at $\pm 536 \mu\text{V}$. Averaged, rectified EMG activity during active treadmill-stepping derived from three able-bodied subjects and recorded with the same set-up as used for subject 1 is displayed in Fig. 4.1B.

In subject 2, the EMG signals were amplified with the Grass 12D-16-OS NEURODATA ACQUISITION SYSTEM (GRASS INSTRUMENTS, Quincy, MA) adjusted to a gain of 2000 over

bandwidth of 30–1000 Hz and digitized at 2048 Hz per channel using a CODAS ADC system (DATAQ INSTRUMENTS, Akron, OH).

A “BMCA event-marker” (a trigger signal) was used to manually mark the stance phases between heel strike and toe-off of one lower limb during assisted treadmill walking. Foot switches or foot pressure sensors were not available.

Data analysis

To find out if the induced EMG bursts were temporally synchronized with the stepping cadence and to illustrate the amount of muscle activity in relation to the phases of the step cycle, the averaged EMG activity versus normalized time was calculated.

The original raw EMG data was rectified. From these data 200 data points were calculated for each stance phase and 100 data points for each swing phase. This was done regardless of the duration of individual stance or swing phases. Thereby each calculated data point represented the muscle activity (integrated EMG) within a time interval of 0.5% of a stance or 1% of a swing phase. After this time normalization, the EMG activity of each stance phase and each swing phase consisted of the same number of data points (200 and 100). This allowed averaging the EMG activity of consecutive stance phases or swing phases.

The EMG activity of 10 stance phases and 10 swing phases was averaged separately. The result was the average muscle activity during the stance and the swing phase versus the percentage of the average stance phase duration and the average swing phase duration, respectively. For the calculations MATLAB 6.1 (THE MATHWORKS, INC., NATIC, MA) was used.

For illustration of the results, the calculated averaged muscle activity during the stance and the swing phase were placed in the order swing-stance-swing-stance to represent two step cycles (Fig. 4.1B).

RESULTS

Effect of spinal cord stimulation on lower limb EMG patterns induced during passive treadmill stepping

Figure 4.2 shows the averaged, rectified EMG activity of the right lower limb muscles with respect to time-normalized stance (marked by gray background) and swing phase. Muscle activity was induced by assisted treadmill walking without (Fig. 4.2A) and with additional epidural stimulation (Fig. 4.2B,C). Data was derived from subject 1. Without epidural stimulation, no activity was induced in quadriceps (Q), while EMG bursts temporally synchronized to the step cycle were induced in hamstrings (H), tibialis anterior (TA), and triceps surae (TS). Triceps surae activity preceded the onset of loading and was active during late swing and the whole stance phase. EMG response of hamstrings and tibialis anterior lagged triceps surae activity for about 10–20% of the swing phase duration and then mainly demonstrated co-activation with triceps surae.

When epidural stimulation was applied at 30 Hz and 6 V during passive treadmill walking (Fig. 4.2B), activity was induced in quadriceps during the whole swing phase. The EMG activity was characterized by components with high amplitudes and low frequency (10 Hz). The EMG burst reached maximum amplitudes at 40% of the swing phase. Hamstrings were mainly active during the swing phase and thus demonstrated a significant change of the

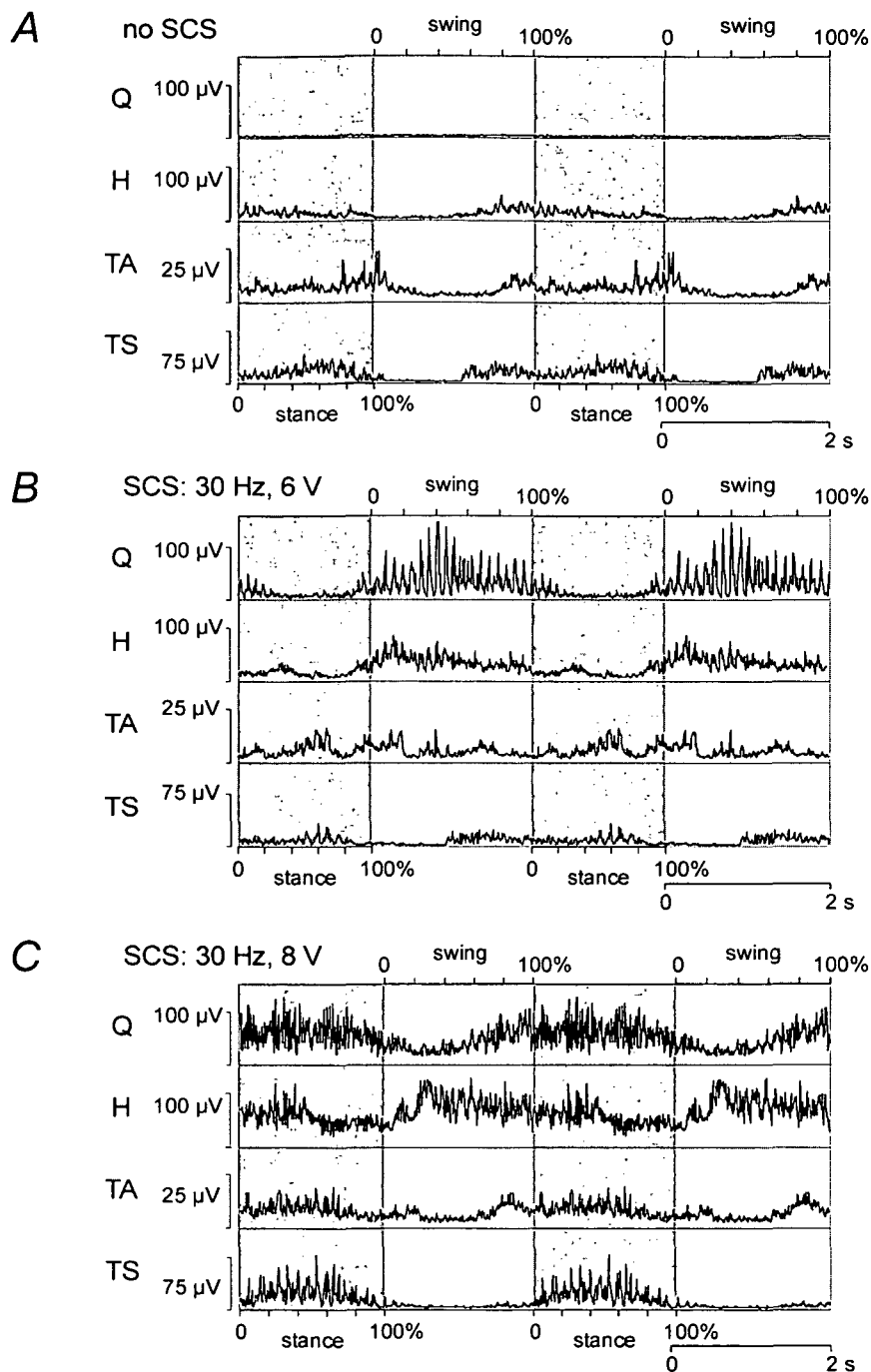


Figure 4.2 Lower limb EMG activity induced by assisted treadmill walking with body weight support (A) and additional spinal cord stimulation (B, C)

Averaged rectified EMG activity relative to normalized step cycle of quadriceps (Q), hamstrings (H), tibialis anterior (TA) and triceps surae (TS) shown for two cycles. Stance phases are marked by gray background. Treadmill speed was 0.8 km/h (0.22 m/s), body weight support was 80%. Data is derived from subject 1.

pattern compared to the trial without stimulation. Tibialis anterior did not show consistent rhythmicity of EMG activity synchronized to any specific phase of the step cycle. There was no apparent change of the triceps surae burst pattern compared to the one recorded during assisted stepping without electrical stimulation.

Increasing the epidural stimulation strength to 8 V at 30 Hz further changed the EMG activation patterns of the paralyzed lower limb muscles (Fig. 4.2C). Quadriceps bursts were prolonged and displayed EMG components evoked at a higher rate than during stimulation with 6 V and 30 Hz. Moreover, the muscle was mainly active during the stance phase and showed a minimum activation between 20 and 40% of the swing phase. During this period of minimum quadriceps activation the hamstrings burst reached highest amplitudes. The EMG burst of triceps surae was primarily present during the stance phase and contained some high-amplitude and low-frequency (10 Hz) components. Tibialis anterior displayed co-activation with triceps surae with some additional components during early and late swing. The EMG patterns in the paralyzed lower limb muscles induced by mechanical stimulation and additional epidural stimulation at 30 Hz and 8 V resembled the patterns recorded in able-bodied subjects (Fig. 4.1B) with the exception of the tibialis anterior activity during the stance phase.

Contributions of mechanical (phasic) and electrical (tonic) stimulation to the induced EMG activities

Figure 4.3 presents the effect of the onset of mechanical stimulation associated with manually assisted treadmill-stepping on the EMG activity of the quadriceps (Q) and triceps surae (TS) muscles under different initial conditions (subject 1). In Fig. 4.3A spinal cord stimulation was off and after the first four seconds of displayed recording the lower limb was manually assisted through the first swing phase. The cyclic mechanical stimulation initiated an EMG burst in triceps surae with a characteristic pattern that was synchronized with the stepping cadence and was consistently preceding the onset of the stance phase (marked by gray background). Passive stepping initially generated some low-amplitude EMG activity in quadriceps without consistent rhythmicity which did not persist more than some step cycles. Before the onset of the recording shown in Fig. 4.3B, epidural stimulation was turned on at 30 Hz and 6 V and was continuously active during the displayed 30 seconds. During supported standing before the first swing was initiated, some low amplitude ($< 30 \mu\text{V}$) CMAPs related to the epidural stimulation were present in quadriceps, while no consistent activation was detected in triceps surae. After completing the first step cycle, amplitudes of the stimulus-related CMAPs in quadriceps increased during the second swing phase. This EMG activity further increased in amplitudes, having burst-like shapes synchronized to the swing phases of the passive stepping. In triceps surae an EMG pattern similar to the one observed in the trial without stimulation was established during the assisted stepping. When epidural stimulation strength was increased to 8 V (Fig. 4.3C) and the lower limbs were not passively moved, each pulse of the 30 Hz-train evoked a single CMAP in the quadriceps muscle with a constant latency of 8 ms. The resulting EMG pattern showed some modulations but without consistent rhythmicity. There was no stimulus-evoked activity recorded in triceps surae. Additional mechanical stimulation associated with assisted stepping had a modulatory effect on the quadriceps activity. The quadriceps EMG activity solely consisted of CMAPs that could be unequivocally related to the electrical stimulation. While the lower limbs were passively moved, the amplitudes of the stimulus-evoked quadriceps-CMAPs during the early stance phases were higher than during supported standing and were attenuated during the swing phases. As in the case of the quadriceps muscle and 6 V-stimulation, 8 V-stimulation induced high-amplitude EMG activity in triceps surae but only in combination with mechanical stimulation. The muscle was solely active during the stance phases.

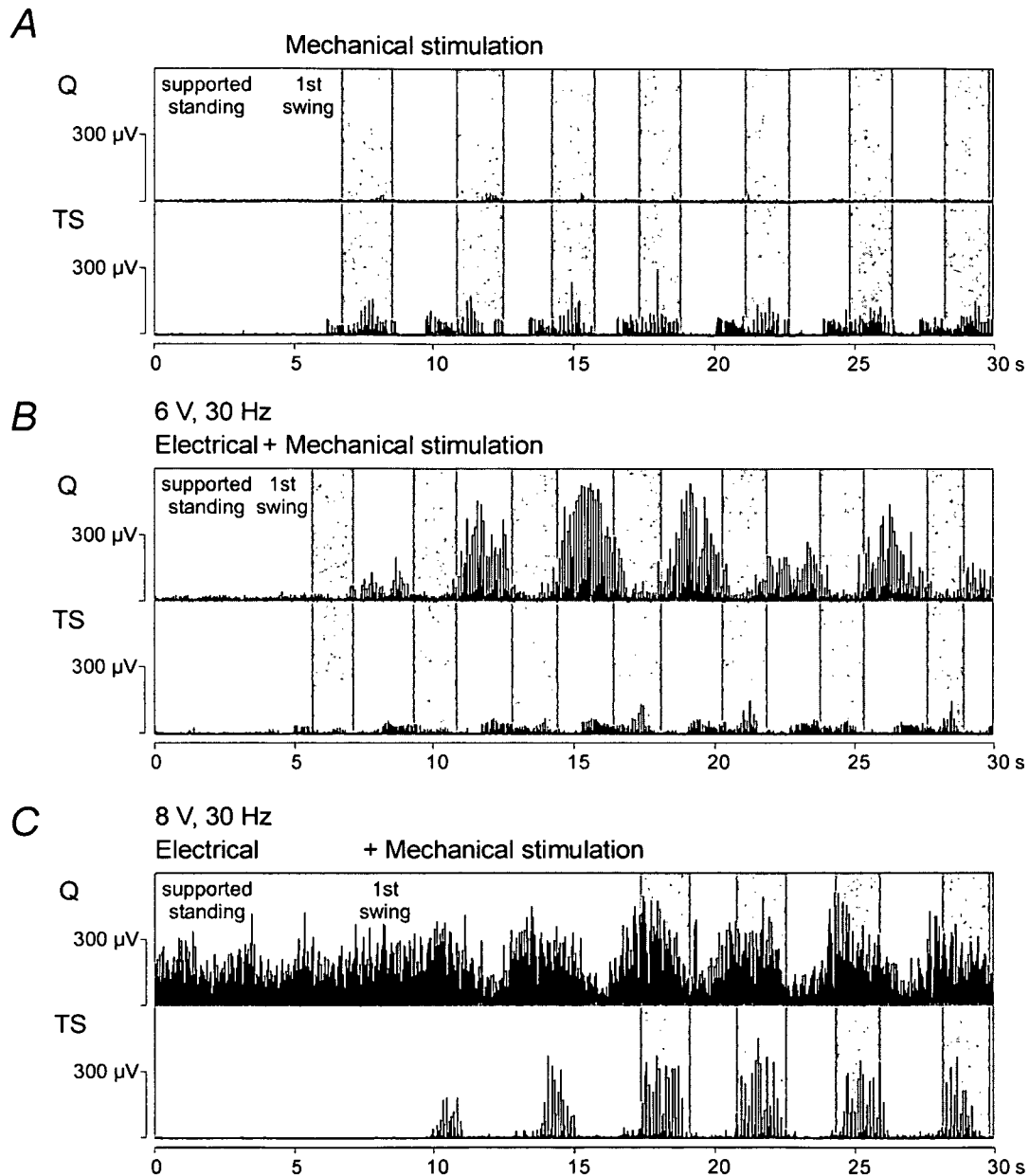


Figure 4.3 Transition from supported standing to passive stepping without (A) and with spinal cord stimulation (B, C)

Continuous rectified EMG activity (1024 samples/s) of quadriceps (Q) and triceps surae (TS) showing the effect of the onset of first manually assisted steps on a treadmill under different initial stimulation conditions. Gray background marks stance phases after a treadmill speed of 0.8 km/h (0.22 m/s) was reached. Data derived from subject 1.

Figure 4.4A demonstrates the enhancing and suppressing effect of mechanical stimulation on the EMG activity of triceps surae (TS) with epidural stimulation continuously active at two different strengths (subject 1). In the top figure, spinal cord stimulation at 8 V and 30 Hz did not initiate an EMG activity before the onset of mechanical stimulation. After the first passive swing of the lower limb, EMG bursts were evoked during the stance phases. The EMG bursts had higher amplitudes than in trials of assisted stepping without epidural stimulation. After the last passive step cycle was performed and a supported standing

position of the subject was established, epidural stimulation was further delivered but was not effective in evoking any activity in triceps surae. In the case illustrated at the bottom of Fig. 4.4A, electrical stimulation was applied at supra-threshold level (10 V, 30 Hz) and continuously elicited high-amplitude EMG responses in triceps surae before the first passive swing was performed. As soon as the lower limb was manually assisted through the first swing phase, epidural stimulation failed to evoke EMG responses during the early swing phases. After the end of passive stepping, epidural stimulation again consistently elicited trains of EMG responses.

In Fig. 4.4B the effect of different strengths of epidural stimulation on the EMG pattern of the evoked quadriceps (Q) activity during passive stepping is outlined (subject 1). Increasing stimulation strength from 6 V to 8 V at 30 Hz significantly changed the timing of the EMG bursts with respect to the phases of the gait cycle. While at 6 V the EMG bursts were induced during the whole swing phase with maximum amplitudes at 40% of the swing phase, at 8 V the muscle showed a maximum activity at the transition from swing to stance and was active during the whole stance phase.

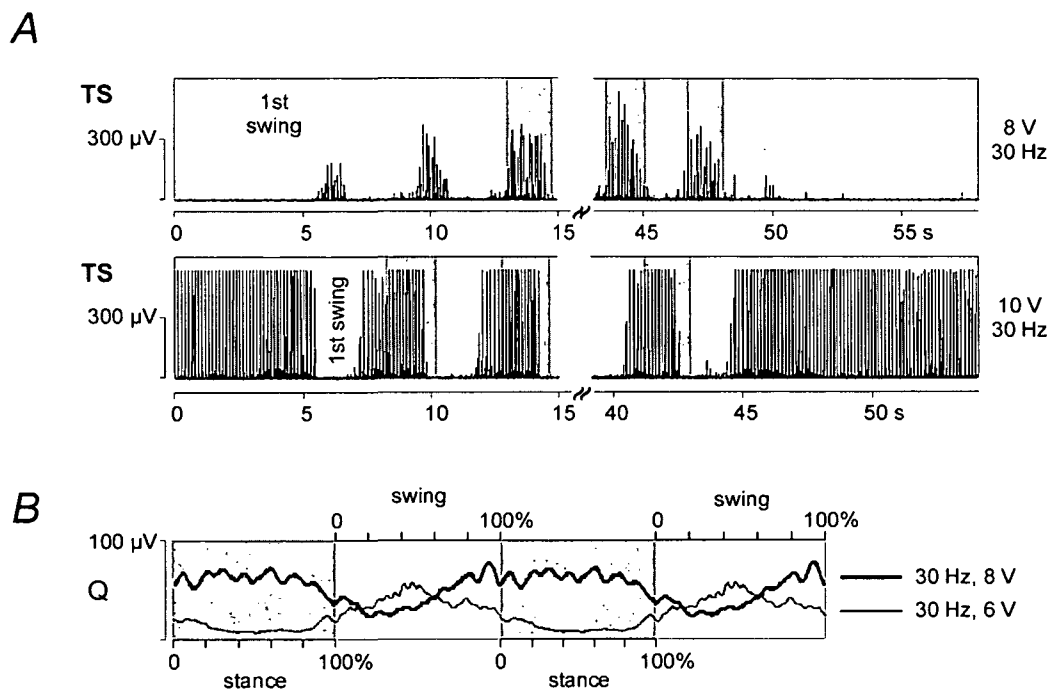


Figure 4.4 Effects of mechanical and electrical stimulation on the EMG patterns during passive treadmill stepping

A, Rectified EMG activity (1024 samples/s) of triceps surae (TS) at the onset and the end of manually assisted treadmill stepping and additional epidural stimulation at 8 V, 30 Hz (top figure) and 10 V, 30 Hz. Stance phases are marked by gray background. EMG signal is cut at $\pm 536 \mu\text{V}$ (see *Methods*). *B*, Averaged EMG activity (μV) with respect to normalized step cycle of the quadriceps (Q) muscle (rectified, low-pass filtered at 5 Hz). Comparison of the effect of 6 V, 30 Hz and 8 V, 30 Hz stimulation, while the same externally controlled maneuver of passive stepping movement is performed.

Figure 4.4 demonstrated the enhancing (Fig 4.4A, top figure) and suppressing (Fig 4.4B, bottom figure) effect of mechanical stimulation in combination with epidural stimulation on the muscle activation pattern during passive treadmill stepping. Furthermore it was shown

that spinal cord stimulation not only induced “test” responses influenced by a dominating conditioning effect of the mechanical stimulation, but could also modulate and change the timing of efferent motor patterns of complete spinal cord injured subjects during manually assisted stepping on a treadmill (Fig 4.4B).

The effect of epidural cathode position on the induced EMG patterns

The optimal cathode levels to initiate stepping-like movements in paralyzed lower limbs, when subjects were lying in a supine position, were identified to be at the L2–L4 segments. In subject 2 the electrode location was more caudal than in subject 1 (see methods). This allowed studying the effect of stimulation with a cathode below the upper lumbar segmental levels. Passive treadmill stepping without epidural stimulation triggered some low-

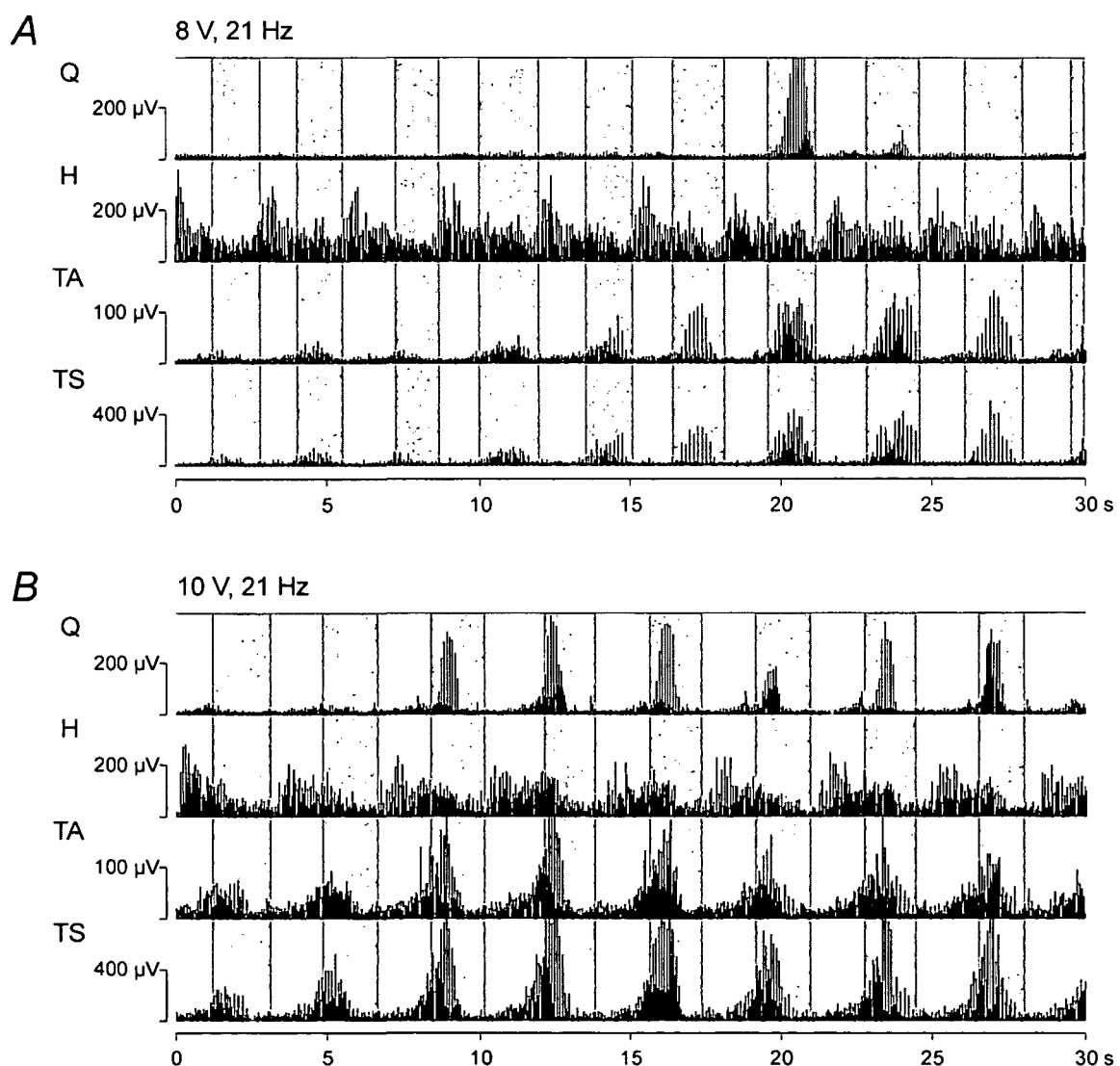


Figure 4.5 Effect of a caudally placed stimulating electrode on the EMG patterns during passive treadmill stepping

Rectified continuous EMG activity (1024 samples/s) of the quadriceps (Q), hamstrings (H), tibialis anterior (TA) and triceps surae (TS) muscles induced by continuous spinal cord stimulation at a constant frequency of 21 Hz and strengths of 8 V (A) and 10 V (B) during passive treadmill stepping displayed for 30 seconds. Treadmill speed was 0.4 km/h (0.11 m/s), body weight support was 80%. Data was derived from subject 2 (recording 3).

amplitude EMG activity mainly in the distal lower limb muscles demonstrating co-activation during the stance phases. Additional spinal cord stimulation at 8 V and 21 Hz (Fig. 4.5A) resulted in EMG bursts in the hamstrings, tibialis anterior and triceps surae muscles temporally synchronized to specific phases of the step cycle. Tibialis anterior and triceps surae showed co-activation during the stance phases (marked by gray background). The corresponding EMG bursts were composed of stimulus-triggered CMAPs with latencies of 16.5 ms. The hamstrings activity consisted of stimulus-evoked CMAPs with latencies of 11 ms and maximum amplitudes during the early swing phases. In the quadriceps muscle only two EMG bursts during the seventh and eighth stance phase of the shown 30 second-trace were evoked. At a stimulation strength of 10 V the EMG amplitudes of the tibialis anterior and triceps surae bursts increased. After the second displayed step cycle, bursts were consistently induced in quadriceps during the early stance phases. The increase in stimulation strength did not enhance the activity in the hamstrings but decreased the amplitude of the induced EMG activity at the transitions from the stance to swing phases.

The recordings derived from subject 2 demonstrated that epidural stimulation during passive treadmill-stepping could induce EMG bursts in the paralyzed lower limb muscles, even if predominantly delivered to cord levels caudal to the L2–L4 segments. However, the burst-style EMG activities did not resemble functional locomotor patterns.

The effect of different frequencies of spinal cord stimulation on the induced EMG patterns

Figure 4.6 shows the effect of “low” stimulation frequencies of 10–30 Hz on the EMG patterns recorded from the quadriceps muscle during manually assisted stepping on a treadmill (subject 2, electrode polarity: c+2–). When spinal cord stimulation was applied with 10 V at 10 Hz without additional mechanical stimulation (supported standing position, first 6 seconds of Fig. 4.6A), stimulus-coupled CMAPs with a constant latency of 9 ms were evoked. Successively elicited CMAPs did not show systematically modulated EMG amplitudes. Mechanical stimulation associated with assisted treadmill walking demonstrated some modulatory effect on the induced EMG activity and increased the amplitudes of the stimulus-evoked CMAPs during the late stance phases. EMG amplitudes of the stimulus-evoked CMAPs decreased when stimulation frequency was increased to 15 Hz (first 6 seconds of Fig. 4.6B). With the onset of mechanical stimulation the EMG amplitudes increased during the late stance and late swing phases. The enhancing effect of the mechanical stimulation which was synchronized with the stepping cadence was more apparent than in the case of 10 Hz-stimulation. Continuous stimulation with 10 V at 30 Hz (Fig. 4.6C) failed to elicit any quadriceps activity when the subject was in a supported standing position. After the first step cycle was carried out passively, a short burst activity was built up during the second stance phase and further increased in amplitude during the following steps. A quasi-stationary condition was reached after the sixth passive step cycle. The short, high-amplitude bursts consisted of frequency-following CMAPs with a latency of 9 ms.

Results of “higher” stimulation frequencies (20–60 Hz) on the induced quadriceps EMG patterns are illustrated in Fig. 4.7 (subject 2, electrode polarity: 0+3–). At a stimulation strength of 10 V, frequencies of 20, 30 and 50 Hz induced EMG bursts during the stance phases of the step cycle. The lowest frequency inducing EMG bursts separated by phases of

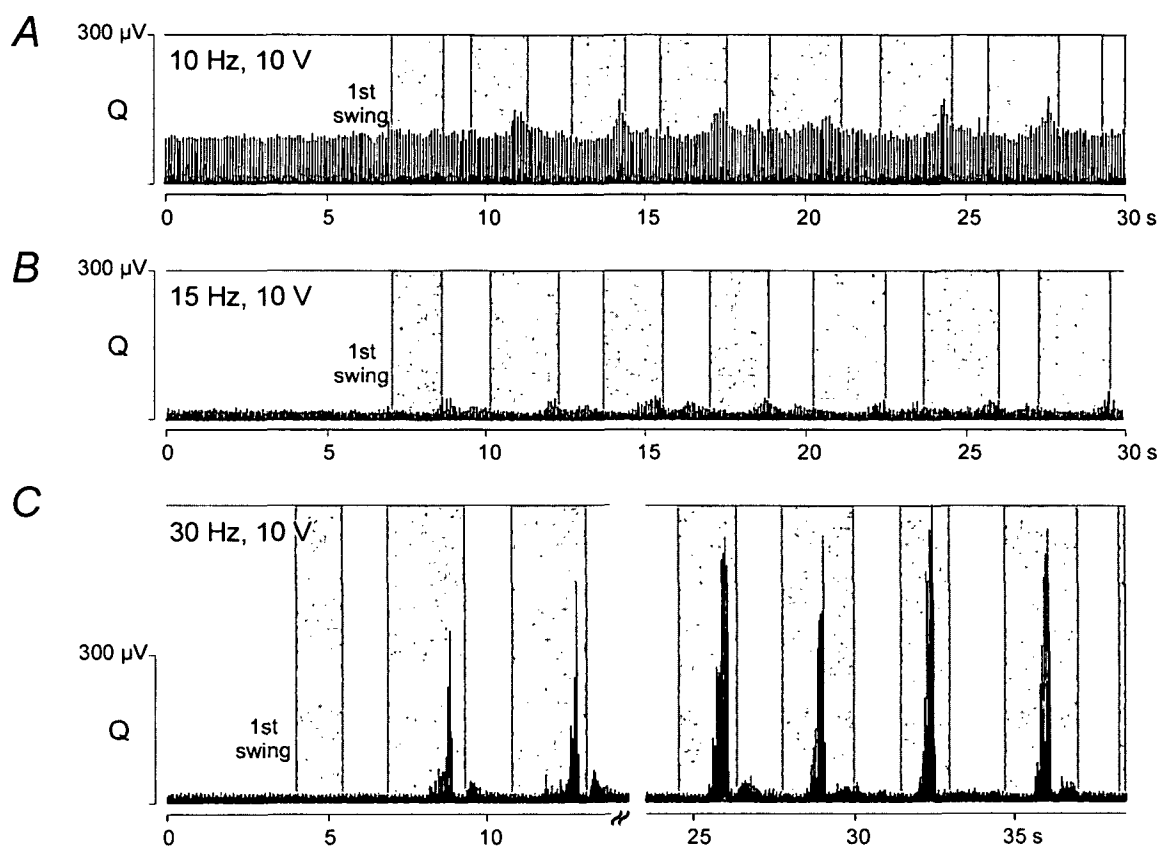


Figure 4.6 Effect of stimulation frequencies of 10–30 Hz on the EMG patterns during passive treadmill stepping

Rectified EMG activity (2048 samples/s) of the left quadriceps muscle induced by mechanical stimulation and additional continuous spinal cord stimulation delivered at a constant strength of 10 V and frequencies of 10, 15 and 30 Hz. At the onset of each displayed trace spinal cord stimulation was on and the subject was in a supported standing position. After some seconds of recording, the lower limb was passively moved through the first step cycle (gray backgrounds mark the stance phases of stepping). Data was derived from subject 2 (recording 2, electrode polarity: c+2–).

inactivity/low activity was 20 Hz. Increasing the frequency to 30 and 50 Hz shifted the EMG burst to the early stance with maximum amplitudes at 20% and 46% of the stance phase, respectively. At 60 Hz epidural stimulation in combination with assisted treadmill stepping did not evoke any systematically modulated EMG activities in the lower limb muscles. This was also the case when frequencies of 80 Hz and 100 Hz were applied at the same strength using the same electrode set-up (not displayed in the figure).

In the subjects 1 and 2, stimulation with 38 different parameter combinations between 1–10 V and 10–100 Hz were applied during four different testing sessions. Eighteen of the combinations induced EMG bursts during passive treadmill stepping, all were within the range of 20–50 Hz and 6–10 V (median: 30 Hz, 10 V, mean: 33.1 Hz, 9 V). The findings were consistent both within and between testing sessions.

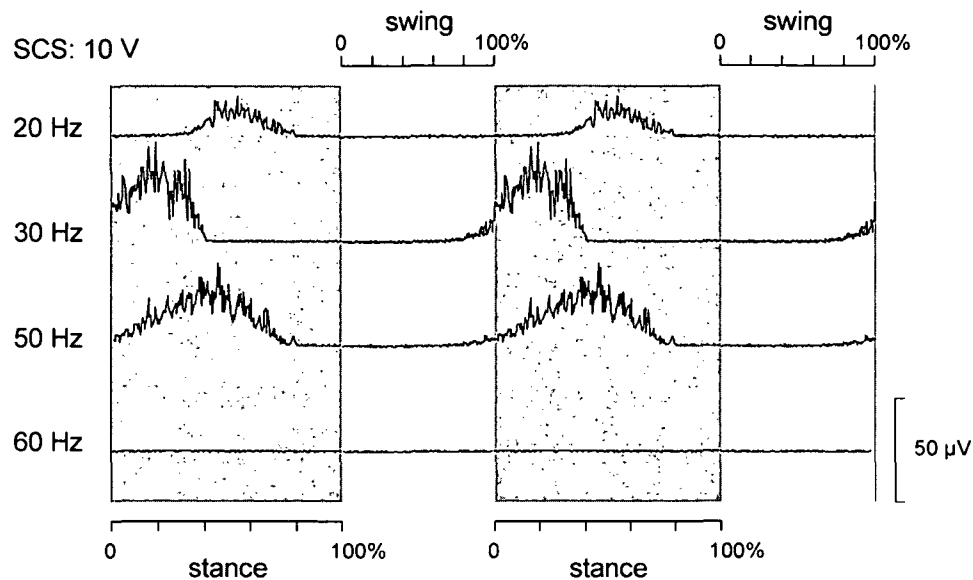


Figure 4.7 Effect of stimulation frequencies of 20–60 Hz on the EMG patterns during passive treadmill stepping

Averaged ($n = 10$ stance and 10 swing phases) rectified EMG activity (μV) with respect to time-normalized stance and swing phase of the step cycle. Stance phases are marked by gray background, the duration of stance and swing phase is displayed with a ratio of 60:40 for all cases. Data is derived from left quadriceps, subject 2 (recording 2, electrode polarity: 0+3–). Stimulation strength was 10 V in the shown cases.

DISCUSSION

Effect of phasic peripheral feedback input to the isolated lumbar cord

Peripheral sensory feedback input to the spinal cord associated with assisted treadmill stepping generated EMG bursts in the paralyzed lower limbs which were characterized by co-activation during the late swing and the whole stance phase (Fig. 4.2A). EMG activity was smallest or even absent in the quadriceps muscle. Thus, proprioceptive feedback input to the isolated spinal cord generated a non-functional EMG burst pattern which was different to the locomotor pattern observed in able-bodied subjects during active treadmill stepping and comparable recording conditions (Fig. 4.1B). Note that the spinal cord injured subjects included in the present study never participated in a locomotor training prior to the recordings.

Effect of tonic input to the lumbar cord generated by spinal cord stimulation

Epidural stimulation applied at strengths above the motor threshold of a given muscle while the subject was in an upright, supported standing position (i.e. without additional proprioceptive input related to passive stepping movements) was not effective in generating EMG bursts in the lower limb muscles (see first seconds of Figs. 4.3C, 4.4A and 4.6). Stimulation at frequencies below 20 Hz (Fig. 4.6A and B) induced a tonic activity consisting of frequency-following CMAPs with short latencies characteristic for monosynaptic Posterior Roots Muscle Reflex Responses (PRMRRs, see Chapter 2;

Minassian *et al.* 2004a). At frequencies between 20–50 Hz and before the onset of passive stepping, modulated tonic EMG patterns were generated in some cases but without consistent rhythmicity or periods of inactivity/low activity (Fig. 4.3C).

On the other hand, rhythmic stepping-like EMG activity could be induced by epidural stimulation in the subjects 1 and 2 when they were lying in a supine position with parameters between 20–50 Hz and 7–10 V (several recordings carried out between 1997 and 1999).

The inefficiency of epidural stimulation to induce stepping-like EMG bursts without additional mechanical stimulation by passive lower limb movements might be due to biophysical and physiological differences resulting from the upright body position of the subject. Since the subjects had subclinically complete spinal cord injuries, any supraspinal influence during the (supported) standing position like additional extrapyramidal control contribution to the excitation of spinal cord motor cell pools can be ruled out.

It is well known in the clinical application of epidural spinal cord stimulation for the control of spasticity that the effect of stimulation depends on the subject's posture. At a given stimulus strength, the effect of stimulation decreases when the subject's position is changed from supine to upright, and from upright to prone position, respectively. The intradural geometry, and primarily the dorsal cerebrospinal fluid layer, strongly influences the effect of epidural spinal cord stimulation (Struijk *et al.* 1993; He *et al.* 1994). The intradural antero-posterior position of the spinal cord, and thus the dorsal cerebrospinal fluid layer-thickness, depends on the subject's posture. The dorsal cerebrospinal fluid layer-thickness is at its minimum when the subject is in a supine position and maximum when the subject is in a prone position (Holsheimer *et al.* 1994). When the subject is upright, the intradural antero-posterior position of the spinal cord is between the situations described by Holsheimer *et al.* (1994). With increasing cerebrospinal fluid layer-thickness, the thresholds for posterior root recruitment increase. Accordingly, during a supported standing position of the subject, the stimulation strength necessary to stimulate lumbar posterior roots sufficiently to activate the Lumbar Locomotor Pattern Generator (LLPG, see Chapter 3; Minassian *et al.* 2004b) might be above the limit (10 V) of the used pulse generator.

Another difference between the supine and supported-standing position of the subjects is the amount of afferent inflow from cutaneous and articular receptors associated with weight-bearing to the spinal cord. During passive standing on the treadmill trainers had one hand on the front of the thigh or knee of the spinal cord injured subject to keep the knee in full extension. Thus, during this supported standing the subject's lower limbs were passively bearing considerable weight (the difference between body weight and body weight support provided by the counterweights). The corresponding sustained proprioceptive input signaling standing could have some suppressive effect on the lumbar spinal interneurons to temporarily combining into locomotor pattern generating networks.

Effect of spinal cord stimulation-evoked tonic input in conjunction with phasic peripheral feedback input to the lumbar cord

When the same externally controlled maneuver of assisted treadmill stepping was performed, very different EMG patterns were induced depending on the frequency of the applied epidural stimulation, namely modulated tonic or burst-type rhythmic activity (Fig. 4.6). When stimulation frequency was increased above 50 Hz, motor output could be even completely suppressed during passive treadmill stepping (Fig. 4.7).

Epidural stimulation applied at frequencies below the range of 20–50 Hz effective to activate the LLPG (Chapter 3; Minassian *et al.* 2004b) could induce a tonic EMG activity during supported standing position. The tonic EMG activity was amplitude-modulated when additional proprioceptive input related to passive stepping was provided to the spinal cord (Figs. 4.6A and B). However, burst-style rhythmic activity could not be induced. It was shown that epidural stimulation with frequencies between 5–15 Hz can set-up an “extension pattern generator”-configuration of the lumbosacral interneuronal networks (Jilge *et al.* 2004), generating a sustained motor output. Once established by the appropriate frequency of stimulation, Figs. 4.6A and B suggest that this set-up of the lumbar internuncial networks cannot be overridden by peripheral phasic feedback input related to passive stepping movements to operate as a locomotor pattern generator.

A mechanism simpler than the contribution of pattern generating spinal networks may account for the amplitude-modulations of the epidurally-evoked tonic EMG activity. In the presented examples in Figs. 4.6A and B the main effect of mechanical stimulation was a periodic augmentation of the tonic quadriceps activity during the late stance phases. During these phases the quadriceps muscle is stretched (imposed knee flexion while the hip is still in an extended position), and the lower limb is loaded. This proprioceptive input to the corresponding lumbar spinal segments may depolarize motoneurons and premotoneuronal spinal structures. These structures would be then closer to threshold and thus more responsive to sustained electrical stimulation during the corresponding phases of the gait cycle. A similar effect was described by Mushahwar and colleagues (2000) in healthy, adult cats. They implanted arrays of microwires in the lumbosacral region of the feline spinal cord to study the quality of lower limb movements that could be elicited from within the active, nonanesthetized spinal cord. The effect of afferent input on stimulus threshold was also described. It was reported that imposed knee flexion increased EMG responses in quadriceps. At a given stimulus intensity of electrical stimulation, EMG responses increased with increasing angular velocities of imposed movement (i.e., the threshold for activating the muscle was reduced). Upon termination of knee flexion, stimulus-evoked EMG activity returned to its pre-stretch levels in the cat.

In Fig. 4.6C, epidural stimulation was applied at 30 Hz while passive stepping movement was performed like in the Figs. 4.6A and B. The modulated tonic EMG activity as induced at frequencies below 20 Hz was replaced by a burst-style rhythmical one at 30 Hz stimulation. This finding indicates that epidural stimulation at appropriate frequencies could facilitate the LLPG set-up of the lumbar internuncial networks. This organization is expressed by generation of rhythmical efferent output.

The stimulation strength and the number of recruited lumbar cord segments determined to what degree the internuncial lumbar cord networks responded to repetitive and regular stimulation at 20–50 Hz by setting up an LLPG organization. The effect of increasing the strength of stimulation at a constant frequency of 30 Hz was demonstrated in the Figs. 4.2 and 4.3. In Fig. 4.3 only quadriceps and triceps surae were considered, since they are the only of the recorded muscle groups with separate segmental innervations (L2–L4 vs. L5–S2). Due to the upper lumbar position of the cathode in subject 1 (see *Methods* and Table 4.2), epidural stimulation predominantly stimulated the segments L2–L4 which were near to the cathode. At 6 V and 30 Hz, epidural stimulation of posterior roots was not strong enough to activate lower limb motor neuron pools during supported standing position (Fig. 4.3B, first 4 seconds of recording). Phasic feedback input related to rhythmic stepping lowered the thresholds of the premotoneuronal spinal structures. During passive stepping,

the 6 V-stimulation induced separate CMAPs in the L2–L4 innervated quadriceps muscle that were subject to well-defined amplitude modulations resulting in burst-like envelopes of the EMG activity (Fig. 4.3B, after the first swing). However, the timing of the burst-style EMG activities was non-functional since they had maximum amplitudes during the swing phases (compare with Fig. 4.1B). The CMAPs composing the burst-style EMG activities in quadriceps were consistently responding at 10 Hz and were not following the stimulation frequency of 30 Hz. (This is in contrast to the findings in supine position, where epidurally-evoked burst-style EMG activities consisted of frequency-following CMAPs, see Minassian *et al.* 2004a,b; Chapters 2 and 3). Due to the cathode position, the current spread in caudal direction was not sufficient at 6 V to activate the more distant posterior roots of the L5 and S1 segments. Consequently, no CMAPs related to the epidural stimulation were detected in triceps surae even during passive treadmill-stepping in the case of 6 V-stimulation. At 8 V and 30 Hz (Fig. 4.3C), a phase shift in the quadriceps activation patterns occurred. The timing of the quadriceps EMG activity was a more functional one. The amplitude-modulated CMAPs composing the burst-style quadriceps activity were elicited with a frequency of 30 Hz and were thus frequency-following. Furthermore, stimulation-related CMAPs were also induced in the triceps surae muscle. These findings suggest that at 6 V the epidural stimulation did not provide strong enough tonic stimuli to sufficiently activate the LLPG. Peripheral feedback input helped to express some features of the LLPG, even when not fully established. The more functional EMG patterns at 8 V indicate that a more complete LLPG set-up was built up by the stronger tonic stimuli.

The importance of a predominant stimulation of upper lumbar cord segments to elicit stepping-like EMG patterns could be deduced from Fig. 4.5. There, epidural stimulation delivered to lower lumbar cord segments during assisted treadmill-walking induced rhythmic EMG activity in the lower limb muscles which mainly co-activated during the stance phases.

Significance of the results

It was shown that subjects with clinically complete spinal cord injuries can generate stepping-like efferent patterns when partially supported over a moving treadmill belt and manually assisted with stepping (Dietz *et al.* 1995; Dobkin *et al.* 1995). These studies were taken as evidence that sensory information associated with weight-bearing passive stepping can activate and coordinate locomotor networks in the spinal cord which can generate stepping-like EMG patterns.

The present study suggests that the peripheral feedback input related to passive treadmill-stepping can make use of pattern generating networks in the isolated lumbar cord to produce rhythmic EMG activities in the lower limb muscles. However, the efficiency of the phasic afferent input in modifying the central state of spinal circuits and to fully develop an LLPG organization was limited. An essential role of the phasic input was that of reinforcing LLPG activities. This could be clearly seen in cases where epidural stimulation was applied at frequencies of 20–50 Hz but at strengths below motor threshold. Another crucial role of peripheral afferent input was a timing function, which was reflected by the temporal synchronization of EMG bursts to specific phases of the step cycle.

Epidural stimulation provided a repetitive, regular input to several lumbar and upper sacral cord segments via the posterior roots to the lumbar spinal cord. While coming from “periphery”, the tonic input at a constant frequency is unlike physiological sensory

feedback information. We speculate that the tonic input of particular frequencies is interpreted by the lumbar interneuronal structures as a central command signal due to its code. This “central” peripheral input was capable of modifying the central state of spinal lumbar networks. At frequencies of 20–50 Hz an LLPG organization could be established. Thereby the responsiveness of the spinal circuits to proprioceptive feedback to generate stepping-like efferent motor patterns was significantly enhanced. This effect could be achieved immediately as soon as the appropriate stimulus parameters were applied.

Originally, evidence has been adduced for the existence of a LLPG in supine individuals (Dimitrijevic *et al.* 1998). With the limited information from periphery to the LLPG, amplitude and timing of the cyclical motor output could only be set to some default level in these studies. The present study provides the significant result, that the LLPG activated by epidural stimulation can adapt its motor output to external demands during passive stepping. The spinal lumbar networks can integrate and interpret the “central” peripheral inputs (provided by epidural stimulation) and the proprioceptive inputs (associated with passive stepping) in order to generate functional locomotor patterns. This also implies that both, the tonic and the phasic afferent inputs – which have very different sources of origin – converge on common components of spinal rhythm-generating networks.

We take the findings of the present study as further evidence that lumbar interneurons can be temporarily incorporated into pattern generating networks for stepping-like activity – the LLPG. The LLPG can be set-up by epidural stimulation even when a massive afferent inflow from various sensory organs in muscles, joints, skin, and connective tissues induced during weight-bearing, manually assisted stepping is delivered to the spinal cord. The internuncial cord network can immediately respond by building up an LLPG circuitry when tonic input at 20–50 Hz is provided to the lumbar cord. To generate and enhance stepping-like EMG activity by solely activating the LLPG with phasic feedback input requires a regular locomotor training for an extended period of time. This might be due to the inappropriate code used to activate the LLPG, i.e. the lack of a tonic component of the mechanical stimulation. Therefore we suggest that sustained electrical stimulation to elicit a multisegmental “central” afferent input to the lumbar spinal cord might be a valuable adjunct to treadmill training in spinal cord injured patients.

REFERENCES

- Dietz V, Colombo G, Jensen L & Baumgartner L (1995). Locomotor capacity of spinal cord in paraplegic patients. *Ann Neurol* **37**, 574-582.
- Dietz V, Muller R & Colombo G (2002). Locomotor activity in spinal man: significance of afferent input from joint and load receptors. *Brain* **125**, 2626-2634.
- Dimitrijevic MR, Gerasimenko Y & Pinter MM (1998a). Evidence for a spinal central pattern generator in humans. In *Neural Mechanisms for Generating Locomotor Activity. Ann N Y Acad Sci Vol. 860*, ed. Kiehn O, Harris-Warrick RM, Jordan LM, Hultborn H & Kudo N, pp. 360-376. New York Academy of Sciences, New York.
- Dimitrijevic MR, Gerasimenko Y & Pinter MM (1998b). Effect of reduced afferent input on lumbar CPG in spinal cord injury subjects. Soc Neurosci Abstr; 24: Program No. 654.23.
- Dobkin BH, Harkema S, Requejo P & Edgerton VR (1995). Modulation of locomotor-like EMG activity in subjects with complete and incomplete spinal cord injury. *J Neurol Rehabil* **9**, 183-190.
- Ferris DP, Gordon KE, Beres-Jones JA & Harkema SJ (2004). Muscle activation during unilateral stepping occurs in the nonstepping limb of humans with clinically complete spinal cord injury. *Spinal Cord* **42**, 14-23.
- Harkema SJ, Hurley SL, Patel UK, Requejo PS, Dobkin BH & Edgerton VR (1997). Human lumbosacral spinal cord interprets loading during stepping. *J Neurophysiol* **77**, 797-811.
- He J, Barolat G, Holsheimer J & Struijk JJ (1994). Perception threshold and electrode position for spinal cord stimulation. *Pain* **59**, 55-63.
- Holsheimer J, den Boer JA, Struijk JJ & Rozeboom AR (1994). MR assessment of the normal position of the spinal cord in the spinal canal. *Am J Neuroradiol* **15**, 951-959.
- Jilge B, Minassian K, Rattay F, Pinter MM, Gerstenbrand F, Binder H & Dimitrijevic MR (2004). Initiating extension of the lower limbs in subjects with complete spinal cord injury by epidural lumbar cord stimulation. *Exp Brain Res* **154**, 308-326.
- Minassian K, Jilge B, Rattay F & Dimitrijevic MR (2004a). Posterior Roots Muscle Reflex Responses elicited by epidural stimulation of the human lumbar cord. *J Physiol*, submitted.
- Minassian K, Jilge B, Rattay F, Pinter MM, Binder H, Gerstenbrand F & Dimitrijevic MR (2004b). Stepping-like movements in humans with complete spinal cord injury induced by epidural stimulation of the lumbar cord: Electromyographic study of compound muscle action potentials. *Spinal Cord* May 4 [Epub ahead of print].
- Murg M, Binder H & Dimitrijevic MR (2000). Epidural electric stimulation of posterior structures of the human lumbar spinal cord: 1. muscle twitches – a functional method to define the site of stimulation. *Spinal Cord* **38**, 394-402.
- Mushahwar VK, Collins DF & Prochazka A (2000). Spinal cord microstimulation generates functional limb movements in chronically implanted cats. *Exp Neurol* **163**, 422-429.
- Struijk JJ, Holsheimer J & Boom HB (1993). Excitation of dorsal root fibers in spinal cord stimulation: A theoretical study. *IEEE Trans Biomed Eng* **40**, 632-639.

Curriculum Vitae

Personal Data

Name Dipl.Ing. Karen Minassian
 Date of Birth 12 April 1974
 Place of Birth Tehran, Iran
 Nationality Austria

Education

Since October 2000 PhD studies at the Vienna University of Technology
 October 1992 – July 2000
 Studies in Technical Physics at the Vienna University of Technology
 1984 – 1992 Secondary School: Bundesrealgymnasium IV, Vienna
 Graduation in June 1992

Internships

June 1998 – July 1998 Internship at the Department of Biomedical Engineering and Physics, Medical University of Vienna
 April 1997 – June 1997 Internship at the Research Department of Hilti, Schaan, Principality of Liechtenstein
 February 1997 – March 1997
 Internship at the Department of Fundamentals and Theory in Electrical Engineering, Vienna University of Technology

Employment Record

Since March 2003 Research associate at the Ludwig Boltzmann Institute for Electrical Stimulation and Physical Rehabilitation, Vienna
 October 2003 – January 2004
 Teaching assistant at the Department for Analysis and Scientific Computing, Vienna University of Technology
 October 2002 – January 2003
 Teaching assistant at the Department for Analysis and Technical Mathematics, Vienna University of Technology
 November 2000 – December 2002
 Research fellow in the project „Neurophysiologische Modellierung der Erregbarkeit der Lokomotionszentren im lumbalen

Rückenmark durch elektrische Stimulation“ (GZ 140.591/4-V/B/9b/2000, Federal Ministry for Transport, Innovation and Technology)

October 2001 – January 2002

Teaching assistant at the Department for Analysis and Technical Mathematics, Vienna University of Technology

List of scientific publications

1. Rattay F & Minassian K (1999). A computer model for the electrical stimulation of the spinal cord. *Med & Biol Eng & Comp* **37**, Suppl. 2: 800-801.
2. Rattay F, Naves Leao R, Minassian K & Markum H (1999). Finite Element Analysis for Electrical Nerve Simulation. Seminarband über Modellbildung und Simulation / MATLAB, Wien: 187-188.
3. Minassian K, Rattay F & Markum H (1999). Modell und Simulation der Rückenmarkstimulation mit implantierten Elektroden. Jahrestagung Österr Physik Ges, Innsbruck: 20.
4. Rattay F, Minassian K & Markum H (1999). The electrical stimulation of the spinal cord: Computer simulation with ANSYS and ACSL. Seminar zu Modellbildung und Simulation, Wien: 65-68.
5. Minassian K, Rattay F & Markum H (2000). The Electrical Stimulation of the Human Spinal Cord: A Computer Model Study. Deutsche Physik Ges.
6. Minassian K, Rattay F & Markum H (2000). The electrical stimulation of the spinal cord: Computer model for electrode positioning. Proc. Poster Session Vol. 3rd Mathmod IMACS Symposium on Math. Modelling: 15.
7. Minassian K, Rattay F & Markum H (2000). 3D Finite Element Approach and Simulation of the Excitation of the Spinal Cord. Jahrestagung Österr Physik Ges, Graz.
8. Rattay F & Minassian K (2000). Excitation of lower spinal cord structures with implanted electrodes: 3D finite element analysis and simulation of neural responses. *Österr Ges Neurowissenschaften-Newsletter* **13**, 27.
9. Minassian K (2000). Excitation of lower spinal cord structures with implanted electrodes: 3D finite element analysis and simulation of neural responses. Diploma Thesis, Vienna University of Technology.
10. Rattay F, Minassian K & Dimitrijevic MR (2000). Epidural electrical stimulation of posterior structures of the human lumbosacral cord: 2. quantitative analysis by computer modeling. *Spinal Cord* **38**, 473-489.
11. Rattay F, Minassian K & Markum H (2001). Simulation of electrical nerve stimulation with ACSL. ARGESIM Report: Modellbildung in der Mechatronik: ACSL, Dymola, ESL: 19-23.
12. Dimitrijevic MR, Minassian K, Murg M, PinterMM, Rattay F, Gerasimenko Y & Binder H (2001). Study of locomotor capabilities induced by spinal cord stimulation (SCS) of the human lumbar cord isolated from the brain control by posttraumatic spinal cord injury (SCI). Soc Neurosci Abstr; 27: Program No. 935.6.
13. Minassian K, Rattay F, Pinter MM, Murg M, Binder H, Sherwood A & Dimitrijevic MR (2001). Effective spinal cord stimulation (SCS) train for evoking stepping locomotor movement of paralyzed human lower limbs due to SCI elicits a late response additionally to the early monosynaptic response. Soc Neurosci Abstr; 27: Program No. 935.12.

14. Minassian K, Rattay F & Dimitrijevic MR (2001). Features of the reflex responses of the human lumbar cord isolated from the brain but during externally controlled locomotor activity. Proceedings of the World Congress on Neuroinformatics, Vienna, Austria; Part I: 55-57.
15. Minassian K, Rattay F & Dimitrijevic MR (2001). Features of the reflex responses of the human lumbar cord isolated from the brain but during externally controlled locomotor activity. Proceedings of the World Congress on Neuroinformatics, Vienna, Austria; Part II: 267-268.
16. Minassian K, Rattay F & Dimitrijevic MR (2001). A computer simulation and electrophysiological methods to identify the primary stimulated spinal cord structures with epidural electrodes. Proceedings of the World Congress on Neuroinformatics, Vienna, Austria; Part II: 284-285.
17. Gilge B, Minassian K, Dimitrijevic MR (2001). Involuntary movements of paralyzed lower limbs and residual brain control below spinal cord injury. Proceedings of the World Congress on Neuroinformatics, Vienna, Austria; Part II: 278-280.
18. Gilge B, Minassian K & Dimitrijevic MR (2001). Electrical stimulation of the human lumbar cord can elicit standing parallel extension of paralysed lower limbs after spinal cord injury. Proceedings of the World Congress on Neuroinformatics, Vienna, Austria; Part II: 281-283.
19. Minassian K, Rattay F, Dimitrijevic MR, Pinter MM, Gerstenbrand F & Binder H (2002). Neurophysiologische Modellierung der Erregbarkeit der Lokomotionszentren im lumbalen Rückenmark durch elektrische Stimulation. 2. Zwischenbericht über das Projekt GZ 140.591/4-V/B/9b/2000.
20. Gilge B, Minassian K, Rattay F & Dimitrijevic MR (2002). Tonic and rhythmic motor units activity of the cord induced by epidural stimulation can alter posterior roots muscle reflex responses. Proceedings of the 7th Annual Conference of the IFESS, Ljubljana, Slovenia: 164-166.
21. Minassian K, Gilge B, Rattay F, Pinter MM, Gerstenbrand F, Binder H & Dimitrijevic MR (2002). Effective spinal cord stimulation (SCS) for evoking stepping movement of paralyzed human lower limbs: study of posterior root muscle reflex responses. Proceedings of the 7th Annual Conference of the IFESS, Ljubljana, Slovenia: 167-169.
22. Dimitrijevic MR, Minassian K, Gilge B & Rattay F (2002). Initiation of standing and locomotion like movements in complete SCI subjects "by mimicking" brain stem control of lumbar network with spinal cord stimulation. Proceedings of the 4th International Symposium on Experimental Spinal Cord Repair and Regeneration, Brescia, Italy: 25-27.
23. Rattay F, Minassian K, Dimitrijevic MR, Pinter MM, Gerstenbrand F & Binder H (2002). Neurophysiologische Modellierung der Erregbarkeit der Lokomotionszentren im lumbalen Rückenmark durch elektrische Stimulation. Endbericht über das Projekt GZ 140.591/4-V/B/9b/2000.
24. Rattay F, Minassian K, Gilge B, Pinter MM, Dimitrijevic MR (2003). EMG analysis of lower limb muscle responses to epidural lumbar cord stimulation. Proceedings of the IEEE EMBS Conference Cancun (Mexico).

25. Rattay F, Resatz S, Lutter P, Minassian K, Gilge B & Dimitrijevic MR (2003). Mechanisms of electrical stimulation with neural prostheses. *Neuromodulation* 6(1), 42-56.
26. Pinter MM, Minassian K, Gilge B, Rattay F, Binder H, Gerstenbrand F & Dimitrijevic MR (2003). Locomotor movements in complete paraplegic subjects evoked by spinal cord stimulation. *European Journal of Neurology* 10(s1), 221.
27. Gilge B, Minassian K, Rattay F, Pinter MM, Gerstenbrand F, Binder H & Dimitrijevic MR (2004). Initiating extension of the lower limbs in subjects with complete spinal cord injury by epidural lumbar cord stimulation. *Exp Brain Res* 154, 308-326.
28. Minassian K, Gilge B, Rattay F, Pinter MM, Binder H, Gerstenbrand F & Dimitrijevic MR (2004) Stepping-like movements in humans with complete spinal cord injury induced by epidural stimulation of the lumbar cord: electromyographic study of compound muscle action potentials. *Spinal Cord* May 4 [Epub ahead of print].
29. Minassian K, Persy I, Rattay F, Binder H, Pinter MM & Dimitrijevic MR (2004). Output induced by manually assisted treadmill stepping of paraplegic individuals can be enhanced by epidural stimulation of the Lumbar Locomotor Pattern Generator. Abstract No. 4770, 34th Annual Meeting of the Society for Neuroscience, San Diego, CA.
30. Dimitrijevic MR, Dimitrijevic MM, Kern H, Minassian K & Rattay F (2004). Electrophysiological characteristics of H-reflexes elicited by percutaneous stimulation of the cauda equina. Abstract No. 4927, 34th Annual Meeting of the Society for Neuroscience, San Diego, CA.